INTEGRATING CROP GROWTH MODELS AND REMOTE SENSING FOR PREDICTING PERFORMANCE IN SORGHUM

by

Kai-Wei Yang

A Dissertation

Submitted to the Faculty of Purdue University

In Partial Fulfillment of the Requirements for the degree of

Doctor of Philosophy

Department of Agronomy

West Lafayette, Indiana

December 2021

THE PURDUE UNIVERSITY GRADUATE SCHOOL
STATEMENT OF COMMITTEE APPROVAL

Dr. Mitchell R Tuinstra, Chair

Department of Agronomy

Dr. Melba Crawford

Department of Agronomy, Civil Engineering, and
Electrical & Computer Engineering

Dr. Tony Vyn

Department of Agronomy

Dr. Scott Chapman

School of Agriculture and Food Sciences, The University of Queensland

Dr. Karthikeyan Natesan Ramamurthy

Thomas J. Watson Research Center, IBM

Approved by:

Dr. Ronald F. Turco

To my family

ACKNOWLEDGMENTS

This dissertation was made possible by the contribution of many. First, I would like to express my sincere gratitude to my advisor Dr. Mitchell Tuinstra. Dr. Tuinstra, thank you so much for giving me an opportunity to join your laboratory and the fantastic project. I really appreciate your guidance and support when I am worried. Thank you for being patient with me, I am very lucky for being your student.

I am grateful for the guidance and intellectual contributions of Dr. Karthikeyan Natesan Ramamurthy, Dr. Melba Crawford, Dr. Scott Chapman, and Dr. Tony Vyn while serving on my committee. Your support and the key insight improved this dissertation and my career.

I appreciate the technical support of the plant science team at Purdue: Dr. Clifford Weil and Dr. Adedayo Adeyanju; the APSIM team at the University of Queensland: Dr. Graeme Hammer, Dr. Greg McLean, Al, Bangyou, Jonathan; and the Purdue TERRA project team: Dr. Edward Delp, Dr. Ayman Habib, Dr. David Ebert, Yuhao, Changye, Meghdad, Ali, Taojun, An-Te, Jieqiong, Claudia, Karoll, Jill, Evan, Larry, Tian. Your support was critical in this research effort.

My dissertation would not be possible without support from the Tuinstra Tigers. Thank you, Andy, Eugene, Addie, Neal, Amrit, Meng-Yang, Seth, Shelby, Brad, Stefanie, Valerie, Elisabeth, Antje, Nicola, and the undergraduate assistants.

I would like to say thank you to my friends for your suggestions and encouragement, Lia, Diana, Jing, Miguel, Patrick, Blake, Rupesh, Fabiana, Savannah, Shams, Josh, Ana, Nick, Paula, Xiaochen, Cheng-Hsien, Matt, Behrokh, Yan, Jacquee, Roselyn, and many others who showed kindness to me.

I also received a lot of help from professors and staff in the Department of Agronomy at Purdue University. Thank you for your support and for making my life easier.

And I would like to thank my family, I could not have been where I am today without your support.

TABLE OF CONTENTS

LIST OF TABLES 8
LIST OF FIGURES 11
ABSTRACT 13
CHAPTER 1. RESEARCH OVERVIEW 15
1.1 Introduction 15
1.2 Genotyping and Phenotyping 17
1.3 Remote sensing benefits breeding programs 19
1.4 Crop growth models 24
1.5 Hypotheses and Objectives 26
CHAPTER 2. INTEGRATING CROP GROWTH MODELS WITH REMOTE SENSING FOR PREDICTING BIOMASS YIELD OF SORGHUM 27
2.1 Abstract 27
2.2 Introduction 28
2.2.1 Importance of forage sorghum in rainfed environments 28
2.2.2 High-throughput phenotyping methods potentially facilitate the measurement of canopy and crop growth through the entire cropping season 29
2.2.3 Crop growth models 30
2.2.4 Bioenergy sorghum 32
2.3 Materials and methods 32
2.3.1 Genotypes and field management 32
2.3.2 Ground validation studies 32
2.3.3 Ground validation data from 2015 and 2017 36
2.3.4 Remote-sensing data collection 36
2.3.5 Agricultural Production Systems sIMulator 37
2.3.6 Model calibration 38
2.3.7 Model validation 40
2.4 Results 40
2.4.1 Field conditions 40
2.4.2 Calibration of APSIM models 41

2.4.3 Validation of APSIM models 42
2.5 Discussion 46
2.5.1 Plant height and final dry biomass of photoperiod-sensitive and -insensitive forage sorghum hybrids are similar and greater than grain sorghum in medium- and short-season environments 46
2.5.2 Sorghum hybrids exhibit diverse canopy structures 47
2.5.3 Photoperiod-sensitive and photoperiod-insensitive forage sorghum hybrids exhibit similar RUE 49
2.5.4 Forage sorghum models perform well in above-ground biomass simulations across years and locations 51
CHAPTER 3. ANALYSIS OF HYBRID SORGHUM BIOMASS YIELDS IN MULTI-YEAR PERFORMANCE TRIALS 55
3.1 Abstract 55
3.2 Introduction 55
3.3 Materials and methods 59
3.3.1 Genotypes and field management 59
3.3.2 Molecular background 60
3.3.3 Field data collection 60
3.3.4 Remote-sensing data collection 61
3.3.5 Statistical analysis 61
3.4 Results 65
3.4.1 Trait heritability and correlations 65
3.4.2 GWAS for biomass traits in sorghum hybrids 67
3.4.3 LiDAR height data description 79
3.4.4 GWAS results of LiDAR height 80
3.5 Discussion 85
3.5.1 The sorghum diversity testcrosses were competitive in yield with commercial sorghum hybrids 85
3.5.2 Trait heritability and correlation between ground reference traits 86
3.5.3 Significant SNPs and candidate genes for hybrid sorghum performance 86
3.5.4 Trait heritability and significant SNPs for LiDAR plant height 92

3.5.5 Favorable and rare alleles for hybrid sorghum biomass productivity 92
3.6 Conclusion 93
CHAPTER 4. ESTIMATING SEASONAL RADIATION USE EFFICIENCY IN SORGHUM USING BIOMASS AND TIME-DEPENDENT MEASUREMENTS OF CANOPY COVER AND DAILY RADIATION 95
4.1 Abstract 95
4.2 Introduction 95
4.3 Materials and methods 98
4.3.1 Genotypes and field management 98
4.3.2 Molecular background 98
4.3.3 Remote-sensing data collection 99
4.3.4 Statistical analysis 100
4.4 Results 101
4.4.1 Estimating seasonal radiation use efficiency 101
4.4.2 Validation using 2018 HybCAL panel 102
4.4.3 Heritability of SRUE and biomass yield 103
4.4.4 Correlations between SRUE and ADB 104
4.4.5 GWAS for canopy cover and SRUE 104
4.5 Discussion 111
4.5.1 SRUE value exhibits a similar range as previous publications 111
4.5.2 SRUE is heritable and stable over seasons 112
4.5.3 Favorable alleles for SRUE and ADB with low allele frequencies 112
4.5.4 Mapping loci associated with canopy cover 113
4.5.5 Mapping loci associated with SRUE 118
4.6 Conclusions 121
CHAPTER 5. GENERAL CONCLUSIONS 122
APPENDIX A. CHAPTER 2 125
APPENDIX B. CHAPTER 3 129
APPENDIX C. CHAPTER 4 143
REFERENCES 158

LIST OF TABLES

Table 2.1 Details of the types and observed data for 18 hybrids in central-west Indiana from May to October. The value in a cell is mean plus minus standard deviation and the results of LSD test. 34

Table 2.2 2018 parameters from the pipeline calculating derived parameters based on observed parameters. K for extinction coefficient and RUE for radiation use efficiency. 38

Table 2.3 The genotypes and management details in Bushland trials. 43

Table 3.1 ANOVA of performance traits measured in sorghum hybrids in replicated trials in 2018, 2019, and 2020. 63

Table 3.2 Heritability of agronomic traits measured in sorghum hybrids in trials conducted in 2018, 2019, and 2020. 65

Table 3.3 Correlations for agronomic traits measured in sorghum hybrids in trials conducted in 2018, 2019, and 2020. Red cell color represents positive correlations, and green color represents negative correlations. 66

Table 3.4 Significant SNPs and candidate genes for apex height identified by GWAS using the FarmCPU model at FDR 0.01. Candidate gene in blue color are not reported in prior QTL studies. 73

Table 3.5 Significant SNPs and candidate genes for top collar height identified by GWAS using the FarmCPU model at FDR 0.01. Candidate genes in blue color are not reported in prior QTL studies. 74

Table 3.6 Significant SNPs and candidate genes for base stem diameter identified by GWAS using the FarmCPU model at FDR 0.01. 75

Table 3.7 Significant SNPs and candidate genes for aboveground dry biomass identified by GWAS using the FarmCPU model at FDR 0.01. 75

Table 3.8 Significant SNPs and candidate genes for flowering time identified by GWAS using the FarmCPU model at FDR 0.01. Candidate genes in blue color are not reported in prior QTL studies. 77

Table 3.9 Significant SNPs and candidate genes for moisture content identified by GWAS using the FarmCPU model at FDR 0.01. Candidate genes in blue color are not reported in prior QTL studies. 78

Table 3.10 GDD of LiDAR height data collection dates. 79

Table 3.11 Heritability of LiDAR plant height at 400GDD, 600GDD, 800GDD, and 1000GDD. 80

Table 3.12 Significant SNPs and candidate genes for LiDAR plant height at 600GDD identified by GWAS using the FarmCPU model at FDR 0.01. Candidate genes in blue color are mapped to

the same position as the dwarfing locus *Dw1*, candidate genes in green color are mapped to the same position as the dwarfing locus *Dw3*. 83

Table 3.13 Significant SNPs and candidate genes for LiDAR plant height at 800GDD identified by GWAS using the FarmCPU model at FDR 0.01. Candidate genes in blue color are mapped to the same position as the dwarfing locus *Dw1*, candidate genes in green color are mapped to the same position as the dwarfing locus *Dw3*. 84

Table 3.14 Significant SNPs and candidate genes for LiDAR plant height at 1000GDD identified by GWAS using the FarmCPU model at FDR 0.01. Candidate genes in blue color are mapped to the same position as the dwarfing locus *Dw1*, candidate genes in green color are mapped to the same position as the dwarfing locus *Dw3*. 84

Table 4.1 Heritability of SRUE and ADB through SpATS 103

Table 4.2 SRUE and ADB correlation between three hybrid years and the average over years. Avg. is the average of three years for each hybrid. 104

Table 4.3 GWAS for canopy cover at 600GDD in the SbDIV TC population of sorghum hybrids with significant SNPs and candidate genes at FDR 0.05. 107

Table 4.4 GWAS for canopy cover at 800GDD in the SbDIV TC population of sorghum hybrids with significant SNPs and candidate genes at FDR 0.05. 108

Table 4.5 GWAS for SRUE in the SbDIV TC population of sorghum hybrids with significant SNPs and candidate genes at FDR 0.05. 110

Table 4.6 Identified candidate genes of RGB canopy cover at 600GDD and published QTLs. 114

Table 4.7 Identified candidate genes of RGB canopy cover at 800GDD and published QTLs. 115

Table 4.8 Identified candidate genes of SRUE and published QTLs. 119

Table B.1 Top 30 significant SNPs for apex height identified by GWAS using the MLM model. The SNP associated with *Dw3* is highlighted in red color..... 129

Table B.2 Top 30 significant SNPs for top collar height identified by GWAS using the MLM model. The SNP identified *Dw3* is highlighted in red color. 130

Table B.3 Top 30 significant SNPs for ADB identified by GWAS using the MLM model. The SNPs identified *Dw3* are highlighted in red color. 131

Table B.4 Significant SNPs and candidate genes for moisture identified by GWAS using the MLM model..... 132

Table B.5 Significant SNPs and candidate genes for apex height identified by GWAS using the FarmCPU model at FDR 0.05..... 133

Table B.6 Significant SNPs and candidate genes for ADB identified by GWAS using the FarmCPU model at FDR 0.05. maf is the minor allele frequency. 135

Table B.7 Top 30 significant SNPs for LiDAR height at 600GDD identified by GWAS using the MLM model. The SNPs identified *Dw3* are highlighted in red color. 137

Table B.8 Top 30 significant SNPs for LiDAR height at 800GDD identified by GWAS using the MLM model. The SNPs identified *Dw3* are highlighted in red color. 138

Table B.9 Top 30 significant SNPs for LiDAR height at 1000GDD identified by GWAS using the MLM model. The SNPs identified *Dw3* are highlighted in red color. 139

Table B.10 Significant SNPs and candidate genes for LiDAR height at 600GDD identified by GWAS using the FarmCPU model at FDR 0.01-0.05. 140

Table B.11 Significant SNPs and candidate genes for LiDAR height at 800GDD identified by GWAS using the FarmCPU model at FDR 0.01-0.05. 141

Table B.12 Significant SNPs and candidate genes for LiDAR height at 1000GDD identified by GWAS using the FarmCPU model at FDR 0.01-0.05. 142

Table C.1 SRUE and ADB values for each genotype in the SbDIV TC in 2018, 2019, 2020, and the average across three years. SRUE is seasonal radiation use efficiency. ADB is aboveground dry biomass. 143

LIST OF FIGURES

Figure 2.1 Leaf size distributions collected from 25 June (48 DAS), 12 July (65 DAS) and 9 August (93 DAS) at West Lafayette, IN, in 2018. Vertical bars indicate ± 1 SEM for measured values. 45

Figure 2.2 The canopy cover (CC) versus leaf area index (LAI) for different types of sorghum. The fitted curve ($CC=1–e^{-k.LAI}$) indicates the extinction coefficient (k) of different types of sorghum and the values shown in Table 2.2. 46

Figure 2.3 Simulated crop leaf area index (LAI) throughout the crop life cycle (lines) compared to measured values (symbols) for six represented hybrids of each sorghum type. The experiments were sown on 8 May 2018 at West Lafayette. Vertical bars indicate ± 1 SEM for measured values. 48

Figure 2.4 Simulated crop attributes throughout the crop life cycle (lines) compared to measured values (symbols) for a range of treatments for the experiments sown on 8 May 2018 at West Lafayette. Vertical bars indicate ± 1 SEM for measured values. For each forage (A–N) and grain (O–R) type hybrid, the panel shows the time course of total and organ (stem, leaf, grain) biomass. The simulated lines are in the same colour as their measured types except the simulated total dry biomass (black line) and the simulated dead leaf dry weight (brown line). 50

Figure 2.5 Simulated crop leaf area index (LAI) throughout the crop life cycle (lines) compared to measured values (symbols) for six represented hybrids of each sorghum type sown on 19 May 2015 and 16 May 2017 at West Lafayette. The simulated lines are in the same colour as their measured types. Vertical bars indicate ± 1 SEM for measured values. 51

Figure 2.6 Model validation through comparing observed and predicted biomass of West Lafayette 2015, West Lafayette 2017 and Bushland data from 2000 to 2017. The P-value is to test the null hypothesis that the fitted line slope is not different from 1. 53

Figure 2.7 Biomass probability exceedance of nine hybrids from 1980 to 2017. The plots from (A) to (C) are harvested on 80, 100 and 120 DAS in Bushland, TX; the plots from (D) to (F) are harvested on 80, 100 and 120 DAS in West Lafayette, IN. 54

Figure 3.1 A screen plot of principal components (x-axis) and their contribution to the variance determined from GBS data of SbDIV TC. 67

Figure 3.2 Quantile-quantile (QQ)-plots of P-values for six agronomic traits using FarmCPU. . 68

Figure 3.3 Manhattan plots of the significant SNPs detected for (A) Apex height, (B) Top collar height, (C) Base diameter, (D) Aboveground dry biomass, (E) Flowering and (F) Moisture. 71

Figure 3.4 Violin plots of LiDAR plant height of the SbDIV TC at 400GDD, 600GDD, 800GDD, and 1000GDD in 2018, 2019, and 2020. 80

Figure 3.5 GWAS results of LiDAR plant height at (A) 600GDD, (B) 800GDD, and (C) 1000GDD. 81

Figure 4.1 Unmanned aerial vehicle (UAV) used in this study. This system acquired hyperspectral, LiDAR, and RGB image. We use RGB data in this study. 99

Figure 4.2 Violin plot of SRUE calculated from RGB canopy cover and aboveground dry biomass of 619 sorghum testcross hybrids. The mean and standard deviation of 2018, 2019, and 2020 are 1.35±0.31, 1.31±0.17, and 1.33±0.18, respectively. 102

Figure 4.3 Comparison of SRUE calculated from RGB canopy cover and aboveground dry biomass with maximum RUE used as input for APSIM in Chapter 2. The blue dashed line is the fitted line, and the black dashed line is one-to-one line. The P-value tests the null hypothesis that there is no relationship between the two types of RUE. 103

Figure 4.4 Manhattan plot from GWAS for RGB canopy cover in 619 sorghum hybrids at (A) 600GDD, (B) 800GDD. 106

Figure 4.5 Manhattan plot from GWAS for seasonal radiation use efficiency in 619 sorghum hybrids..... 107

Figure A.1 The canopy cover (CC) versus leaf area index (LAI) for 18 sorghum hybrids. The fitted curve ($CC = 1 - e^{-k \cdot LAI)}$ indicates the extinction coefficient (k) of different types of sorghum and the values shown in Table 2.3. 125

Figure A.2 Simulated crop leaf area index (LAI) throughout the crop life cycle (lines) compared to measured values (symbols) for all sorghum hybrids of each sorghum type. The experiments were sown on 8 May 2018 at West Lafayette. Vertical bars indicate ± 1 SEM for measured values. 126

Figure A.3 Simulated crop leaf area index (LAI) throughout the crop life cycle (lines) compared to measured values (symbols) for all sorghum hybrids of each sorghum type sown on 19 May 2015 and 16 May 2017 at West Lafayette. The simulated lines are in the same colour as their measured types. Vertical bars indicate ± 1 SEM for measured values. 127

ABSTRACT

Evaluating large numbers of genotypes and phenotypes in multi-environment trials is key to crop improvement for biomass performance in sorghum. In this dissertation, we developed an approach that integrates crop growth models with remote-sensing data and genetic information for modeling and predicting sorghum biomass yield. The goal of studies described in Chapter 2 was to parameterize the Agricultural Production Systems sIMulator (APSIM) crop growth models with remote-sensing and ground-reference data to predict variation in phenology and yield-related traits for 18 commercial grain and biomass sorghum hybrids. These studies showed that (i) biomass sorghum hybrids tended to have higher maximum plant height, final dry biomass and radiation use efficiency (RUE) than grain sorghum, (ii) photoperiod-sensitive sorghum hybrids exhibited greater biomass potential in longer growing environments and (iii) the parameterized APSIM models performed well in above-ground biomass simulations across years and locations. Crop growth models that integrate remote-sensing data offer an efficient approach to parameterize models for larger plant breeding populations. Understanding the genetic architecture of biomass productivity and bioenergy-related traits is another key aspect of bioenergy sorghum breeding programs. In Chapter 3, 619 sorghum genotypes from the sorghum diversity panel were individually crossed to ATx623 to create a half-sib population that was planted and evaluated in field trials in three consecutive years. Single-nucleotide polymorphisms (SNPs) were used in a genome-wide association study (GWAS) to identify genetic loci associated with variation in plant architecture and biomass productivity. A few SNPs associated with these traits were located in previously described genes including the sorghum dwarfing genes *Dw1* and *Dw3* and stay-green QTLs *Stg1* and *Stg4*. Of particular interest were seven genetic loci that were discovered for biomass yield. For three of these loci, the minor or uncommon allele exhibited a favorable effect on productivity suggesting opportunities to further improve the crop for biomass accumulation through plant breeding. Marker-assisted and genomic selection strategies may provide tools to introgress and exploit these genes for bioenergy sorghum development. Since parameterizing biophysical crop models requires extensive time and manual effort, a simple model was developed in Chapter 4 that used time-dependent measurements of RGB canopy cover and daily radiation coupled with end-of-season biomass for estimating seasonal radiation use efficiency (SRUE) in 619 sorghum hybrids. SRUE was shown to be a stable and heritable trait that has a positive relationship with aboveground

dry biomass (ADB) over seasons. GWAS identified 11 SNPs associated with SRUE with the favorable effect represented by the minor allele for seven of these SNPs. Increasing the frequency of these favorable alleles may improve the breeding population. These results demonstrated that the simple model for calculating SRUE can be used in genetic studies and for parameterizing biophysical crop models. The studies integrating crop growth models with remote sensing technologies provide an opportunity to evaluate a large number of phenotypes for the target population to understand the underlying genetic variation of bioenergy sorghum.

CHAPTER 1. RESEARCH OVERVIEW

1.1 Introduction

Sorghum is a genus of angiosperms in the grass family Poaceae, the subfamily Panicoideae and the tribe Andropogoneae (Hamby and Zimmer 1988). *Sorghum bicolor* is one of the sorghum species that is native to Africa. All the cultivated sorghums belong to *Sorghum bicolor* subsp. *bicolor*, which can be classified into five races based on their physical characteristics: bicolor, guinea, kafir, caudatum, and durra (Harlan and Wet 1972; Smith and Frederiksen 2000). This crop serves as a staple food for millions of people in India and sub-Saharan Africa, especially for semi-arid environments (FAOSTAT, 2019). Sorghum is also a major crop in the USA, India, Argentina, Mexico, Africa, China and Australia that is used for food, feed, forage, and biofuel production (Smith and Frederiksen 2000; Arendt and Zannini 2013; Singh et al. 2014; Borrell et al. 2014a).

As a C4 crop, sorghum has higher light, nitrogen, and water use efficiency than C3 crops in hotter and drier conditions (Carpita and McCann 2008; Byrt et al. 2011). Compared with corn, another C4 crop, sorghum exhibits excellent drought and heat stress tolerance and produces acceptable yields in stressful environments and high yields in favorable environments (Jordan et al. 2012).

Other than their scientific names, sorghum varieties can also be separated into several different types based on usage by growers, such as grain sorghum, sweet sorghum, Sorghum-Sudangrass, forage sorghum, and biomass sorghum (Stefaniak et al. 2012). There are many shapes, sizes, and heights of sorghum. For example, some grain sorghums have a tightly-packed, round-shaped panicles while others have open, droopy panicles. Sorghum grains can also be many different colors including red, orange, bronze, cream, yellow, white, and black. Traditionally, red, white, and bronze sorghums are used in all segments of the sorghum industry in the United States. Yellow, cream and white colored sorghum varieties are used to make flour, while black and burgundy varieties contain beneficial antioxidant properties and are utilized in other food applications (Harlan and Wet 1972; Smith and Frederiksen 2000). Sweet sorghums accumulate sugars in the stalk after flowering and are grown for production of sorghum syrup. Sweet sorghums are also used for biofuel and chemical production (Reddy et al. 2005).

Bioenergy is defined as a liquid or gaseous fuel that is produced from plant biomass. To enhance biomass yield of bioenergy sorghums, a new type of sorghum hybrid was designed for long growing seasons (Gill et al. 2014; Olson et al. 2012; Rooney et al. 2007; Truong et al. 2017). Olson et al. (2012) found that drought-tolerant, annual energy sorghum hybrids have the genetic yield potential to contribute significantly to bioenergy production. Derived from forage sorghum varieties, biomass sorghum hybrids may be used for bioenergy production. This type of sorghum primarily is defined by high-biomass yields. Biomass sorghum variety development has prioritized cellulosic biomass yield, not sugar levels or grain production. This type of sorghum can reach a height of 6 meters in a normal growing season (Rocateli et al. 2012).

The U.S. Environmental Protection Agency (EPA) defines biomass sorghum as *Sorghum bicolor* varieties that contain at least 75 percent cellulosic content. If a *Sorghum bicolor* and sudangrass cross contains at least 75 percent cellulosic content, then EPA also considers the cross to be biomass sorghum (EPA, 2015). Biomass sorghum is not commercially produced in the U.S. at this time. Its production has been limited to test plots for research. Biomass sorghum has potential throughout the Corn Belt and the southern U.S. Rooney et al. (2007) and Mullet et al. (2014) developed high biomass sorghum hybrids that were photoperiod sensitive. The later flowering times allowed the hybrids have longer vegetative growth duration and produce higher biomass yields in water-limited growing environments.

The starches and sugars of sorghum can both be used as feedstocks for biofuel production. However, there are co-localizations between grain and stem sugar yield quantitative trait locus (QTLs) with height and flowering time QTLs. Some tradeoff may need to be considered (Murray et al. 2008). Structural carbohydrates provide a third source of biomass for energy production and are the only type that is produced in quantities sufficient to meet future energy demands (Tilman et al. 2006; Rubin 2008). Sorghum is efficient at producing structural carbohydrates for biofuel conversion including crop residue remaining from a sorghum grain crop, bagasse from sweet sorghum or forage sorghums, and biomass from a dedicated bioenergy crop (Rooney et al. 2007; Carpita and McCann 2008; Olson et al. 2012).

Bioenergy sorghum hybrids are defined by high total dry biomass, plant height, and stem radial growth and low stem water contents. These traits may affect the structural carbohydrates in plants and ethanol production (Tilman et al. 2006; Rooney et al. 2007; Rubin 2008; Kong et al. 2020). Biomass is a complex secondary trait that is affected by other yield related components,

such as plant height (Wilson and Eastin 1982; van Oosterom and Hammer 2008; George-Jaeggli et al. 2011; Olson et al. 2012), days to flowering (Rooney et al. 2007; Olson et al. 2012; Murphy et al. 2014; Meki et al. 2017), and leaf morphology (Sieglinger 1936; Rooney et al. 2007; Olson et al. 2012; Gill et al. 2014; Truong et al. 2017). Biomass production is also driven by radiation use efficiency multiplied by light intercepted (Falster and Westoby 2003), so radiation use efficiency is important for bioenergy sorghum (Kiniry et al. 1989; Narayanan et al. 2013). Leaf number, leaf area and leaf angle are key traits for radiation use efficiency since they play an important role in determination of light interception (Cho and Son 2007; Falster and Westoby 2003).

Bioenergy sorghum is targeted for production in water-limited areas; therefore, water use efficiency and drought tolerance are key traits (Narayanan et al. 2013). Plant water use efficiency is impacted by multiple physiological mechanisms and is affected by numerous genes and environmental factors (Han et al. 2015; Murray et al. 2008). Stay-green is one of the best studied drought tolerance traits of sorghum and has a direct impact on biomass production (Borrell et al. 2014a). This complex trait can affect early canopy development, which allows crops to save water during the vegetative growth stage (Hammer et al., 2010; van Oosterom et al., 2010), photosynthesize for longer periods (Borrell et al. 2014), and yield more.

1.2 Genotyping and Phenotyping

Traditional plant breeding and genomic selection are two major strategies to improve or develop new cultivars. Marker-assisted selection (MAS) and genomic selection strategies use molecular markers for indirect selection of traits in crop improvement (Lande and Thompson 1990). In recent decades, several types of molecular markers have been developed, such as the restriction fragment length polymorphism (RFLP) (Botstein et al. 1980), random amplification of polymorphic DNA (RAPD) (Williams et al. 1990), cleaved amplified polymorphic sequences (CAPS) (Konieczny and Ausubel 1993), simple sequence repeats (SSRs) (Litt and Luty 1989; Salimath et al. 1995), and amplified fragment length polymorphisms (AFLPs) (Vos et al. 1995). However, these types of molecular markers are limited and genotyping costs are high. Lander (1996) proposed single nucleotide polymorphisms (SNPs) as DNA markers. SNPs are abundant in a genome and appropriate for genome-wide analysis (Rafalski 2002). SNPs are identified by DNA sequencing. The application of next-generation sequencing (NGS) technologies coupled with

Genotyping-by-sequencing (GBS) approaches provides high-throughput and low-cost sequencing data for plant genotyping and breeding (Elshire et al. 2011; Pareek et al. 2011; He et al. 2014). Researchers can analyze and interpret GBS datasets for implementing genome-wide association studies (GWAS), genomic diversity studies, genetic linkage analyses, molecular marker discovery and genomic selection (He et al. 2014; Huang and Han 2014).

GWAS is an approach to scan genome to find the statistically significant associations between genetic and phenotypic variations (Myles et al. 2009). The first GWAS publication in plants appeared in the model plant *Arabidopsis thaliana* (Atwell et al. 2010). Since then GWAS studies were successfully used to identify significant markers and traits associations in cereal crops including rice (Huang et al. 2012), barley (Cockram et al. 2010), wheat (Neumann et al. 2011; Sukumaran et al. 2015), maize (Tian et al. 2011), and sorghum (Sukumaran et al. 2012; Morris et al. 2013). The pace of genotyping has increased exponentially, and the cost of sequencing has dramatically decreased. These advances provide the tools to better understand the biological determinants of quantitative phenotypic variation.

The costs to obtaining high-quality phenotype data on thousands of plants is a bottleneck to variety development. While technical advances have accelerated the pace of genomic research, phenotyping has lagged behind and currently limits prospects for association mapping, gene discovery, and predictive genomic selection (GS) for crop improvement (Cobb et al. 2013, 2019). In conventional field trials, many crop breeding programs only have a single end-of-season biomass yield measurement for diverse environments over multiple seasons (Furbank and Tester 2011). However, biomass yield is a complex trait and affected by many other related traits, such as height, days to flowering, and leaf morphology (Rooney et al. 2007; Olson et al. 2012). Biomass yield also generally exhibits lower heritability than other traits in sorghum breeding (Kenga et al. 2006; Shiringani and Friedt 2011). This kind of low-throughput field phenotyping is a bottleneck and has driven intense interest in applying remote sensing technologies to measuring plant phenotypes.

Most high-throughput phenotyping research programs use sensors and other imaging technologies to support rapid, low-cost measurements of plants across time and space (Furbank 2009; Pauli et al. 2016). There are two basic phenotyping approaches called forward and reverse phenomics. Forward phenomics is defined as selecting collections of germplasm for trait analyses with phenotyping tools under certain condition. Depending on the breeding or experimental goals,

the phenotyping methods could be either high-throughput with low resolution or lower-throughput with higher-resolution. Treatments could include abiotic stresses such as drought, flooding, heat, or cold, or biotic stresses such as fungal or bacterial diseases. On the other hand, reverse phenomics involves the dissection of traits to reveal biological mechanisms. This can link a physiological trait to biochemical or biophysical processes including translational or post-translational regulation of genes, or even epigenetic control (Furbank and Tester 2011).

High-throughput phenotyping research requires multi-disciplinary collaborations between plant biologists, computer scientists, statisticians and engineers (Cobb et al. 2013). Most phenotyping systems have been developed to measure phenotypes of individual plants with high frequency using platforms that combine robotics and image analysis with controlled environment, such as greenhouse and growth chamber (Furbank and Tester 2011). Although these systems could be applicable for certain research goals, the use of controlled environments to represent field environments has limitations. Limited space in greenhouse or growth chamber often results in plants not grown for a whole cycle, making it impossible to assess effects of biological or abiotic stresses during reproductive stage. The substrate volume for plant growth in pots or trays is far less than that available to plants in the field; therefore, differences in nutrient content and water availability alters normal patterns of growth and development (White et al. 2012). Solar radiation, air temperature, wind speed and evaporation rates typically are lower in controlled environment systems than under open-air field situations. Mechanical vibrations caused by wind can also affect plant growth and development (Biddington 1986; Chehab et al. 2009).

Field-based phenotyping is more realistic for genetic improvements in yield potential of field crops, such as sorghum (Campos et al. 2004). Field-based phenotyping is gaining popularity as an appropriate approach to accurately describe traits developed in real cropping conditions in short time for plants at vegetative and reproductive stages (White et al. 2012).

1.3 Remote sensing benefits breeding programs

Quantifying variation in agronomic traits for crop improvement or association studies is a bottleneck in most plant breeding programs. Field-based phenotyping approaches that carry sensors to plants utilize remote and proximal sensing systems to capture variation in spectral or geometric features (White et al. 2012; Fiorani et al. 2012; Li et al. 2014). These systems rely on

different sensors such as RGB (Chen et al. 2017; Ribera et al. 2018; Freitas Moreira et al. 2021; Lin et al. 2021), multispectral (Potgieter et al. 2017), hyperspectral (Masjedi et al. 2020), and light detection and ranging (LiDAR) (Masjedi et al. 2020; Lin and Habib, 2021; Zhou et al. 2021) cameras. These instruments can be mounted on unmanned aerial vehicles (UAV) (Chen et al. 2017; Ribera et al. 2018; Ravi et al. 2019) or ground-based platforms (Ravi et al. 2018).

The most commonly used remote sensing instruments include RGB, LiDAR, and hyperspectral sensors. RGB imaging is based on visible light, which captures the information from red (~600 nm), green (~550 nm), and blue (~450 nm) spectral bands (Großkinsky et al. 2015). Compared with other types of sensing, RGB is widely used since it is reliable, low cost, easy to operate, and relatively simple in data processing (Zhao et al. 2019). LiDAR has been introduced in plant phenotyping platforms to measure geometric features of plants such as crop height (Hoffmeister et al. 2016). LiDAR measurements exhibit higher spatial resolution, higher throughput and independence from air temperature and wind speed (Tumbo et al. 2002; Escolà et al. 2011; Llorens et al. 2011). Since the laser beams can penetrate into canopies, computing the difference between the digital surface model and the digital terrain model can be used to estimate variations in plant height (Madec et al. 2017). The accuracy of plant height measurements derived from LiDAR techniques can be a few centimeters (Deery et al. 2014; Virlet et al. 2016). Hyperspectral imaging is able to capture a large number of spectral bands across the whole spectrum (Furbank et al. 2019). Based on its high spectral resolution, hyperspectral imaging has been used in different scales of agricultural studies, such as plant biochemical composition, vegetation mapping, nutrient content, moisture content, crop stress or disease, and yield estimation (Dale et al. 2013; Zhao et al. 2019). Hyperspectral imaging could also couple with LiDAR or RGB imaging to increase the spatial resolution and improve crop biomass prediction through regression models (Masjedi et al. 2020; Wang et al. 2021).

As ground-based and UAV-based data acquisition systems continue to improve, data processing and feature extraction have become increasingly important (Pauli et al. 2016; Tardieu et al. 2017). Image and data processing includes georeferencing, geometric calibration, and spectral calibration to prepare the appropriate images. Some common methods include binarization, thresholding, resizing, normalization etc. reapplied on the sampled images (Kumar and Bhatia 2014). Ravi et al. (2018b) proposed a calibration procedure for cameras based on using the conjugate points and linear or planar features in images and point clouds to align data derived from

different flight lines. For accurate georeferencing, establishing the angular relationship between the scanner and GNSS/INS coordinate systems is important. Habib et al. (2018) introduced three approaches to estimate this angular relationship for the hyperspectral push-broom scanner. After the calibration, the orthophotos were significantly improved. Hasheminasab et al. (2021) and Zhou et al. (2021) proposed new approaches for automated geometric calibration of RGB and hyperspectral cameras through tightly coupled camera/LiDAR integration for GNSS/INS coordinate systems mounted on UAV. For most applications of high-throughput plant phenotyping, accurate georeferencing is important in plant feature extraction, such as plant height, canopy cover (Ravi et al. 2018), plant count (Ribera et al. 2017), maize tassel detection (Olsen et al. 2018; Karami et al. 2021), sorghum panicle counting (Cai et al. 2021), leaf segmentation (Chen et al. 2017; Chen et al. 2019), and plant location (Chen et al. 2018; Cai et al. 2020). He et al. (2018), Hasheminasab et al. (2020), and Lin et al. (2021) introduced modified Structure from Motion (SfM) strategies that are able to generate more accurate orthophotos for plant feature extraction. Lin and Habib (2021) also proposed an approach that can be used detect rows and alleys from LiDAR point cloud data.

Feature extraction techniques are used to identify geometric and spectral features. Phenotypes are traditionally associated with both structural and spectral characteristics of plants, some of which can be measured directly, while others must be inferred from empirical or biophysical models (White et al., 2012; Holzworth et al., 2014). RGB imaging is a useful tool for plant morphological traits (Großkinsky et al. 2015; Zhao et al. 2019). This technology was successfully implemented for estimation of canopy cover in diverse crops. Hoyos-Villegas et al. (2014) used RGB images acquired each week to estimate soybean canopy cover and total aboveground biomass. Their study demonstrated that this digital imaging method has the potential to determine the dynamics of canopy cover and biomass accumulation. Duan et al. (2016) developed a workflow based on RGB images to monitor the dynamic growth and development of the wheat canopy. Guo et al. (2017) used a large number of RGB images to evaluate the ground coverage ratio of rice under variable field conditions. Ribera et al. (2018) presented methods to estimate sorghum leaf number, plant location, and leaf segmentation for canopy cover in RGB images. Similarly, Zhou et al. (2019) extracted coverage information of maize from RGB images through an image-segmentation method based on machine learning. Chen (2019) segmented sorghum plants from soil using HSV color information and estimated canopy cover in RGB images.

All of these approaches utilize RGB imaging to collect canopy-based phenotypes. Ribera et al. (2017) introduced a method to count sorghum plants in the field using RGB images and Convolutional Neural Networks (CNN). Karami et al. (2020a; 2020b) successfully using deep learning techniques to identify maize plant count and locations in RGB images acquired from UAV. These results exhibited an overall precision > 95% when the training and testing sets were from the same field. Cai et al. (2020) proposed a method to estimate plant centers using RGB images acquired by UAV coupled with transfer learning models. Karami et al. (2021) used deep learning methods to detect and count maize tassels in RGB images acquired by UAV. Yang et al. (2021) proposed a method that assumes the maize and sorghum were planted in a grid fashion to detect field row and range in UAV RGB images. The results demonstrated that the new approach increased plot extraction accuracy. Cai et al. (2021) introduced an approach to detect sorghum panicles and estimate flowering time using RGB images acquired by UAV and deep neural network structures.

Plant height is one of the important and well-characterized quantitative traits in sorghum and maize (Salas Fernandez et al. 2009). It exhibits higher heritability and is highly correlated with biomass yield. Since data collection for plant height is more cost-effective than biomass, some indirect selection strategies may be conducted (Burks et al. 2015; Castro et al. 2015; Fernandes et al. 2018; Monk, Miller, and McBee 1984). Measuring height manually in the field is laborious and is typically obtained at only one terminal time point of growing season. Ravi et al. (2018) provided an approach that focused on wheel-based LiDAR data acquired by a ground-based platform for estimating sorghum plant height and canopy cover. Masjedi et al. (2020) used geometric features derived from LiDAR to characterize plant structure, such as plant height percentile, canopy volume, and canopy cover. In wheat, LiDAR based estimates of plant heights were highly heritable and exhibited good consistency with manual measurements (Madec et al. 2017). LiDAR was also used for estimating height of sorghum and maize breeding programs over time to elucidate new phenotypes such as the growth curve (Pugh et al. 2018). Chu et al. (2018) used UAS structure-from-motion photogrammetry to characterize canopy height of maize and reported that the 99th percentile height provided the best canopy height estimation accuracy. These research support that LiDAR technology is a useful tool for estimating plant height at multiple time points throughout the growing season and can add value in breeding programs. Masjedi and Crawford (2020) developed models for sorghum biomass prediction based on LiDAR and hyperspectral inputs

through Recurrent Neural Networks (RNNs). Masjedi et al. (2020) evaluated the impacts of sorghum biomass prediction using diverse models with HS-VNIR, HS-SWIR, and LiDAR data collected over time and reported that the data source was most important. Wang and Crawford (2021) introduced another approach that uses k-means assisted transfer learning to improve RNN models for sorghum biomass prediction based on features extracted from LiDAR, hyperspectral and weather data.

High-throughput phenotyping enables breeders to evaluate thousands of genotypes in multi-environment field trials with non-destructive monitoring through the growing season (Zhao et al. 2019; Großkinsky et al. 2015). Remote sensing instrumentation can be used to collect phenotypes faster and cheaper and with less manpower. This also provides an efficient way to capture the temporal expression patterns of interesting phenotypes (Pauli et al. 2016), which can be used to evaluate time-dependent traits such as height (Campbell et al. 2019). Approaches for identifying genetic variation through plant height extracted from remote sensing data were successfully applied in maize and sorghum (Anderson et al. 2020; Miao et al. 2020).

Biophysical crop models can be used to incorporate environmental factors into predictions of crop performance. However, challenges with parameterizing models for hundreds or thousands of genotypes have limited applications in plant breeding programs. Incorporating remote sensing into crop simulation models had been used either as a forcing function or simulation steering (Bouman 1995; Ines et al. 2013). The forcing function is applied to replace the input variable for simulation with the remote sensing observation. And the simulation steering is used to re-initialize by using sowing date and planting density, or re-parameterize the crop model by using canopy and growth parameters in a way that minimizes the differences between simulated and measured data (Ines et al. 2013). Most field-based phenotyping systems have focused on rapid assessment of individual traits or suites of traits with limited sensor and data processing capacity. Remote sensing can provide spatial information and improve the accuracy of crop models prediction, while crop models can derive time series or hard-to-measure phenotypes (Kasampalis et al. 2018; Yang et al. 2021). Incorporating environment and plant physiology factors as input information using crop modeling could be the solution for modeling high-throughput phenotyping data.

1.4 Crop growth models

In recent years, growers, the government, and companies have demanded more agricultural information to help make decisions on planting, growing and marketing crops. These needs from different groups are growing because of increased demands for agricultural products and limited land, water, and other natural resources, especially under climate change stresses (Wheeler and von Braun 2013). The data generated from traditional agricultural research methods do not meet these increasing needs. Traditional agronomic experiments are conducted at a specific point in a certain time and space, making results location- and time-specific, and data collection for these studies is laborious and expensive. Biophysical crop models are being developed to address this challenge to simulate crop production at a regional or country scale using inputs that are important for plant physiological and morphological functions (Bouman et al. 1996). Crop models vary in sophistication for integrating components across scales including gene interactions, metabolic pathways, cellular organization, tissue, and whole plant development (Zhu et al. 2016). Building models for complex crop phenotypes combine biological insights and mathematics to drive simple yet accurate equations to target processes of crop growth. Approaches that use a bottom-up approach without a fundamental plant sciences framework cannot provide more robust results than existing models in simulating phenotypes (Yin et al. 2021).

Crop growth models integrate knowledge about soil, weather, crops, and field management to simulate crop production in diverse locations under a range of environmental conditions (Jones et al. 2003). Crop model systems provide a framework to understand how the system and its components function. Then we can integrate this understanding into crop growth models that predict the behavior of the system for given conditions. Once models are parameterized and well-developed for simulation, large number of simulations can be performed for given environments to determine the best combination of management. Models that integrate quantitative genetics and gene-to-phenotype knowledge of traits are providing new tools for plant improvement because there are limitations to predicting plant phenotypes based solely on genotype, especially for complex adaptive traits. Crop models that are suitably constructed and well-tested have the potential to bridge this predictability gap by integrating solar radiation, water, and nitrogen inputs within a framework that predicts biomass accumulation and potential (Cooper et al. 2014).

Simulation models are becoming increasingly popular tools for addressing research questions for growers, government, and companies. Several different dynamic crop growth models

are currently available for modelling and simulation including WOFOST (Diepen et al. 1989), DSSAT (Jones et al. 2003), APSIM (Holzworth et al. 2018; Keating et al. 2003), CROPSYST (Stöckle 2003), and EPIC (Williams et al. 1989; Williams et al. 1983; Bouman et al. 1996; Jones et al. 2017). These crop growth models provide valuable tools in research, crop management, and in policy decisions (Boote et al. 1996). Even though crop modeling has considerable potential, care must be taken to avoid misrepresentation, misuse, and misunderstanding of the tools. Despite concerns about validating models, crop models proposed for broader crop management applications should be tested widely and in diverse field environments.

Agricultural Production Systems Simulator (APSIM) is a bio-physical modelling framework that was designed to simulate the dynamics of crop growth in response to soil, climate, and management conditions (Wang et al. 2002; Keating et al. 2003). This model has been used to investigate diverse questions related to food security, climate change adaptation and mitigation, economic risk evaluation, simulation of gene expression, and multi-trial simulation (Holzworth 2014).

Crop models can also be used to explore genotype by environment interactions affecting crop performance (Chapman et al. 2000a; Chapman et al. 2000b) in real-world and simulated plant breeding trials (Chapman 2008). Similar models were effective for prediction of heading dates in rice (Onogi et al. 2016), assessment of VPD-limited transpiration traits to enhance biomass yield in water-limited environments (Truong et al. 2017), and opportunities to exploit G×E×M interactions for maize improvement in Ethiopia (Seyoum et al. 2018). Plant breeding has been revolutionized by genomic selection strategies that support a prediction of performance across environments for traits with additive gene effects (Jonas and de Koning 2013; Desta and Ortiz 2014; Crossa et al. 2017). However, prediction of traits with non-additive gene effects and prediction of genotype by environment interactions (G×E) continues to be a challenge. Approximate Bayesian computation, a novel and powerful computational procedure to incorporate crop growth models directly into the estimation of whole-genome marker effects in whole-genome prediction, has been used to integrate crop growth models into whole genome prediction models (Technow et al. 2015).

1.5 Hypotheses and Objectives

Well-developed crop growth models and high-throughput phenotyping approaches have been developed in recent years (Baret et al. 2018; Blancon et al. 2019; Casa et al. 2010; Demarez et al. 2008; Jiang et al. 2019; Parent et al. 2019); however, strategies that accommodate crop growth models and high-throughput phenotyping as part of breeding pipelines have not been thoroughly explored. We hypothesize that high-throughput phenotyping and crop growth modeling can offer effective approaches for modeling performance in bioenergy sorghum. The hypotheses and corresponding objectives that will be addressed in this dissertation include:

1. Integration of remote sensing with ground reference data can be used to parameterize Agricultural Production Systems sIMulator (APSIM) crop growth models to predict biomass yield and related traits. The parameterized APSIM model can be used to predict sorghum performance across geographical regions through historical weather data. The objectives of this study were to develop a crop model for biomass sorghum that can predict seasonal biomass production of diverse hybrids over multiple seasons at different locations by combining high-throughput phenotyping and crop growth models.
2. Genome wide association studies can identify genetic variation underlying important agronomic traits for bioenergy sorghum breeding programs including biomass yield. The objectives of this study were to (a) evaluate hybrid performance in multi-year trials, (b) explore favorable alleles for aboveground dry biomass (ADB) (c) identify candidate genes for each trait, and (d) compare these identified candidate genes with published QTLs.
3. Estimates of RGB canopy cover, daily radiation, and end-of season ADB can be used in simplified crop models for estimating seasonal radiation use efficiency (SRUE). Specific objectives that will be addressed in this study include (a) introduce a simplified crop growth model to estimate SRUE using time-dependent measurements of RGB canopy cover and daily radiation coupled with end-of-season biomass, (b) validate SRUE estimates with maximum RUE as APSIM inputs, (c) quantify heritability and stability of SRUE over seasons, and (d) conduct GWAS of SRUE in sorghum germplasm collections.

CHAPTER 2. INTEGRATING CROP GROWTH MODELS WITH REMOTE SENSING FOR PREDICTING BIOMASS YIELD OF SORGHUM

A version of this chapter has been published in *in silico* Plants (Yang et al., 2021).

Kai-Wei Yang[1], Scott Chapman[2,3], Neal Carpenter[1], Graeme Hammer[4], Greg McLean[4], Bangyou Zheng[3], Yuhao Chen[5], Edward Delp[5], Ali Masjedi[6], Melba Crawford[1,6], David Ebert[5], Ayman Habib[6], Addie Thompson[1,7], Clifford Weil[1] and Mitchell R. Tuinstra[1*]

1 Department of Agronomy, Purdue University, 915 West State Street, West Lafayette, IN 47907, USA
2 School of Agriculture and Food Sciences, The University of Queensland, Gatton, QLD 4343, Australia
3 CSIRO Agriculture and Food, Queensland Biosciences Precinct, 306 Carmody Road, St Lucia, QLD 4067, Australia
4 Queensland Alliance for Agriculture and Food Innovation (QAAFI), The University of Queensland, Brisbane, QLD 4072, Australia
5 School of Electrical and Computer Engineering, Purdue University, 465 Northwestern Avenue, West Lafayette, IN 47907, USA
6 Lyles School of Civil Engineering, Purdue University, 550 Stadium Mall Drive, West Lafayette, IN 47907, USA
7 Plant Soil and Microbial Sciences Department, Michigan State University, 1066 Bogue Street, East Lansing, MI 48824, USA
*Corresponding author's e-mail address: mtuinstr@purdue.edu

Authors contributions

K.-W. Yang contributed to data collection, data analysis and writing (original draft). S.C. contributed to conceptualization, software, writing (review & editing), supervision and methodology. N.C. contributed to data collection and data analysis. G.H. contributed to conceptualization, software and resources. G.M. and B.Z. contributed to technical support of analyses in R and APSIM. Y.C. and E.D. contributed to extraction of canopy cover from RGB images. A.M., M.C., D.E. and A.H. contributed to remote-sensing data collection and processing as well as writing (review & editing). A.T. contributed to establishment of the preliminary data collection and analysis protocol. C.W. contributed to generation of the plant materials used in this study and edited the manuscript. M.R.T. contributed to conceptualization, writing (review & editing), supervision, project administration, funding acquisition, methodology and resources.

2.1 Abstract

Plant phenotypes are often descriptive, rather than predictive of crop performance. As a result, extensive testing is required in plant breeding programs to develop varieties aimed at performance in the target environments. Crop models can improve this testing regime by providing a predictive framework to (i) augment field phenotyping data and derive hard-to-measure phenotypes and (ii)

estimate performance across geographical regions using historical weather data. The goal of this study was to parameterize the Agricultural Production Systems sIMulator (APSIM) crop growth models with remote-sensing and ground-reference data to predict variation in phenology and yield-related traits in 18 commercial grain and biomass sorghum hybrids. Genotype parameters for each hybrid were estimated using remote-sensing measurements combined with manual phenotyping in West Lafayette, IN, in 2018. The models were validated in hybrid performance trials in two additional seasons at that site and against yield trials conducted in Bushland, TX, between 2001 and 2018. These trials demonstrated that (i) maximum plant height, final dry biomass and radiation use efficiency (RUE) of photoperiod- sensitive and -insensitive forage sorghum hybrids tended to be higher than observed in grain sorghum, (ii) photoperiod-sensitive sorghum hybrids exhibited greater biomass production in longer growing environments and (iii) the parameterized and validated models perform well in above-ground biomass simulations across years and locations. Crop growth models that integrate remote-sensing data offer an efficient approach to parameterize larger plant breeding populations.

2.2 Introduction

2.2.1 Importance of forage sorghum in rainfed environments

Sorghum (*Sorghum bicolor*) is commercially important in semi-arid environments due to its substantial heat and drought tolerance. Grain sorghum is the fifth most important cereal in global production with over 57 million tons of grain produced on 40 million ha in 2017 (FAOSTAT). Sorghum also is an important forage and sugar crop and can be utilized to produce plant-based biofuels including starch from sorghum grain, sugar from sweet-stemmed sorghum and cellulose from plant leaves and stems. In the USA, almost one-third of the sorghum grain crop is processed through grain-based ethanol production systems. Limited quantities of sugar-based and cellulose-based biofuel are produced currently, but these are considered important feedstocks for the future, minimizing direct competition with food production (Tilman et al. 2006; Rubin 2008).

Biomass sorghums can reach heights of 4–5 m with biomass yields maximized by high crop growth rates throughout the available growing season (Rocateli et al. 2012). When planted at high density, commercial sorghum hybrids exhibit a diversity of plant and canopy types to quickly

reach maximum radiation interception (Rooney et al. 2007; Olson et al. 2012; Gill et al. 2014; Truong et al. 2017). Total leaf number was found to be highly correlated with length of vegetative period. Hence, early maturing sorghum has fewer leaves and lower biomass production (Sieglinger 1936). In contrast, at high latitudes, spring-sown photoperiod-sensitive sorghum hybrids exhibit extended vegetative periods resulting in high biomass yields. Moreover, since sorghum exhibits better drought tolerance during vegetative growth stages, the longer period of vegetative growth results in better drought tolerance or drought avoidance in rainfed environments (Rooney et al. 2007).

2.2.2 High-throughput phenotyping methods potentially facilitate the measurement of canopy and crop growth through the entire cropping season

Marker-assisted selection (MAS), next-generation sequencing (NGS) technologies and data analytics pipelines have contributed to the implementation of genome-wide association studies (GWAS), genomic diversity studies, genetic linkage analyses, molecular marker discovery and genomic selection in large-scale plant breeding programs (He et al. 2014). Although genomic technologies are developing quickly, understanding the biological determinants of quantitative phenotype variation remains the central challenge of modern genetic analysis. New, high-throughput phenotyping (HTP) technologies are expected to be the next step in developing association mapping, gene discovery and developing predictive genomic selection models in crop improvement (Cobb et al. 2013).

High labor costs often constrain crop breeding programs to single measurements of final yield in diverse testing environments over multiple seasons. This bottleneck in field phenotyping has driven intense interest in applying remote-sensing technologies to field crop monitoring (Furbank and Tester 2011). Remote sensing of crops includes passive and active sensing of plants to acquire and interpret data to extract information about features, objects and classes in the area of interest (Konare et al. 2003). Data are processed through an analysis pipeline to calibrate and convert digital data into interpretable information (Campbell 2006). For example, the dynamics of canopy cover influence the pattern of crop growth rate and eventual yield. Remote-sensing images acquired by unmanned aerial vehicles (UAVs) can be used directly for large-scale estimation of leaf coverage and are key components of high-throughput field phenotyping (Duan et al. 2014,

2017; Gouache et al. 2016; Stanton et al. 2017; Zhang et al. 2017; Masjedi et al. 2018; Ribera et al. 2018).

Multiple remote-sensing approaches focused on quantifying variations in canopy cover and its dynamics have been investigated. An image-based workflow to monitor the growth and development of the wheat canopy dynamically using RGB cameras was developed by Duan et al. (2016). Similarly, Guo et al. (2017) evaluated the ground coverage ratio of rice from a large number of RGB images under variable field conditions. Light Detection and Ranging (LiDAR) has also been used to estimate canopy cover and above-ground biomass (Jimenez- Berni et al. 2018). Masjedi et al. (2019) introduced a strategy that incorporates multi-sensor time series data, environmental inputs and use Recurrent Neural Networks to predict sorghum biomass. Blancon et al. (2019) reported a high-throughput, model-assisted method for quantifying green leaf area (GLAI) dynamics in maize using multispectral imagery. Zhou et al. (2019) used an image-segmentation method based on machine learning to extract relatively accurate coverage information from RGB images. All of these approaches utilize remote-sensing technology to collect canopy-based phenotypes. However, interpreting dynamics of change is not easily done in empirical models.

2.2.3 Crop growth models

Dynamic crop growth modelling and simulation have become accepted tools for agricultural research (e.g. WOFOST (Diepen et al. 1989), DSSAT (Jones et al. 2003), APSIM (Keating et al. 2003; Holzworth et al. 2018), CROPSYST (Stöckle et al. 2003), EPIC (Williams et al. 1983, 1989)) (Bouman et al. 1996; Jones et al. 2017). Unlike purely statistical approaches, these models have functions that respond to external drivers and how those responses affect other components in the system (Wallach et al. 2018). Well-developed crop growth models as well as HTP approaches have been developed in recent years (Demarez et al. 2008; Casa et al. 2010; Baret et al. 2018; Blancon et al. 2019; Jiang et al. 2019; Parent et al. 2019); however, strategies that accommodate crop growth models as part of HTP pipelines have not been thoroughly explored.

Agricultural Production Systems sIMulator (APSIM) is a biophysical simulation model for cropping systems that was designed to predict the dynamics of crop growth, including biomass and grain yield, in response to climate and management conditions (Keating et al. 2003). Agricultural Production Systems sIMulator incorporates a generic crop model that utilizes a library

of routines for simulating crop growth and development processes (Wang et al. 2002) and has been used to investigate diverse questions related to food security, climate change adaptation and mitigation, simulation of gene expression and multitrial simulation (Holzworth 2014).

In the investigation of biomass growth in crops like biomass sorghum, the key physiological processes are phenology, leaf area development and crop growth rate as affected by weather and soil conditions. Simulated phenology in APSIM is based on thermal time elapsed in growth stages. Thermal time is calculated from a piecewise linear function of the mean air temperature, depending on base, optimum and maximal temperatures, which are 11, 30 and 42 °C for sorghum, respectively (Hammer et al. 1993). Panicle initiation (conversion of the meristem from production of vegetative initials to reproductive initials) is triggered at a genotype-specific thermal time, which can be further influenced by a genotype-specific photoperiod response. The accumulated thermal time between emergence and simulated panicle initiation determines the value of the total leaf number when divided by the plastochron (°Cd per leaf), period between the appearances of two successive leaf primordia. Leaves are expanded at a rate determined by the phyllochron (°Cd per leaf), period between the appearance of two successive leaves, and thus the product of total leaf number and phyllochron determines the thermal time to reach flag leaf stage (°Cd) (Hammer et al. 2010). The duration of growth stages such as flag leaf to anthesis, anthesis to start of grain filling and start to end of grain filling are also simulated in the model by accumulation of thermal time to reach genotype-specific target values (Muchow and Carberry 1990; Hammer and Muchow 1994; Ravi Kumar et al. 2009).

Canopy development is simulated based on the relationship between total plant leaf area (TPLA) and thermal time. Total plant leaf area accounts for the number of fully expanded leaves, size of each leaf and tiller number (Hammer et al. 1993, 2010). The model provides flexibility to simulate canopy development using other options such as leaf size distribution (Carberry et al. 1993; van Oosterom et al. 2001; Hammer et al. 2010) or the extension rate of each leaf (Hammer et al. 2010; Chenu et al. 2018). In the standard version of APSIM, the above-ground dry biomass accumulation is simulated as the minimum of light-limited or water-limited growth, then biomass is partitioned in different ratios to plant parts depending on the plant developmental stages through founded functions (Hammer et al. 2010).

2.2.4 Bioenergy sorghum

The objectives of this study were to develop a crop model for biomass sorghum that can predict seasonal biomass production of diverse hybrids over multiple seasons at different locations by combining HTP and crop growth models. Canopy cover estimated from RGB images was used to estimate key parameters describing leaf cover dynamics, light interception and radiation use efficiency (RUE). Other canopy properties were derived as outputs of the APSIM model. This method provides a new approach for understanding the adaptation of biomass sorghum and its interaction with the environment to identify trait targets for plant breeding.

2.3 Materials and methods

2.3.1 Genotypes and field management

A set of 18 sorghum hybrids (S. bicolor) (Table 2.1) were grown in 2015, 2017 and 2018 at the Agronomy Center for Research and Education (ACRE) of Purdue University in West Lafayette, IN, USA. Daily solar radiation, maximum and minimum temperatures and precipitation were recorded at the experimental site. Field trials were conducted each year using a randomized complete block design with four replicates. The hybrid entries were evaluated in 12-row plots with 76 cm spacing between rows measuring 3.81 m long. Seeds were sown at 30-mm depth on 19 May in 2015, 16 May in 2017 and 8 May in 2018 with emerged densities as shown (Table 2.1). Weeds and pests were controlled as required and there was negligible pest damage to the photosynthetic leaf surface throughout growth.

2.3.2 Ground validation studies

Ground-reference data from trials conducted in 2018 were used to parameterize the APSIM model. Plant population density was determined from row 2 and row 3 of each 12-row plot at 31 days after sowing (DAS). Days to flowering were measured as the number of days from sowing to when 50 % of the panicles in the plot were at 50 % anthesis. Plant height was measured after flowering.

Destructive harvests at four different stages of development were used to determine biomass yields; leaf, stem, tiller and panicle weights of individual plants; and leaf size distribution.

Four plants were harvested manually from plot row 11 on 7 June (31 DAS), two plants from plot rows 8 and 9 on 25 June (49 DAS), two plants from plot rows 5 and 6 on 12 July (66 DAS) and two plants from plot rows 2 and 3 on 9 August (94 DAS). After harvesting, each plant was dissected to determine the weight of the collared leaves, leaves that had not fully emerged, stems, tillers and panicle fractions. Leaves were removed from each plant in order and scanned individually to determine leaf size distribution using a LI-3100C Leaf Area Meter (LI-COR, Lincoln, NE, USA). The final tiller number was estimated from the tiller dry weight and total plant dry weight. Percent moisture of each plant was determined from the combined fresh weights and, later, dry weights of all fractions from each plant.

Repeated non-destructive measurements of plant development were also made during the vegetative period including the number of fully expanded leaves (collared leaves) of four tagged plants in rows 2 and 3 of each plot. Collection dates were 7 June (31 DAS), 19 June (43 DAS), 28 June (52 DAS), 5 July (59 DAS), 11 July (65 DAS) and 26 July (80 DAS). The final leaf numbers were the maximum value of leaf collar counts of each plot across dates. Final tiller number per plant was determined on 12 July (66 DAS). The average leaf biomass fraction and specific leaf weight (SLW) were used to compute leaf area and leaf area index (LAI) for each plot and sampling date.

Total biomass yields were measured in each plot on 7 June (31 DAS), plot rows 8 and 9 on 25 June (49 DAS), plot rows 5 and 6 on 12 July (66 DAS) and plot rows 2 and 3 on 9 August (94 DAS); one replicate was not harvested at 49 DAS due to inclement weather. On 7 June (31 DAS), a 2-m section of row segment 11 was hand-harvested, weighed and dried to compare fresh weights and dry weights. For the next three harvest dates, the entire 2-row segment of each plot was harvested with a Wintersteiger Cibus 2-row Biomass Harvester (Wintersteiger Inc., Salt Lake City, UT, USA). After harvesting a plot, ~500 g of the shredded plant material from each plot was taken to determine fresh weight, dry weight and moisture content. For the mechanically harvested plots, a 0.614-kg fresh weight correction factor was added back to the biomass estimate of each plot to account for the short stem segments that were left behind after machine harvesting. At the last sampling date (94 DAS), several plots were lodged and could not be harvested.

Table 2.1 Details of the types and observed data for 18 hybrids in central-west Indiana from May to October. The value in a cell is mean plus minus standard deviation and the results of LSD test.

Genotype†	Type	2015 plant density	2017 plant density	2018 plant density	2017 flowering date	2018 flowering date	2015 final dry biomass	2017 final dry biomass	2018 final dry biomass	2015 max height	2017 max height	2018 max height
		stand count/m^2			DAS		g/m^2			cm		
PH 849F	Forage Sorghum	15.5 ±1.3 abcde	15.9 ±1.3 def	18.3 ±0.8 defg	72.8 ±9.2 ef	74.0 ±4.0 ef	1670 ±194 bc	2258 ±382 cde	2040 ±111 abc	244.6 ±10.4 Def	242.5 ±29.7 de	273.8 ±11.1 bcd
PH 877F	Forage Sorghum	16.1 ±1.6 abc	19.5 ±1.7 a	19.6 ±0.5 ab	66.3 ±1.9 gh	66.8 ±1.7 gh	1497 ±72 cde	2217 ±448.7 cde	2006 ±187 abcd	265.0 ±7.9 C	224.0 ±52.8 ef	294.7 ±13.5 ab
RS 327x36 BMR	Forage Sorghum	15.6 ±1.1 abcd	18.5 ±2.0 abc	19.1 ±0.8 abcde	91.0 ±NA c	83.8 ±12.5 d	1343 ±269 def	2245 ±401 cde	1645 ±118 defg	255.8 ±12.7 Cde	246.2 ±19.7 de	250.0 ±9.6 d
RS 341x10	Food Grain white	15.5 ±0.8 abcde	16.7 ±1.3 cde	17.4 ±1.1 g	68.8 ±0.5 fgh	65.5 ±1.3 gh	973 ±82 g	1465 ±191 h	1138 ±17 h	77.5 ±1.6 J	82.7 ±1.9 I	126.0 ±1.8 h
RS 366x58	Food Grain white	12.9 ±1.8 f	12.7 ±0.3 g	15.9 ±0.7 h	77.3 ±3.1 de	73.8 ±2.1 ef	1139 ±85 fg	1939 ±160 efg	1366 ±173 gh	123.5 ±8.2 I	139.3 ±7.0 H	153.3 ±9.4 g
RS 374x66	Forage Sorghum	14.2 ±1.2 cdef	13.9 ±0.6 fg	17.5 ±0.9 fg	75.0 ±4.8 def	69.8 ±2.1 efg	1634 ±143 bc	2049 ±346 defg	1988 ±211 abcd	263.1 ±21.2 Cd	264.7 ±8.9 Cd	263.9 ±3.0 cd
RS 392x105 BMR	Forage Sorghum	16.4 ±1.0 ab	17.8 ±1.9 abcd	19.6 ±0.7 abc	91.0 ±0.0 c	90.0 ±0.0 c	1117 ±99 fg	2318 ±358 bcd	1563 ±196 efg	163.0 ±5.8 H	203.4 ±31.2 fg	190.5 ±13.5 f
RS 400x38 BMR	Sorghum-sudangrass	16.3 ±0.9 ab	17.7 ±1.8 abcd	18.6 ±1.0 bcdef	74.8 ±1.9 def	73.0 ±1.4 ef	1151 ±148 fg	1962 ±102 defg	1516 ±55 fgh	190.1 ±11.0 G	220.9 ± 7.3 ef	216.5 ±3.6 e
RS 400x82 BMR	Sorghum-sudangrass	13.7 ±1.3 def	14.1 ±0.8 fg	15.0 ±0.8 h	76.0 ±NA def	104.0 ±5.7 b	1248 ±305 efg	2128 ±59 cdefg	1569 ±403 efg	242.6 ±6.0 Def	191.7 ±27.7 g	202.8 ±6.4 ef
SP HIKANE II	Forage Sorghum	15.5 ±0.6 abcde	18.7 ±1.6 abc	20.1 ±0.7 a	74.0 ±2.6 def	70.3 ±1.3 efg	1607 ±237 bc	2230 ±372 cde	2080 ±203 abc	239.4 ±14.8 Ef	244.9 ±6.0 de	254.5 ±30.1 d
SP NK300	Forage Sorghum	16.8 ±2.1 a	19.4 ±2.0 ab	19.4 ±1.0 abcd	79.3 ±1.0 d	75.3 ±3.3 e	1570 ±232 bcd	2140 ±290 cdef	1919 ±188 bcd	180.0 ±10.9 Gh	189.4 ±5.0 G	189.6 ±13.1 f
SP NK5418	Grain Sorghum	15.4 ±1.0 abcde	18.7 ±1.2 abc	19.4 ±0.5 abcd	68.0 ±1.0 fgh	65.3 ±1.9 gh	1069 ±94 g	1754 ±164 gh	1210±170 h	66.8 ±2.8 J	73.8 ±5.2 I	116.0 ±1.8 h
SP NK8416	Grain Sorghum	13.5 ±1.7 ef	15.2 ±2.2 ef	15.4 ±1.1 h	79.3 ±1.7 d	70.3 ±1.3 efg	1183 ±151 fg	1929 ±222 efg	1364 ±310 gh	125.1 ±9.6 I	128.1 ±5.9 H	167.4 ±8.9 g
SP Sordan 79	Forage Sorghum	14.8 ±0.7 abcdef	18.2 ±2.3 abcd	17.7 ±0.8 fg	71.0 ±2.3 fg	69.3 ±2.9 fg	1795 ±134 ab	1942 ±111 efg	2209 ±221 ab	291.0 ±17.4 B	261.4 ±15.1 cd	307.5 ±1.1 a

Table 2.1 continued

SP Sordan Headless	Forage Sorghum Photoperiod Sensitive	15.1 ±1.2 abcde	18.0 ±1.3 abcd	18.5 ±0.4 cdefg	138.0 ±0.0 a	NA	1525 ±217 cde	3117 ±98 a	1882 ±218 cde	240.9 ±20.7 Ef	297.6 ±7.4 B	257.8 ±13.5 d
SP SS405	Forage Sorghum	14.2 ±1.3 cdef	17.4 ±0.8 abcde	18.1 ±0.5 efg	NA	108.0 ±0.0 b	1976 ±70 a	2466 ±299 bc	2288 ±339 a	338.5 ±28.7 A	342.0 ±19.5 a	296.0 ±13.8 ab
SP Trudan 8	Forage Sorghum	12.9 ±1.6 f	17.1 ±2.3 bcde	15.2 ±0.3 h	63.7 ±0.6 h	62.8 ±0.5 h	1523 ±319 cde	1803 ±104 fgh	1834 ±300 cdef	227.1 ±11.4 F	200.8 ±18.7 fg	287.7 ±1.7 abc
SP Trudan Headless	Forage Sorghum Photoperiod Sensitive	14.5 ±2.8 bcdef	16.6 ±2.8 cde	15.2 ±0.8 h	131.5 ±7.5 b	120.0 ±NA a	1628 ±165 bc	2634 ±191 b	1766 ±66 cdef	251.1 ±11.8 Cde	277.3 ±15.8 Bc	262.3 ±30.1 d
DF		53	54	54	43	44	53	53	47	53	52	30
Mean		15.0	17.0	17.78	82.6	75.1	1427	2143	1777	209.8	212.2	224.1
CV		9.6	9.9	4.4	4.5	5.2	13	12	13	6.5	9.0	5.8
p-value from ANOVA		3.3e-03	1.2e-06	<2e-16	<2e-16	<2e-16	1.0e-10	5.4e-09	1.3e-08	<2e-16	<2e-16	<2e-16
significance		**	**	**	**	**	**	**	**	**	**	**

** Significant at the 0.001 probability level.

† PH, Seeds from Pioneer Hi-Bred; RS, Seeds from Richardson Seeds; SP, Seeds from Sorghum Partners.

2.3.3 Ground validation data from 2015 and 2017

Replicated trials conducted in 2015 and 2017 were used to validate the parameterized APSIM models for each hybrid. Total above-ground biomass was measured by manual sampling and by machine harvesting. Manual sampling was conducted at 65 and 93 DAS in 2015, and 42, 63, 84 DAS in 2017 by harvesting plants from three 1-m sections of row in rows 5–8 of the 12-row plot. Plant count and biomass fresh weight and dry weight were measured for each sample. An individual plant from each sample was dissected to measure leaf, stem, tiller and panicle weights. The leaf sizes were determined using ImageJ, an open source software package developed by NIH for the analysis of scientific images (Schneider et al. 2012). The leaves were laid on a white board in leaf order from top to bottom. RGB images of the leaves were acquired using a Cannon EOS 6D camera with a Canon 35-mm lens under a white light source and ~1.5 m height. Leaves were segmented by thresholding in HSB (Hue, Saturation, Brightness) colour space with four thresholds. Total leaf area per plant and plant stand information were used to calculate the LAI. A Wintersteiger Cibus 2-row Biomass Harvester (Wintersteiger Inc., Salt Lake City, UT, USA) was also used to mechanically harvest plants from plot rows 10 and 11 on 25 August 2015 (99 DAS) and 31 July 2017 (77 DAS) and from plot rows 2 and 3 on 27 September 2017 (135 DAS) as described above.

2.3.4 Remote-sensing data collection

Remote-sensing data were used to measure canopy cover for each plot. RGB images were collected in 2017 and 2018 using a DJI Matrice M600 Pro UAV as a platform, equipped with an APX-15 V2 as the GNSS (Global Navigation Satellite System)/INS (Inertial Navigation System) unit for direct geo-referencing. Images were collected using a Sony Alpha 7R (ILCE-7R) camera with a Sony 35-mm lens at a height of 50 m, resulting in a ground sampling distance of 0.7 cm. Spatial and temporal calibration of the imaging systems in this study were done by methods described in Ravi et al. (2018). The RGB images were collected in 2017 on 6 June (22 DAS), 21 June (37 DAS), 28 June (44 DAS), 5 July (51 DAS), 11 July (57 DAS), 17 July (63 DAS), 25 July (71 DAS), 2 August (79 DAS), 8 August (85 DAS), 16 August (93 DAS) and 30 August (107 DAS). RGB images were taken in 2018 on 16 May (9 DAS), 22 May (15 DAS), 29 May (22 DAS),

4 June (28 DAS), 11 June (35 DAS), 20 June (44 DAS), 27 June (51 DAS), 2 July (56 DAS), 11 July (65 DAS), 18 July (72 DAS), 23 July (77 DAS), 1 August (86 DAS) and 6 August (91 DAS). The RGB images were collected in 2015 using a DJI Phantom 2 platform, and a GoPro Hero3+ camera at a height of 15 m, with ground sampling distance of 0.7 cm. The images were acquired on 15 June (28 DAS), 26 June (39 DAS), 6 July (49 DAS), 15 July (58 DAS) and 25 July (68 DAS).

Orthomosaics were obtained using modified Structure from Motion (SfM) strategies introduced in He et al. (2018) with ground control targets, and then used to identify the coordinates of the plots and row segments. While multiple photos may have overlapping plot coverage, the image coordinates for the same row segment vary from photo to photo. Row segments at the image border suffer more lens and perspective distortion than the row segments at the photo centre, which will have a big impact on canopy cover calculation. Therefore, the photo where the plot is closest to the centre of the image was used for canopy cover estimation. Each row segment was defined by a rectangle whose dimensions were 0.76 m × 3.81 m on average, and then 0.4 m was trimmed from each end of the row to minimize effects of the alley between plots. The canopy cover was estimated for rows 2 and 3 as the ratio of vegetative to non-vegetative pixels within the box, using segmentation methods described previously (Ribera et al. 2018) and canopy cover for each plot taken as the average of the two rows.

2.3.5 Agricultural Production Systems sIMulator

Weather data, soil data, field management and sorghum physiological parameters were used to parameterize the APSIM model for West Lafayette. Weather data included daily solar radiation (MJ), maximum and minimum temperatures (°C) and precipitation (mm). Field management parameters included sowing date, sowing depth and plant density (Table 2.1). The sorghum physiological parameters included observed parameters (final leaf number, final tiller number, maximum leaf area (m2) and maximum leaf multiplier) and derived parameters (extinction coefficient of canopy (k) and RUE (g MJ−1)) determined from the 2018 data set (Table 2.2, see explanation of computation of k and RUE below).

Table 2.2 2018 parameters from the pipeline calculating derived parameters based on observed parameters. K for extinction coefficient and RUE for radiation use efficiency.

Genotype	K	RUE (g / MJ)
PH 849F	0.57	1.47
PH 877F	0.98	1.53
RS 327x36 BMR	0.35	1.36
RS 341x10	0.46	1.15
RS 366x58	0.58	1.15
RS 374x66	0.48	1.60
RS 392x105 BMR	0.44	1.29
RS 400x38 BMR	0.46	1.27
RS 400x82 BMR	0.65	1.28
SP HIKANE II	0.54	1.61
SP NK300	0.84	1.40
SP NK5418	0.79	0.97
SP NK8416	0.55	1.10
SP Sordan 79	0.69	1.64
SP Sordan Headless	0.38	1.40
SP SS405	0.35	1.70
SP Trudan 8	1.43	1.44
SP Trudan Headless	0.38	1.40

2.3.6 Model calibration

An R pipeline for APSIM parameters calculation was developed to process the 2018 data set. The input data included of weather data and sorghum physiological parameters by plot. Weather data were comprised of maximum daily temperature, minimum daily temperature, precipitation and solar radiation. The sorghum physiological parameters for APSIM: observed leaf number, final tiller number, two leaf size distribution parameters, observed canopy cover and observed biomass, were extracted after spatial analysis of the variable values using spline fits (Rodríguez-Álvarez et al. 2018). Two leaf size distribution parameters, maximum leaf area (aMaxI) and maximum leaf multiplier (aX0) were determined for each hybrid. The leaf size functions were computed as follows (Carberry et al. 1993; Chenu et al. 2008):

$$aMax = aMaxS \times Final\ leaf\ number\ (FLN) + aMax$$

For these data, we assume $aMaxS \times FLN = 0$ so,

$$aMax = aMaxI$$

$$Leaf\ Size = aMax \times \exp(a \times (Leaf\ number - Largest\ leaf\ position)^2 + b \times (Leaf\ number - Largest\ leaf\ position)^3) \times 100;$$

$$Largest\ leaf\ position = aX0 \times FLN;$$

$$a = a_0 - \exp(a_1 * FLN);$$

$$b = b_0 - \exp(b_1 * FLN);$$

$$a_0 = -0.009 \qquad a_1 = -0.2$$

$$b_0 = 0.0006 \qquad b_1 = -0.43$$

Using the leaf size function, the largest leaf area and the position multiplier of this leaf within the whole plant of each hybrid were determined. Leaf appearance rate was calculated using an assistant function created with global optimization through DEoptim from Package 'RcppDE' and read in the R pipeline. The leaf appearance rate was determined by plotting number of fully expanded leaves from the weekly measurements plotted against accumulated thermal time. The leaf appearance rate during the early vegetative stage is typically different from the late vegetative stage, so the regression was split into two parts, with the last four leaves set apart. Leaf appearance rates were determined from the estimated slope of a linear regression, leaf appearance rate 1 (early vegetative) and leaf appearance rate 2 (late vegetative). The fraction of incident radiation intercepted (RI) was computed as described previously (Charles-Edwards 1982; Lafarge and Hammer 2002):

$$\mathrm{RI} = 1 - \mathrm{e}^{-\mathrm{k}*\mathrm{LAI}}$$

RI is a function of the LAI and the canopy extinction coefficient (k), which is related to canopy structure. Each day the value of LAI was computed from a sigmoidal curve as a function of leaf number, leaf appearance rate, final tiller number and leaf size distribution through accumulated thermal time, and observed canopy cover was then used to derive k based on the RI

equation. To avoid any effects of senescent leaves, the canopy cover data collected after anthesis were not used for k calculation.

The RUE is defined as the quantity of dry biomass produced under non-stressed conditions based on the amount of intercepted radiation (IR). The maximum RUE for each variety was determined using the slope of the estimated linear relationship between above-ground biomass and cumulative IR, which was derived from the calculated k, calculated LAI and daily radiation.

2.3.7 Model validation

The APSIM models were validated using the performance trials conducted in West Lafayette, IN, in 2015 and 2017. Agricultural Production Systems sIMulator models were also validated for nine of the hybrids evaluated in multi-year trials in Bushland, Texas as part of the Texas A&M Forage Sorghum Test (https://amarillo.tamu.edu/amarillo-center-programs/agronomy/forage-sorghum/). For each hybrid, there were different sowing and harvesting dates. When plant stand count was not collected, we applied 90 % germination rate to the seeding rate as the assumed plant density (Table 2.3). Regression was used to compare predicted and observed values and slope and intercept parameters against the 1:1 line (Piñeiro et al. 2008).

The validated models were used to run a long-term simulation for these hybrids from 1980 to 2017 in both locations. In the simulation, we assumed the sowing date for all years in both locations was 1 June and the plant density was 20 plants per m2 with no irrigation in the West Lafayette simulation and with irrigation in the Bushland simulation. The simulation harvest dates were 80, 100 and 120 DAS.

2.4 Results

2.4.1 Field conditions

The average maximum temperature from sowing to the end of October in 2015, 2017 and 2018 were 26.1, 26.6 and 27.1 °C, respectively. The average minimum temperatures were 13.2, 13.8 and 14.6 °C, respectively. Total precipitation from sowing date to the end of October in 2015, 2017 and 2018 was 471.9, 628.4 and 722.2 mm, respectively, and the crops did not experience

water stress. 2015 and 2017 were slightly cooler and dryer years than 2018, but there were no extreme differences between the 3 years.

2.4.2 Calibration of APSIM models

The commercial sorghum hybrids were compared for variations in plant density, flowering date, final dry biomass and max height (Table 2.1). Significant variations in plant density were detected among hybrids within and between trials. These results demonstrated that plant stand count is an important parameter and should not be replaced by seeding rate. Most of the 18 hybrids flowered at ~75 DAS, except Sordan Headless, Trudan Headless, SP SS405 and RS 400x82 BMR, which exhibited substantially later flowering dates. Analyses of variation in plant height among hybrids revealed that forage sorghum hybrids were taller (average height ~200 cm) while the grain sorghum hybrids were shorter (average height ~100 cm). These differences in morphology between the two types of sorghum represent alternate ideotypes that optimize biomass production versus grain. Final dry biomass was collected on 25 August 2015 (98 DAS), 27 September 2017 (134 DAS) and 9 August 2018 (93 DAS). In all 3 years, SP SS405 exhibited the highest final dry biomass and RS 341x10 exhibited the lowest final dry biomass.

In addition to variation in plant development and productivity, the 18 sorghum hybrids also exhibited surprising variations in leaf size distribution (Fig. 2.1). Maximum leaf area of these hybrids ranged from 300 to 600 cm2. SP SS405 was late-flowering and exhibited the largest maximum leaf area while SP Trudan 8 was an early-flowering type and exhibited the smallest maximum leaf area (Fig. 2.1; Table 2.1). For most hybrids, the maximum leaf size occurred close to the middle leaf of the plant (Fig. 2.1). However, SP Sordan Headless and SP Trudan Headless are photoperiod sensitive and flower very late in temperate environments (120 to 138 DAS in West Lafayette, respectively; Table 2.1). During the data collection from 49 to 94 DAS, these two hybrids were in vegetative growth stage and produced more fullsize leaves than other hybrids. While the photoperiod-insensitive hybrids exhibit a clear, bell-shaped leaf size distribution with the largest leaf in the middle of the plant, the leaf size distribution for the photoperiod-sensitive hybrids show that each hybrid achieves a near-maximum leaf size at leaf 11 or 12, then continues to produce similar-sized leaves while the plant maintains vegetative growth (Fig. 2.1). This pattern of development is similar to what has been observed and parameterized for the APSIM sugarcane

model (Keating et al. 1999, 2003). Leaf size distributions show that each hybrid has a unique canopy structure.

The management practices and biophysiological characteristics of each hybrid, including sowing date, sowing depth, plant density, observed final leaf number, final tiller number, two leaf size distribution parameters, leaf number, observed canopy cover and observed biomass were input to the pipeline for the APSIM simulation. The extinction coefficients (k) of the hybrids (Fig. 2.2) and estimates of RUE (Table 2.2) indicated that, whether photoperiod-sensitive or -insensitive, forage sorghum hybrids exhibited higher RUE. For k of all 18 hybrids, please see Supporting Information—Fig. A1. Thus, given the same amount of solar radiation, forage sorghum can fix more CO2 and produce more biomass per unit of land compared to dwarf or semi-dwarf grain sorghum hybrids or to sorghum-sudan hybrids used for hay production.

To evaluate the accuracy of the parameterized and calibrated models, simulated and observed traits were evaluated over years and environments. For LAI, the six hybrids shown in Fig. 2.3 are representative of hybrids of different types of sorghum that farmers produce. The LAI for all 18 hybrids is in the Supporting Information—Fig. A2. Most of the simulation lines fall within 1 SEM, except under late-season conditions, when LAI is underestimated.

Simulations of total plant biomass production and biomass partitioning into leaves, stems and panicles are shown in Fig. 2.4. The APSIM simulations report green stem and leaf weights; however, senesced and non-senesced leaves and stems were not differentiated in the observed data. Therefore, some leaf and stem simulation results are underestimated in the late-season data points. The simulations of senesced leaves show that the observed leaf dry biomass is close to the simulated green leaf dry biomass plus dead leaf dry biomass. The parameterized APSIM models performed well for most of the different types of sorghum; however, there are some differences between forage sorghum and grain sorghum hybrids. When we consider the stem and leaf dry biomass simulations, the simulations of grain sorghum (Fig. 2.4, O–R) exhibit a better fit than in the forage sorghum hybrids (Fig. 2.4, A–N). For the panicle dry biomass simulations, the models perform better for forage sorghum.

2.4.3 Validation of APSIM models

To validate the parameterized APSIM models over environments, LAI was simulated in West Lafayette using 2015 and 2017 weather data. The models performed well in both years with

simulations for six of the hybrids shown in Fig. 2.5. Model performance of 2015 and 2017 LAI for all 18 hybrids are shown in the Supporting Information—Fig. A3. Leaf area index was overestimated in hybrids with later flowering dates such as SP SS405 and SP Sordan Headless.

Given these results, above-ground dry biomass production was simulated for West Lafayette, IN and Bushland, TX representing two very different production environments (Fig. 2.6). The P-values in the plot test the null hypothesis that the fitted line slope is not different from 1. Only SP SS405 exhibited a slope significantly lower than 1.

Table 2.3 The genotypes and management details in Bushland trials.

Genotype	Year	Sowing date	Harvest date	Stand count (Plts/m^2)
849F	2017	6/13	10/4	16.7
849F	2016	6/8	9/15	17.8
849F	2014	6/13	9/8	22.2
849F	2011	5/19	9/2	22.2
849F	2010	5/28	9/7	22.2
849F	2009	5/28	9/9	22.2
849F	2008	5/27	9/22	22.2
849F	2007	5/30	9/25	20.0
877F	2006	5/25	10/6	28.5
HIKANE II	2016	6/8	8/27	17.8
HIKANE II	2011	5/19	9/2	22.2
HIKANE II	2009	5/28	9/16	22.2
HIKANE II	2008	5/27	9/17	22.2
HIKANE II	2007	5/30	9/25	20.0
HIKANE II	2006	5/25	9/11	26.1
HIKANE II	2005	5/25	9/8	26.7
HIKANE II	2004	5/24	9/9	26.7
HIKANE II	2003	5/21	9/5	26.7
HIKANE II	2002	5/23	8/28	26.7
NK 300	2016	6/8	9/26	17.8
NK 300	2011	5/19	9/22	22.2
NK 300	2009	5/28	10/14	22.2
NK 300	2006	5/25	9/14	25.7
NK 300	2004	5/24	9/9	26.7
NK 300	2003	5/21	9/22	26.7
NK 300	2002	5/23	9/27	26.7
Sordan 79	2006	5/25	9/14	25.4
Sordan 79	2005	5/25	9/29	26.7
Sordan 79	2004	5/24	10/13	26.7

Table 2.3 continued

Sordan Headless	2016	6/8	10/25	17.8
Sordan Headless	2014	6/13	10/6	22.2
Sordan Headless	2008	5/27	10/26	22.2
Sordan Headless	2006	5/25	10/6	22.5
Sordan Headless	2005	5/25	9/29	26.7
Sordan Headless	2004	5/24	10/13	26.7
Sordan Headless	2003	5/21	10/15	26.7
Sordan Headless	2002	5/23	10/11	26.7
SS405	2017	6/13	10/26	16.7
SS405	2016	6/8	10/15	17.8
SS405	2014	6/13	9/17	22.2
SS405	2011	5/19	10/6	22.2
SS405	2009	5/28	10/14	22.2
SS405	2008	5/27	10/26	22.2
SS405	2007	5/30	9/25	20.0
SS405	2006	5/25	9/28	29.1
SS405	2005	5/25	9/29	26.7
SS405	2004	5/24	9/30	26.7
SS405	2002	5/23	9/27	26.7
SS405	2000	5/24	9/27	26.7
Trudan 8	2006	5/25	8/31	23.8
Trudan 8	2005	5/25	9/1	26.7
Trudan 8	2004	5/24	9/9	26.7
Trudan Headless	2014	6/13	10/6	22.2
Trudan Headless	2008	5/27	10/26	22.2
Trudan Headless	2006	5/25	10/6	24.5
Trudan Headless	2005	5/25	9/29	26.7
Trudan Headless	2004	5/24	10/13	26.7
Trudan Headless	2003	5/21	10/15	26.7
Trudan Headless	2002	5/23	10/11	26.7

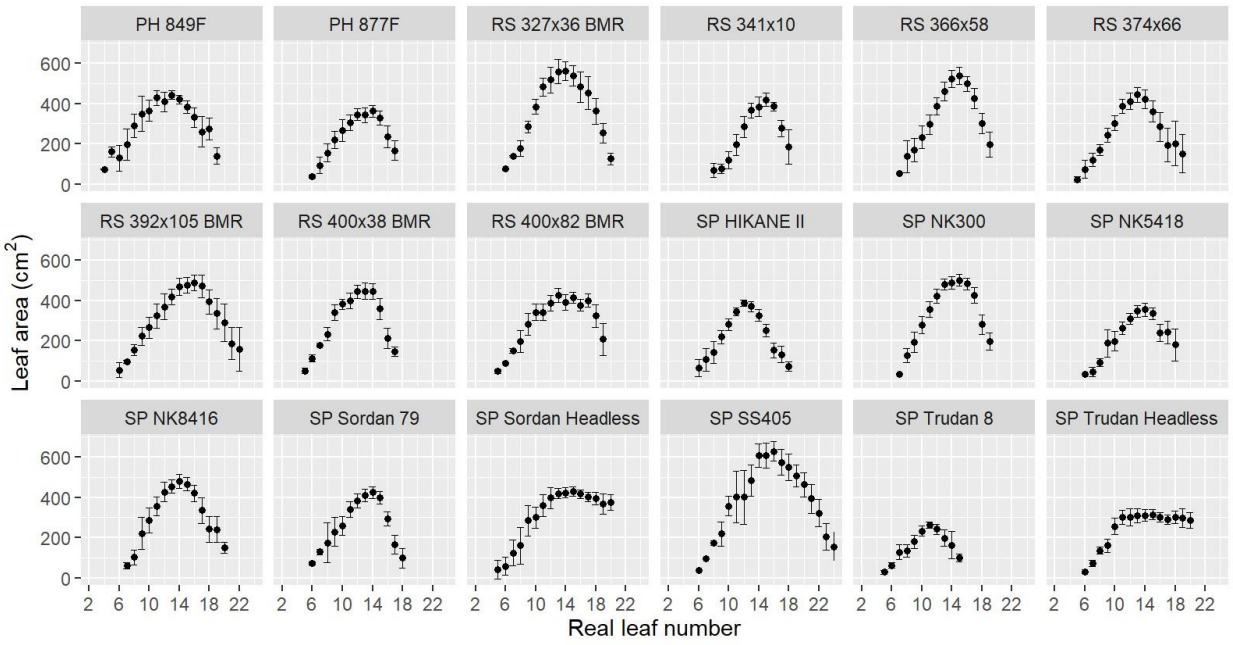

Figure 2.1 Leaf size distributions collected from 25 June (48 DAS), 12 July (65 DAS) and 9 August (93 DAS) at West Lafayette, IN, in 2018. Vertical bars indicate ± 1 SEM for measured values.

Given that APSIM models can simulate above-ground biomass in multiple years and different regions, the above-ground biomass for nine hybrids was simulated in West Lafayette, IN and Bushland, TX using historical weather data from 1980 to 2017. Results are shown in a biomass probability exceedance plot across years (Fig. 2.7). Overall, the simulated biomass in West Lafayette, IN was larger than in Bushland, TX for each of three different harvest dates. The patterns of hybrid biomass performance in the two locations differed. Considering the rank performance of hybrids, the ranks over the three harvest dates do not change much in Bushland, TX but show considerable variation from year-to-year in West Lafayette, IN. SP SS405 and the SP Sordan 79 hybrids had the highest simulated biomass, and SP Trudan Headless had the lowest biomass. Under early harvesting conditions in Bushland, TX, PH 849F, PH 877F, SP HIKANE II and SP Sordan Headless had similar simulated biomass production but indicated more variation when harvested later in the season. Plots of simulated biomass production in West Lafayette, IN showed that SP SS405 and SP Sordan 79 had highest simulated biomass yields and the SP Trudan Headless had the lowest simulated biomass at 80 DAS and 100 DAS. However, the hybrids with the highest biomass also have a large range of potential biomass. For example, SP SS405 has potential biomass between 2200 (g m−2) and 3950 (g m−2) at 120 DAS simulation, which has

larger range than other hybrids (Fig. 2.7, F). SP SS405, SP Sordan 79 and SP Sordan Headless had the highest simulated biomass in West Lafayette at 120 DAS. Other hybrids exhibited a similar range of simulated biomass yields.

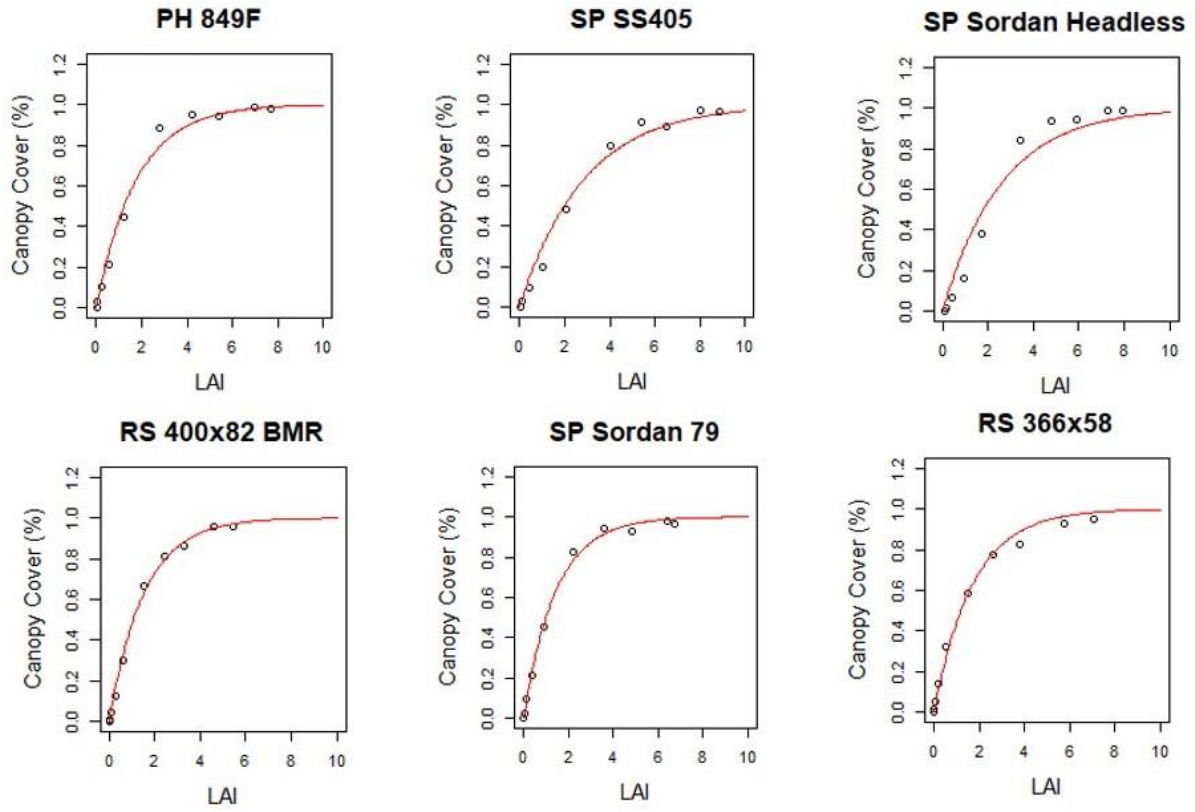

Figure 2.2 The canopy cover (CC) versus leaf area index (LAI) for different types of sorghum. The fitted curve ($CC=1–e^{-k.LAI}$) indicates the extinction coefficient (k) of different types of sorghum and the values shown in Table 2.2.

2.5 Discussion

2.5.1 Plant height and final dry biomass of photoperiod-sensitive and -insensitive forage sorghum hybrids are similar and greater than grain sorghum in medium- and short-season environments

Renewable fuels produced from plants could help to ensure future energy sustainability. Different feedstocks are used in starch-based, sugar-based and cellulose-based ethanol production. Whereas starch and sugar-based ethanol compete with food production (Tilman et al. 2006),

lignocellulosic biofuels do not have a potential negative influence on food production (Rubin 2008).

Not surprisingly, the yield trials and simulation studies of biomass sorghum hybrids reported in this study showed that photoperiod-sensitive and photoperiod-insensitive forage sorghum hybrids have larger max height and final dry biomass than grain sorghum. This indicates that these types of sorghum can produce more lignocellulosic biomass for ethanol and are better choices as feedstocks compared to grain sorghum. Based on our final harvest data in 2018 (Fig. 2.4), the proportion of stem to total biomass for forage sorghum and grain sorghum are 0.70 and 0.37, respectively. Variation in maximum height and final dry biomass of these hybrid cultivars depends on the length of the growing season. The final dry biomass of the photoperiod-insensitive forage hybrids was higher than the photoperiod-sensitive sorghum in 2018 at 94 DAS, while the photoperiod-sensitive hybrids outperformed the photoperiod-insensitive hybrids at 99 DAS in 2015 and 135 DAS in 2017 (Table 2.1). This is consistent with observations that the photoperiod-sensitive sorghum extends pre-floral development up to 8 months, resulting in taller plants with more leaves (Rooney 2004; Rooney et al. 2007; Clerget et al. 2008; Olson et al. 2012). Photoperiod-sensitive sorghum hybrids maximize the yield of lignocellulosic material not only directly through delay of reproductive growth stage but also indirectly through enhancement of drought tolerance or drought avoidance in rainfed environments (Rooney et al. 2007). Our results suggest that photoperiod-sensitive sorghum improves biomass production in longer growing periods by inhibiting the transition from vegetative to reproductive growth, which can add value to bioenergy production in locations that have longer growing periods with sufficiently warm temperatures.

2.5.2 Sorghum hybrids exhibit diverse canopy structures

In conditions of sufficient water supply, the crop biomass is determined by the accumulated radiation interception and the efficiency with which radiant energy is converted to dry matter (Monteith et al. 1977; Muchow 1989). The amount of RI is a function of the pattern of leaf area development. Therefore, leaf size distribution is an important determinant of crop growth. In maize, Hammer et al. (2009) found that the change in canopy architecture may also have indirect effects via leaf area retention and partitioning of carbohydrate to the ear.

The leaf size distributions vary considerably among the hybrids reported in this study (Fig. 2.1). Some hybrids with larger leaf areas may produce more biomass in stress-free environments while hybrids with smaller leaf areas may perform better under drought stress. Hammer et al. (2009) found that crops with smaller leaf area have a yield advantage because they can reduce water use before flowering and conserve subsoil moisture that can then be accessed during the critical grain-filling period under drought stress (He et al. 2017). Borrell et al. (2014a, b) also found that the size of the crop canopy has important consequences for water use in sorghum, where the stay-green trait contributes to drought tolerance by conferring reduced tillering and smaller plant leaf areas before flowering.

Photoperiod-sensitive sorghum can achieve higher biomass when there is a longer vegetative growth supporting its potential value as a feedstock for lignocellulosic biofuel. Photoperiod-sensitive sorghum hybrids exhibit a unique pattern of leaf size distribution (Fig. 2.1). These hybrids remain vegetative throughout the growing season and do not produce a flag leaf or have a clear maximum leaf in the leaf size distributions. These hybrids continued growing and producing more leaves until the last harvest date in 2018 at 94 DAS. This pattern may explain why the photoperiod-sensitive sorghum had larger final dry biomass when harvested at later dates (99 DAS in 2015 and 135 DAS in 2017).

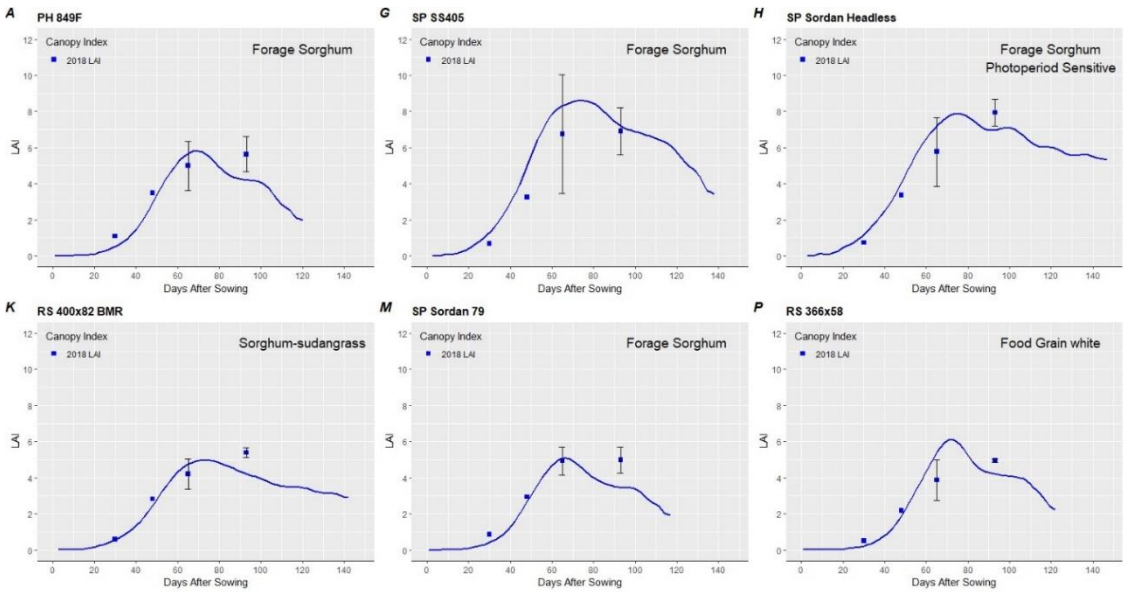

Figure 2.3 Simulated crop leaf area index (LAI) throughout the crop life cycle (lines) compared to measured values (symbols) for six represented hybrids of each sorghum type. The experiments were sown on 8 May 2018 at West Lafayette. Vertical bars indicate ± 1 SEM for measured values.

2.5.3 Photoperiod-sensitive and photoperiod-insensitive forage sorghum hybrids exhibit similar RUE

Radiation use efficiency is a robust and theoretically appropriate parameter for describing crop growth. The total production of dry matter is strongly correlated with intercepted solar radiation in many different species (Monteith et al. 1977). DeWit (1965) and Goudriaan (1982) found that RUE values are essentially stable throughout the growing season and over a wide range of production conditions for most crop species. Further analyses suggested that RUE is not particularly sensitive to leaf angle even with extreme leaf angles (Duncan 1971). Consistent with these findings, some of the hybrids in this study have relatively high extinction coefficients (k) and still have reasonable RUE (Table 2.2). In general, RUE is higher for C4 plants than C3 plants; Kiniry et al. (1989) reported the RUE for both C4 plants and C3 plants showing that C4 plants exhibited the highest RUE, with maize at 1.75 g MJ−1 and sorghum at 1.4 g MJ−1 of intercepted short-wave solar radiation. Other studies have shown maximum RUE of maize in the range 1.6–1.7 g MJ−1 during vegetative growth and 1.2– 1.4 g MJ−1 for sorghum during vegetative growth, suggesting the range of potential RUE for sorghum is less than that of maize (Muchow and Davis 1988; Muchow 1989; Muchow and Sinclair 1994; Sinclair and Muchow 1999; Lindquist et al. 2005).

Most of the RUE studies in sorghum are for grain cultivars; however, our studies in photoperiod-sensitive and photoperiodinsensitive forage hybrids showed that these hybrids have similar RUE to one another and higher RUEs than reported for grain sorghums. Within commercial forage sorghum hybrids, the observed RUE ranged from 1.29 to 1.70 g MJ−1 with the highest RUE similar to reports in maize (Sinclair and Muchow 1999). The sorghum hybrid with highest RUE of the 18 commercial grain and biomass sorghum hybrids in our studies was SP SS405 (Table 2.2). This hybrid also exhibits a larger max height and greater final dry biomass. Other studies have reported similar findings of tall sorghum hybrids exhibiting 1.65 g MJ−1 RUE (Hammer et al. 2010). Narayanan et al. (2013) also reported that two taller sorghum hybrids had the highest biomass and RUE in their study. Conversely, to test the hypothesis that height affects RUE in sorghum, George-Jaeggli et al. (2011) used dwarf sorghum to examine the effects of plant height on RUE. They found that sorghum dwarfing genes negatively affect radiation capture and in some cases RUE.

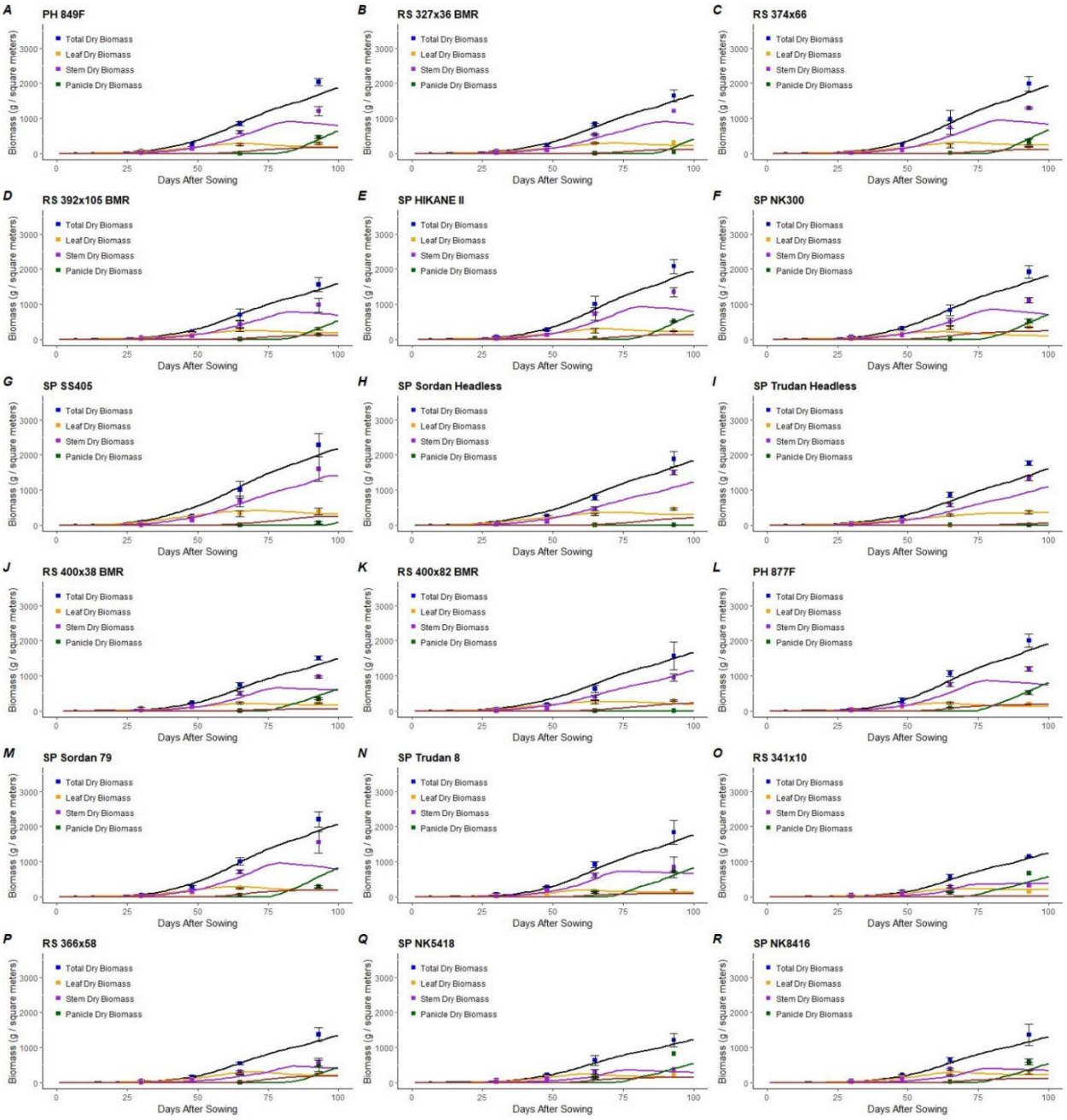

Figure 2.4 Simulated crop attributes throughout the crop life cycle (lines) compared to measured values (symbols) for a range of treatments for the experiments sown on 8 May 2018 at West Lafayette. Vertical bars indicate ± 1 SEM for measured values. For each forage (A–N) and grain (O–R) type hybrid, the panel shows the time course of total and organ (stem, leaf, grain) biomass. The simulated lines are in the same colour as their measured types except the simulated total dry biomass (black line) and the simulated dead leaf dry weight (brown line).

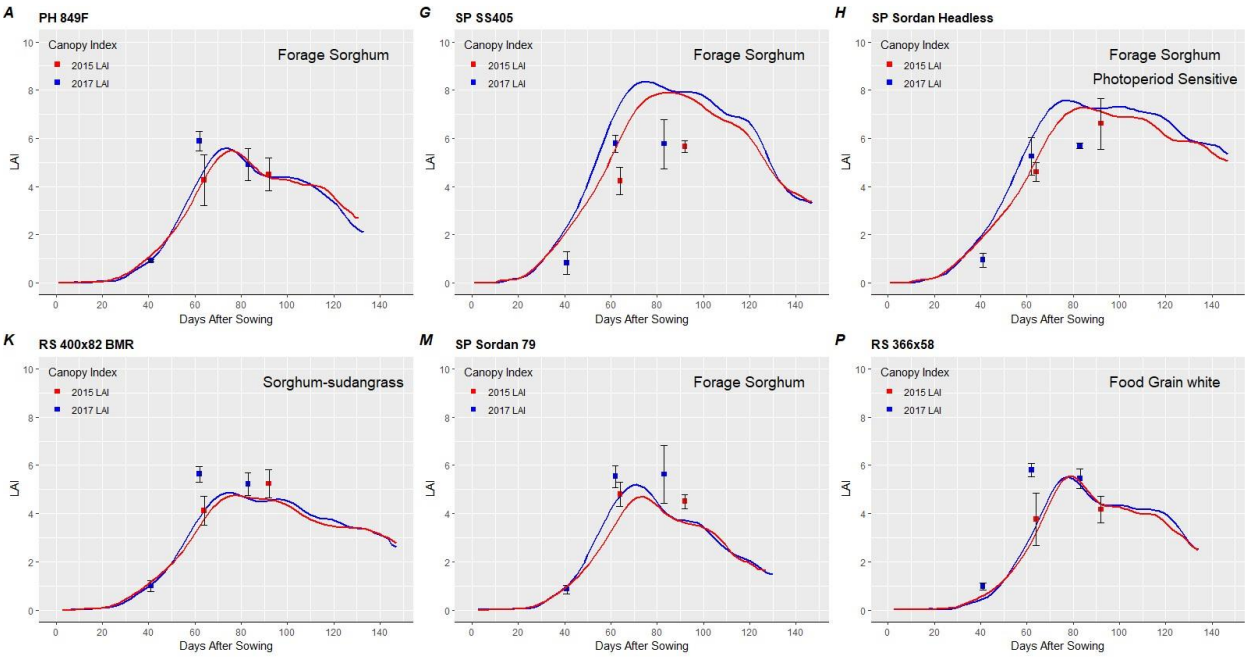

Figure 2.5 Simulated crop leaf area index (LAI) throughout the crop life cycle (lines) compared to measured values (symbols) for six represented hybrids of each sorghum type sown on 19 May 2015 and 16 May 2017 at West Lafayette. The simulated lines are in the same colour as their measured types. Vertical bars indicate ± 1 SEM for measured values.

2.5.4 Forage sorghum models perform well in above-ground biomass simulations across years and locations

The forage and grain sorghum biomass models described in this study performed well in simulations in both West Lafayette, IN and Bushland, TX. These studies showed that the simulated aboveground biomass was higher in West Lafayette than in Bushland over multiple years. Within the set of nine hybrids evaluated at both locations, SP SS405 and SP Sordan 79 exhibited the highest RUE and simulated biomass in both locations. The photoperiod-sensitive sorghum hybrids exhibited the highest predicted biomass yields over time. Interestingly, the photoperiod-sensitive sorghum hybrids did not perform as well in Bushland as in West Lafayette. This may be because West Lafayette has comparatively higher rainfall, and the photoperiod-sensitive sorghum hybrids had more vegetative growing time to produce biomass in West Lafayette than in Bushland.

The APSIM models reported in this study can be used to explore differences in productivity among sorghum hybrids through long-term simulation. Hammer et al. (2014) have used APSIM to study locally optimal G × M combinations and demonstrated that significant improvements in yield and or reduction in failure risk are possible. Hammer et al. (2009) used the past 50 years of

climate data to simulate canopy and root system architecture effects for maize that was planted at a range of densities at three representative locations throughout the US Corn Belt. Their results indicated that change in canopy architecture had little direct effect on biomass accumulation and historical yield trends, but likely had important, indirect effects via leaf area retention and partitioning of carbohydrate to the ear (Hammer et al. 2009).

Applying the APSIM model to sorghum can have similar benefits. White et al. (2015) simulated a rainfed sorghum–winter wheat rotation at Bushland, TX, from 1958 to 1999 comparing no-till versus tillage. The simulated grain sorghum biomass was lower than the one observed. Agricultural Production Systems sIMulator should also be able to improve mid-season predictions of yield. Soler et al. (2007) used CERES-Maize to simulate the impacts of different planting dates on four different maize hybrids under rainfed and irrigated conditions in a subtropical region of Brazil. These studies showed that an accurate yield forecast could be provided at ~45 days prior to the harvest date for all four maize hybrids (Soler et al. 2007). These kinds of studies are promising for farmers, decision makers and researchers, as they could provide longer-term information for strategic management decisions, without extensive yield trials. In the future, our adapted biomass sorghum models can be applied to diverse areas and provide credible simulations for sorghum crop growth and development across a range of environments and management practices.

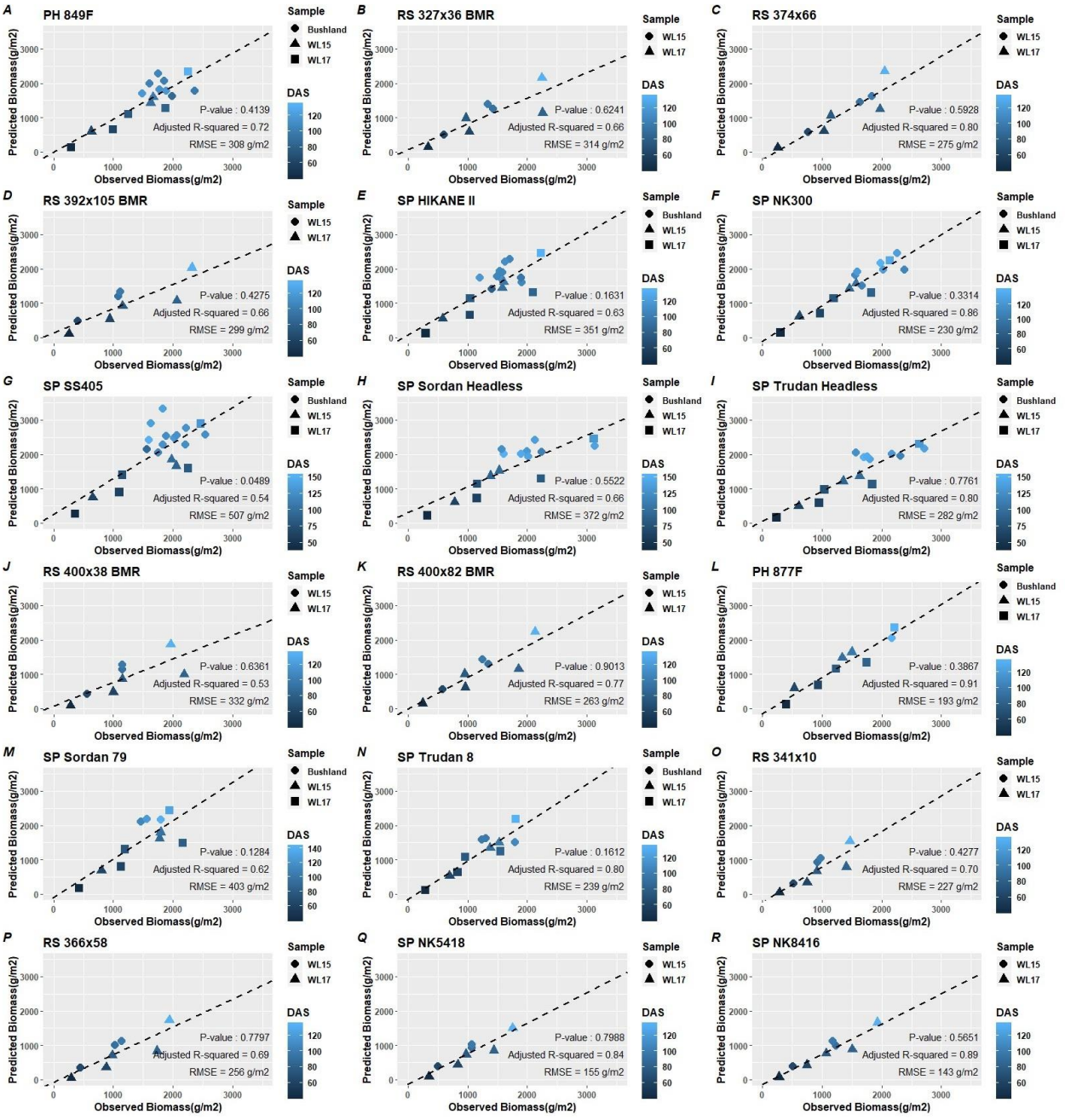

Figure 2.6 Model validation through comparing observed and predicted biomass of West Lafayette 2015, West Lafayette 2017 and Bushland data from 2000 to 2017. The P-value is to test the null hypothesis that the fitted line slope is not different from 1.

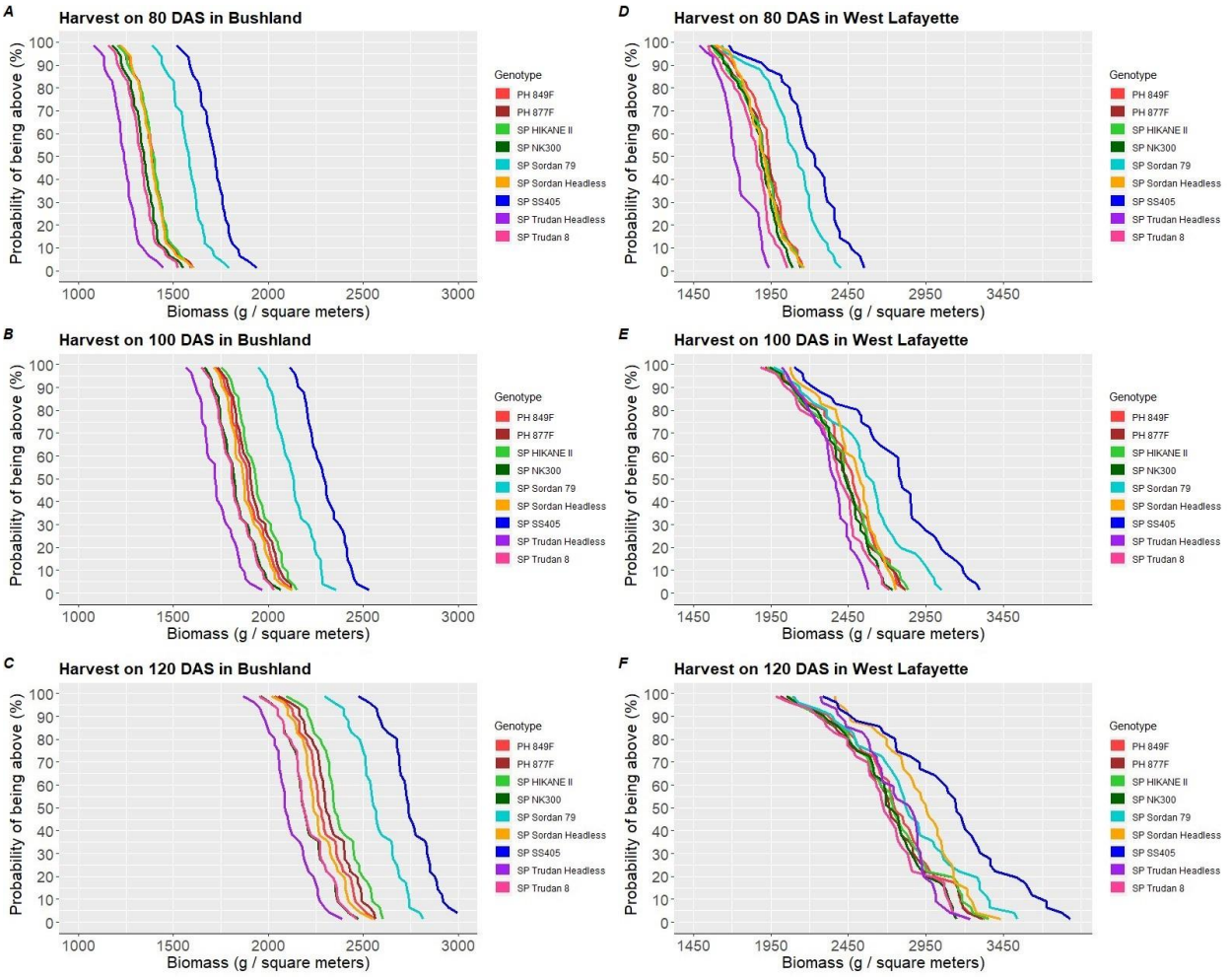

Figure 2.7 Biomass probability exceedance of nine hybrids from 1980 to 2017. The plots from (A) to (C) are harvested on 80, 100 and 120 DAS in Bushland, TX; the plots from (D) to (F) are harvested on 80, 100 and 120 DAS in West Lafayette, IN.

CHAPTER 3. ANALYSIS OF HYBRID SORGHUM BIOMASS YIELDS IN MULTI-YEAR PERFORMANCE TRIALS

3.1 Abstract

Sorghum is a productive, heat-tolerant and drought-tolerant crop that can be used for biomass and bioenergy production. However, few sorghum breeding programs focus on the improvement of traits related to bioenergy production. The objective of this study was to study the genetic architecture of biomass productivity and bioenergy-related traits in a large population of testcross hybrids representing genetically diverse accessions from the sorghum conversion program. A set of 619 sorghum genotypes was individually crossed to ATx623 to create a half-sib population that was planted and evaluated in field trials in three consecutive years. Single-nucleotide polymorphisms (SNPs) were used in a genome-wide association study (GWAS) to identify genetic loci associated with plant architecture and productivity using fixed and random model circulating probability unification (FarmCPU) strategies. GWAS identified 9, 6, 7, 8, 6, and 2 SNPs that were significantly associated with apex height, top collar height, aboveground dry biomass (ADB), moisture, days to flowering (FL) and stem base diameter, respectively. Several of the quantitative trait loci (QTLs) for apex height, top collar height and ADB mapped to previously described dwarfing genes *Dw1* and *Dw3.* Genes associated with top collar height mapped to maturity gene *Ma2*. Genes for harvest moisture mapped to the stay-green loci *Stg1* and *Stg4*. Other loci with significant effects on ADB were mapped to chromosomes 1, 2, 6, 7, 8, 9 with favorable alleles often represented at low frequencies in the sorghum germplasm collection. Dwarf Yellow Milo and Spur Feterita were shown to have favorable alleles for multiple SNPs for ADB and are unique resources for crop improvement. Most genetic studies in sorghum focus on inbred line performance, this study provided one of the first comprehensive assessments of genes contributing to biomass accumulation in hybrid sorghum.

3.2 Introduction

Sorghum (*Sorghum bicolor* (L.) Moench) is tolerant to abiotic stresses (such as drought and heat) and serves as a major food for millions of people in India and sub-Saharan Africa (Smith and Frederiksen 2000; Singh et al. 2014; Borrell, Oosterom, et al. 2014). It is also an important

grain crop for animal feed and biomass for biofuel markets (FAOSTAT, 2019; Jordan et al. 2012). The resilience of sorghum may be attributed to the breadth of genetic resources contributing to variation in physiological, anatomical, and agronomic traits for crop improvement (Morris et al. 2013).

Sorghum also is an important forage and biomass crop that can be used to feed livestock and produce plant-based biofuels. As a C4 plant, sorghum exhibits high maximum photosynthetic rates and high water use efficiency. Based on these attributes, sorghum was proposed as a good candidate for bioenergy feedstock production (Smith 1986). This highly productive, heat-tolerant, and drought-tolerant crop has a history in lignocellulose, sugar and starch improvement. Total dry biomass affects ethanol yield potential and is important target for bioenergy sorghum breeding (Tilman et al. 2006; Rooney et al. 2007; Rubin 2008; Kong et al. 2020). Few genetic studies have addressed the inheritance and expression of biomass production and adaptation traits in sorghum hybrids.

Aboveground dry biomass (ADB) is a complex trait and the primary target for sorghum biomass breeding programs (Gill et al. 2014; Pfeiffer et al. 2019; de Oliveira et al. 2020). However, ADB generally exhibits low heritability. Shiringani and Friedt (2011) reported that broad-sense heritability for sorghum dry biomass was 0.13. Sorghum dry biomass may be affected by plant height (Wilson and Eastin 1982; van Oosterom and Hammer 2008; George-Jaeggli et al. 2011; Olson et al. 2012), days to flowering (Rooney et al. 2007; Olson et al. 2012; Murphy et al. 2014; Meki et al. 2017), and leaf morphology (Sieglinger 1936; Rooney et al. 2007; Olson et al. 2012; Gill et al. 2014; Truong et al. 2017). Plant height affects biomass accumulation and partitioning to grain yield (van Oosterom and Hammer 2008; Wilson and Eastin 1982). Days to flowering affects the length of vegetative growth and is a key trait associated with high biomass yield (Olson et al. 2012; Rooney et al. 2007). Leaf morphology traits, such as leaf area and leaf number, contribute to a diversity of plant and canopy types thereby affecting radiation interception and biomass accumulation (Sieglinger 1936; Rooney et al. 2007; Olson et al. 2012). Incorporating these traits into a selection index while evaluating ADB may be a good approach for crop improvement. Usually, these traits exhibit higher heritability than biomass yield. Sami (2013) found the heritability of plant height was 0.69, and days to flowering was 0.83 in sweet sorghum. Kenga et al. (2006) found that heritability of plant height was 0.77, days to anthesis was 0.42, and grain yield was 0.14 in hybrid sorghum populations.

Plant height is often reported as one of the most important traits driving variation in ADB. Since measurements of plant height are easy and inexpensive, indirect selection strategies have been developed (Burks et al. 2015; Castro et al. 2015; Fernandes et al. 2018; Monk et al. 1984). Four major genes (*Dw1-Dw4*) have been reported for plant height with dwarfism exhibiting recessive inheritance (Quinby and Karper 1953). *Dw1* (*Sobic.009G230800*) was identified in two different genetic studies (Hilley et al. 2016; Yamaguchi et al. 2016). *Dw1* plays a role in the brassinosteroid signaling pathway and affects plant height by reducing cell proliferation activity in the internodes (Hirano et al. 2017). *Dw3* (*Sobic.007G163800*) encodes a MDR transporter that plays a role in polar auxin transport and affects plant height by decreasing cell length and reducing length of the lower internodes. This transporter is orthologous to *brachytic2* in maize (Multani et al. 2003). Some published studies report that there is epistatic interaction between *Dw1* and *Dw3* (Brown et al. 2008; Hilley et al. 2016; Yamaguchi et al. 2016).

Photoperiod sensitivity and flowering time have a major impact on biomass accumulation. Six genes (*Ma1-Ma6*) corresponding to flowering time or photoperiod sensitivity have been described in previous studies. Five of these gene have been cloned. *Ma1* (*Sobic.006G057866*) is the major gene with the greatest influence on flowering time and encodes *SbPRR37*, a pseudo-response regulator that inhibits flowering in long days for grain and bioenergy sorghum (Murphy et al. 2011). *Ma2* (*Sobic.002G302700*) affects sorghum maturity and selectively enhances *Ma1* (*Sobic.006G057866*) expression to delay flowering in long days (Casto et al. 2019). *Ma3* (*Sobic.001G394400*) encodes a phytochrome B (Childs et al. 1997), and *Ma5* (*Sobic.001G087100*) encodes *phytochrome C* (Yang et al. 2014). *Ma6* (*Sobic.006G004400*) encodes *Ghd7* and is a repressor of flowering in long days (Murphy et al. 2014).

Stem diameter and water content are also salient plant traits in biofuel breeding programs (Kong et al. 2020). Plant water content is affected by many genes and environmental factors (Han et al. 2015; Murray et al. 2008). Stem diameter is associated with lodging resistance in plants with larger diameters of basal internodes (Esechie et al. 1977). Some co-localizations of genes impacting water content and other biomass-related traits, such as plant height and flowering time, have been reported. This suggests that the inheritance of these traits may be functionally or physically linked (Kong et al. 2020). The dry stalk (*D*) locus (*Sobic.006G147400*) maps to chromosome 6 and plays a major role in controlling plant water content (Zhang et al. 2018). *D* (*D_*) is dominant and produces a white and dry stem, while the recessive allele (*dd*) produces a

green and juicy stem (Smith and Frederiksen 2000). The *D* locus was reported to have a significant effect on juice volume and stalk moisture in a sweet sorghum mapping population (Burks et al. 2015). Stay-green, an integrated drought-tolerance trait in sorghum, also influences water content (Borrell et al. 2014a). This complex trait also can affect early canopy development, contributes to reduced water use before flowering (Hammer et al., 2010; van Oosterom et al., 2010), and late-season photosynthesis (Borrell et al. 2014a). The stay-green trait is an important component of crop performance under drought stresses.

The genetic architecture of complex polygenic traits can be investigated in genome-wide association studies (GWAS). *Arabidopsis thaliana* is the first plant used in GWAS study (Atwell et al. 2010). Subsequently, GWAS was used to explore significant marker and trait associations in many cereal crops including rice (Huang et al. 2012), barley (Cockram et al. 2010), wheat (Neumann et al. 2011; Sukumaran et al. 2015), maize (Tian et al. 2011), and sorghum (Sukumaran et al. 2012; Morris et al. 2013). False positives in GWAS can be controlled using the mixed linear model (MLM) that corrects for population structure (Q) + relative kinship (K) (Yu et al. 2006). The MLM model has been widely used in association mapping studies (Cruet-Burgos et al. 2020; Huang et al. 2012; Morris et al. 2013; Rhodes et al. 2017); however, this method may miss some true positives. The fixed and random model circulating probability unification (FarmCPU) approach was developed to address this challenge. FarmCPU uses the associated markers to define kinship to avoid over-fitting, which results in higher statistical power compared with other methods (Liu et al. 2016; Habyarimana et al. 2020; Wang et al. 2020; Kavuluko et al. 2021).

The sorghum conversion program was initiated in the 1960s to convert tall, photoperiod-sensitive, exotic sorghums from the world collection into short, photoperiod insensitive, early-maturing sorghums (Rosenow et al. 1997; Stephens et al. 1967). The collection of sorghum conversion lines (SC lines) was developed to represent the genetic diversity of the crop (Hayes et al. 2015). The population exhibits genetic and phenotypic variation for most traits and has been used in GWAS to find the statistically significant associations between sequence variation in the genome and phenotypes of interest (Myles et al. 2009).

In this study, GWAS approaches were used to identify genetic loci controlling biomass yield and adaptation traits in hybrid sorghum. For traits like biomass yield, end-of-season measurements provide an indication of differences in productivity at that time point; however, most agronomically important traits are dynamic and change throughout plant development. Field-

based phenotyping technologies provide efficient tools for capturing spatial and temporal variation in plant phenotypes of crops like maize and sorghum (Pauli et al. 2016; Masjedi et al. 2018; Masjedi et al. 2019; Anderson et al. 2020; Miao et al. 2020; Masjedi et al. 2020). Relative differences in traits like plant height and biomass may be regulated by different sets of genes throughout the growing season (Campbell et al. 2019).

Specific objectives of this study are (1) assess hybrid performance in multi-year trials via heritability and correlation, (2) identify candidate genes for important biomass production traits in sorghum hybrid, (3) explore favorable alleles for biomass yield, and (4) compare identified candidate genes for these traits with published QTLs.

3.3 Materials and methods

3.3.1 Genotypes and field management

The sorghum conversion program converted tall and photoperiod sensitive alien sorghums from U.S. and international collections into short, photoperiod-insensitive, early-maturing sorghums (Rosenow et al. 1997; Rosenow et al. 1997; Stephens et al. 1967). The collection of sorghum conversion lines (SbDIV) was developed to represent the genetic diversity of the crop (Hayes et al. 2015). To study genes controlling variation in hybrid sorghum performance, SbDIV was testcrossed to tester ATx623 to create a population of testcross hybrids (SbDIV TC). In 2018, 2019, and 2020, a set of 619 sorghum F1 hybrids were grown at the Agronomy Center for Research and Education (ACRE) in West Lafayette, IN. Field trials were conducted each year using a randomized complete block design with two replicates. The hybrids were evaluated in 4-row plots with 0.76 m spacing between rows with 3.05 m long. Seeds were sown on 8 May in 2018, 4 June 2019 and 12 May 2020 with a planting rate of 22 plants/m^2. For 2018, 28% liquid UAN fertilizer at 16 g N/m^2 was applied on June 7. For 2019, 34 g/m^2 of potash 0-0-60 (for potassium) and 1121 g/m^2 of lime were applied in October 2018 and 18 g N/m^2 as anhydrous ammonia was applied on May 9. For 2020, 18 g N/m^2 as anhydrous ammonia was applied on April 6. In each study, the experiment was planted with fields managed with a sorghum-soybean rotation.

3.3.2 Molecular background

The SbDIV population was genotyped using genotype-by-sequencing (GBS) with enzyme PSTI. GBS data were aligned to reference genome *Sorghum bicolor* version 3 from Phytozome (Goodstein et al. 2012; McCormick et al. 2018) and imputed using Beagle version 4 (Browning and Browning 2007). The 80,103 single nucleotide polymorphism (SNP) markers were called on reference genome *Sorghum bicolor* version 3 and were filtered for a minor allele frequency (MAF) of 0.025. These SNPs were used in genome-wide association studies (GWAS).

3.3.3 Field data collection

Ground-reference traits include in-season and end-of-season performance traits that were used in trait correlations and GWAS. Plant stand counts were determined from row 2 and 3 of each 4-row plot on 15 June in 2018 (38 days after sowing (DAS)), 24 June in 2019 (20 DAS), and 10 June in 2020 (29 DAS). Days to flowering (FL) were measured as the number of days from planting to when 50% of the panicles in the plot were at 50% anthesis. ADB was measured on rows 2 and 3 in each plot on 14 August in 2018 (98 DAS), 12 September in 2019 (100 DAS) and 19 August in 2020 (99 DAS). All plants in the entire 2-row segment (2 rows x 0.76m x 3.05m) of each plot were harvested with a Wintersteiger Cibus 2-row Biomass Harvester (Wintersteiger Inc., Salt Lake City, UT, USA). After harvesting a plot, ~500 g of the chopped biomass from each plot was taken to determine the fresh weight, dry weight, and moisture content. The moisture contents were defined as $(weight_{wet} - weight_{dry})/weight_{wet} \times 100\%$. Tissue samples were dried at 72 ℃ for 10 d. In the biomass estimation, a 0.614-kg fresh weight correction factor was added back to each plot to account for the short stem segments that were left behind after machine harvesting. The end-of-season (around 1067 ℃d) phenotyping was conducted after machine harvest on plants in rows 1 and 4 in each plot on 19 September in 2019 (107 DAS) and 20 August 2020 (100 DAS). In 2018, we did not record the exact date, but the data collection immediately followed harvest operations. Two plants from rows 1 and 4 of each plot were selected to measure the apex height, top collar height, stem base diameter and stem top collar diameter using rulers and calipers.

3.3.4 Remote-sensing data collection

UAV platforms were used to collect multi-modal and multi-temporal remote sensing data in field trials conducted in 2018, 2019, and 2020 as described in Masjedi et al. (2020). Data were collected using a DJI Matrice M600 Pro UAV as a platform, equipped with an APX-15 V2 as the GNSS (Global Navigation Satellite System)/INS (Inertial Navigation System) unit for direct geo-referencing. LiDAR data were acquired using a Velodyne VLP-16 Puck Lite laser scanner with a range accuracy of ±3 cm. Geometric calibration of the imaging systems in this study were performed using methods described in Ravi et al. (2018b).

A data analytics pipeline was used to accommodate processing of remote sensing data. Orthomosaics were obtained using modified Structure from Motion (SfM) strategies (He et al. 2018; Hasheminasab et al. 2020; Lin et al. 2021) with ground control targets and then used to identify the coordinates of the plots and row segments. Each row segment was defined by a rectangle whose dimensions were 0.76 m × 3.81 m on average, and then 0.4 m was trimmed from each end of the row to minimize effects of the alley between plots.

The first LiDAR data each year were acquired before plants emerged. It was assumed all points belong to the ground and were used to generate a DEM for later dates to extract non-ground points. Height was defined as the 99-percentile height of the non-ground points in rows 2 and 3 of each plot. The python code for extracting LiDAR features can be found in https://hackmd.io/@LiDAR-Feature-Extraction/r1HAB9Wuu/%2FDZXuQH1pQf-KF0ZD0FrJAg.

Daily maximum and minimum temperature data used to calculate growing degree days (GDDs) was downloaded from Midwestern Regional Climate Center (https://mrcc.illinois.edu/). Accumulated GDDs were calculated from the piecewise linear function of the mean air temperatures using the methods introduced in Hammer et al. (1993). There were multiple data acquisition dates in the three years. We selected dates near 400, 600, 800, and 1000 GDDs each year to represent different growth stages of hybrids to evaluate time-dependent LiDAR height.

3.3.5 Statistical analysis

Field trait data collected in 2018, 2019, and 2020 were analyzed for spatial variation by row, column, and replicate based on modeling spatial trends using two-dimensional Penalised

splines (P-spline) models through SpATS R-package (Rodríguez-Álvarez et al. 2018). The generalized heritability of traits was calculated using Oakey's methods that set the genotypes as a random effect in splines through SpATS R-package (Oakey et al. 2007; Rodríguez-Álvarez et al. 2018). After spatial correction, Pearson correlation coefficients between traits were calculated using corrplot R-package version 0.90 (Taiyun 2021).

The genotype main effects and genotype x year interaction effects were evaluated by a nested analysis of variance (ANOVA) using the lm function in R (Table 3.1). The genotype effects were larger than genotype x year interaction effects for most traits, so a combined analysis for the three years was conducted. The best linear unbiased prediction (BLUP) of each genotype was estimated using the lmer function in lme4 R-package (Bates et al. 2015). A mixed linear model was fitted to the data as described by Tolley et al. (2021):

$$Y_{ijkl} = \mu + H_i + Y_j + HY_{ij} + R/Y_{jk} + \varepsilon_{ijkl} \qquad (1)$$

Where Y_{ijkl} is the phenotypic measurement of the i^{th}hybrid, in the j^{th}year, in the k^{th}rep. μ is the overall mean; H_i is the random effect of the i^{th} hybrid; Y_j is the fixed effect of j^{th} year; HY_{ij} is random interaction effect of the i^{th} hybrid in the j^{th} year; R/Y_{jk} is the fixed effect of the k^{th}rep nested in the j^{th} year, and ε_{ijkl} is the random effect of error.

The BLUP values from the combined analysis were used as input phenotypes for GWAS using FarmCPU (Liu et al. 2016) and Mixed Linear Model (MLM) (Yu et al. 2006) with 80,103 SNP markers. GWAS in this study was conducted by Genomic Association and Prediction Integrated Tool (GAPIT) (Zhang et al. 2010; Lipka et al. 2012; Wang and Zhang 2020). The FarmCPU and MLM in GAPIT were run with default settings. The threshold of significant SNPs was determined using FDR of adjusted p-values at 0.01 (Benjamini and Hochberg 1995). The candidate gene search window was set to 15kb upstream and downstream of each significant SNP with FDR of P-value at 0.01. Manhattan plots of GWAS results were created using the R package "qqman" (Turner 2014). Sorghum QTL publications was searched through the Sorghum QTL Atlas (Mace et al. 2019).

Table 3.1 ANOVA of performance traits measured in sorghum hybrids in replicated trials in 2018, 2019, and 2020.

Apex Height					
Source of variation	Degrees of freedom	Sums of squares	Mean square	F value	Pr(>F)
Genotype	628	6410547	10208	39.2977	< 2e-16 ***
Year	1	71590	71590	257.6040	< 2e-16 ***
Rep nested in Year	1	22067	22067	84.9510	< 2e-16 ***
Genotype by Year	628	142212	226	0.8718	0.9835
Residuals	2515	653291	260		

Top Collar Height					
Source of variation	Degrees of freedom	Sums of squares	Mean square	F value	Pr(>F)
Genotype	628	6572507	10466	59.5250	< 2.2e-16 ***
Year	1	27449	27449	156.1163	< 2.2e-16 ***
Rep nested in Year	1	17388	17388	98.8946	< 2.2e-16 ***
Genotype by Year	628	144844	231	1.3118	4.73e-06 ***
Residuals	2515	442191	176		

Stem Base Diameter					
Source of variation	Degrees of freedom	Sums of squares	Mean square	F value	Pr(>F)
Genotype	628	6749.2	10.75	7.3081	< 2.2e-16 ***
Year	1	440.1	440.05	299.2378	< 2.2e-16 ***
Rep nested in Year	1	335.0	335.04	227.8302	< 2.2e-16 ***
Genotype by Year	628	3545.6	5.65	3.8392	< 2.2e-16 ***
Residuals	2515	3698.5	1.47		

Aboveground Dry Biomass					
Source of variation	Degrees of freedom	Sums of squares	Mean square	F value	Pr(>F)
Genotype	628	172648672	274918	6.6255	< 2e-16 ***
Year	1	1735	1735	0.0418	0.838
Rep nested in Year	1	30344448	30344448	731.3029	< 2e-16 ***
Genotype by Year	628	51942577	82711	1.9933	< 2e-16 ***
Residuals	2515	104356598	41494		

Table 3.1 continued

Flowering					
Source of variation	Degrees of freedom	Sums of squares	Mean square	F value	Pr(>F)
Genotype	628	30202.4	48.1	16.3135	<2e-16 ***
Year	1	16694.1	16694.1	5662.7906	<2e-16 ***
Rep nested in Year	1	2.7	2.7	0.9088	0.3405
Genotype by Year	628	4471.3	7.1	2.4151	<2e-16 ***
Residuals	2515	7414.3	2.9		

Moisture					
Source of variation	Degrees of freedom	Sums of squares	Mean square	F value	Pr(>F)
Genotype	628	3.3397	0.005318	7.4278	< 2.2e-16 ***
Year	1	0.0001	0.000129	0.1800	< 2.2e-16 ***
Rep nested in Year	1	0.0797	0.079725	111.3556	< 2.2e-16 ***
Genotype by Year	628	0.9883	0.001574	2.1981	< 2.2e-16 ***
Residuals	2515	1.8006	0.000716		

Stem Top Collar Diameter					
Source of variation	Degrees of freedom	Sums of squares	Mean square	F value	Pr(>F)
Genotype	628	1589.79	2.532	4.46664	< 2.2e-16 ***
Year	1	196.24	196.236	361.7285	< 2.2e-16 ***
Rep nested in Year	1	72.15	72.148	132.9928	< 2.2e-16 ***
Genotype by Year	628	974.56	1.552	2.8606	< 2.2e-16 ***
Residuals	2515	1364.38	0.542		

Stand Count					
Source of variation	Degrees of freedom	Sums of squares	Mean square	F value	Pr(>F)
Genotype	628	20759	33	4.3584	< 2.2e-16 ***
Year	1	48608	48608	6408.9434	< 2.2e-16 ***
Rep nested in Year	1	5854	5854	771.7937	< 2.2e-16 ***
Genotype by Year	628	14387	23	3.0206	< 2.2e-16 ***
Residuals	2515	19075	8		

Signif. codes: 0 ‘***’ 0.001 ‘**’ 0.01 ‘*’ 0.05 ‘.’ 0.1 ‘ ’ 1

3.4 Results

3.4.1 Trait heritability and correlations

Analyses of heritability of important agronomic traits indicated apex height, top collar height, and FL have the highest heritability compared with other traits (Table 3.2). ADB is a secondary and more complex trait and the heritability was 0.5-0.67. The heritability of moisture were high in 2019 (0.65) and 2020 (0.71). However, the moisture heritability of 2018 (0.1) was much lower than the other two years. In 2018, the biomass harvesting began on 1 August, but mechanical and rain delays slowed progress until 13 August. The moisture measurement relies on environments. Delayed harvest times may be the reason for the 0.1 heritability of 2018. The stem top collar diameter, stem base diameter, and stand count are lower heritable than other traits (Table 3.2).

Table 3.2 Heritability of agronomic traits measured in sorghum hybrids in trials conducted in 2018, 2019, and 2020.

	Heritability							
Year	Moisture	ADB	FL	Stand count	Apex height	Top collar height	Top collar diameter	Base diameter
2018	0.10	0.50	0.79	0.30	0.94	0.95	0.17	0.22
2019	0.65	0.57	0.84	0.47	0.97	0.98	0.41	0.35
2020	0.71	0.67	0.83	0.41	0.97	0.98	0.45	0.47

Table 3.3 shows the correlation between agronomic traits. Moisture exhibited a strong and positive correlation with flowering date as well as top collar diameter and base diameter. ADB exhibited a strong and positive correlation with apex height and top collar height, and top collar diameter. Flowering time exhibited a highly significant and positive correlation with moisture and base diameter and was also correlated with ABD. Apex height exhibited a near perfect correlation with top collar height and both measures of plant height were positively correlated with ADB. Although top collar diameter and base diameter were positively correlated, top collar diameter was positively correlated with biomass yield and base diameter was negatively correlated with biomass yield. The results indicate a complex relationship between stem diameter and biomass accumulation in this population.

Table 3.3 Correlations for agronomic traits measured in sorghum hybrids in trials conducted in 2018, 2019, and 2020. Red cell color represents positive correlations, and green color represents negative correlations.

	Moisture	ADB	FL	Stand count	Apex height	Top collar height	Top collar diameter	Base diameter
Moisture								
ADB	-0.07							
FL	0.52**	0.13*						
Stand count	0.06	0.1*	0.12*					
Apex height	-0.1*	0.77**	0.02	0				
Top collar height	-0.09*	0.79**	0.01	0.01	0.99**			
Top collar diameter	0.15**	0.18**	0.12*	-0.12*	0.07	0.11*		
Base diameter	0.29**	-0.08*	0.37**	-0.15**	-0.16**	-0.19**	0.49**	

*Significant at the 0.05 probability level.

** Significant at the 0.001 probability level.

3.4.2 GWAS for biomass traits in sorghum hybrids

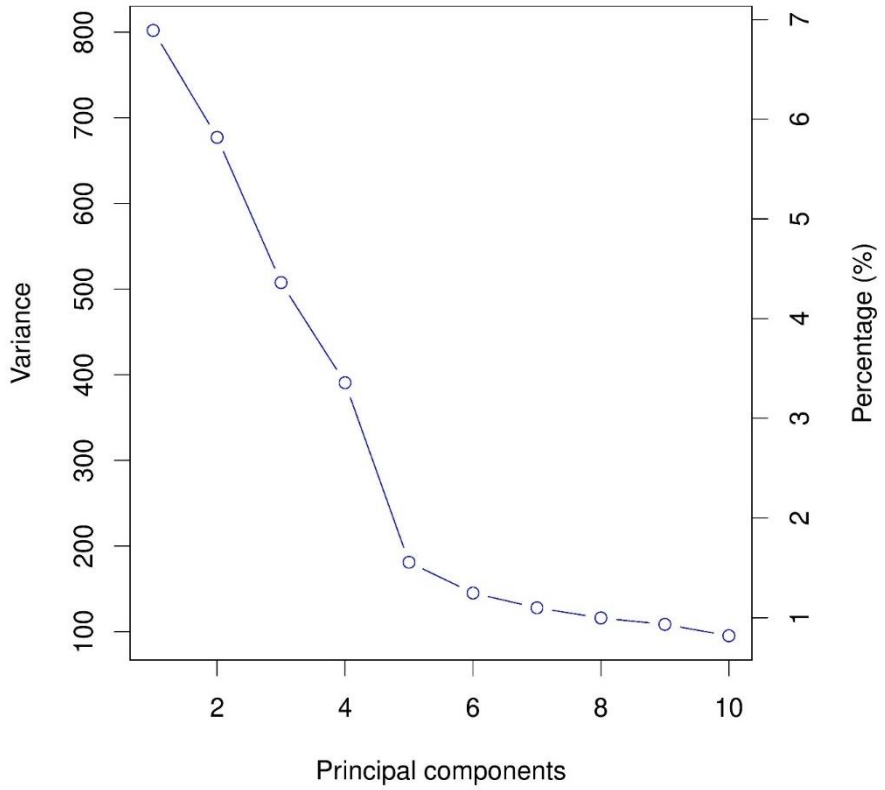

Figure 3.1 A screen plot of principal components (x-axis) and their contribution to the variance determined from GBS data of SbDIV TC.

The BLUPs of each trait and hybrid were used as input phenotypes in GWAS. The principal components (PCs) were calculated using GAPIT and set to 5 based on the number of PCs and their contribution to the variance as shown in Figure 3.1. The FarmCPU and MLM GWAS models were evaluated. As previously reported, the FarmCPU model generally exhibited better performance and higher statistical power than MLM (Liu et al. 2016). The Quantile-quantile (QQ)-plots of P-values for six agronomic traits with significant SNPs detected by FarmCPU are shown in Figure 3.2. The X-axis is the expected P-values which assumed uniform [0,1] distribution. The dotted line shows the 95% confidence interval under the null hypothesis that there is no association between the SNPs and the trait. The FarmCPU models detected SNPs associated with apex height, top collar height, base diameter, ADB, FL and moisture but no significant SNPs were discovered for stand count and top collar diameter.

A. Apex height

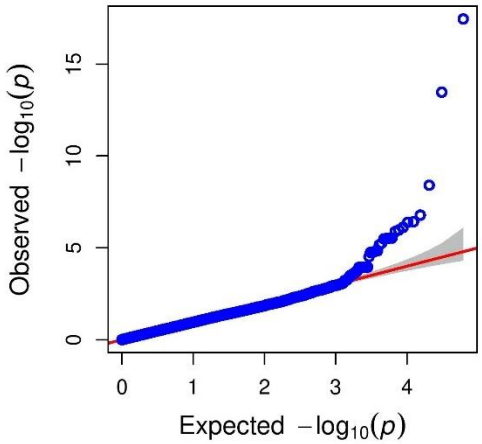

B. Top collar height

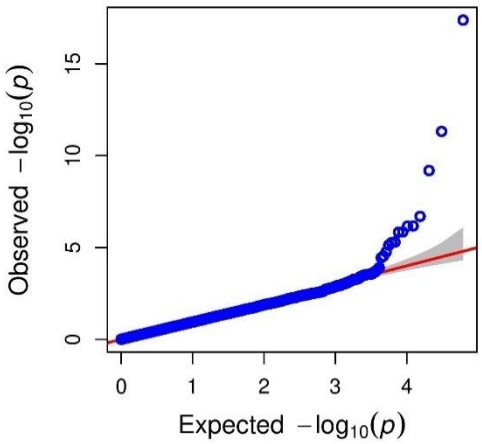

C. Base diameter

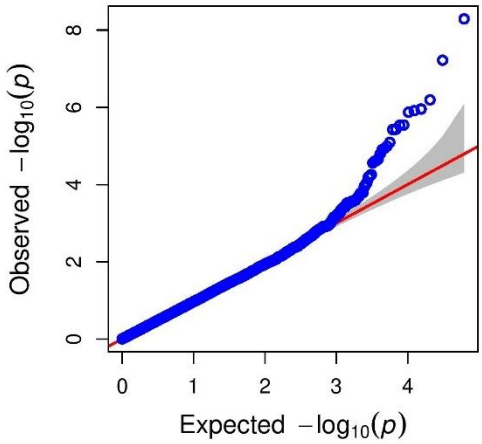

D. Aboveground dry biomass

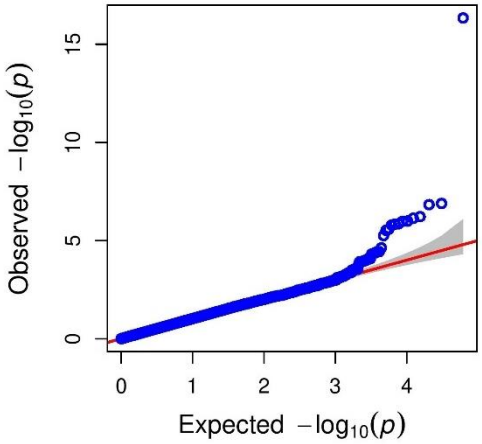

E. Flowering

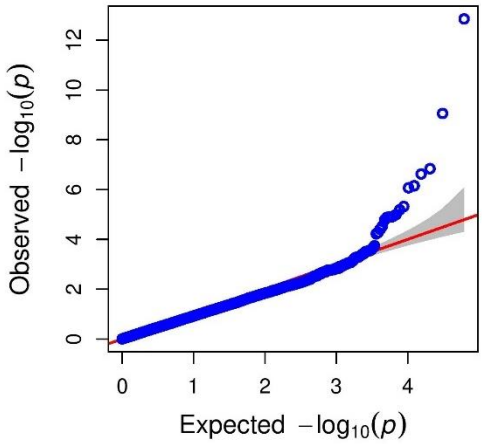

F. Moisture

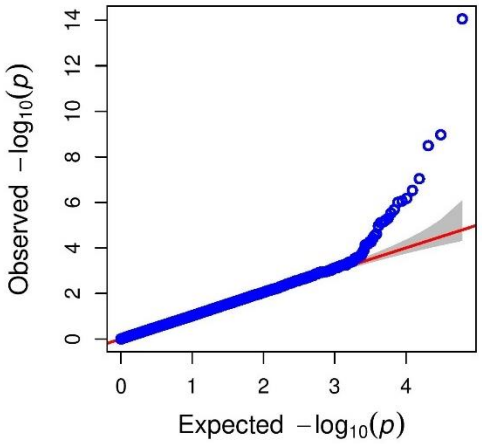

Figure 3.2 Quantile-quantile (QQ)-plots of P-values for six agronomic traits using FarmCPU.

Manhattan plots of the significant SNPs detected for apex height, top collar height, base diameter, ADB, FL and moisture using FarmCPU are shown in Figure 3.3. GWAS results using the MLM model are shown in Appendix B.

A. Apex Height

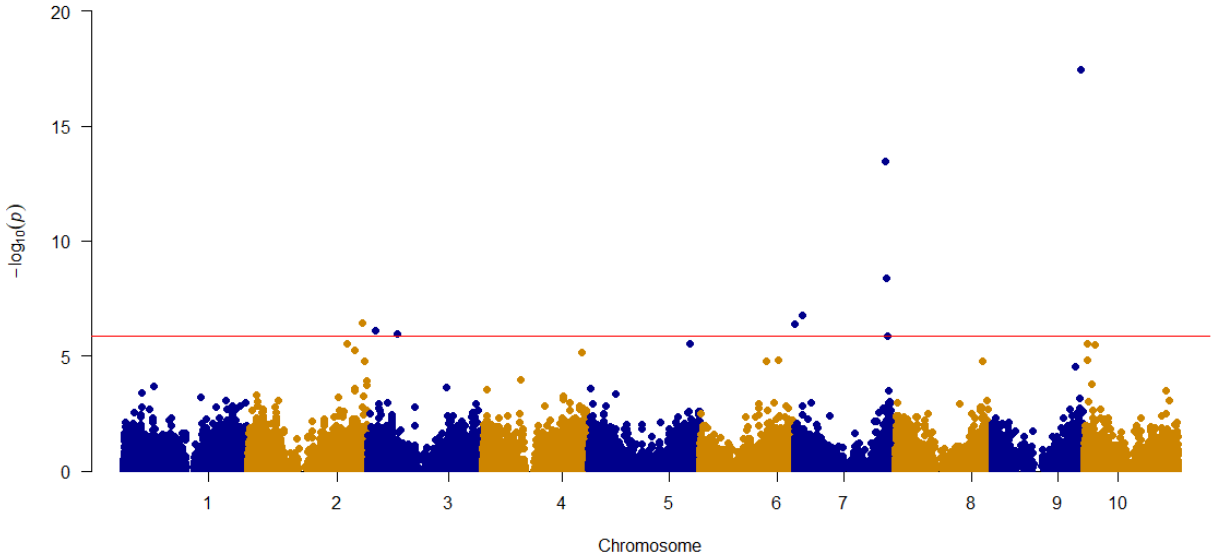

B. Top collar height

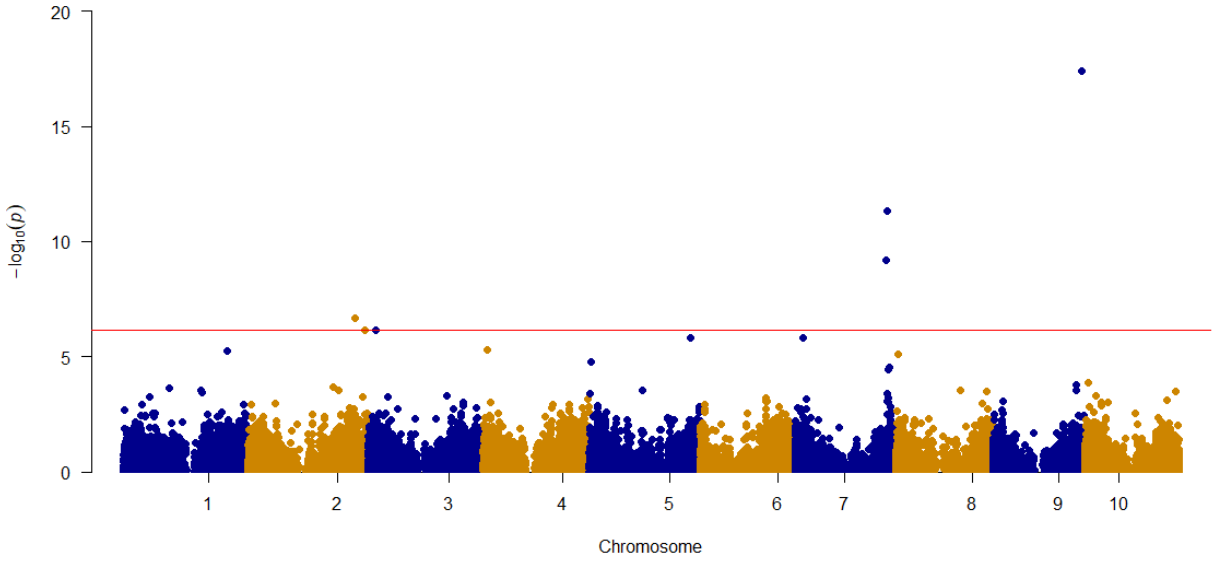

Figure 3.3 continued

C. Base diameter

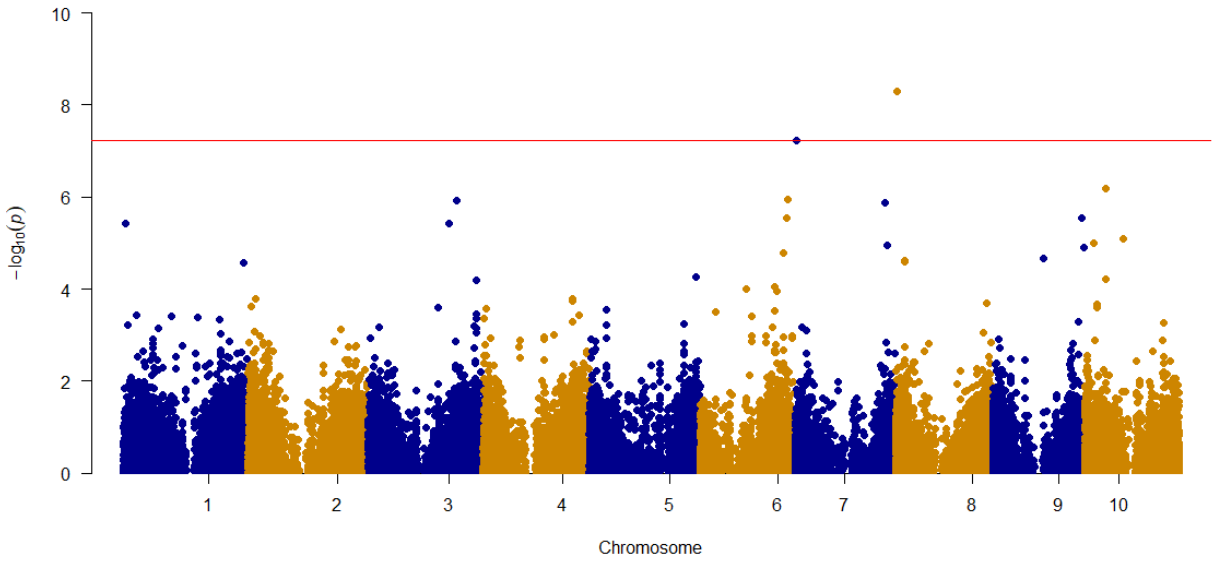

D. Aboveground dry biomass

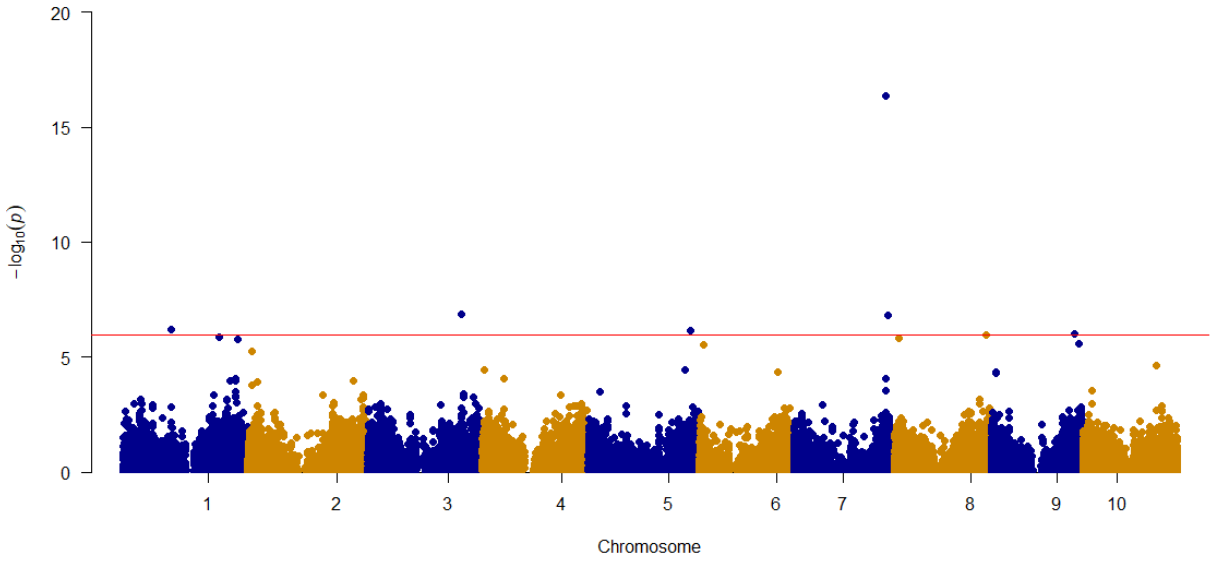

Figure 3.3 continued

E. Flowering

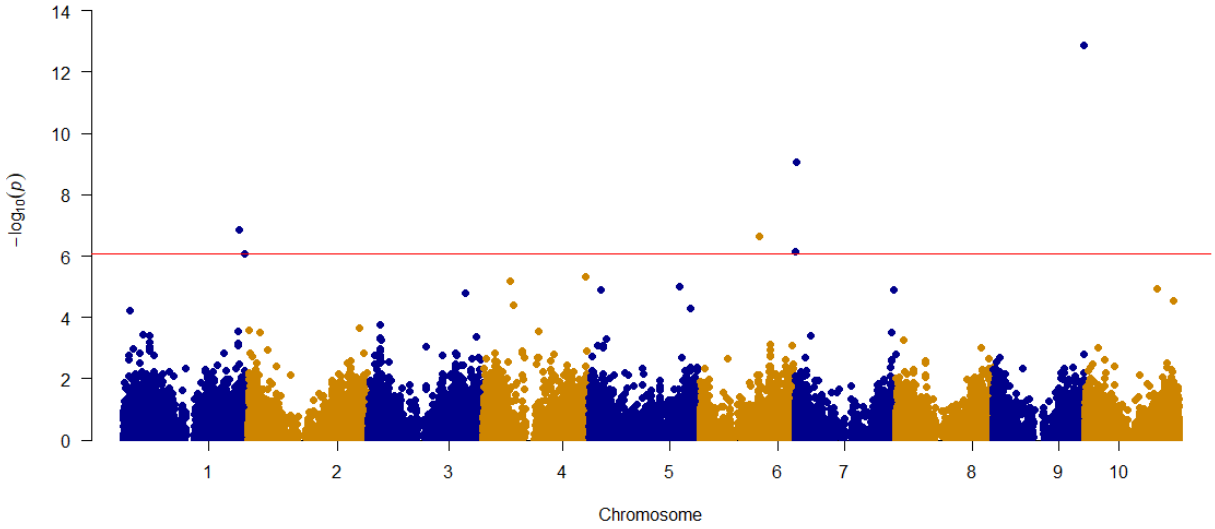

F. Moisture

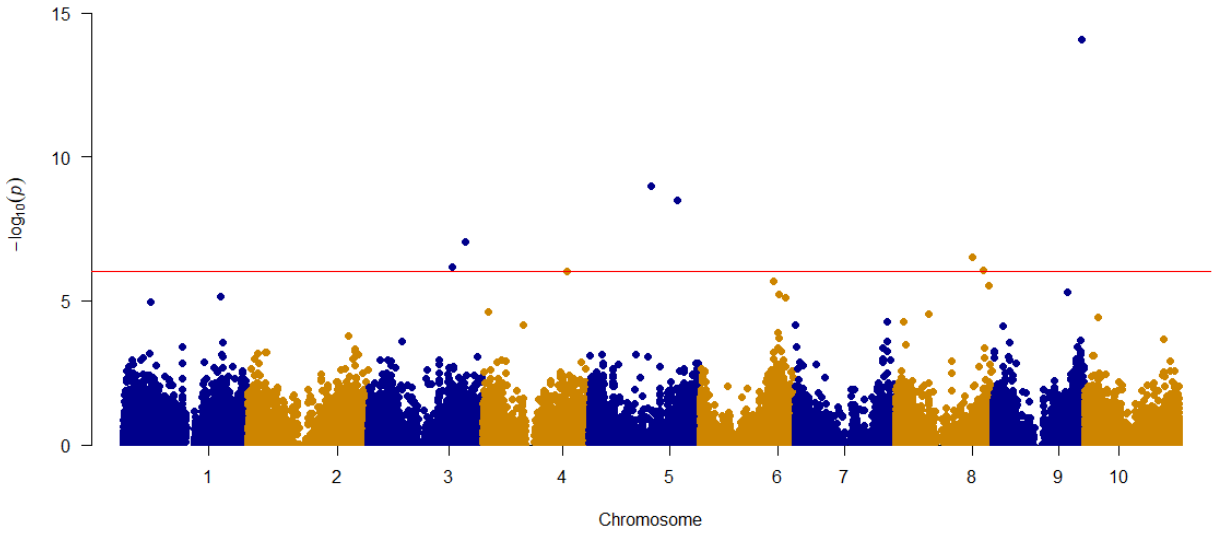

Figure 3.3 Manhattan plots of the significant SNPs detected for (A) Apex height, (B) Top collar height, (C) Base diameter, (D) Aboveground dry biomass, (E) Flowering and (F) Moisture.

GWAS using FarmCPU identified nine significant SNPs for apex height, six significant SNPs for top collar height, two significant SNPs for base diameter, seven significant SNPs for ADB, six significant SNPs for FL, and eight significant SNPs for moisture (Fig. 3.3). Some SNPs were significantly related to more than one trait. SNP S09_57212498 was significant in apex height

(Table 3.4) and top collar height (Table 3.5); SNP S07_59366675 was significant in apex height (Table 3.4), top collar height (Table 3.5), and ADB (MLM results in Table B.2); SNP S07_59768820 was significant in apex height (Table 3.4), top collar height (Table 3.5) and ADB (Table 3.7); SNP S07_61080813 was significant for apex height (Table B.1), top collar height (Table B.3), and ADB (Table 3.7); SNP S07_1078618 was significant for base diameter (Table 3.6) and FL (Table 3.8).

Linkage Disequilibrium (LD) decay in the SbDIV TC was estimated using GAPIT at approximated 12kb (Griebel et al. 2021). Therefore, a candidate gene search window was set to 15kb upstream and downstream of each significant SNP with FDR of P-value at 0.01. One or more candidate genes were discovered flanking each of the SNPs associated with apex height (Table 3.4), top collar height (Table 3.5), base diameter (Table 3.6), aboveground dry biomass (Table 3.7), flowering (Table 3.8), and moisture content (Table 3.9). Significant SNPs and identified candidate genes were on each sorghum chromosome except Chromosome 10.

GWAS using MLM produced similar results (Appendix B). Of particular note, the gene for *Dw3 (Sobic.007G163800)* was identified as a candidate for apex height (Table B.1), top collar height (Table B.2), and ADB (Table B.3). A SNP located 3.96kbp downstream of the previously reported Dry Midrib (D) locus was identified as a candidate gene for moisture content in the SbDIV TC (Table B.4).

For each SNP discovered by GWAS, either the major or minor allele contributed to the favorable effect. If the SNP effect had a positive value, the minor allele was favorable, and if the SNP effect had a negative value, the major allele was favorable. A more in-depth analysis of the genes and alleles controlling aboveground dry biomass in the SbDIV TC indicated the minor allele for three of the SNPs discovered by FarmCPU contributed to increased biomass yield in hybrid sorghum (Table 3.7). The minor alleles for S07_59768820, S07_61080813 and S08_59178415 had positive effects on hybrid performance and were present at frequencies of 0.18, 0.18, and 0.35, respectively, in the SbDIV population. The minor allele for three additional SNPs discovered by FarmCPU under FDR p-value between 0.01 and 0.05 also contributed favorable effects (Table B.6). The minor alleles for S01_ 74145303, S09_56521150, S06_2686264, and S02_2417641 also had positive effects on hybrid performance and were present at even lower frequencies of 0.12, 0.31, 0.03, 0.04, respectively, in the SbDIV population.

Table 3.4 Significant SNPs and candidate genes for apex height identified by GWAS using the FarmCPU model at FDR 0.01. Candidate gene in blue color are not reported in prior QTL studies.

SNP	Chr.	Position	FDR_Adjusted _P-values	Effect	CandidateGene	Annotation
S09_57212498	9	57212498	2.14E-13	19.36	Sobic.009G231900	SUMO-PROTEIN LIGASE
					Sobic.009G232000	RIBOSOME BIOGENESIS PROTEIN
					Sobic.009G232100	Fasciclin domain
					Sobic.009G232200	Fasciclin domain
					Sobic.009G232266	GLUTAREDOXIN
S07_59366675	7	59366675	1.04E-09	19.36	Sobic.007G158800	Galactolipase
					Sobic.007G158900	SODIUM CHANNEL MODIFIER 1
					Sobic.007G159000	CHAPERONE DNAJ-DOMAIN CONTAINING PROTEIN
					Sobic.007G159100	Tetraspanin family
					Sobic.007G159200	PWWP domain
S07_59768820	7	59768820	8.11E-05	15.25	Sobic.007G163300	-
S07_5435798	7	5435798	0.002566026	11.84	Sobic.007G053500	MOB kinase activator 1
					Sobic.007G053600	DNA POLYMERASE DELTA SUBUNIT 4
					Sobic.007G053700	GB
					Sobic.007G053800	RNA POLYMERASE SIGMA FACTOR
					Sobic.007G053900	-
					Sobic.007G054000	LEUCINE-RICH REPEAT-CONTAINING PROTEIN
S02_73983796	2	73983796	0.004214251	-16.21	Sobic.002G384500	-
					Sobic.002G384600	-
					Sobic.002G384700	small subunit ribosomal protein S9e
					Sobic.002G384800	PPR repeat family
					Sobic.002G384900	-
					Sobic.002G385000	-
					Sobic.002G385100	small subunit ribosomal protein S9e
					Sobic.002G385200	PPR repeat family
S07_162826	7	162826	0.004214251	14.18	Sobic.007G001800	Late embryogenesis abundant protein
					Sobic.007G001900	Late embryogenesis abundant protein
					Sobic.007G002000	COPPER TRANSPORT PROTEIN
S03_4997705	3	4997705	0.006740849	13.07	Sobic.003G055500	SOLUTE CARRIER FAMILY 35
					Sobic.003G055600	MINI-CHROMOSOME MAINTENANCE COMPLEX-BINDING PROTEIN
					Sobic.003G055700	saposin

Table 3.4 continued

					Sobic.003G055800	-
					Sobic.003G055900	phosphatidylinositol glycan, class H
					Sobic.003G056000	Micrococcal nuclease / Micrococcal endonuclease
S03_19146851	3	19146851	0.008286311	-24.05	Sobic.003G160500	THIAMIN PYROPHOSPHOKINASE
					Sobic.003G160600	-
					Sobic.003G160700	PROTEIN RALF-LIKE 22
					Sobic.003G160800	MITOCHONDRIAL OUTER MEMBRANE PROTEIN 25
					Sobic.003G160900	small subunit ribosomal protein S4e
					Sobic.003G161000	LEUCINE-RICH REPEAT-CONTAINING PROTEIN
S07_60179636	7	60179636	0.008984154	11.38	Sobic.007G166600	SUPEROXIDE DISMUTASE
					Sobic.007G166701	-
					Sobic.007G166800	Domain of unknown function (DUF966)
					Sobic.007G166900	PROTEIN WALLS ARE THIN 1

Table 3.5 Significant SNPs and candidate genes for top collar height identified by GWAS using the FarmCPU model at FDR 0.01. Candidate genes in blue color are not reported in prior QTL studies.

SNP	Chr.	Position	FDR_Adjusted _P-values	Effect	CandidateGene	Annotation
S09_57212498	9	57212498	2.57E-13	20.04	Sobic.009G231900	SUMO-PROTEIN LIGASE
					Sobic.009G232000	RIBOSOMAL PROTEIN
					Sobic.009G232100	Fasciclin domain
					Sobic.009G232200	Fasciclin domain
					Sobic.009G232266	GLUTAREDOXIN
S07_59768820	7	59768820	1.49E-07	19.92	Sobic.007G163300	-
S07_59366675	7	59366675	1.33E-05	16.87	Sobic.007G158800	Galactolipase
					Sobic.007G158900	SODIUM CHANNEL MODIFIER 1
					Sobic.007G159000	CHAPERONE DNAJ-DOMAIN CONTAINING PROTEIN
					Sobic.007G159100	Tetraspanin family
					Sobic.007G159200	PWWP domain
S02_69475078	2	69475078	0.003139243	-10.28	Sobic.002G323400	Lipase
					Sobic.002G323500	-
					Sobic.002G323600	-
					Sobic.002G323700	SYNTAXIN
					Sobic.002G323800	Protein of unknown function (DUF1668)
					Sobic.002G323900	Proline-rich nuclear receptor coactivator

Table 3.5 continued

					Sobic.002G324000	Isocitrate lyase / Isocitritase
S02_75333122	2	75333122	0.007096102	-15.87	Sobic.002G402900	-
					Sobic.002G403000	ASPARTYL PROTEASES
					Sobic.002G403100	PHOSPHATIDYLINOSITOL 4-PHOSPHATE 5-KINASE 6
S03_4997705	3	4997705	0.007096102	14.53	Sobic.003G055500	SOLUTE CARRIER FAMILY 35
					Sobic.003G055600	MINI-CHROMOSOME MAINTENANCE COMPLEX-BINDING PROTEIN
					Sobic.003G055700	saposin
					Sobic.003G055800	-
					Sobic.003G055900	phosphatidylinositol glycan, class H
					Sobic.003G056000	Micrococcal nuclease / Micrococcal endonuclease

Table 3.6 Significant SNPs and candidate genes for base stem diameter identified by GWAS using the FarmCPU model at FDR 0.01.

SNP	Chr.	Position	FDR_Adjusted _P-values	Effect	CandidateGene	Annotation
S08_882967	8	882967	0.000316375	0.47	Sobic.008G010500	PEROXIDASE 52
					Sobic.008G010600	EPIDIDYMAL MEMBRANE PROTEIN
					Sobic.008G010700	LEUCINE-RICH REPEAT-CONTAINING PROTEIN
					Sobic.008G010750	-
					Sobic.008G010800	PROTEIN ACS-13, ISOFORM C
S07_1078618	7	1078618	0.001866466	-0.28	Sobic.007G011500	F-box domain
					Sobic.007G011600	branch point binding protein (RRM superfamily)
					Sobic.007G011700	BILE ACID BETA-GLUCOSIDASE-RELATED

Table 3.7 Significant SNPs and candidate genes for aboveground dry biomass identified by GWAS using the FarmCPU model at FDR 0.01.

SNP	Chr.	Position	FDR_Adjusted _P-values	maf†	Effect	CandidateGene	Annotation
S07_59768820	7	59768820	2.84E-12	0.18	88.39	Sobic.007G163300	-
S03_60588984	3	60588984	0.0030591	0.44	-72.51	Sobic.003G268900	MITOGEN-ACTIVATED KINASE
						Sobic.003G269000	MITOGEN-ACTIVATED KINASE
						Sobic.003G269100	AWPM-19-like family
						Sobic.003G269200	-
S07_61080813	7	61080813	0.0030591	0.18	49.23	Sobic.007G176900	BETA-GALACTOSIDASE 11-RELATED

Table 3.7 continued

						Sobic.007G177000	L-ASCORBATE PEROXIDASE 3
						Sobic.007G177100	MYB-LIKE DNA-BINDING PROTEIN
						Sobic.007G177150	-
S01_30652981	1	30652981	0.00902187	0.05	-70.95	Sobic.001G258200	SERINE/THREONINE PROTEIN PHOSPHATASE
						Sobic.001G258300	ZINC FINGER FYVE DOMAIN CONTAINING PROTEIN
S05_66379531	5	66379531	0.00902187	0.05	-60.13	Sobic.005G180700	ZINC FINGER-CONTAINING PROTEIN
						Sobic.005G180800	PHOSDUCIN-LIKE PROTEIN 1
						Sobic.005G180850	-
						Sobic.005G180900	Protein of unknown function (DUF632)
						Sobic.005G181000	ACYL-COENZYME A OXIDASE 2, PEROXISOMAL
						Sobic.005G181100	-
S09_54144857	9	54144857	0.00919189	0.14	-42.94	Sobic.009G189400	Assimilatory sulfite reductase / Sulfite reductase (ferredoxin)
						Sobic.009G189501	-
						Sobic.009G189600	-
						Sobic.009G189700	-
S08_59178415	8	59178415	0.00919189	0.35	48.62	Sobic.008G158666	Protease inhibitor
						Sobic.008G158732	Protease inhibitor
						Sobic.008G158800	Protease inhibitor
						Sobic.008G158900	CHITINASE
						Sobic.008G159000	-

† Minor allele frequency

Table 3.8 Significant SNPs and candidate genes for flowering time identified by GWAS using the FarmCPU model at FDR 0.01. Candidate genes in blue color are not reported in prior QTL studies.

SNP	Chr.	Position	FDR_Adjusted _P-values	Effect	CandidateGene	Annotation
S09_58649847	9	58649847	8.53E-09	1.12	Sobic.009G251400	LYSOPHOSPHOLIPASE-RELATED
					Sobic.009G251500	structural maintenance of chromosome 3 (chondroitin sulfate proteoglycan 6)
					Sobic.009G251600	Cytochrome c oxidase
					Sobic.009G251700	Helix-hairpin-helix domain
S07_1078618	7	1078618	2.69E-05	-1.00	Sobic.007G011500	F-box domain
					Sobic.007G011600	branch point binding protein (RRM superfamily)
					Sobic.007G011700	BILE ACID BETA-GLUCOSIDASE-RELATED
S01_74762373	1	74762373	0.002963546	1.27	Sobic.001G475200	Trypsin-like peptidase domain
					Sobic.001G475300	ubiquitin carboxyl-terminal hydrolase
S06_38161198	6	38161198	0.003654368	0.82	Sobic.006G051700	NB-ARC domain
					Sobic.006G051750	-
					Sobic.006G051800	CALMODULIN-BINDING TRANSCRIPTION ACTIVATOR 4
S07_156957	7	156957	0.008657447	0.93	Sobic.007G001700	Transcriptional repressor
					Sobic.007G001800	Late embryogenesis abundant protein
					Sobic.007G001900	Late embryogenesis abundant protein
					Sobic.007G002000	COPPER TRANSPORT PROTEIN
S01_77989586	1	77989586	0.008732666	-0.82	Sobic.001G512000	CYCLIN-DEPENDENT KINASE INHIBITOR 1
					Sobic.001G512100	MAGNESIUM TRANSPORTER
					Sobic.001G512200	EXPRESSED PROTEIN

Table 3.9 Significant SNPs and candidate genes for moisture content identified by GWAS using the FarmCPU model at FDR 0.01. Candidate genes in blue color are not reported in prior QTL studies.

SNP	Chr.	Position	FDR_Adjusted _P-values	Effect	CandidateGene	Annotation
S09_57846253	9	57846253	5.35E-10	0.01	Sobic.009G241300	EXPRESSED PROTEIN
					Sobic.009G241400	-
					Sobic.009G241500	-
					Sobic.009G241600	butyrate response factor 1
					Sobic.009G241700	2OG-FE II OXYGENASE FAMILY PROTEIN
					Sobic.009G241801	-
S05_39908079	5	39908079	3.31E-05	-0.01	NA	-
S05_57225839	5	57225839	6.62E-05	0.01	Sobic.005G131400	-
					Sobic.005G131500	Nucleoside diphosphate phosphatase
					Sobic.005G131550	-
					Sobic.005G131600	Leucine Rich Repeat/ Protein tyrosine kinase
S03_62788762	3	62788762	0.001410978	-0.01	Sobic.003G295400	MACPF DOMAIN-CONTAINING PROTEIN CAD1
					Sobic.003G295500	OLIGOPEPTIDE TRANSPORTER-RELATED
					Sobic.003G295600	Protein of unknown function (DUF1264)
					Sobic.003G295700	ALKALINE CERAMIDASE-RELATED
					Sobic.003G295800	RIBOSOMAL PROTEIN L13
					Sobic.003G295900	HEAT SHOCK TRANSCRIPTION FACTOR
					Sobic.003G296000	TREHALOSE-6-PHOSPHATE SYNTHASE
S08_49686141	8	49686141	0.003688284	-0.01	Sobic.008G105432	-
S03_54134664	3	54134664	0.00687297	0.00	Sobic.003G209200	PROTEIN PHOSPHATASE PP2A REGULATORY SUBUNIT B
					Sobic.003G209300	-
					Sobic.003G209400	-
					Sobic.003G209500	-
					Sobic.003G209600	PHOSPHATASE, ORPHAN 1, 2
S08_56311247	8	56311247	0.007633331	0.02	Sobic.008G134500	Receptor protein-tyrosine kinase
					Sobic.008G134600	-
S04_54073211	4	54073211	0.007633331	-0.01	Sobic.004G188600	ubiquitin carboxyl-terminal hydrolase 12/46
					Sobic.004G188701	KOG0254 - Predicted transporter
					Sobic.004G188800	Sugar (and other) transporter
					Sobic.004G188900	PUMILIO HOMOLOG 11-RELATED

3.4.3 LiDAR height data description

Variation in LiDAR plant height was estimated at four different time points at approximately 400GDD, 600GDD, 800GDD, and 1000GDD in 2018, 2019, and 2020 (Table 3.10). These time points correspond to different growth stages with floral initiation occurring between 400GDD and 600GDD, flag leaf appearance at approximately 800GDD, average flowering time at 850GDD, and mid-grain filling at approximately 1000GDD based on NK300 performance.

Table 3.10 GDD of LiDAR height data collection dates.

Hybrids					
2018 SbDIV TC		2019 SbDIV TC		2020 SbDIV TC	
Date	GDD ($℃d$)	Date	GDD ($℃d$)	Date	GDD ($℃d$)
6/11/2018	333.04	7/12/2019	411.21	6/19/2020	342.29
7/2/2018	595.3	7/23/2019	562.43	7/8/2020	583.69
7/11/2018	704.81	8/10/2019	751.89	7/25/2020	789.8
8/1/2018	920.2	8/24/2019	913.26	8/6/2020	910.24

Variations in LiDAR plant height at these time points are shown in Figure 3.4. At 400GDD and 600GDD, the population exhibited less variation in plant heights with most of the hybrids close the median. At later stages of development at 800GDD and 1000GDD, the population exhibited considerably more variation in plant height for all years. The median plant height at 1000 GDD in 2018, 2019, and 2020 were 2.3m, 1.9m, and 2.2m, respectively.

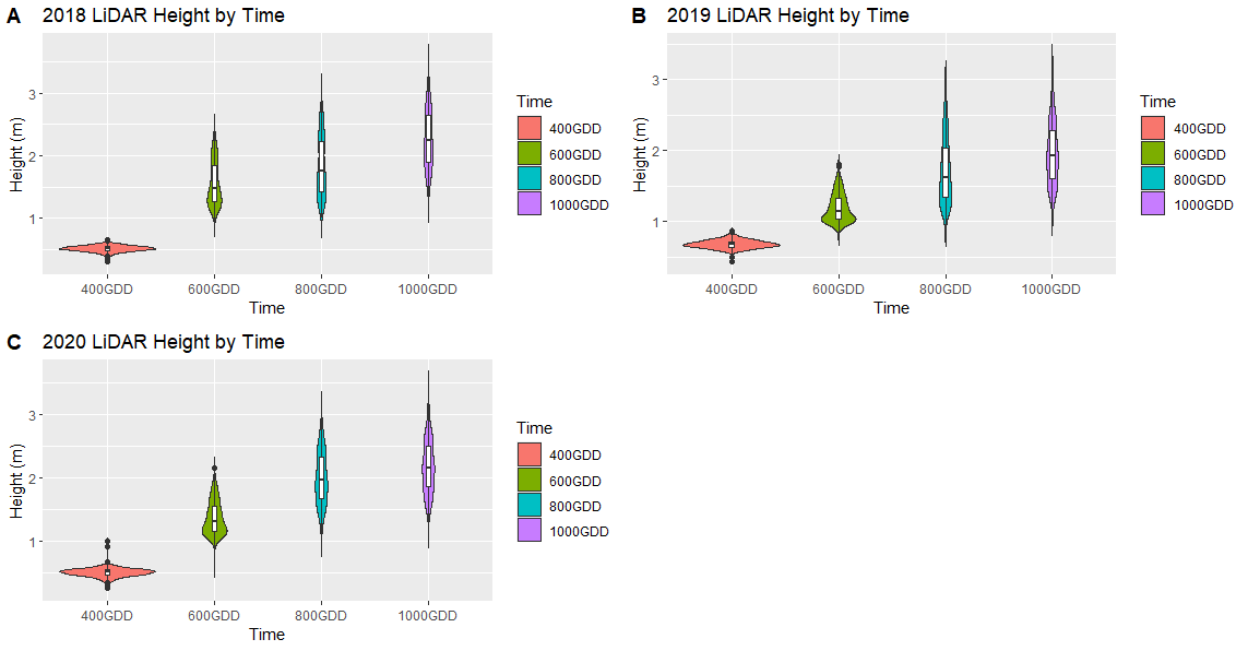

Figure 3.4 Violin plots of LiDAR plant height of the SbDIV TC at 400GDD, 600GDD, 800GDD, and 1000GDD in 2018, 2019, and 2020.

The heritability for LiDAR plant height at 400GDD, 600GDD, 800GDD, and 1000GDD are shown in Table 3.11. Higher heritabilities were observed in the later growing season in all three years.

Table 3.11 Heritability of LiDAR plant height at 400GDD, 600GDD, 800GDD, and 1000GDD.

	LiDAR Height		
	2018	2019	2020
400GDD	0.72	0.78	0.48
600GDD	0.95	0.97	0.93
800GDD	0.96	0.98	0.96
1000GDD	0.96	0.96	0.96

3.4.4 GWAS results of LiDAR height

GWAS using the FarmCPU model identified four significant SNPs associated with LiDAR plant height at 600GDD, three significant SNPs at 800GDD, and seven significant SNPs at 1000GDD (Figure 3.5). No significant SNPs were identified in 400GDD. Several of the SNP markers were significant over time points.

A. LiDAR height at 600GDD

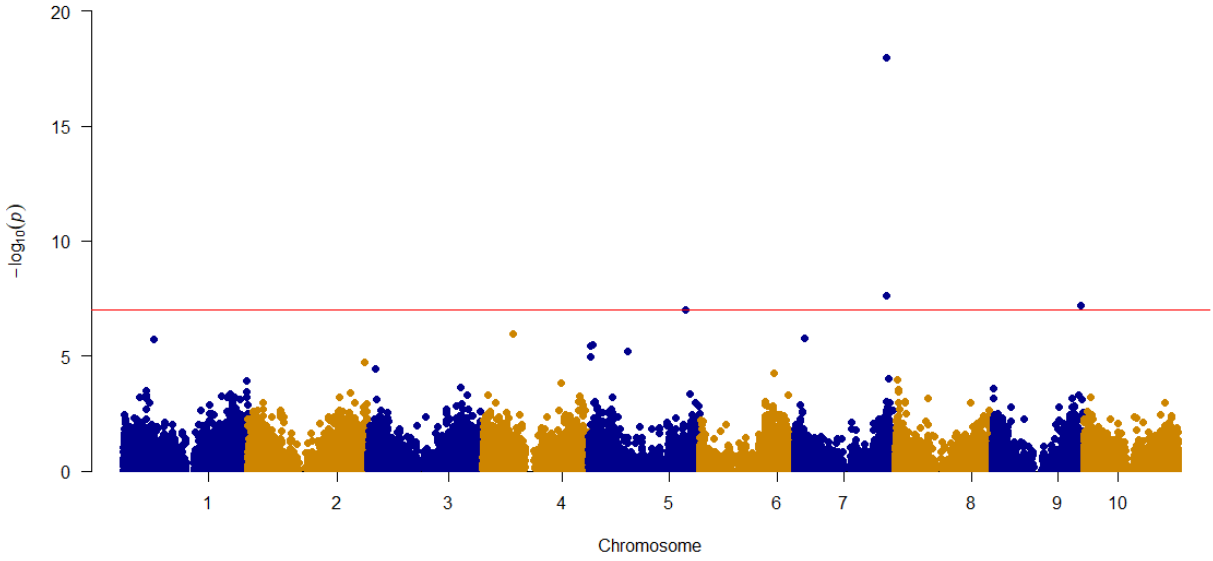

B. LiDAR height at 800GDD

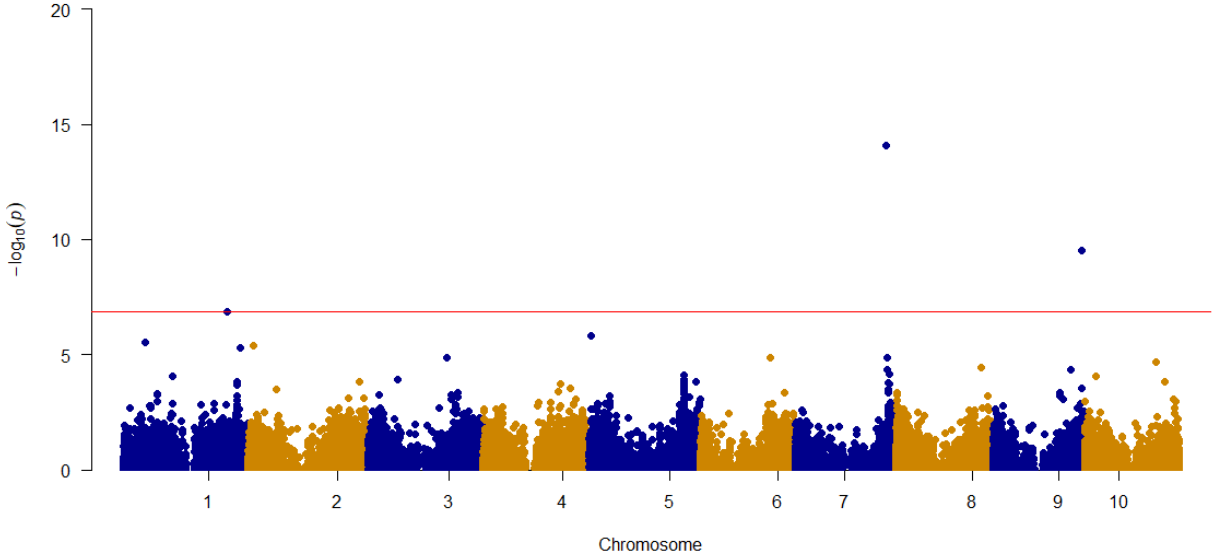

Figure 3.5 GWAS results of LiDAR plant height at (A) 600GDD, (B) 800GDD, and (C) 1000GDD.

Figure 3.5 continued

C. LiDAR height at 1000GDD

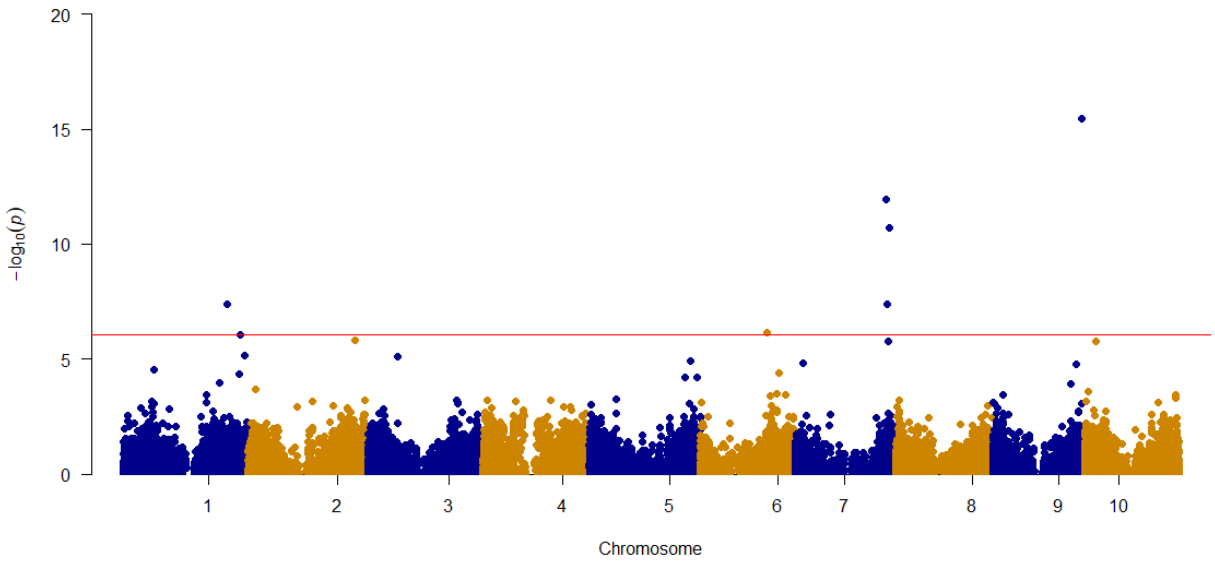

One or more candidate genes were discovered flanking each of the SNPs associated with LiDAR plant height at 600GDD (Table 3.12), at 800GDD (Table 3.13), and at 1000GDD (Table 3.14). Significant SNPs and candidate genes were on sorghum chromosomes 1, 5, 7, and 9.

Some SNPs for LiDAR plant height were significant at more than one time point. SNP S07_59366675 was significant at 800GDD (Table 3.13) and 1000GDD (Table 3.14) with effects 0.21 and 0.19, respectively. SNP S07_59768820 was significant in 600GDD (Table 3.12) and 1000GDD (Table 3.14) with effects of 0.13 and 0.14, respectively. SNP S09_57212498 was significant in 600GDD (Table 3.12), 800GDD (Table 3.13) and 1000GDD (Table 3.14) with effects of 0.06, 0.12 and 0.17, respectively.

The candidate genes in the search window for S09_57212498 included *Sobic.009G231900, Sobic.009G232000, Sobic.009G232100, Sobic.009G232200,* and *Sobic.009G232266* that map to the same region as the *Dw1* gene. Five candidate genes were discovered in the search window for S07_59366675 including *Sobic.007G158800, Sobic.007G158900, Sobic.007G159000, Sobic.007G159100,* and *Sobic.007G159200* that map to the same region as the *Dw3* gene. Although *Dw1* and *Dw3* were not identifieid directly using FarmCPU, candidate gene *Sobic.009G231900* is 99.74kb downstream to *Dw1* and candidate gene *Sobic.007G163300* is 53.08kb upstream to *Dw3*.

Table 3.12 Significant SNPs and candidate genes for LiDAR plant height at 600GDD identified by GWAS using the FarmCPU model at FDR 0.01. Candidate genes in blue color are mapped to the same position as the dwarfing locus *Dw1*, candidate genes in green color are mapped to the same position as the dwarfing locus *Dw3*.

SNP	Chr.	Position	FDR_Adjusted _P-values	Effect	CandidateGene	Annotation
S07_59768820	7	59768820	7.00E-14	0.13	Sobic.007G163300	-
S07_59418009	7	59418009	0.000723628	0.08	Sobic.007G159500	IMPACT-RELATED
					Sobic.007G159700	F-type H+-transporting ATPase subunit d
					Sobic.007G159800	Domain of unknown function (DUF296)
					Sobic.007G159900	ubiquitin carboxyl-terminal hydrolase 36/42
S09_57212498	9	57212498	0.001282308	0.06	Sobic.009G231900	SUMO-PROTEIN LIGASE
					Sobic.009G232000	RIBOSOME BIOGENESIS PROTEIN
					Sobic.009G232100	Fasciclin domain
					Sobic.009G232200	Fasciclin domain
					Sobic.009G232266	GLUTAREDOXIN
S05_62313708	5	62313708	0.001480724	-0.07	Sobic.005G152100	SUBGROUP I AMINOTRANSFERASE RELATED
					Sobic.005G152200	SUBGROUP I AMINOTRANSFERASE RELATED
					Sobic.005G152250	-
					Sobic.005G152300	-
					Sobic.005G152400	Protein of unknown function (DUF2667)
					Sobic.005G152500	-
					Sobic.005G152550	Adenylyl-sulfate reductase (glutathione)

Table 3.13 Significant SNPs and candidate genes for LiDAR plant height at 800GDD identified by GWAS using the FarmCPU model at FDR 0.01. Candidate genes in blue color are mapped to the same position as the dwarfing locus *Dw1*, candidate genes in green color are mapped to the same position as the dwarfing locus *Dw3*.

SNP	Chr.	Position	FDR_Adjusted _P-values	Effect	CandidateGene	Annotation
S07_59366675	7	59366675	4.92E-10	0.21	Sobic.007G158800	Galactolipase
					Sobic.007G158900	SODIUM CHANNEL MODIFIER 1
					Sobic.007G159000	CHAPERONE DNAJ-DOMAIN CONTAINING PROTEIN
					Sobic.007G159100	Tetraspanin family
					Sobic.007G159200	PWWP domain
S09_57212498	9	57212498	9.53E-06	0.12	Sobic.009G231900	SUMO-PROTEIN LIGASE
					Sobic.009G232000	RIBOSOME BIOGENESIS PROTEIN
					Sobic.009G232100	Fasciclin domain
					Sobic.009G232200	Fasciclin domain
					Sobic.009G232266	GLUTAREDOXIN
S01_66709805	1	66709805	0.00284104	-0.11	Sobic.001G378600	RING FINGER DOMAIN-CONTAINING
					Sobic.001G378700	Glutathione peroxidase
					Sobic.001G378800	Fumarate hydratase / Fumarase
					Sobic.001G378900	AP2 domain

Table 3.14 Significant SNPs and candidate genes for LiDAR plant height at 1000GDD identified by GWAS using the FarmCPU model at FDR 0.01. Candidate genes in blue color are mapped to the same position as the dwarfing locus *Dw1*, candidate genes in green color are mapped to the same position as the dwarfing locus *Dw3*.

SNP	Chr.	Position	FDR_Adjusted _P-values	Effect	CandidateGene	Annotation
S09_57212498	9	57212498	2.20E-11	0.17	Sobic.009G231900	SUMO-PROTEIN LIGASE
					Sobic.009G232000	RIBOSOME BIOGENESIS PROTEIN
					Sobic.009G232100	Fasciclin domain
					Sobic.009G232200	Fasciclin domain
					Sobic.009G232266	GLUTAREDOXIN
S07_59366675	7	59366675	3.52E-08	0.19	Sobic.007G158800	Galactolipase
					Sobic.007G158900	SODIUM CHANNEL MODIFIER 1
					Sobic.007G159000	CHAPERONE DNAJ-DOMAIN CONTAINING PROTEIN
					Sobic.007G159100	Tetraspanin family
					Sobic.007G159200	PWWP domain
S07_61080813	7	61080813	3.93E-07	0.15	Sobic.007G176900	BETA-GALACTOSIDASE 11-RELATED
					Sobic.007G177000	L-ASCORBATE PEROXIDASE 3, PEROXISOMAL

Table 3.14 continued

					Sobic.007G177100	MYB-LIKE DNA-BINDING PROTEIN
					Sobic.007G177150	-
S07_59768820	7	59768820	0.000535332	0.14	Sobic.007G163300	-
					Sobic.001G378500	RING FINGER DOMAIN-CONTAINING
S01_66681653	1	66681653	0.000535332	-0.12	Sobic.001G378550	-
					Sobic.001G378600	RING FINGER DOMAIN-CONTAINING
					Sobic.006G068700	ALPHA/BETA HYDROLASE FOLD-CONTAINING PROTEIN
					Sobic.006G068800	Dihydrolipoyllysine-residue acetyltransferase / Transacetylase X
S06_43189859	6	43189859	0.00728713	0.14	Sobic.006G068900	-
					Sobic.006G069000	FERREDOXIN-3, CHLOROPLASTIC
					Sobic.001G485200	AP2-LIKE ETHYLENE-RESPONSIVE TRANSCRIPTION FACTOR AIL1
S01_75602579	1	75602579	0.00764457	0.10	Sobic.001G485300	transcription initiation factor TFIIE subunit beta (TFIIE2, GTF2E2, TFA2)

3.5 Discussion

3.5.1 The sorghum diversity testcrosses were competitive in yield with commercial sorghum hybrids

The biomass yields of the sorghum diversity testcrosses (SbDIV TC) evaluated in 2018, 2019, and 2020 ranged from 929 to 3309 g/m^2, 1214 to 2548 g/m^2, and 1061 to 2549 g/m^2, respectively. The larger variation in 2018 may be due to the late fertilizer application after planting that year. In 2019 and 2020, the applied rate of N was a little higher than in 2018, but it was applied about 1 month prior to planting whereas in 2018 it was applied about 1 month after planting. The SbDIV TC hybrids were surprisingly productive compared with commercial hybrids evaluated in multi-environment trials in recent years. Ferraris (1981) reported the total dry biomass yield of sweet sorghum was around 1588 g/m^2 under irrigation at Ayr, North Queensland. Felderhoff et al. (2012) found that the total dry biomass of sweet sorghum population in College Station, TX with irrigation ranged from 734 g/m^2 to 2444 g/m^2 in 2009 and from 417g/m^2 to 2285g/m^2 in 2010. Gill et al. (2014) studied the dry biomass of six sorghum genotypes (include sorghum-sudan forage hybrid and PS bioenergy hybrid) in seven locations. The range of dry biomass yield at these locations was 399 g/m^2 to 2232 g/m^2 in Kansas, 136 g/m^2 to 2341 g/m^2 in Texas, 435 g/m^2 to 2794

g/m^2 in Kentucky, 372 g/m^2 to 3094 g/m^2 in Mississippi, 807 g/m^2 to 2585 g/m^2 in Iowa, and 526 g/m^2 to 3729 g/m^2 in North Carolina.

3.5.2 Trait heritability and correlation between ground reference traits

Apex height, top collar height, and flowering date of the SbDIV TC exhibited the highest heritability across the three years compared to other agronomic traits. Other studies have reported similar or somewhat lower heritabilities. Sami (2013) reported a heritability of H=0.69 for plant height and H=0.83 days to flowering in a sweet sorghum population. Kenga et al. (2006) reported similar heritabilities for plant height (H = 0.77) and days to anthesis (H = 0.42) in hybrid sorghum.

Heritability for dry biomass yield was somewhat lower (H = 0.5-0.67) than height and flowering time but still higher than reported in many recent studies (Table 3.2). Shiringani and Friedt (2011) reported a broad sense heritability of 0.13 for sorghum dry biomass. Plant height was highly correlated with dry biomass, exhibited higher heritability, and data collection is much easier (Burks et al. 2015; Castro et al. 2015; Fernandes et al. 2018; Monk et al. 1984). Higher heritabilities for these traits indicate they are likely to respond to selection and may provide an indirect selection strategy for biomass yield. Other stem morphology traits were also correlated biomass yields with top collar diameter positively correlated with ADB and base diameter positively correlated with moisture content. Kong et al. (2020) also found a similar relationship between basal stem diameter and rachis diameter (r = 0.56) and positive correlations with stem water content.

3.5.3 Significant SNPs and candidate genes for hybrid sorghum performance

GWAS using the FarmCPU and MLM models provided good control of false positives and supported identification of candidate genes for numerous traits. Taken together, these GWAS studies provide some of the first insights into genes that control hybrid performance since most prior association studies have used populations of inbred sorghum lines.

GWAS for plant height identified nine significant SNPs associated with apex height and six SNPs associated with top collar height on chromosomes 2, 3, 7, 9. The SNP associated with top collar height on chromosome 2 maps to the previously reported plant height QTL *qHGHT2.12*

(Liu et al. 2019). This QTL maps to the same region as the maturity locus *Ma2* (Liu et al. 2019). The *Ma2* gene *(Sobic.002G302700)* affects sorghum maturity and selectively enhances the *Ma1* gene *(Sobic.006G057866)* expression to delay flowering under long days (Casto et al. 2019). Since the plant reached their maximum height after flowering, flowering time would affect vegetative growth, the flag leaf appearance and plant height (Ciampitti and Prasad 2020).

The SNPs associated with apex height and top collar height on chromosome 3 maps to the same region as the plant height QTLs *qHGHT3.5* (Hart et al. 2001) and *qHGHT3.4* (Phuong 2013). The SNP and candidate genes *Sobic.007G158800, Sobic.007G158900, Sobic.007G159000, Sobic.007G159100,* and *Sobic.007G159200* on chromosome 7 associated with apex plant height map to the same position as plant height QTLs *qHGHT7.62* (Zhang et al. 2015) and *qHGHT7.91* (Liu et al. 2019). Candidate genes *Sobic.007G163300, Sobic.007G166600, Sobic.007G166701, Sobic.007G166800,* and *Sobic.007G166900* were reported as plant height QTL *qHGHT7.45* (Pereira and Lee 1995), *qHGHT7.46* (Madhusudhana and Patil 2013), *qHGHT7.62* (Zhang et al. 2015), *qHGHT7.76* (Yamaguchi et al. 2016), *qHGHT7.83* (Girma et al. 2019), *qHGHT7.91* and *qHGHT7.92* (Liu et al. 2019), *qHGHT7.93*, *qHGHT7.95*, *qHGHT7.96* and *qHGHT7.97* (Marla et al. 2019). These QTLs map to the same position as the dwarfing locus *Dw3* (Karper 1932). The *Dw3* gene (*Sobic.007G163800*) is orthologous to *brachytic2* in maize and encodes an MDR transporter that plays a role in polar auxin transport, hence influencing cell elongation and plant height (Multani et al. 2003). *Dw3* affects height by reducing the lengths of lower internodes by decreasing cell lengths (Multani et al. 2003). In this study, the *Dw3* locus showed a strong association with apex height, top collar height, and biomass yield. The other SNPs associated with apex plant height on chromosome 7 were previously reported as QTLs *qHGHT7.2* (Wang et al. 2014) and *qHGHT7.3* (Shiringani et al. 2010). The SNPs associated with plant height on chromosome 9 map to the same positions as previously reported as plant height QTLs *qHGHT9.10* (Lin et al 1995); *qHGHT9.64* and *qHGHT9.65* (Zhang et al. 2015); *qHGHT9.20, qHGHT9.21, qHGHT9.29, qHGHT9.30, qHGHT9.45* and *qHGHT9.46* (Felderhoff et al. 2012); *qHGHT9.16* and *qHGHT9.31* (Takai et al. 2012); *qHGHT9.12* and *qHGHT9.19* (Wang et al. 2014); and *qHGHT9.81* (Boyles et al. 2017). These SNPs and QTL map to the same position as the *Dw1* locus (Yamaguchi et al. 2016). The *Dw1* gene plays a role in the brassinosteroid signaling pathway and reduce cell proliferation activity in the internodes, hence influencing plant height (Yamaguchi et al. 2016).

GWAS for LiDAR plant height at 600GDD identified SNPs located on chromosomes 5, 7, 9. The SNPs and candidate genes identified on chromosome 5 map to the previously reported QTLs *qDMGR5.13* and *qDMGR5.14*, which are related to the initial dry matter growth rate (Fiedler et al. 2016). SNPs and candidate genes identified on chromosome 7 map to the same region as *Dw3* (Karper 1932; Multani et al. 2003). The SNPs on chromosome 9 map to the *Dw1* locus (Yamaguchi et al. 2016). SNPs for LiDAR plant height at 800GDD are located on chromosomes 1, 7, 9. Candidate genes identified on chromosome 1 are *Sobic.001G378600, Sobic.001G378700, Sobic.001G378800*, and *Sobic.001G378900* and map to the same position as previously reported QTL *qSLIN1.1*, which is related to stem internode length (Hilley et al. 2016); *qDTFL1.25* (Mace et al. 2013), *qDTFL1.26* (Srinivas et al. 2009), *qDTFL1.27* (El Mannai et al. 2011), and *qDTFL1.65* (Guindo et al. 2019). Candidate genes on chromosomes 7 and 9 map to *Dw1* and *Dw3*. SNPs for LiDAR plant height at 1000GDD are located on chromosomes 1, 6, 7, 9. Candidate genes on chromosome 1 are *Sobic.001G485200* and *Sobic.001G485300* and map to previously reported height QTLs *qHGHT1.16* (Kebede et al. 2001), *qHGHT1.17* (Wang et al. 2014), and *qHGHT1.18* (Lin et al. 1995). Candidate genes on chromosomes 7 and 9 map to *Dw1* and *Dw3*.

Biomass productivity is the most important trait for many sorghum breeding programs (Gill et al. 2014; Pfeiffer et al. 2019; de Oliveira et al. 2020) and is affected by numerous traits, such as plant height (Wilson and Eastin 1982; van Oosterom and Hammer 2008; George-Jaeggli et al. 2011; Olson et al. 2012), days to flowering (Rooney et al. 2007; Olson et al. 2012; Murphy et al. 2014; Meki et al. 2017), and leaf morphology (Sieglinger 1936; Rooney et al. 2007; Olson et al. 2012; Gill et al. 2014; Truong et al. 2017). The candidate genes associated with biomass yield mapped to chromosomes 1, 3, 5, 7, 8, and 9. Candidate genes *Sobic.001G258200,* and *Sobic.001G258300* map to the same region as previously reported in height QTLs *qHGHT1.5* (Hart et al. 2001) and *qHGHT1.6* (Nagaraja Reddy et al. 2013); and in stem dry weight QTL *qSDWT1.1* (Kapanigowda et al. 2014). Candidate genes *Sobic.003G268900, Sobic.003G269000, Sobic.003G269100,* and *Sobic.003G269200* map to the same regions of chromosome 3 as previously reported plant height QTLs *qHGHT3.11* (Lin et al. 1995), *qHGHT3.17* (Bai et al. 2017), and *qHGHT3.14* (Phuong et al. 2013); days to flowering QTLs *qDTFL3.22* (Feltus et al. 2006) and *qDTFL3.37* (Guindo et al. 2019); green leaf area QTL *qGLFA3.9* (Rama Reddy et al. 2014); leaf number QTL *qLNUM3.6* (Nagaraja Reddy et al. 2013); leaf width QTLs *qLFWD3.2* and

qLFWD3.3 (Shehzad and Okuno 2015); grain weight QTL *qGWGT3.17* (Liu et al. 2019), and tiller number QTL *qTNUM3.8* (Kong et al. 2014). Candidate genes *Sobic.005G180700, Sobic.005G180800, Sobic.005G180850, Sobic.005G180900, Sobic.005G181000,* and *Sobic.005G181100* map to the same regions of chromosome 5 as previously reported in grain yield QTLs *qGYLD5.5* (Gelli et al. 2016) and *qGYLD5.7* (Guindo et al. 2019). Candidate genes *Sobic.007G176900, Sobic.007G177000, Sobic.007G177100,* and *Sobic.007G177150* map to the same regions of chromosome 7 as previously reported dry stem biomass QTL *qTDBM7.6* (Murray et al. 2008); plant height QTLs *qHGHT7.59, qHGHT7.60* and *qHGHT7.62* (Zhang et al. 2015), *qHGHT7.91* and *qHGHT7.92* (Liu et al. 2019), *qHGHT7.45* (Pereira and Lee 1995), *qHGHT7.46* (Madhusudhana and Patil 2013), *qHGHT7.76* (Yamaguchi et al. 2016), *qHGHT7.83* (Girma et al. 2019), *qHGHT7.93, qHGHT7.95, qHGHT7.96,* and *qHGHT7.97* (Marla et al. 2019). These candidate genes and QTL all map to the *Dw3* locus that has a major effect on plant architecture and productivity (Multani et al., 2003). Candidate genes *Sobic.008G158666, Sobic.008G158732, Sobic.008G158800, Sobic.008G158900,* and *Sobic.008G159000* map to the same region on chromosome 8 as previously reported in grain yield QTL *qGYLD8.4* (Felderhoff et al. 2012), height QTL *qHGHT8.4* (Shehzad and Okuno 2015), and stem and leaf fresh weight QTL *qFBMS8.1* (Guan et al. 2011). Candidate genes *Sobic.009G189400, Sobic.009G189501, Sobic.009G189600,* and *Sobic.009G189700* map to the same region of chromosome 9 as previously reported in plant height QTLs *qHGHT9.10* (Lin et al. 1995), *qHGHT9.64* and *qHGHT9.65* (Zhang et al. 2015), *qHGHT9.20* (Felderhoff et al. 2012); grain yield QTL *qGYLD9.11* (Sabadin et al. 2012), and vegetative dry biomass QTL *qTDBM9.1* (Felderhoff et al. 2012). These SNPs and QTL map to the previously described *Dw1* locus (Yamaguchi et al. 2016).

GWAS for base stem diameter discovered candidate genes on chromosomes 7 and 8. On chromosome 7, candidate genes *Sobic.007G011500, Sobic.007G011600,* and *Sobic.007G011700* were identified for both base diameter and flowering time and map to the same positions as previously reported in QTLs *qTNUM7.1, qBRPN7.2,* and *qTNUM7.2* related to tiller number (Kong et al. 2014) and *qDTFL7.2, qDTFL7.3, qDTFL7.4* (Wang et al. 2014) and *qDTF7.1* (Mace et al. 2013) related to days to flowering. The candidate gene *Sobic.007G011500* belongs to a family of auxin receptors and contains an F-box domain (Dharmasiri et al. 2005). Auxin appears to be a multi-function trigger in different plant developmental stages, such as shoot and flower development (Vanneste and Friml 2009). This may explain why this candidate gene was identified

for base diameter and FL. Candidate genes for base diameter on chromosome 8 include *Sobic.008G010500, Sobic.008G010600, Sobic.008G010700, Sobic.008G010750,* and *Sobic.008G010800*. These candidate genes map to the same regions as QTLs *qBRPN8.1, qTNUM8.2, qTNUM8.3, qTNUM8.4,* and *qTNUM8.5* related to tiller number (Kong et al. 2014). Previous studies found that auxin from the shoot apical meristem inhibits the outgrowth of axillary buds of tillers, while acropetal movement of cytokinin promotes the outgrowth of tiller buds (Beveridge 2006; Ongaro et al. 2008). Between main stem and tillers, there is a competitive relationship in nutrient and biomass partitioning. Narrow main stems were associated with high tiller numbers (Alam et al. 2014). This suggests that stem diameter is affected by plant hormones and hence the tiller numbers.

Candidate genes for flowering time were located on chromosomes 1, 6, 7, and 9. Candidate genes *Sobic.001G512000, Sobic.001G512100,* and *Sobic.001G512200* from chromosome 1 map to the same position as QTL for days to flowering *qDTFL1.45* (Bangbol Sangma 2013) and *qDTFL1.64* (Cuevas and Prom 2020). On chromosome 6, candidate genes *Sobic.006G051700, Sobic.006G051750,* and *Sobic.006G051800* map to the same position as flowering time QTLs *qDTFL6.12* (Wang et al. 2014); *qDTFL6.64* and *qDTFL6.65* (Zhang et al. 2015); *qDTFL6.71, qDTFL6.73, qDTFL6.69* (Sukumaran et al. 2016); *qDTFL6.13* (Mace et al. 2013), and *qDTFL6.83* (Cuevas et al. 2016). Candidate genes for flowering time on chromosome 9 include *Sobic.009G251400, Sobic.009G251500, Sobic.009G251600,* and *Sobic.009G251700* and map to flowering time QTLs *qDTFL9.33* and *qDTFL9.34* (Zhang et al. 2015); *qDTFL9.29* and *qDTFL9.30* (Nagaraja Reddy et al. 2013); *qDTFL9.24, qDTFL9.25, qDTFL9.26, qDTFL9.27* and *qDTFL9.28* (Higgins et al. 2014). Although the genes and gene functions that control flowering time in sorghum are not yet clear, genes controlling flowering time of sorghum hybrids appear to be largely consistent with genes controlling flowering timing in inbred lines.

Moisture content is related to multiple physiological mechanisms and can be affected by many genes and environmental factors (Han et al. 2015; Murray et al. 2008). Candidate genes identified for moisture content were located on chromosomes 3, 4, 5, 8, and 9. Candidate genes on chromosome 3 include *Sobic.003G295400, Sobic.003G295500, Sobic.003G295600, Sobic.003G295700, Sobic.003G295800, Sobic.003G295900,* and *Sobic.003G296000* and map to the same genomic region as stay-green QTL *Stg1* (Xu et al. 2000). These candidate genes also map to QTL for chlorophyll content *qSTGR3.1* and *qCHLC3.12* (Xu et al. 2000) and *qCHLC3.11*

(Rama Reddy et al. 2014). Candidate genes for moisture content on chromosome 4 include *Sobic.004G188600, Sobic.004G188701, Sobic.004G188800,* and *Sobic.004G188900* and map to the same region as QTL for juice weight *qJYLD4.2* (Guan et al. 2011); stay green *qSTGR4.3* (Kebede et al. 2001); transpiration rate *qLFTE4.9* (Ortiz 2017), and stomatal conductance *qSTCD4.1* (Ortiz et al. 2017). Candidate genes *Sobic.005G131400, Sobic.005G131500, Sobic.005G131550,* and *Sobic.005G131600* on chromosome 5 map to the stay-green QTLs *Stg4* (Xu et al. 2000), *qSTGR5.3* (Subudhi 2000), and *qSTGR5.5* (Kebede et al. 2001). Candidate gene *Sobic.008G105432* on chromosome 8 maps to the same positions as QTL for transpiration rate *qLFTE8.1, qLFTE8.2, qLFTE8.59, qLFTE8.60, qLFTE8.3, qLFTE8.4, qLFTE8.28, qLFTE8.29, qLFTE8.5, qLFTE8.6, qLFTE8.7, qLFTE8.8, qLFTE8.9, qLFTE8.10,* and *qLFTE8.11* and QTL for stomatal conductance *qSTCD8.14, qSTCD8.15, qSTCD8.16, qSTCD8.23,* and *qSTCD8.24* (Ortiz et al. 2017). Candidate genes *Sobic.009G241300, Sobic.009G241400, Sobic.009G241500, Sobic.009G241600, Sobic.009G241700,* and *Sobic.009G241801* map to the same position as *Dw1* and QTL *qHGHT9.10* related to plant height (Lin et al. 1995). These candidate genes also map to the same position as QTL for transpiration rate *qLFTE9.9*, stomatal conductance *qSTCD9.2* (Ortiz et al. 2017), and juice yield *qJYLD9.2* (Felderhoff et al. 2012). One of the candidate genes for moisture discovered using the MLM model on chromosome 6 was *Sobic.006G147450*, which is 3.96kb downstream from the Dry stalk (*D*) locus (Sobic.006G147400) (Zhang et al. 2018) (Table B.4). The *D* locus conditions a white and dry stem by a dominant allele (*D*-), while green and juicy stem by recessive genotypes (*dd*) (Smith and Frederiksen 2000). Another GWAS study in sweet sorghum mapped QTL with a significant effect for juice volume and stalk moisture on *D* locus (Burks et al. 2015). Since the female parent Tx623 carries the recessive green midrib allele (*d*) (Xia et al. 2018), we can evaluate which male parents carry the dominant allele (*D*-). These results verify earlier studies that moisture is influenced by QTLs with diverse functions and multiple physiological mechanisms.

Many identified candidate genes in this study are also reported in previous published QTLs with similar functions; this supports the power of the method for gene discovery that was used in this study. We also identified many other candidate genes with unknown functions and not previously reported in other publications.

3.5.4 Trait heritability and significant SNPs for LiDAR plant height

The average heritability of LiDAR height across 400, 600, 800, and 1000GDDs are 0.66, 0.95, 0.97, and 0.96. Higher heritability occurs in the later growing season of all three years. Campbell et al. (2019) found that shoot growth of rice is dynamic and changes throughout growth stages. Genes controlling plant height in maize were also reported to be time-dependent with varying contributions over time (Anderson et al. 2020). GWAS for LiDAR plant height revealed a similar pattern in sorghum with four, three, and seven SNPs identified at 600GDD, 800GDD, and 1000GDD, respectively (Figure 3.5). No significant SNPs were identified at 400GDD, perhaps reflecting the narrow range of variation in plant height observed during the earlier vegetative period. Some of the SNPs were significant for a particular time point and other SNPs were significant across time points. For example, S07_59366675, a marker for *Dw3*, was significant at 600GDD, 800GDD, and 1000GDD but had the largest effect at 800GDD, corresponding to the early flowering period. *Dw3* is a polar auxin transporter that impacts cell elongation (Multani et al. 2003). In contrast, the effects of S09_57212498, representing *Dw1*, increased over time with the largest effect at 1000GDD. *Dw1* plays a role in brassinosteroid signaling (Yamaguchi et al. 2016). These results demonstrate that plant height is dynamic with relative differences in plant height controlled by different genes at different stages of development.

3.5.5 Favorable and rare alleles for hybrid sorghum biomass productivity

Biomass accumulation is an important agronomic trait for many breeding programs. However, low heritability causes difficulty in biomass simulation and selection in breeding populations. This study revealed that height is highly correlated with biomass and has high heritability. Incorporating variation in plant height into biomass predictions may offer more accurate results. This could benefit bioenergy sorghum breeding programs in biomass improvement based on indirect selection. For bioenergy breeding programs, canopy development, juice yield, flowering time, stem diameter and moisture represent other key traits. However, not many publications evaluate these traits. The results of this chapter provide insight into trait correlations and information on candidate genes that may contribute to understanding the relationship between these agronomic traits in hybrids. Kong et al. (2020) reported similar results

with co-localizations between certain biomass-related traits. This may reveal that the inheritance of these traits may be functionally or physically linked.

Genetic diversity is the life blood of plant breeding programs. New genes and alleles must be continuously infused into the elite gene pool to support long term improvement of a crop. In this study, seven different genetic loci were discovered that influence biomass accumulation with the minor or uncommon allele exhibiting positive affects at three of these genetic loci. In this scenario, the minor allele is the favorable allele. The minor allele frequencies for S07_59768820, S07_61080813, and S08_59178415 were 0.18, 0.18, and 0.35, respectively. Since there were 619 hybrids in the population, there were around 111 hybrids with a favorable allele at the S07_59768820 and S07_61080813, plus around 217 hybrids with a favorable allele at the S08_59178415. Other SNPs with significant minor allele associations with biomass accumulation are S01_ 74145303, S09_56521150, S06_2686264, and S02_2417641 with minor allele frequencies of 0.12, 0.31, 0.03, and 0.04, respectively (Table B.6). These unique genes and alleles may play an important role in population improvement. More work is needed to introduce these genetic resources into our population to diversify the gene pool and increase the favorable allele frequency for biomass accumulation.

In the sorghum diversity panel, Dwarf Yellow Milo exhibited minor and favorable alleles at the S02_2417641, S07_59768820, S07_61080813, and S08_59178415 and Spur Feterita exhibited the minor and favorable alleles at S01_74145303, S06_2686264, S07_59768820, S07_61080813, S08_59178415, and S09_56521150. These genotypes may represent unique genetic resources for future population improvement efforts.

3.6 Conclusion

This study provided one of the first comprehensive assessments of genes controlling biomass productivity in hybrid sorghum. Some genes and trait correlations were known from prior studies. *Dw1* and *Dw3* were associated with apex height, top collar height, and ADB. The maturity gene *Ma2* was associated with variation in top collar height. Genes for moisture content mapped to stay-green loci *Stg1* and *Stg4* and to the Dry (D) locus. Many other SNP markers and candidate genes were not previously reported. GWAS for LiDAR plant height demonstrated that some SNPs associated with final plant height may not contribute to variation in the early growing season and exhibit a temporal-dependency. Genetic mapping studies for biomass yield indicated that some

favorable alleles exhibit low frequencies in the sorghum germplasm collections suggesting future targets for genetic selection. Dwarf Yellow Milo and Spur Feterita exhibited favorable alleles for multiple SNPs for biomass yield and are unique resources for future sorghum crop improvement.

CHAPTER 4. ESTIMATING SEASONAL RADIATION USE EFFICIENCY IN SORGHUM USING BIOMASS AND TIME-DEPENDENT MEASUREMENTS OF CANOPY COVER AND DAILY RADIATION

4.1 Abstract

The APSIM crop growth model can simulate sorghum biomass based on biophysiological information, such as radiation use efficiency (RUE). However, the parameterization of APSIM is challenging due to difficulties in acquiring radiation interception for calculating RUE, especially in large breeding populations. With the development of UAV-based RGB imaging systems, radiation interception can be efficiently derived based on measurements of canopy cover. Using time-series canopy cover and daily radiation coupled with end-of-season biomass, we proposed a simple model for estimating seasonal radiation use efficiency (SRUE). Studies of commercial sorghum hybrids showed that estimates of SRUE were highly coorelated with estimates of maximum RUE used in APSIM. Analyses of SRUE in 619 genetically diverse sorghum hybrids indicated heritabilities of 0.45, 0.51 and 0.63 in 2018, 2019 and 2020, respectively. Genome wide association studies identified 11 single-nucleotide polymorphisms (SNPs) that were associated with SRUE using a fixed and random model circulating probability unification model. These SNPs mapped to previously reported quantitative trait loci related to leaf angle, green leaf area, leaf chlorophyll content and fluorescence, the efficiency of energy captured by open PSII reaction centers, leaf senescence, plant height, tiller number, vegetative dry biomass, dry matter growth rate, and days to flowering. Moreover, the positive effect alleles for seven of these SNPs were present at low frequencies in the sorghum diversity panel, which suggests that changing the frequency of these alleles could improve SRUE in the population. The proposed model for calculating SRUE may be useful in parameterizing biophysical crop models like APSIM for simulating sorghum biomass in large breeding populations.

4.2 Introduction

Agronomically important traits of bioenergy sorghum were evaluated to identify candidate genes that drive biomass accumulation in Chapter 3. Genome wide association studies (GWAS) for LiDAR plant height provided a glimpse of the underlying time-dependency for developmental

characteristics; however, the rest of the traits evaluated in that study were based on end-of-season performance with little insight into the biophysical bases for observed differences in productivity.

Bioenergy sorghums produce more leaves and a larger amount of stem biomass than other sorghum types. The higher leaf area increases the radiation interception and radiation use efficiency (RUE) resulting in more than twice the biomass of grain sorghum (Olson et al. 2012). The biomass yield of a crop is determined by the sum of radiation interception by its green leaf area through the growing season and the efficiency with which radiant energy is converted to dry matter in an environment without water stress (Monteith et al. 1977; Muchow 1989). The ratio of green leaf area is an estimation of radiation interception of crop canopy, and the slope of the regression line of biomass versus accumulated intercepted radiation is defined as RUE (Cooper 1970; Sinclair and Muchow 1999). RUE is an important trait for biomass simulation since it quantifies the radiation captured by the crop and the efficiency of the crop to fix carbon without stress (Hatfield and Dold 2019). Improving RUE is one of the promising approaches to increase potential biomass yield (Asseng et al. 2019). The relationship between improving RUE and increasing biomass was found in wheat (Shearman et al. 2005a; Aisawi et al. 2015), maize (Luque et al. 2006; Messina et al. 2009), and sorghum (Curt et al. 1998; Borrell et al. 2021).

Variation in the RUE of 18 commercial sorghum hybrids was reported in Chapter 2. The RUE of the five types of sorghum ranged from 0.97 g MJ^{-1} to 1.7 g MJ^{-1} with forage sorghums and photoperiod sensitive sorghums exhibiting higher RUE than grain sorghums. This reveals that RUE is a genotype-specific trait and can be an input parameter for biomass simulation. The APSIM model is a good tool to dissect the components of biomass. Remote sensing was integrated into the steps for parameterizing the crop growth model and was successfully applied in biomass sorghum simulation in different environments in the United States (Yang et al. 2021). Other approaches that combine genetic information and crop growth models also perform well in simulation of multi-environment trials (Chapman et al. 2003; Löffler et al. 2005; Cooper et al. 2016; Meki et al. 2017; Cooper et al. 2020; Pokhrel et al. 2021). However, it is difficult to parameterize crop growth models for large breeding populations because the calculation of input parameters for RUE is complex with calculations involving daily LAI, canopy cover, daily radiation, k, and biomass harvested at multiple time points. RUE is measured at a canopy scale and is related to photosynthesis (McGrath and Long 2014), respiration, dry matter partitioning, canopy architecture (Sinclair and Muchow 1999; George-Jaeggli et al. 2013), vertical distribution

of radiation and N (Dreccer et al. 2000), dry matter assimilation rate and leaf nitrogen concentration (Sinclair and Horie 1989; Sinclair and Muchow 1999).

Furbank et al. (2019) suggested that since current methods for estimating RUE are laborious, new techniques such as predictive models based on remote sensing features may be used to estimate the complex canopy-related traits. Chapman and Edmeades (1996) introduced a method for estimating seasonal RUE based on radiation interception and final biomass of tropical maize. Since the RUE represents the sum of many sub-traits that play a role in photosynthetic performance, dividing biomass accumulation by the sum of radiation intercepted during the growing season could be used to estimate the seasonal RUE of a crop (Murchie et al. 2018). Nevertheless, measuring canopy photosynthetic capacity rapidly and frequently on hundreds of germplasm entries in a breeding population is virtually impossible and estimates of canopy cover and RUE have not been a major focus of cereal breeding programs (Murchie et al. 2018).

Field-based high-throughput phenotyping approaches may provide a solution for easily obtaining canopy structure traits. This approach relies on remote sensing to record spectral and/or geometric plant features throughout the growing season (White et al. 2012). RGB imaging is widely used for measuring plant morphological traits related to yield (Großkinsky et al. 2015) since it is reliable, inexpensive, and relatively simple in data processing (Zhao et al. 2019). RGB imaging from UAV platforms provides an efficient method to evaluate time-dependent traits such as canopy cover (Pauli et al. 2016). This approach has been successfully used in diverse crops including soybean (Hoyos-Villegas et al. 2014), wheat (Duan et al. 2016), rice (Guo et al. 2017), and maize (Zhou et al. 2019).

Compared with the other cereal crops, there are fewer publications that report canopy structure in bioenergy sorghum; however, a well-developed data acquisition and processing pipeline has been developed for RGB imaging through UAV systems to extract canopy cover of bioenergy sorghum (Chen et al. 2017; Ribera et al. 2018). Using these systems, it is now possible to acquire canopy cover at multiple time points for hundreds of genotypes throughout the growing season and use these data to calculate seasonal RUE.

Genome-wide association study (GWAS) is an approach to identify genomic differences and discover statistical associations between genetic and phenotypic variations (Myles et al. 2009). GWAS have been successfully implemented in recognizing marker and trait associations in multiple cereal crops including rice (Huang et al. 2012), barley (Cockram et al. 2010), wheat

(Neumann et al. 2011; Sukumaran et al. 2015), maize (Tian et al. 2011), and sorghum (Sukumaran et al. 2012; Morris et al. 2013). The Fixed and random model circulating probability unification (FarmCPU) model for GWAS uses the associated markers to define kinship to avoid over-fitting and resulting in higher statistical power compared with other existing methods (Liu et al. 2016; Habyarimana et al. 2020; Wang et al. 2020; Kavuluko et al. 2021).

In this study, we explore the use of simplified crop models for estimating seasonal radiation use efficiency (SRUE) in large-scale sorghum breeding populations. Specific objectives that were addressed in this study include (1) estimation of SRUE using time-dependent measurements of canopy cover and daily radiation coupled with end-of-season biomass, (2) validation of our new SRUE method with inputs used in APSIM, (3) quantification of heritability and stability of SRUE over seasons, and (4) conducting GWAS for SRUE in sorghum germplasm collections. Comparing the candidate genes for canopy cover and SRUE discovered in this study with reported QTLs provided insight into the bases for variation in SRUE.

4.3 Materials and methods

4.3.1 Genotypes and field management

Selected sorghum parent lines and inbred lines from the sorghum conversion program (Rosenow et al. 1997; Stephens et al. 1967) were used to represent the genetic diversity of sorghum (Hayes et al. 2015). These inbred lines were crossed to the tester ATx623 to create a population of 619 half-sib sorghum hybrids. This population of F1 hybrids was grown in 2018, 2019 and 2020 at the Agronomy Center for Research and Education (ACRE) of Purdue University in West Lafayette, IN, USA. Field trials were conducted each year using a randomized complete block design with two replicates. The plant materials were evaluated in 4-row plots with 0.76 m spacing between rows with 3.05 m long. Seeds were sown on 8 May in 2018, 4 June 2019 and 12 May 2020 with a planting rate at 22 plants/m^2. Aboveground dry biomass (ADB) measurements and the field fertilizer programs were described in Chapter 3.

4.3.2 Molecular background

The molecular markers used in Chapter 3 and 4 were the same. More detailed information of the genetic structure of the inbred lines can be found in Griebel et al. (2021).

4.3.3 Remote-sensing data collection

UAV platforms were used to collect multi-modal and multi-temporal remote sensing data in field trials conducted in 2018, 2019, and 2020 as described in Masjedi et al. (2020) (Figure 4.1). In 2018, data were collected using a DJI Matrice M600 Pro UAV as a platform, equipped with an APX-15 V2 as the GNSS (Global Navigation Satellite System)/INS (Inertial Navigation System) unit for direct geo-referencing. Images were collected using a Sony Alpha 7R (ILCE-7R) camera with a Sony 35-mm lens at a height of 50 m, resulting in a ground sampling distance of 0.7 cm. Geometric calibration of the imaging systems were performed by methods described in Ravi et al. (2018b). The RGB images were collected in 2018 on May 16 (8 DAS), May 22 (14 DAS), May 29 (21 DAS), June 4 (27 DAS), June 11 (34 DAS), June 20 (43 DAS), June 27 (50 DAS), July 2 (55 DAS), July 10 (63 DAS), July 18 (71 DAS), July 23 (76 DAS), and Aug 1 (85 DAS).

Figure 4.1 Unmanned aerial vehicle (UAV) used in this study. This system acquired hyperspectral, LiDAR, and RGB image. We use RGB data in this study.

RGB images were collected in 2019 and 2020 using a DJI Matrice M600 Pro UAV as a platform, equipped with an APX-15 V3 as the GNSS (Global Navigation Satellite System)/INS (Inertial Navigation System) unit for direct geo-referencing. Images were collected using a Sony Alpha 7R III (ILCE-7R) camera with a Sony 35-mm lens at a height of 44 m, resulting in a ground sampling distance of 0.6 cm. System calibration was performed as described previously. The RGB images were collected in 2019 on June 14 (10 DAS), June 18 (14 DAS), June 26 (22 DAS), July 12 (38 DAS), July 23 (49 DAS), August 2 (59 DAS), August 10 (67 DAS), August 24 (81 DAS), and September 5 (93 DAS). RGB images were taken in 2020 on June 6 (25 DAS), June 12 (31

DAS), June 19 (38 DAS), June 25 (44 DAS), July 2 (51 DAS), July 8 (57 DAS), July 20 (69 DAS), July 25 (74 DAS), July 28 (77 DAS), August 6 (86 DAS), August 13 (93 DAS).

Orthomosaics were obtained using a modified Structure from Motion (SfM) strategy that is conducive to high throughput phenotyping, as introduced Hasheminasab et al. (2020). Since the row segments at the image border suffer more lens and perspective distortion than the row segments at the center of the photo, the photos where the plot is closest to the center of the image were used for canopy cover estimation. Each row segment was defined by a rectangle whose dimensions were 0.76 m x 3.05 m on average, and then 0.4 m was trimmed from each end of the row to minimize effects of the alley between plots. The canopy cover was estimated for rows 2 and 3 as the ratio of vegetative to non-vegetative pixels within the box, using segmentation methods described previously (Ribera et al. 2018; Chen 2019) and canopy cover for each plot taken as the average of the two rows.

4.3.4 Statistical analysis

The multiple dates of RGB canopy cover from trials in 2018, 2019, and 2020 were used to calculate SRUE. Spatial correction by row, column, and replicate was conducted based on modelling spatial trends using the two dimensional Penalised spline (P-spline) models through SpATS R-package (Rodríguez-Álvarez et al. 2018). The generalized heritability of traits were calculated using Oakey's methods, which set the genotypes as a random effect in splines through the SpATS R-package (Oakey et al. 2007; Rodríguez-Álvarez et al. 2018).

In SRUE (g/MJ) calculation, the estimation of the fraction of radiation interception (*f*) each day was fitted by a self-start logistic function against time:

$$f = Asym/(1 + e^{(xmid-input)/scal}) \qquad (4.1)$$

Asym, xmid, and scale are parameters determined using the self-start logistic model through the SSlogis function in the R package stats version 3.6.3 (R Core Team 2020). Asym represents the asymptote, xmid represents the input value at the inflection point of the curve, scal represents a scale on the input axis. The radiation intercepted each day was estimated by multiplying the *f* and daily solar radiation (MJ/m^2) from the Epply sensor. SRUE was calculated as end-of-season ADB over the sum of seasonal radiation interception between emergence and harvest. The end-of-season ADB data was described in Chapter 3.

Comparison of the maximum RUE (method of Chapter 2) and SRUE (method of Chapter 4) of commercial sorghum hybrids (Hybcal panel) was conducted to validate the SRUE methodology. The maximum RUE of 18 commercial sorghum hybrids from trials in 2018 were reported in Table 2.2. For SRUE calculation, the RGB canopy cover, daily radiation, and final harvest dry biomass data using the same data set as maximum RUE calculation. The fitted line of SRUE and maximum RUE was estimated by the lm function, and RMSE of fitted values was calculated by the rmse function of the R package stats version 3.6.3 (R Core Team 2020). P-value was used to test the null hypothesis that there is no relationship between the SRUE and maximum RUE with results plotted by the R package ggplot2 (Villanueva and Chen 2019).

After spatial correction, trait correlations between SRUE and ADB over seasons were calculated using the corrplot R-package version 0.90 (Taiyun 2021). Given similarities in response over years, a combined analysis of 2018, 2019, and 2020 was conducted by estimating the best linear unbiased prediction (BLUP) of each genotype using the lmer function in the lme4 R-package (Bates et al. 2015). The mixed linear model for fitting the data was described as formula (3.1) in Chapter 3.

The fitted canopy cover at 400 GDD, 600 GDD, 800 GDD, and 1000 GDD and SRUE values of each hybrid genotype were used as input phenotypes for GWAS using FarmCPU (Liu et al. 2016) with 80,103 SNP markers. GWAS was conducted using the Genomic Association and Prediction Integrated Tool (GAPIT) (Zhang et al. 2010; Lipka et al. 2012; Wang and Zhang 2020). FarmCPU model was selected in GWAS since it uses the associated markers to avoid over-fitting, and has higher statistical power compared with other methods (Liu et al. 2016). The FarmCPU model in GAPIT was run with default settings. Thresholds of significant SNPs were determined using FDR of adjusted p-values at 0.05 (Benjamini and Hochberg 1995). Manhattan plots of GWAS results were created using the R package “qqman” (Turner 2014). Sorghum QTL publications was searched through the Sorghum QTL Atlas (Mace et al. 2019).

4.4 Results

4.4.1 Estimating seasonal radiation use efficiency

The variation in SRUE calculated from RGB canopy cover and aboveground dry biomass in a collection of 619 diverse sorghum hybrids is presented in Figure 4.2. The mean values of the

SRUE of 2018, 2019, and 2020 are 1.35, 1.31, and 1.33 (g/MJ), respectively. Although the three years have a similar median value for RUE, the standard deviation was larger in 2018.

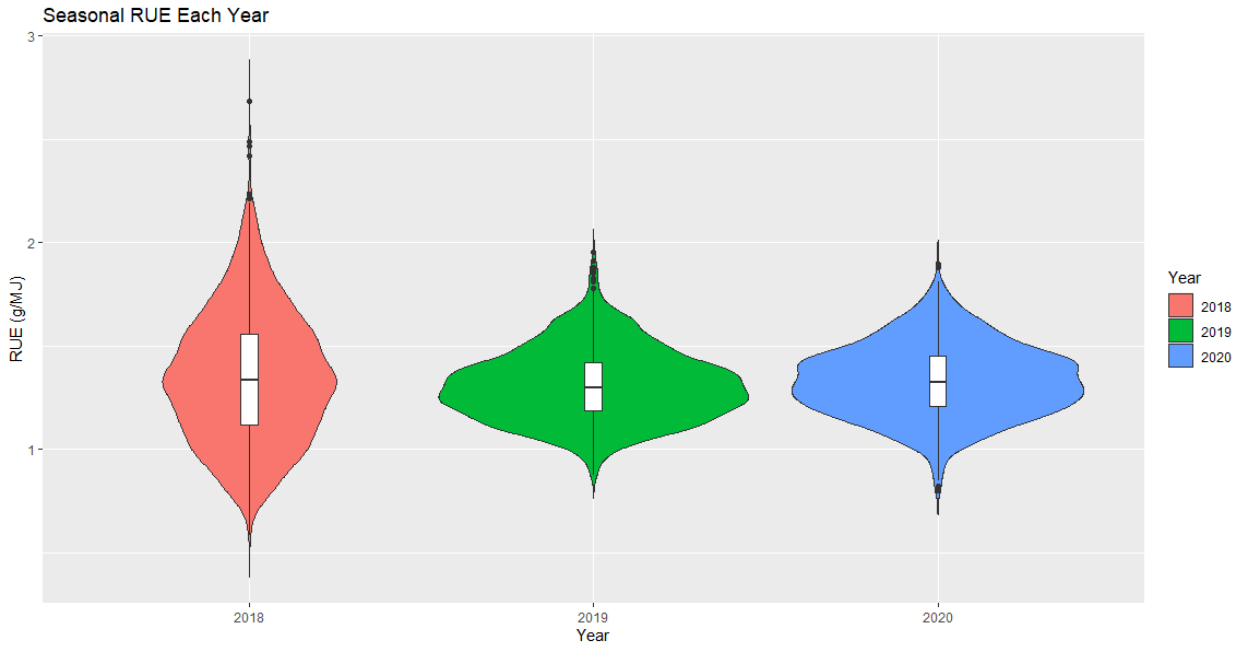

Figure 4.2 Violin plot of SRUE calculated from RGB canopy cover and aboveground dry biomass of 619 sorghum testcross hybrids. The mean and standard deviation of 2018, 2019, and 2020 are 1.35±0.31, 1.31±0.17, and 1.33±0.18, respectively.

4.4.2 Validation using 2018 HybCAL panel

Maximum RUE values were calculated with 18 commercial hybrids as an input parameter for APSIM in Chapter 2. The biophysical crop models for these commercial hybrids exhibited excellent performance; however, the estimation of maximum RUE was complex and required the time-series leaf area index (LAI), extinction coefficient (k), RGB canopy cover, daily radiation, and three ADB data points. Using the SRUE method may be a good alternative for large breeding population such as SbDIV TC since it only requires RGB canopy cover, daily radiation, and end-of-season ADB. The relationships between maximum RUE and seasonal RUE for these 18 commercial sorghum hybrids are shown in Figure 4.3. Maximum and seasonal RUE were highly and positively correlated (r = 0.97) with an RMSE of 0.04 (g/MJ). These data suggest that SRUE may provide a useful approximation for estimating maximum RUE. Given the high-throughput

methodology for estimating canopy cover and ABD, this method will be particularly useful when parameterizing crop models for larger populations of lines or hybrids.

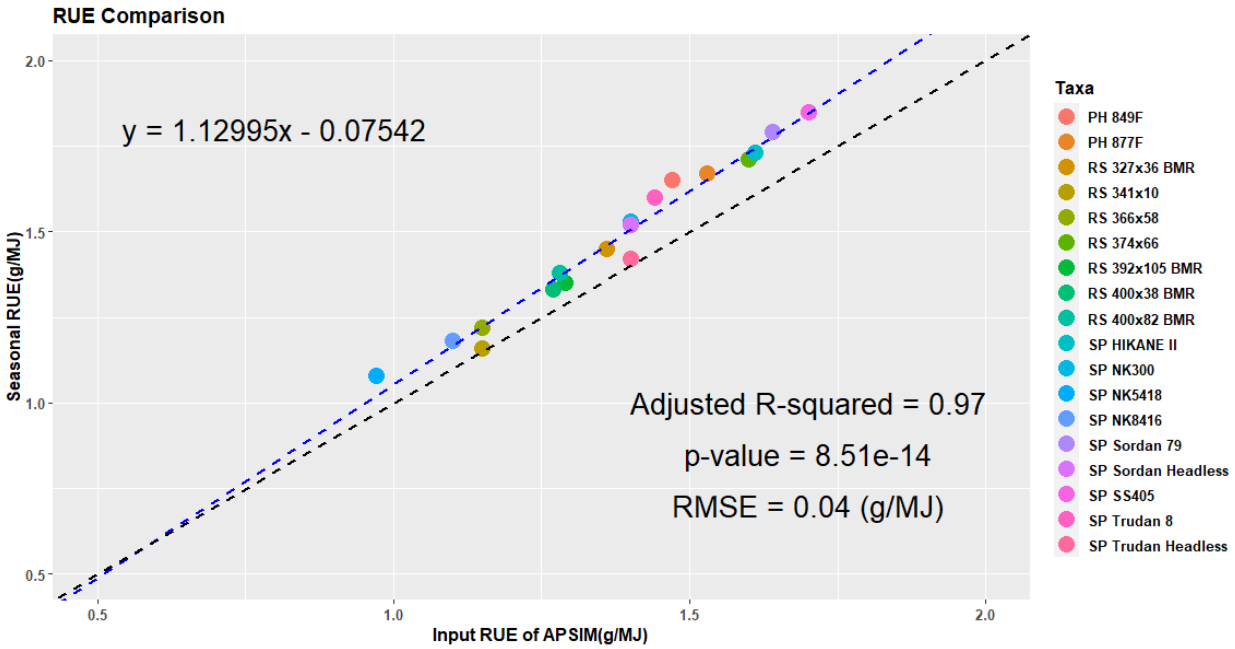

Figure 4.3 Comparison of SRUE calculated from RGB canopy cover and aboveground dry biomass with maximum RUE used as input for APSIM in Chapter 2. The blue dashed line is the fitted line, and the black dashed line is one-to-one line. The P-value tests the null hypothesis that there is no relationship between the two types of RUE.

4.4.3 Heritability of SRUE and biomass yield

The heritability of SRUE and ADB are shown in Table 4.1. The heritability of SRUE ranged from 0.45 to 0.63. Comparisons between heritability of ADB and SRUE show that SRUE is a heritable trait with similar or slightly lower heritability than ADB.

Table 4.1 Heritability of SRUE and ADB through SpATS

	Heritability		
Traits	2018	2019	2020
SRUE	0.45	0.51	0.63

ADB	0.51	0.57	0.67

4.4.4 Correlations between SRUE and ADB

Table 4.2 shows correlations between SRUE and ADB in 2018, 2019, and 2020. The average SRUE was positively correlated with SRUE2018, SRUE2019, and SRUE2020. Average SRUE was also highly correlated with average ADB, ADB 2018, ADB 2019, and ADB 2020. All correlation values were highly significant. These results show that SRUE is stable and exhibits a positive relationship with ADB over seasons.

Hybrid SRUE and ADB values for each line of 2018, 2019, 2020, and the average across three years are shown in Table C.1.

Table 4.2 SRUE and ADB correlation between three hybrid years and the average over years. Avg. is the average of three years for each hybrid.

	ADB 2018	ADB 2019	ADB 2020	Avg. ADB	SRUE2018	SRUE2019	SRUE2020	Avg. SRUE
ADB 2018								
ADB 2019	0.4*							
ADB 2020	0.52*	0.48*						
Avg. ADB	0.85*	0.74*	0.81*					
SRUE2018	0.98**	0.37*	0.49*	0.82*				
SRUE2019	0.33*	0.97**	0.43*	0.68*	0.32*			
SRUE2020	0.48*	0.45*	0.96**	0.77*	0.47*	0.42*		
Avg. SRUE	0.83*	0.73*	0.79*	0.98**	0.83*	0.7*	0.79*	

*Significant at the 0.001 probability level.

**Significant at the 0 probability level.

4.4.5 GWAS for canopy cover and SRUE

GWAS identified significant associations for differences in canopy cover (Figure 4.4) and SRUE (Figure 4.5). Seven SNPs were detected for canopy cover at 600GDD and 13 SNPs were detected for canopy cover at 800GDD. No significant associations for canopy cover were detected at 400GDD when the plants were small and weed and soil reflectance may have resulted in some noise in RGB imaging. No significant SNPs for canopy cover were detected at 1000GDD when the canopy was essentially closed with plants in the grain filling stage. Eleven SNPs were detected

for SRUE (Figure 4.5). A candidate gene search window was set to 15kb upstream and downstream of each significant SNP with FDR of P-value at 0.05. One or more candidate genes were discovered flanking each of the SNPs identified in GWAS. SNP S03_4483384 was significant at both 600GDD (Table 4.3) and 800GDD (Table 4.4) with effects of -1.78 and -0.79, respectively. Four candidate genes were found in the search window including *Sobic.003G048500, Sobic.003G048600, Sobic.003G048700,* and *Sobic.003G048900*. SNP S09_57062019 was significant for canopy cover at 800GDD (Table 4.4) and identified candidate genes *Sobic.009G230000, Sobic.009G230100, Sobic.009G230200, Sobic.009G230300, Sobic.009G230400, Sobic.009G230500, Sobic.009G230600,* and *Sobic.009G230700* in the search window.

Seven SNPs were significant for both SRUE (Table 4.5) and ADB (Table B.6). These SNPs were located on chromosomes 1, 6, 7, 8, and 9. SNP S01_74145303 identified candidate genes *Sobic.001G468400, Sobic.001G468500, Sobic.001G468600,* and *Sobic.001G468700*. SNP S06_2686264 identified candidate genes *Sobic.006G017000, Sobic.006G017100,* and *Sobic.006G017200*. SNP S07_59768820 identified candidate gene *Sobic.007G163300*. SNP S08_2579008 identified candidate genes *Sobic.008G028700, Sobic.008G028800, Sobic.008G028850,* and *Sobic.008G028900*. SNP S08_59178415 identified candidate genes *Sobic.008G158666, Sobic.008G158732, Sobic.008G158800, Sobic.008G158900,* and *Sobic.008G159000*. SNP S09_54144857 identified candidate genes *Sobic.009G189400, Sobic.009G189501, Sobic.009G189600,* and *Sobic.009G189700*. SNP S09_56521150 identified candidate genes *Sobic.009G222200, Sobic.009G222400, Sobic.009G222500,* and *Sobic.009G222600*. Five of the seven SNPs associated with SRUE and ADB show that the minor allele or low frequency allele exhibited the favorable effect on sorghum hybrid performance suggesting opportunities for future crop improvement for SRUE and ADB in sorghum.

A.

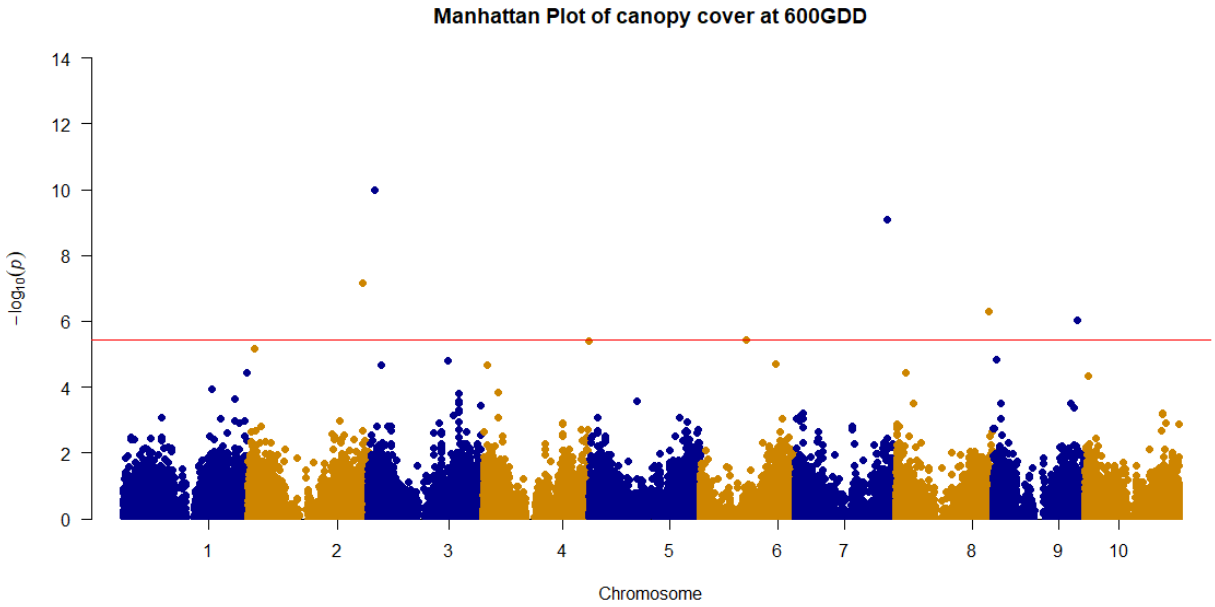

B.

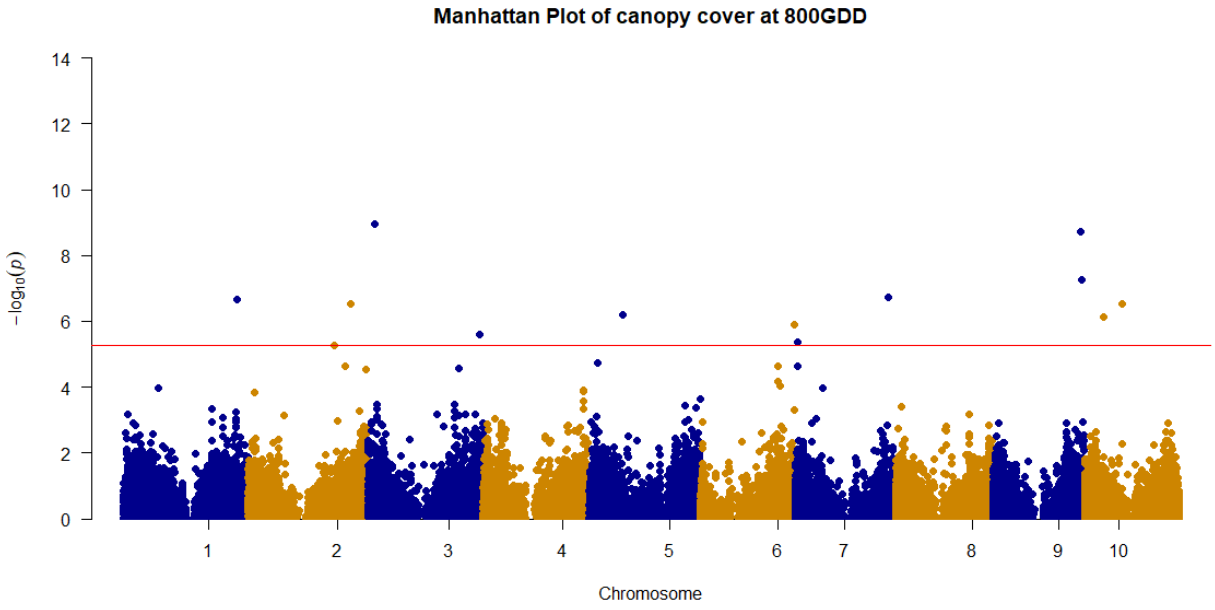

Figure 4.4 Manhattan plot from GWAS for RGB canopy cover in 619 sorghum hybrids at (A) 600GDD, (B) 800GDD.

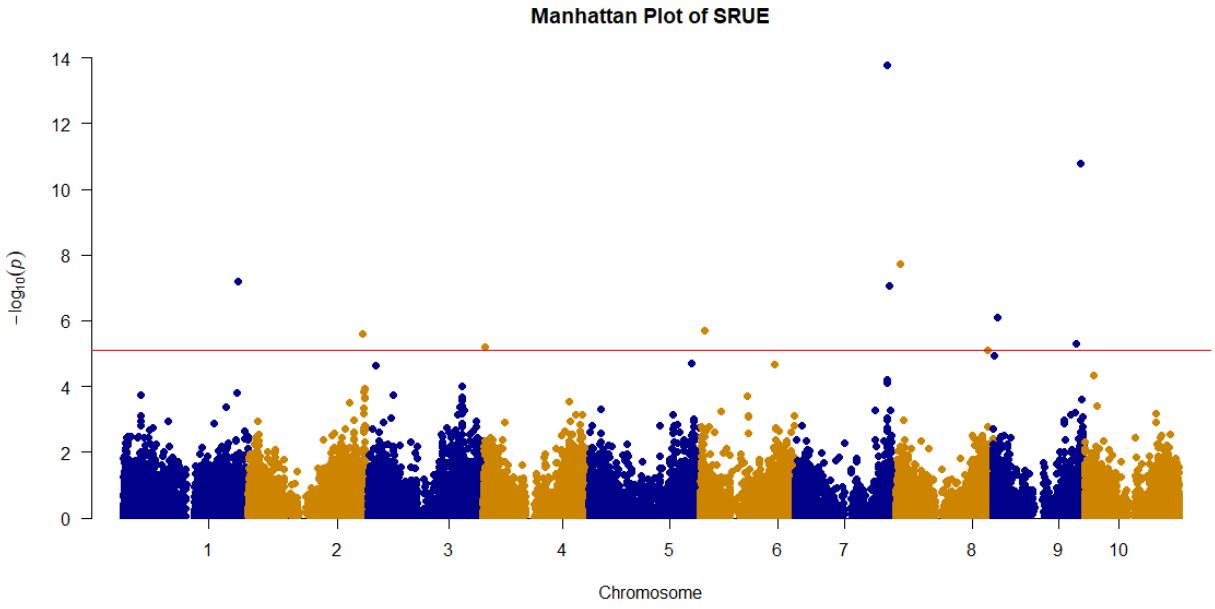

Figure 4.5 Manhattan plot from GWAS for seasonal radiation use efficiency in 619 sorghum hybrids.

Table 4.3 GWAS for canopy cover at 600GDD in the SbDIV TC population of sorghum hybrids with significant SNPs and candidate genes at FDR 0.05.

SNP	Chr.	Position	FDR_Adjusted _P-values	Effect	Candidate Gene	Annotation
S03_4483384	3	4483384	6.39E-06	-1.78	Sobic.003G048500	LYSOPHOSPHOLIPASE-RELATED
					Sobic.003G048600	GLUTAREDOXIN-RELATED PROTEIN
					Sobic.003G048700	RIBOSOMAL PROTEIN S6 KINASE
					Sobic.003G048900	-
S07_59768820	7	59768820	2.50E-05	0.55	Sobic.007G163300	-
S02_73763983	2	73763983	0.001469942	-0.78	NA	-
S08_60159594	8	60159594	0.007667636	0.78	Sobic.008G167401	-
					Sobic.008G167500	LEUCINE-RICH REPEAT-CONTAINING PROTEIN
					Sobic.008G167400	Gamma-thionin family
					Sobic.008G167600	GDP-L-galactose phosphorylase
					Sobic.008G167700	-
S09_54911979	9	54911979	0.011182793	-0.65	Sobic.009G198700	RAS-RELATED PROTEIN RABA1A
					Sobic.009G198800	Transcriptional repressor, Ovate
					Sobic.009G198900	TREHALOSE-6-PHOSPHATE SYNTHASE
					Sobic.009G199001	Gamma-glutamyl hydrolase

Table 4.3 continued

					Sobic.009G199100	gamma-glutamyl hydrolase (GGH)
S06_29459729	6	29459729	0.036249821	0.56	NA	-
S04_68243431	4	68243431	0.036249821	-0.55	Sobic.004G354800	-
					Sobic.004G355000	Phosphoinositide 5-phosphatase
					Sobic.004G355101	-
					Sobic.004G355200	lysine-specific demethylase 3 (KDM3)

Table 4.4 GWAS for canopy cover at 800GDD in the SbDIV TC population of sorghum hybrids with significant SNPs and candidate genes at FDR 0.05.

SNP	Chr.	Position	FDR_Adjusted _P-values	Effect	Candidate Gene	Annotation
S03_4483384	3	4483384	5.92E-05	-0.79	Sobic.003G048500	LYSOPHOSPHOLIPASE-RELATED
					Sobic.003G048600	GLUTAREDOXIN-RELATED PROTEIN
					Sobic.003G048700	RIBOSOMAL PROTEIN S6 KINASE
					Sobic.003G048900	-
S09_57062019	9	57062019	5.92E-05	-0.52	Sobic.009G230000	CAMP-RESPONSE ELEMENT BINDING PROTEIN-RELATED
					Sobic.009G230100	LRR RECEPTOR-LIKE SERINE/THREONINE-PROTEIN KINASE MRH1-RELATED
					Sobic.009G230200	Galactose oxidase
					Sobic.009G230300	-
					Sobic.009G230400	GLUCOSYL/GLUCURONOSYL TRANSFERASES
					Sobic.009G230500	TUBBY-RELATED
					Sobic.009G230600	-
					Sobic.009G230700	Transcription factor GT-2 and related proteins, contains trihelix DNA-binding/SANT domain
S09_57576171	9	57576171	0.001164059	-0.37	Sobic.009G237350	F-box domain (F-box)
					Sobic.009G237400	timeless
					Sobic.009G237500	Protein of unknown function (DUF3143)
					Sobic.009G237600	CAMP-RESPONSE ELEMENT BINDING PROTEIN-RELATED
S07_60408666	7	60408666	0.002667182	0.21	Sobic.007G169300	-
					Sobic.007G169500	large subunit ribosomal protein L10Ae (RP-L10Ae, RPL10A)
					Sobic.007G169533	large subunit ribosomal protein L10Ae (RP-L10Ae, RPL10A)
					Sobic.007G169566	-
S01_73258930	1	73258930	0.002667182	0.51	Sobic.001G456100	SOLUTE CARRIER FAMILY 35
					Sobic.001G456200	-
					Sobic.001G456300	GLYCOSYLTRANSFERASE

Table 4.4 continued

					Sobic.001G456400	Putative nuclear localisation signal (NINJA_B)
S02_66173624	2	66173624	0.002695331	-0.25	Sobic.002G279900	BETA-GALACTOSIDASE RELATED
					Sobic.002G280001	-
					Sobic.002G280100	minichromosome maintenance protein 10 (MCM10)
					Sobic.002G280200	SKP1
					Sobic.002G280300	Cotton fibre expressed protein (DUF761)
					Sobic.002G280400	ACYL CARRIER PROTEIN/ZINC FINGER PROTEIN 593-RELATED
					Sobic.002G280500	ZINC FINGER FYVE DOMAIN CONTAINING PROTEIN
					Sobic.002G280600	MEDIATOR OF RNA POLYMERASE II TRANSCRIPTION SUBUNIT 4
S10_24107416	10	24107416	0.002695331	-0.38	Sobic.010G139550	Putative gypsy type transposon
S05_21444078	5	21444078	0.004974387	-0.16	NA	-
S10_12178788	10	12178788	0.005016464	0.20	Sobic.010G114700	HEAT SHOCK FACTOR BINDING PROTEIN 1
					Sobic.010G114800	CELL DIVISION PROTEIN KINASE
S06_61183041	6	61183041	0.008058085	-0.24	Sobic.006G281800	Ras-related protein Rab-18 (RAB18)
					Sobic.006G281900	No apical meristem (NAM) protein
S03_72075544	3	72075544	0.013864257	-0.47	Sobic.003G413300	-
					Sobic.003G413400	-
					Sobic.003G413500	-
					Sobic.003G413550	-
					Sobic.003G413600	K+ POTASSIUM TRANSPORTER
					Sobic.003G413700	K+ POTASSIUM TRANSPORTER
S07_1657858	7	1657858	0.021880467	0.14	Sobic.007G018100	NAC DOMAIN-CONTAINING PROTEIN 12
S02_55714395	2	55714395	0.02639782	-0.40	Sobic.002G177200	PHOSPHOLIPASE A1-IIDELTA
					Sobic.002G177300	Premnaspirodiene oxygenase
					Sobic.002G177400	Plant family of unknown function (DUF810)
					Sobic.002G177500	SAWADEE domain

Table 4.5 GWAS for SRUE in the SbDIV TC population of sorghum hybrids with significant SNPs and candidate genes at FDR 0.05.

SNP	Chr.	Position	maf	FDR_Adjusted _P-values	Effect	Candidate Gene	Annotation
S07_59768820	7	59768820	0.18	1.00E-09	0.05	Sobic.007G163300	-
S09_56521150	9	56521150	0.31	4.92E-07	0.02	Sobic.009G222200	RING FINGER AND CHY ZINC FINGER DOMAIN-CONTAINING PROTEIN 1
						Sobic.009G222400	PHOSPHATIDYLINOSITOL N-ACETYLGLUCOSAMINYLTRANSFERASE SUBUNIT P DOWN SYNDROME CRITICAL REGION PROTEIN 5 -RELATED
						Sobic.009G222500	Uncharacterized conserved protein
						Sobic.009G222600	Protein of unknown function (DUF1639)
S08_2579008	8	2579008	0.39	0.000387114	-0.05	Sobic.008G028700	SET DOMAIN PROTEINS
						Sobic.008G028800	WRKY DNA -binding domain
						Sobic.008G028850	-
						Sobic.008G028900	RING ZINC FINGER PROTEIN
S01_74145303	1	74145303	0.12	0.001004336	0.04	Sobic.001G468400	Homeobox domain
						Sobic.001G468500	Uncharacterized conserved protein
						Sobic.001G468600	SERYL-TRNA SYNTHETASE
						Sobic.001G468700	AUXILIN/CYCLIN G-ASSOCIATED KINASE-RELATED
S07_61435836	7	61435836	0.28	0.001052593	0.03	Sobic.007G181100	MULTIDRUG RESISTANCE PROTEIN
S09_2949146	9	2949146	0.07	0.007975731	0.03	Sobic.009G032500	RNA POLYMERASE II SUBUNIT B1 CTD PHOSPHATASE RPAP2-RELATED
						Sobic.009G032533	-
						Sobic.009G032566	-
						Sobic.009G032600	Peroxidase / Lactoperoxidase
						Sobic.009G032700	Peroxidase / Lactoperoxidase
S06_2686264	6	2686264	0.03	0.017836345	0.05	Sobic.006G017000	pleiotropic regulator 1 (PLRG1, PRL1, PRP46)
						Sobic.006G017100	RIBOSOMAL PROTEIN L18
						Sobic.006G017200	LEUCINE-RICH REPEAT-CONTAINING PROTEIN
S02_73819709	2	73819709	0.33	0.019769415	-0.03	Sobic.002G381700	WD40 repeat-containing protein
						Sobic.002G381750	SKP1
						Sobic.002G381800	-
						Sobic.002G381900	Casein Kinase 2 substrate (CK2S)
						Sobic.002G382001	-
						Sobic.002G382100	Probable lipid transfer (LTP_2)
S09_54144857	9	54144857	0.14	0.033770119	-0.02	Sobic.009G189400	Assimilatory sulfite reductase (ferredoxin)
						Sobic.009G189501	-
						Sobic.009G189600	-
						Sobic.009G189700	-
S04_1304873	4	1304873	0.18	0.037372688	-0.03	Sobic.004G016250	-

Table 4.5 continued

						Sobic.004G016200	-
						Sobic.004G016300	PPR repeat family
						Sobic.004G016400	Ethanolaminephosphotransferase
						Sobic.004G016600	ZINC FINGER FYVE DOMAIN CONTAINING PROTEIN
						Sobic.004G016500	PPR repeat
S08_59178415	8	59178415	0.35	0.044238154	0.03	Sobic.008G158666	Protease inhibitor/seed storage/LTP family (Tryp_alpha_amyl)
						Sobic.008G158732	Protease inhibitor/seed storage/LTP family (Tryp_alpha_amyl)
						Sobic.008G158800	Protease inhibitor/seed storage/LTP family (Tryp_alpha_amyl)
						Sobic.008G158900	CHITINASE
						Sobic.008G159000	-

4.5 Discussion

4.5.1 SRUE value exhibits a similar range as previous publications

Acquiring multiple time points of canopy cover increases the fit of logistic function and makes the estimation of SRUE possible. This estimation was under the assumption that there is no water stress in the environment. If there is water stress, dry biomass accumulation would decrease and affect the SRUE calculation. The SRUE values measured in a large set of genetically diverse testcross hybrids representing the sorghum diversity panel are presented in Figure 4.2. The median of the SRUE values in 2018, 2019, and 2020 are 1.35, 1.31, and 1.33 (g/MJ), respectively. Although the three years have a similar median of RUE, 2018 has a larger standard deviation than observed in 2019 and 2020. This may because that the nitrogen application of 2018 was one month after planting, while 2019 and 2020 were applied one month before planting. C4 plants like sorghum generally exhibit higher RUE (Sinclair and Muchow 1999) than C3 crops. Kiniry et al. (1989) reported that two important C4 crops, maize and sorghum, exhibited RUE of 1.75 g MJ^{-1} and 1.4 g MJ^{-1} of intercepted short-wave solar radiation, respectively. Hammer et al. (2010b) found that RUE ranged between 1.2 and 1.4 g MJ^{-1} during vegetative growth. Some publications also reported that maximum RUE of maize in the range 1.6 to 1.7 g MJ^{-1} and 1.2 to 1.4 g MJ^{-1} for sorghum during vegetative growth. It suggests that the sorghum potential RUE is less than maize (Muchow and Davis, 1988; Muchow, 1989; Muchow and Sinclair, 1994; Sinclair and Muchow, 1999; Lindquist et al., 2005). However, analyses of RUE and SRUE of commercial sorghum hybrids revealed variations from approximately 1.0 to 1.9 g MJ^{-1} with commercial forage hybrids

exhibiting values similar or higher than RUE and SRUE reported for maize. Variation in SRUE calculated by the simple model provided in this study exhibits a similar range as previous publications.

4.5.2 SRUE is heritable and stable over seasons

Across three hybrid years, SRUEs have heritability close to 0.5 (Table 4.1). This indicated that SRUE is heritable and can be used in genetic studies or as a selection criterion in sorghum breeding programs (Furbank et al. 2019). Since the SRUE calculation used RGB canopy cover, and it had lower heritability than ADB, SRUE has slightly lower heritability than ADB.

Given the moderate heritability reported for SRUE and positive correlations with ADB over years (Table 4.2), SRUE appears to be a valuable trait that can be used in genetic studies and for exploration of components of ADB. Narayanan et al. (2013) reported that RUE has $R^2 = 0.9$ with dry biomass in sorghum. Some cereal breeding programs have successfully increased RUE with gains in grain yield (Shearman et al. 2005b; Sadras et al. 2011; Sadras et al. 2012). Other studies suggested that increased RUE may improve grain yield (Zhu et al. 2016; Asseng et al. 2019).

4.5.3 Favorable alleles for SRUE and ADB with low allele frequencies

GWAS identified 11 SNPs associated with SRUE under FDR 0.05 significance level with the minor allele contributing the favorable effect for seven of these loci (Table 4.5). The minor allele frequencies of S07_59768820, S09_56521150, S01_74145303, S07_61435836, S09_2949146, S06_2686264, and S08_59178415 are 0.18, 0.31, 0.12, 0.28, 0.07, 0.03, and 0.35, respectively. Selection for these minor alleles will provide considerable opportunities for improving SRUE through breeding.

GWAS identified 13 SNPs associated with ADB under FDR 0.05 significant level with the minor allele contributing the favorable effect for seven of these loci (Table B.6). Five of the SNPs (S07_59768820, S09_56521150, S01_74145303, S06_2686264, and S08_59178415) with minor alleles as favorable alleles were significant for SRUE and ADB under FDR p-value 0.05 probability. SNPs S07_61080813 and S02_2417641 were only significant in ADB. This reveals that within the population, there are five SNPs that provide positive effects for both SRUE and

ADB with allele frequencies below 0.5. Efforts to increase these allele frequencies through breeding could simultaneously improve the germplasm for SRUE and ADB.

Further analyses of sorghum accessions having favorable alleles represented in the SbDIV sorghum diversity panel showed that Dwarf Yellow Milo has minor and favorable alleles at the S07_59768820, S07_61435836, S08_59178415, and S09_2949146; KS19 has minor and favorable alleles at the S07_59768820, S07_61435836, S08_59178415, and S09_56521150; San Chi San has minor and favorable alleles at the S07_59768820, S07_61435836, S08_59178415, and S09_56521150; Spur Feterita has minor and favorable alleles at the S01_74145303, S06_2686264, S07_59768820, S07_61435836, S08_59178415, and S09_56521150. These genotypes represent valuable resources for future sorghum hybrid breeding efforts for improve SRUE.

4.5.4 Mapping loci associated with canopy cover

Canopy cover is a complex trait that reflects canopy level structure. The genes impacting canopy cover may be related to variation in an array of traits including leaf angle, leaf appearance rate, leaf area, chlorophyll content, leaf chlorophyll fluorescence, tiller number, plant height, amount of vegetative biomass, dry matter growth rate, and days to flowering. Many of the SNPs identified for canopy cover in this study mapped to the same genomic locations as QTL for these other traits.

GWAS for canopy cover at 600GDD identified SNPs and candidate genes on chromosomes 3, 4, 7, 8, and 9. Identified candidate genes and published QTLs are in Table 4.6.

Table 4.6 Identified candidate genes of RGB canopy cover at 600GDD and published QTLs.

RGB canopy cover candidate genes at 600 GDD	Chr.	position (bp)	Published QTLs	QTL Related Traits	Note
Sobic.003G048500 Sobic.003G048600 Sobic.003G048700 Sobic.003G048900	3	4469846-4506317	*qLFAR3.13* (Fiedler et al. 2016); *qCHLC3.30* (Fiedler et al. 2016); *qCHLF3.13*, *qCHLF3.14*, *qCHLF3.15* (Fiedler et al. 2016); *qHGHT3.3* (Feltus et al. 2006), *qHGHT3.4* (Phuong et al. 2013), *qHGHT3.5* (Hart et al. 2001); *qTNUM3.5* (Kong et al. 2014); *qDTFL3.3* (Wang et al. 2014); *qDMGR3.13*, *qDMGR3.14* (Fiedler et al. 2016)	leaf appearance rate; leaf chlorophyll content; leaf chlorophyll fluorescence; plant height; tiller number; days to flowering; dry matter growth rate	
Sobic.004G354800 Sobic.004G355000 Sobic.004G355101 Sobic.004G355200	4	68228025-68263930	*qCHLF4.23* (Fiedler et al. 2016)	leaf chlorophyll fluorescence	
Sobic.007G163300	7	59767412-59768828	*qLANG7.10*, *qLANG7.11*, *qLANG7.12*, *qLANG7.13* (McCormick et al. 2016); *qCHLC7.17*, *qCHLC7.20* (Gelli et al. 2016); *qHGHT7.45* (Pereira and Lee 1995), *qHGHT7.46* (Madhusudhana and Patil 2013), *qHGHT7.62* (Zhang et al. 2015), *qHGHT7.76* (Yamaguchi et al. 2016), *qHGHT7.83* (Girma et al. 2019), *qHGHT7.91*, *qHGHT7.92* (Liu et al. 2019), *qHGHT7.93*, *qHGHT7.95*, *qHGHT7.96*, *qHGHT7.97* (Marla et al. 2019); *qTDBM7.6* (Murray et al. 2008)	leaf angle; leaf chlorophyll content; plant height; stem dry biomass	*Dw3* gene is in the same height QTLs.
Sobic.008G167401 Sobic.008G167500 Sobic.008G167400 Sobic.008G167600 Sobic.008G167700	8	60151302-60171528	*qLFAR8.16* (Fiedler et al. 2016); *qLFLN8.3* (Shehzad and Okuno 2015); *qCHLF8.29*, *qCHLF8.30* (Fiedler et al. 2016); *qGLFA8.4* (Haussmann et al. 2002); *qDTFL8.23* (Feltus et al. 2006);	leaf appearance rate; leaf length; leaf chlorophyll fluorescence; green leaf area; days to flowering	
Sobic.009G198700 Sobic.009G198800 Sobic.009G198900 Sobic.009G199001 Sobic.009G199100	9	54895227-54925186	*qLFAR9.9* (Fiedler et al. 2016); *qCHLC9.30* (Gelli et al. 2016); *qHGHT9.20*, *qHGHT9.21*, *qHGHT9.46* (Felderhoff et al. 2012), *qHGHT9.64*, *qHGHT9.65* (Zhang et al. 2015), *qHGHT9.8* (Feltus et al. 2006), *qHGHT9.10* (Lin et al. 1995), *qHGHT9.75* (Bai et al. 2017); *qDTFL9.15* (Feltus et al. 2006); *qTDBM9.1* (Felderhoff et al. 2012), *qSDWT9.4* (Zhang et al. 2015)	leaf appearance rate; leaf chlorophyll content; plant height; days to flowering; vegetative dry biomass	

GWAS for canopy cover at 800GDD identified SNPs and candidate genes on chromosomes 1, 2, 3, 6, 7, 9, 10. Identified candidate genes and published QTLs are in Table 4.7.

Table 4.7 Identified candidate genes of RGB canopy cover at 800GDD and published QTLs.

RGB canopy cover candidate genes at 800 GDD	Chr.	position (bp)	Published QTLs	QTL Related Traits	Note
Sobic.001G456100 Sobic.001G456200 Sobic.001G456300 Sobic.001G456400	1	73254804-73274411	*qCHLF1.32* (Fiedler et al. 2016); *qHGHT1.21* (Mocoeur et al. 2015); *qTNUM1.24*, *qTNUM1.25*, *qTNUM1.26* (Kong et al. 2014); *qSTGR1.3* (Wang et al. 2014); *qDTFL1.34* (El Mannai et al. 2011), *qDTFL1.35* (Bangbol Sangma 2013), *qDTFL1.37* (Srinivas et al. 2009); *qDMGR1.21* (Fiedler et al. 2016)	leaf chlorophyll fluorescence; plant height; tiller number; stay-green; days to flowering; dry matter growth rate	*Ma3* is also in QTL *qDTFL1.35* .
Sobic.002G279900 Sobic.002G280001 Sobic.002G280100 Sobic.002G280200 Sobic.002G280300 Sobic.002G280400 Sobic.002G280500 Sobic.002G280600	2	66153611-66189183	*qLFAR2.11* (Fiedler et al. 2016); *qCHLC2.14*, *qCHLC2.16*, *qCHLC2.17* (Sukumaran et al. 2016); *qCHLF2.28*, *qCHLF2.29*, *qCHLF2.30* (Fiedler et al. 2016); *qHGHT2.12* (Liu et al. 2019); *qDTFL2.20* (Mace et al. 2013), *qDTFL2.22*, *qDTFL2.23* (Srinivas et al. 2009), *qDTFL2.24* (Phuong et al. 2013), *qDTFL2.45* (Marla et al. 2019); *qDMGR2.15* (Fiedler et al. 2016)	leaf appearance rate; leaf chlorophyll content; leaf chlorophyll fluorescence; plant height; days to flowering; dry matter growth rate	
Sobic.002G177200 Sobic.002G177300 Sobic.002G177400 Sobic.002G177500	2	55708840-55733484	*qGLFA2.11* (Sabadin et al. 2012); *qDTFL2.3* (Bangbol Sangma 2013), *qDTFL2.34* (Mocoeur et al. 2015), *qDTFL2.4*, *qDTFL2.5*, *qDTFL2.6* (Wang et al. 2014)	green leaf area; days to flowering	
Sobic.003G048500 Sobic.003G048600 Sobic.003G048700 Sobic.003G048900	3	4469846-4506317	*qLFAR3.13* (Fiedler et al. 2016); *qCHLC3.30* (Fiedler et al. 2016); *qCHLF3.13*, *qCHLF3.14*, *qCHLF3.15* (Fiedler et al. 2016); *qHGHT3.3* (Feltus et al. 2006), *qHGHT3.4* (Phuong et al. 2013), *qHGHT3.5* (Hart et al. 2001); *qTNUM3.5* (Kong et al. 2014); *qDTFL3.3* (Wang et al. 2014); *qDMGR3.13*, *qDMGR3.14* (Fiedler et al. 2016)	leaf appearance rate; leaf chlorophyll content; leaf chlorophyll fluorescence; plant height; tiller number; days to flowering; dry matter growth rate	
Sobic.003G413300 Sobic.003G413400 Sobic.003G413500 Sobic.003G413550 Sobic.003G413600 Sobic.003G413700	3	72060603-72093980	*qLFWD3.2*, *qLFWD3.3* (Shehzad and Okuno 2015), *qLFWD3.4* (Feltus et al. 2006); *qCHLC3.27* (Sukumaran et al. 2016); *qHGHT3.16* (Nagaraja Reddy et al. 2013), *qHGHT3.24* (Liu et al. 2019); *qTNUM3.8* (Kong et al. 2014); *qDTFL3.31* (Wang et al. 2014)	leaf width; leaf chlorophyll content; plant height; tiller number; days to flowering	
Sobic.006G281800 Sobic.006G281900	6	61166869-61179561	*qCHLC6.13* (Sukumaran et al. 2016); *qCHLF6.17* (Fiedler et al. 2016); *qDTFL6.59* (Bangbol Sangma 2013), *qDTFL6.74* (Sukumaran et al. 2016); *qSDWT6.3* (Shiringani and Friedt 2011)	leaf chlorophyll content; leaf chlorophyll fluorescence; days to flowering; vegetative dry biomass	

Table 4.7 continued

Sobic.007G169300 Sobic.007G169500 Sobic.007G169533 Sobic.007G169566	7	60392556-60419781	*qLANG7.10*, *qLANG7.11*, *qLANG7.12*, *qLANG7.13* (McCormick et al. 2016); *qCHLC7.17*, *qCHLC7.20* (Gelli et al. 2016); *qHGHT7.45* (Pereira and Lee 1995), *qHGHT7.46* (Madhusudhana and Patil 2013), *qHGHT7.62* (Zhang et al. 2015), *qHGHT7.76* (Yamaguchi et al. 2016), *qHGHT7.83* (Girma et al. 2019), *qHGHT7.91* (Liu et al. 2019), *qHGHT7.93*, *qHGHT7.95*, *qHGHT7.96*, *qHGHT7.97* (Marla et al. 2019); *qTDBM7.6* (Murray et al. 2008)	leaf angle; leaf chlorophyll content; plant height; vegetative dry biomass	*Dw3* is in the same height QTLs.
Sobic.007G018100	7	1663031-1668132	*qCHLC7.2* (Rama Reddy et al. 2014); *qCHLF7.18* (Fiedler et al. 2016); *qTNUM7.1*, *qTNUM7.2* (Kong et al. 2014); *qSTGR7.1* (Subudhi et al. 2000); *qDTFL7.2*, *qDTFL7.3*, *qDTFL7.4* (Wang et al. 2014)	leaf chlorophyll content; leaf chlorophyll fluorescence; tiller number; stay-green; days to flowering	
Sobic.009G230000 Sobic.009G230100 Sobic.009G230200 Sobic.009G230300 Sobic.009G230400 Sobic.009G230500 Sobic.009G230600 Sobic.009G230700	9	57045813-57076364	*qLFAR9.9* (Fiedler et al. 2016); *qCHLC9.30* (Gelli et al. 2016); *qGLFA9.6* (Sabadin et al. 2012); *qHGHT9.10* (Lin et al. 1995), *qHGHT9.103* (Marla et al. 2019), *qHGHT9.16* (Takai et al. 2012), *qHGHT9.12*, *qHGHT9.19* (Wang et al. 2014), *qHGHT9.64*, *qHGHT9.65* (Zhang et al. 2015), *qHGHT9.20*, *qHGHT9.21*, *qHGHT9.29*, *qHGHT9.30*, *qHGHT9.45*, *qHGHT9.46* (Felderhoff et al. 2012), *qHGHT9.81* (Boyles et al. 2017); *qTNUM9.7*, *qTNUM9.8* (Zhang et al. 2015); *qDTFL9.15* (Feltus et al. 2006), *qDTFL9.33*, *qDTFL9.34* (Zhang et al. 2015); *qTDBM9.1*, *qTDBM9.4* (Felderhoff et al. 2012), *qSDWT9.4*, *qSDWT9.5* (Zhang et al. 2015)	leaf appearance rate; leaf chlorophyll content; green leaf area; plant height; tiller number; days to flowering; vegetative dry biomass	*Dw1* is in the same height loci. This gene can affect plant height by reducing cell proliferation activity in the internodes (Hirano et al. 2017).
Sobic.009G237350 Sobic.009G237400 Sobic.009G237500 Sobic.009G237600	9	57557464-57585953	*qLFAR9.9* (Fiedler et al. 2016); *qCHLC9.30* (Gelli et al. 2016); *qGLFA9.6* (Sabadin et al. 2012), *qGLFA9.2* (Rama Reddy et al. 2014); *qTNGL9.1* (Rama Reddy et al. 2014); *qHGHT9.10* (Lin et al. 1995), *qHGHT9.16* (Takai et al. 2012), *qHGHT9.19* (Wang et al. 2014), *qHGHT9.20*, *qHGHT9.21*, *qHGHT9.29*, *qHGHT9.30*, *qHGHT9.44*, *qHGHT9.45*, *qHGHT9.46* (Felderhoff et al. 2012), *qHGHT9.22*, *qHGHT9.23*, *qHGHT9.24*, *qHGHT9.25*, *qHGHT9.26*, *qHGHT9.27*, *qHGHT9.28*, *qHGHT9.32*, *qHGHT9.33*, *qHGHT9.34*, *qHGHT9.35*, *qHGHT9.36*, *qHGHT9.37*, *qHGHT9.38*, *qHGHT9.39* (Higgins et al. 2014), *qHGHT9.31*, *qHGHT9.49* (Takai et al. 2012), *qHGHT9.56* (Pereira and Lee 1995), *qHGHT9.64*, *qHGHT9.65* (Zhang et al. 2015), *qHGHT9.68* (Zhao et al. 2016), *qHGHT9.73*, *qHGHT9.74* (Wang et al. 2016), *qHGHT9.81* (Boyles et al. 2017);	leaf appearance rate; leaf chlorophyll content; green leaf area; total leaf number; plant height; tiller number; days to flowering; vegetative dry biomass	

Table 4.7 continued

			qTNUM9.7, *qTNUM9.8* (Zhang et al. 2015); *qDTFL9.15* (Feltus et al. 2006), *qDTFL9.33*, *qDTFL9.34* (Zhang et al. 2015); *qTDBM9.1*, *qTDBM9.4* (Felderhoff et al. 2012), *qSDWT9.4*, *qSDWT9.5* (Zhang et al. 2015)		
Sobic.010G139550	10	24112634-24115120	*qLFAR10.7*, *qLFAR10.8* (Fiedler et al. 2014), *qLFAR10.15* (Fiedler et al. 2016); *qRLSN10.1* (Rama Reddy et al. 2014); *qLNUM10.1* (Rajkumar et al. 2013); *qCHLF10.17*, *qCHLF10.18*, *qCHLF10.19* (Fiedler et al. 2014), *qCHLF10.24* (Fiedler et al. 2016); *qHGHT10.2* (Pereira and Lee 1995), *qHGHT10.17*, *qHGHT10.18* (Liu et al. 2019), *qHGHT10.5* (Shiringani et al. 2010); *qTNUM10.1* (Shiringani et al. 2010), *qTNUM10.2*, *qTNUM10.3*, *qTNUM10.4* (M. M. Alam et al. 2014); *qDTFL10.13* (Felderhoff et al. 2012), *qDTFL10.15* (Crasta et al. 1999), *qDTFL10.18* (Bangbol Sangma 2013), *qDTFL10.19*, *qDTFL10.20*, *qDTFL10.21* (Wang et al. 2014), *qDTFL10.22* (Nagaraja Reddy et al. 2013), *qDTFL10.24* (Wang et al. 2014), *qDTFL10.25* (Mace et al. 2013), *qDTFL10.38* (Mocoeur et al. 2015), *qDTFL10.43* (Guindo et al. 2019), *qDTFL10.45*, *qDTFL10.46* (Liu et al. 2019); *qDMGR10.29* (Fiedler et al. 2016); *qTDBM10.1*, *qTDBM10.2* (Felderhoff et al. 2012)	leaf appearance rate; rate of leaf senescence; leaf number; leaf chlorophyll fluorescence; plant height; tiller number; days to flowering; dry matter growth rate; vegetative dry biomass	
Sobic.010G114700 Sobic.010G114800	10	12181779-12188720	*qLFAR10.6* (Fiedler et al. 2014), *qLFAR10.15* (Fiedler et al. 2016); *qRLSN10.1* (Rama Reddy et al. 2014); *qCHLF10.24* (Fiedler et al. 2016); *qHGHT10.2* (Pereira and Lee 1995), *qHGHT10.16* (Kong et al. 2018), *qHGHT10.17*, *qHGHT10.18* (Liu et al. 2019), *qHGHT10.5* (Shiringani et al. 2010); *qTNUM10.1* (Shiringani et al. 2010), *qTNUM10.2*, *qTNUM10.3*, *qTNUM10.4* (M. M. Alam et al. 2014); *qDTFL10.13* (Felderhoff et al. 2012), *qDTFL10.15* (Crasta et al. 1999), *qDTFL10.22* (Nagaraja Reddy et al. 2013), *qDTFL10.25* (Mace et al. 2013), *qDTFL10.38* (Mocoeur et al. 2015), *qDTFL10.39* (Miao et al. 2020), *qDTFL10.43* (Guindo et al. 2019), *qDTFL10.45*, *qDTFL10.46* (Liu et al. 2019); *qDMGR10.16*, *qDMGR10.17* (Fiedler et al. 2014), *qDMGR10.29* (Fiedler et al. 2016); *qTDBM10.1*, *qTDBM10.2* (Felderhoff et al. 2012)	leaf appearance rate; rate of leaf senescence; leaf chlorophyll fluorescence; plant height; tiller number; days to flowering; dry matter growth rate; vegetative dry biomass	

All identified candidate genes of RGB canopy cover were also reported in the traits related to canopy structure, such as leaf morphology, chlorophyll content and fluorescence, plant height, tiller number, vegetative biomass, and days to flowering. These results are not surprising since our approach for estimating SRUE involved multi-date canopy cover extracted from RGB images and fitted to logistic regression by days after sowing to estimate seasonal radiation interception for the SRUE calculation. The candidate genes for canopy cover from GWAS are consistent with published QTLs functions. This support that the remote sensing approach used in this study is reliable since it was supported by the genetic aspect.

4.5.5 Mapping loci associated with SRUE

SNPs associated with SRUE also show considerable overlap with QTLs related to canopy cover and ADB and previously reported QTL for leaf angle, green leaf area, leaf chlorophyll content and fluorescence, the efficiency of energy captured by open PSII reaction centers, leaf senescence, plant height, tiller number, vegetative dry biomass, dry matter growth rate, and days to flowering. A cluster of these QTLs map near the *Dw3* locus, which is consistent with previous reports that sorghum dwarfing genes can affect light interception, canopy extinction coefficient (k), and RUE (George-Jaeggli et al. 2013). McCormick et al. (2016) reported that *Dw3* can also influence leaf inclination angle and shoot height. This influence is time-dependent since leaf angle is affected prior to shoot height.

GWAS for SRUE identified SNPs and candidate genes on chromosomes 1, 2, 4, 6, 7, 8, and 9. Identified candidate genes and published QTLs are in Table 4.8. Some of these genes and genetic loci were already discussed in Chapter 3 since these candidate genes were also identified for ADB. The major candidate gene on chromosome 7, *Sobic.007G163300*, mapped to same region of *Dw3*. A cluster of QTL have been mapped to this locus including four leaf angle QTLs (McCormick et al. 2016), two leaf chlorophyll content QTLs (Gelli et al. 2016), eleven plant height QTLs (Pereira and Lee 1995; Madhusudhana and Patil 2013; Zhang et al. 2015; Yamaguchi et al. 2016; Marla et al. 2019; Girma et al. 2019; Liu et al. 2019), one stem dry biomass QTL (Murray et al. 2008). Another cluster of QTL have been mapped to the candidate gene on chromosome 8 including a grain yield QTL (Felderhoff et al. 2012), height QTL (Shehzad and Okuno 2015), and stem and leaf fresh weight QTL (Guan et al. 2011). The QTL for SRUE on chromosome 9 map to the same region as a cluster of QTL for plant height QTLs (Lin et al. 1995; Felderhoff et al. 2012;

Zhang et al. 2015), a grain yield QTL (Sabadin et al. 2012), and a vegetative dry biomass QTL (Felderhoff et al. 2012). Other SNPs for SRUE are indicated in Table 4.8.

Table 4.8 Identified candidate genes of SRUE and published QTLs.

SRUE candidate genes	Chr.	position (bp)	Published QTLs	QTL Related Traits	Note
Sobic.001G468400 Sobic.001G468500 Sobic.001G468600 Sobic.001G468700	1	74135477-74157363	*qGLFA1.12*, *qGLFA1.13* (Haussmann et al. 2002); *qPSII1.30* (Ortiz et al. 2017); *qCHLF1.32* (Fiedler et al. 2016); *qHGHT1.21* (Mocoeur et al. 2015); *qTNUM 1.24*, *qTNUM 1.25*, *qTNUM 1.26* (Kong et al. 2014); *qDMGR1.21* (Fiedler et al. 2016)	green leaf area; efficiency of energy captured by open PSII reaction centers; leaf chlorophyll fluorescence; plant height; tiller number; dry matter growth rate	
Sobic.002G381700 Sobic.002G381750 Sobic.002G381800 Sobic.002G381900 Sobic.002G382001 Sobic.002G382100	2	73808198-73833394	*qLSNS2.1* (Feltus et al. 2006); *qCHLC2.19* (Fiedler et al. 2016); *qTNUM2.15*, *qTNUM2.16* (Liu et al. 2019); *qDTFL2.31* (Wang et al. 2014); *qTDBM2.4* (Mocoeur et al. 2015)	leaf senescence; leaf chlorophyll content; tiller number; days to flowering; vegetative fresh biomass	
Sobic.004G016250 Sobic.004G016200 Sobic.004G016300 Sobic.004G016400 Sobic.004G016600 Sobic.004G016500	4	1291907-1320592	*qGLFA4.1* (Srinivas et al. 2009); *qCHLF4.18* (Fiedler et al. 2016); *qHGHT4.22* (Liu et al. 2019); *qDMGR4.9* (Fiedler et al. 2016); *qTDBM4.1* (Felderhoff et al. 2012)	green leaf area; leaf chlorophyll fluorescence; plant height; dry matter growth rate; vegetative dry biomass	
Sobic.006G017000 Sobic.006G017100 Sobic.006G017200	6	2673409-2688955	*qGLFA6.2* (Sabadin et al. 2012); *qCHLC6.14* (Fiedler et al. 2016); *qHGHT6.4* (Takai et al. 2012); *qDTFL6.10* (Bangbol Sangma 2013), *qDTFL6.70*, *qDTFL6.72* (Sukumaran et al. 2016); *qFBM6.6* (Wang et al. 2016)	green leaf area; leaf chlorophyll content; plant height; days to flowering; vegetative fresh biomass	
Sobic.007G163300	7	59767412-59768828	*qLANG7.10*, *qLANG7.11*, *qLANG7.12*, *qLANG7.13* (McCormick et al. 2016); *qCHLC7.17*, *qCHLC7.20* (Gelli et al. 2016); *qHGHT7.45* (Pereira and Lee 1995), *qHGHT7.46* (Madhusudhana and Patil 2013), *qHGHT7.62* (Zhang et al. 2015), *qHGHT7.76* (Yamaguchi et al. 2016), *qHGHT7.83* (Girma et al. 2019), *qHGHT7.91*, *qHGHT7.92* (Liu et al. 2019), *qHGHT7.93*, *qHGHT7.95*, *qHGHT7.96*, *qHGHT7.97* (Marla et al. 2019); *qTDBM7.6* (Murray et al. 2008)	leaf angle; leaf chlorophyll content; plant height; stem dry biomass	*Dw3* gene is in the same height QTLs.
Sobic.007G181100	7	61437163-61442361	*qLFAR7.6* (Kapanigowda et al. 2014); *qCHLC7.17* (Gelli et al. 2016); *qHGHT7.45* (Pereira and Lee 1995), *qHGHT7.46*, *qHGHT7.47*, *qHGHT7.48*, *qHGHT7.49*, *qHGHT7.50* (Madhusudhana and Patil 2013), *qHGHT7.76* (Yamaguchi et al. 2016), *qHGHT7.91* (Liu et al. 2019);	leaf area; leaf chlorophyll content; plant height	*Dw3* is also in QTLs *qHGHT7.45*, *qHGHT7.46*, *qHGHT7.76*, and *qHGHT7.91*

Table 4.8 continued

Sobic.008G028700 Sobic.008G028800 Sobic.008G028850 Sobic.008G028900	8	2546275-2588560	*qLFAR8.4* (Fiedler et al. 2014); *qCHLC8.4*, *qCHLC8.5* (Fiedler et al. 2014), *qCHLC8.16* (Fiedler et al. 2016); *qCHLF8.9*, *qCHLF8.10*, *qCHLF8.11*, *qCHLF8.12* (Fiedler et al. 2014); *qTNUM8.2*, *qTNUM8.3*, *qTNUM8.4*, *qTNUM8.5* (Kong et al. 2014), *qTNUM8.6* (Mohammad Mobashwer Alam et al. 2014); *qDTFL8.5*, *qDTFL8.6*, *qDTFL8.7* (Wang et al. 2014), *qDTFL8.8* (Mace et al. 2013)	leaf appearance rate; leaf chlorophyll content; leaf chlorophyll fluorescence; tiller number; days to flowering	
Sobic.008G158666 Sobic.008G158732 Sobic.008G158800 Sobic.008G158900 Sobic.008G159000	8	59163745-59184476	*qHGHT8.4* (Shehzad and Okuno 2015); *qGYLD8.4* (Felderhoff et al. 2012); *qFBMS8.1* (Guan et al. 2011)	plant height; grain yield; stem and leaf fresh weight;	
Sobic.009G189400 Sobic.009G189501 Sobic.009G189600 Sobic.009G189700	9	54132845-54157512	*qHGHT9.10* (Lin et al. 1995), *qHGHT9.64*, *qHGHT9.65* (Zhang et al. 2015), *qHGHT9.20* (Felderhoff et al. 2012); *qGYLD9.11* (Sabadin et al. 2012); *qTDBM9.1* (Felderhoff et al. 2012)	plant height; grain yield; vegetative dry biomass	
Sobic.009G222200 Sobic.009G222400 Sobic.009G222500 Sobic.009G222600	9	56508971-56534265	*qLFAR9.9* (Fiedler et al. 2016); *qGLFA9.6* (Sabadin et al. 2012); *qTNGL9.1* (Rama Reddy et al. 2014); *qCHLC9.30* (Gelli et al. 2016); *qCHLF9.13* (Fiedler et al. 2014); *qHGHT9.64*, *qHGHT9.65* (Zhang et al. 2015), *qHGHT9.8* (Feltus et al. 2006), *qHGHT9.10* (Lin et al. 1995), *qHGHT9.16* (Takai et al. 2012), *qHGHT9.19* (Wang et al. 2014), *qHGHT9.20*, *qHGHT9.21*, *qHGHT9.30*, *qHGHT9.45*, *qHGHT9.46* (Felderhoff et al. 2012); *qTNUM9.7*, *qTNUM9.8* (Zhang et al. 2015); *qDTFL9.15* (Feltus et al. 2006), *qDTFL9.16* (Lin et al. 1995), *qDTFL9.33*, *qDTFL9.34* (Zhang et al. 2015); *qDMGR9.17* (Fiedler et al. 2014); *qTDBM9.1*, *qTDBM9.4* (Felderhoff et al. 2012), *qSDWT9.4* (Zhang et al. 2015)	leaf appearance rate; green leaf area; total number of green leaves; leaf chlorophyll content; leaf chlorophyll fluorescence; plant height; tiller number; days to flowering; dry matter growth rate; vegetative dry biomass	*Dw1* is in the QTLs: *qHGHT9.10*, *qHGHT9.16*, *qHGHT9.19*, *qHGHT9.20*, *qHGHT9.21*, *qHGHT9.30*, *qHGHT9.45*, *qHGHT9.46*, *qHGHT9.64*, *qHGHT9.65*.
Sobic.009G032500 Sobic.009G032533 Sobic.009G032566 Sobic.009G032600 Sobic.009G032700	9	2931347-2961761	*qDMGR9.19* (Fiedler et al. 2016)	dry matter growth rate	

The co-mapping of genes impacting SRUE with known QTL or genes impacting canopy cover and ADB and previously reported QTL for leaf angle, green leaf area, leaf chlorophyll content and fluorescence, the efficiency of energy captured by open PSII reaction centers, leaf senescence, plant height, tiller number, vegetative dry biomass, dry matter growth rate, and days

to flowering suggest that these loci represent genes or clusters of genes that have pleiotropic effects on multiple traits that are important for SRUE.

4.6 Conclusions

SRUE calculated from RGB canopy cover, accumulated radiation, and aboveground dry biomass exhibited similar values and ranges of variation in sorghum as the maximum RUE method reported in Chapter 2. Multi-year analyses in a panel of diverse sorghum hybrids indicated that the methodology for SRUE calculation is reliable and repeatable. SRUE had significant and positive relationships with ADB over seasons and similar heritabilities. Taken together, these studies reveal that SRUE is a valuable trait for crop improvement. Within the hybrid population, there are five low frequency SNPs that provide positive effects for both SRUE and ADB. Increasing the allele frequencies for these SNPs could improve the germplasm for SRUE and ADB.

The candidate genes for canopy cover and SRUE from GWAS are consistent with published QTLs functions. This supports the assertion that the remote sensing approach, the simplified crop growth model for SRUE estimation, and model selected in GWAS were reliable, and applying our SRUE approach to a large breeding population is feasible. Moreover, the simple model for SRUE calculation can also be used to parameterize sophisticated biophysical crop models like APSIM.

CHAPTER 5. GENERAL CONCLUSIONS

Evaluating a large number of genotypes and phenotypes in multiple environments is key to understanding the underlying genetic variation for agronomically important traits related to biomass in bioenergy sorghum breeding programs.

An approach integrating crop growth models with RGB imaging for predicting dynamic sorghum leaf area index and biomass yield in Indiana and Texas across years was presented in Chapter 2. These models for 18 commercial sorghum hybrids, including biomass sorghum, indicated that (i) biomass sorghum hybrids tended to have higher maximum plant height, final dry biomass and RUE than grain sorghum, (ii) photoperiod-sensitive sorghum hybrids exhibited greater biomass potential in longer growing environments and (iii) the adapted APSIM models perform well in above-ground biomass simulations across years and locations. Crop growth models that integrate remote-sensing data offer an efficient approach to evaluate sorghum biomass-related traits in diverse environments.

GWAS using FarmCPU was used to identify SNPs and candidate genes for bioenergy sorghum related traits including apex height, top collar height, ADB, moisture, FL, stem base diameter, top collar diameter, and stand count. The results presented in Chapter 3 confirm that SNPs associated with apex height, top collar height and ADB were located in dwarf QTLs *Dw1* and *Dw3*. SNPs associated with moisture were located in stay-green QTLs *Stg1* and *Stg4*. SNPs and genes associated with top collar height mapped to maturity gene *Ma2*. Seven SNPs were detected for biomass productivity on chromosomes 1, 2, 6, 7, 8, 9. The genotypes such as Dwarf Yellow Milo and Spur Feterita exhibited favorable alleles for these SNPs and may represent unique resources for crop improvement. This chapter also evaluated LiDAR height at 400GDD, 600GDD, 800GDD, and 1000GDD and demonstrated that the effects of height-related genes vary over the season. Many of the candidate genes were reported in published QTLs that have related functions indicating that our methodology was appropriate. The remaining candidate genes have not yet been published and may represent new deployment genes. Additional research for confirmation will be needed.

The parameterized APSIM models introduced in Chapter 2 provided an approach to phenotype predictions in multiple environment trials. However, applying these models to large breeding populations is challenging. Therefore, we proposed a simple model for estimating SRUE

using time-dependent measurements of RGB canopy cover and daily radiation coupled with end-of-season biomass in Chapter 4. This estimate of SRUE was stable and heritable with significant and positive relationships with ADB over seasons. All identified candidate genes for SRUE map to the same positions as previously reported QTLs for related traits. Increasing the allele frequencies for these loci may add value to SRUE and ADB in sorghum breeding programs. Taken together, these studies demonstrated that the simple model for calculating SRUE can be used in genetic studies and for parameterizing sophisticated crop models.

Future studies that integrate crop growth models with remote sensing technologies provide an opportunity to extend these tools to larger numbers of genotypes and phenotypes in the target population of environments to improve our understanding of genetic variation for bioenergy sorghum improvement. Possible future work to extend these research findings include:

1. Parameterize and validate APSIM models for SbDIV TC Cal using the pipeline described in Chapter 2 using 2019 and 2020 data. In the model validation, comparing the APSIM simulated results with remote sensing predicted biomass may be worth trying since people could use the remote sensing predicted biomass for parameterizing SbDIV TC, the larger population.
2. Parameterize and validate the APSIM models for the SbDIV TC with 619 genotypes. The SRUE for these entries were already calculated for this population in Chapter 4 and the biomass of each genotype in different stages can be provided from remote sensing predictions. Since the SbDIV TC Cal is the subset of SbDIV TC, the rest of the input parameters of APSIM for SbDIV TC could be estimated from SbDIV TC Cal. There are two possible ways to estimate inputs from the SbDIV TC. The first approach involves classifying the range of input parameters from the SbDIV TC Cal and then assigning the value for SbDIV TC based on genetic cluster analyses. The other approach involves training and testing the genomic prediction models for the SbDIV TC Cal, and then applying the genomic prediction models for input parameters of the SbDIV TC.
3. After the APSIM models for the SbDIV TC are developed and validated, performance of some or all of the hybrids could be simulated across the USA. Using these simulated phenotypes in GWAS could be useful for evaluating environment-dependent and time-dependent SNPs at a low cost.

4. Predicted biomass and canopy cover from remote sensing should be used to calculate SRUE. If these predictions are accurate, the SRUE calculation only needs the remote sensing inputs for RGB canopy cover and predicted final biomass and daily radiation.

APPENDIX A. CHAPTER 2

SUPPORTING INFORMATION

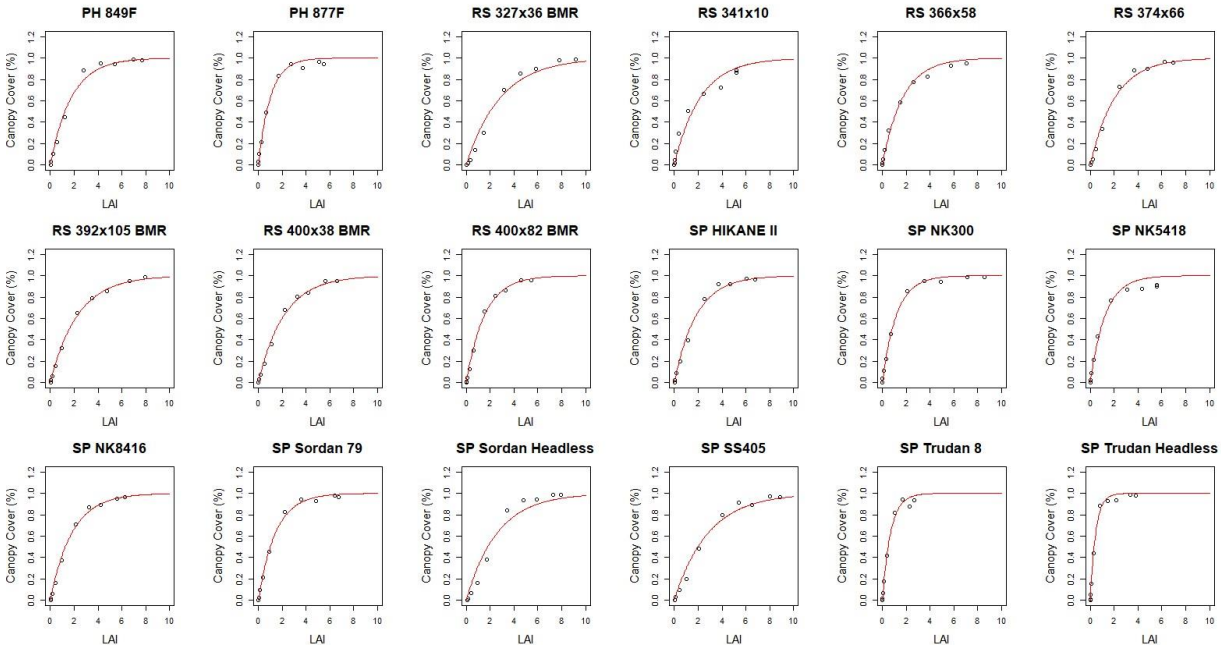

Figure A.1 The canopy cover (CC) versus leaf area index (LAI) for 18 sorghum hybrids. The fitted curve ($CC = 1 - e^{-k \cdot LAI}$) indicates the extinction coefficient (k) of different types of sorghum and the values shown in Table 2.3.

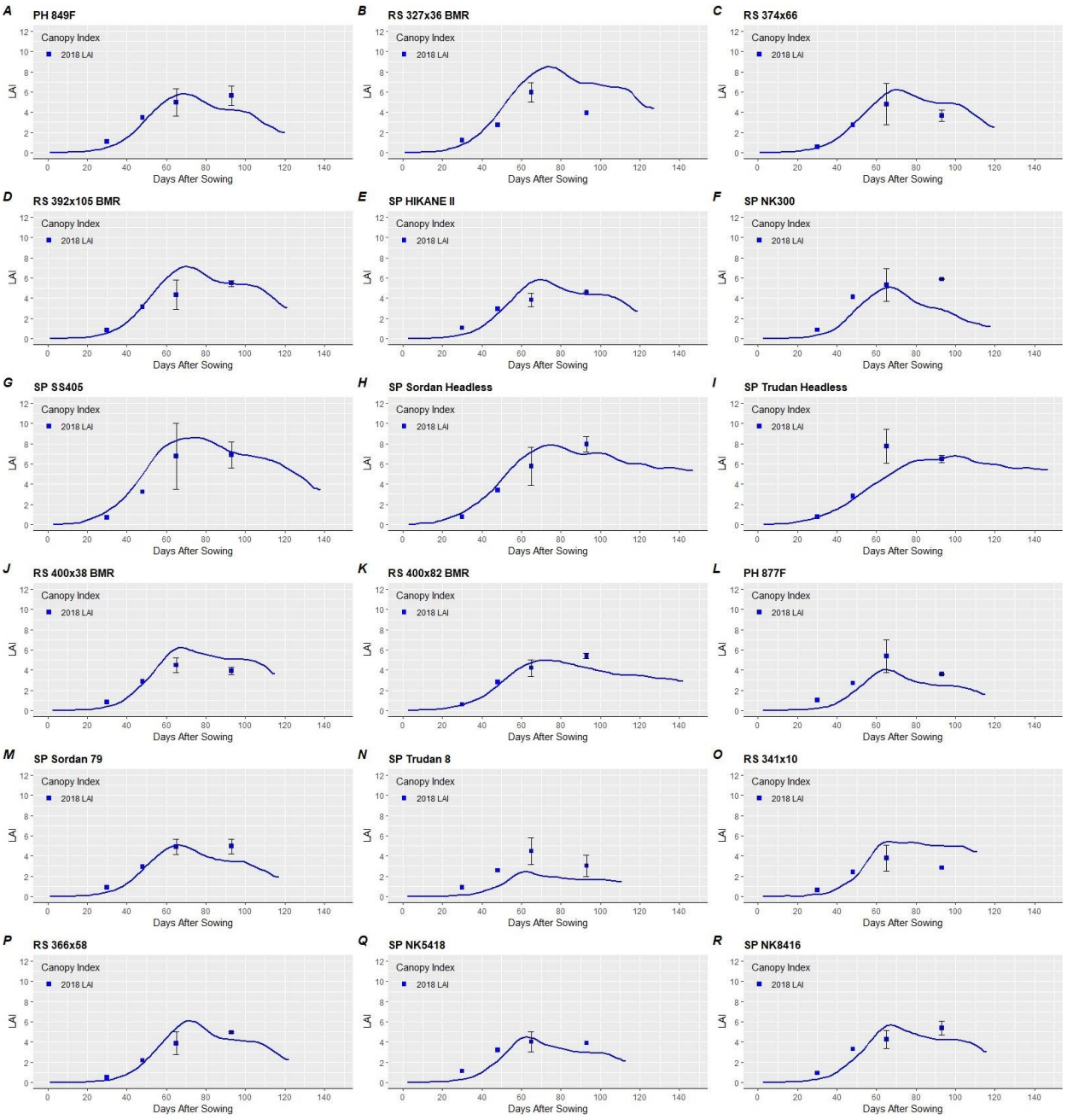

Figure A.2 Simulated crop leaf area index (LAI) throughout the crop life cycle (lines) compared to measured values (symbols) for all sorghum hybrids of each sorghum type. The experiments were sown on 8 May 2018 at West Lafayette. Vertical bars indicate ± 1 SEM for measured values.

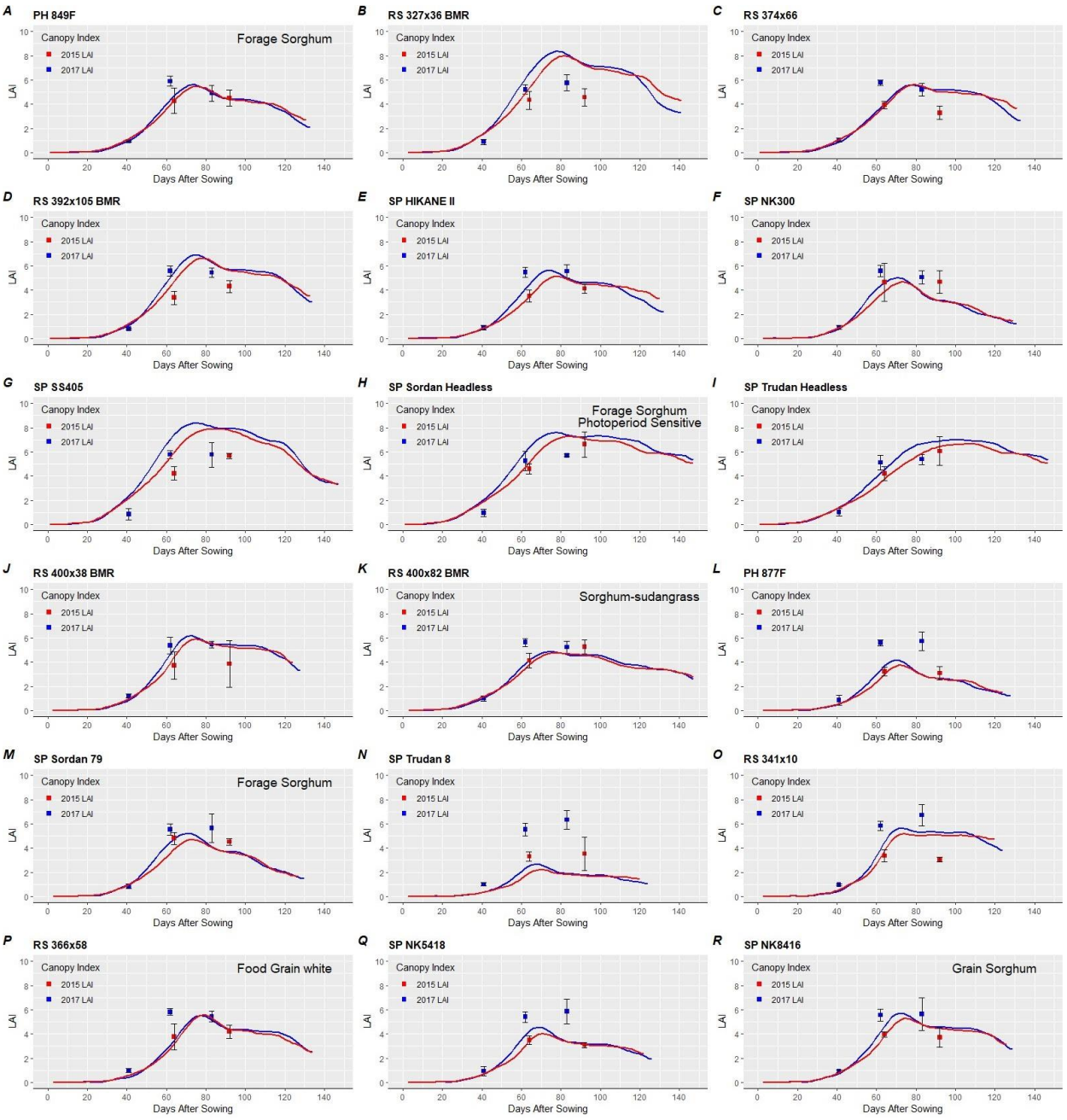

Figure A.3 Simulated crop leaf area index (LAI) throughout the crop life cycle (lines) compared to measured values (symbols) for all sorghum hybrids of each sorghum type sown on 19 May 2015 and 16 May 2017 at West Lafayette. The simulated lines are in the same colour as their measured types. Vertical bars indicate ± 1 SEM for measured values.

DATA AVAILABILITY

The 'R Pipeline for Calculation of APSIM Parameters and Generating the XML File' is stored at the Purdue University Research Repository and includes the data processing pipeline,

data for model input parameters and outputs comparisons, and R-codes for generating or processing central data sets (Yang et al. 2020a). The APSIM files used in the model calibration procedures are stored at the Purdue University Research Repository in '2018 West Lafayette Simulation of 18 Sorghum Hybrids' (Yang et al. 2020b). The APSIM files used for model validations are stored at the Purdue University Research Repository in the '2015 West Lafayette Simulation of 18 Sorghum Hybrids' (Yang et al. 2020c) and '2017 West Lafayette Simulation of 18 Sorghum Hybrids' (Yang et al. 2020d). The APSIM files used for the scenario simulations are stored at the Purdue University Research Repository in the 'Texas Simulation of Sorghum Hybrids Using Historical Weather Data' (Yang et al. 2020e) and 'West Lafayette Scenario Simulation of Sorghum Hybrids Using Historical Weather Data' (Yang et al. 2020f) using multi-year historical weather data of Bushland, TX, and West Lafayette, IN.

APPENDIX B. CHAPTER 3

Table B.1 Top 30 significant SNPs for apex height identified by GWAS using the MLM model. The SNP associated with *Dw3* is highlighted in red color.

SNP	Chromosome	Position	FDR_Adjusted_P-values	Effect	Candidate Gene
S07_59418009	7	59418009	1.32E-15	33.92189161	
S07_59406473	7	59406473	1.32E-15	33.60260527	
S07_59406503	7	59406503	1.32E-15	33.60260527	
S07_59366675	7	59366675	2.07E-15	32.84948767	
S07_59396111	7	59396111	1.03E-14	32.66580435	
S07_59404098	7	59404098	1.03E-14	32.09894474	
S07_59768820	7	59768820	1.03E-14	30.85283116	
S07_59519118	7	59519118	3.39E-14	18.67697807	
S07_59417972	7	59417972	8.29E-12	28.13954901	
S07_59439884	7	59439884	2.83E-11	27.6283758	
S07_59456813	7	59456813	6.90E-11	14.48470446	
S07_59456807	7	59456807	1.88E-09	25.30640307	
S07_59512451	7	59512451	5.62E-09	29.91113092	
S07_59858203	7	59858203	2.87E-08	25.58685947	
S07_59177463	7	59177463	7.97E-06	20.32407942	
S07_61080813	7	61080813	2.26E-05	20.98017729	
S07_59419274	7	59419274	3.09E-05	20.37433902	
S07_60179636	7	60179636	7.22E-05	20.7888479	
S07_61098841	7	61098841	8.25E-05	19.21926228	
S07_59867803	7	59867803	8.25E-05	22.94405957	
S07_59867807	7	59867807	8.25E-05	22.94405957	
S07_59867808	7	59867808	8.25E-05	22.94405957	
S07_59867811	7	59867811	8.25E-05	22.94405957	
S07_60104728	7	60104728	0.000126242	20.090935	
S07_59808206	7	59808206	0.000148646	22.96385605	Dw3 (Sobic.007G163800)
S07_60734373	7	60734373	0.000325148	19.43527099	
S03_12923320	3	12923320	0.000419087	23.01086475	
S03_12923423	3	12923423	0.001202258	21.16817999	
S07_59953003	7	59953003	0.001499968	20.87815555	
S03_12923421	3	12923421	0.00161679	20.67916815	

Table B.2 Top 30 significant SNPs for top collar height identified by GWAS using the MLM model. The SNP identified *Dw3* is highlighted in red color.

SNP	Chromosome	Position	FDR_Adjusted_P-values	Effect	Candidate Gene
S07_59418009	7	59418009	2.64E-17	37.29117909	
S07_59768820	7	59768820	2.94E-17	35.06698942	
S07_59406473	7	59406473	2.94E-17	36.67021174	
S07_59406503	7	59406503	2.94E-17	36.67021174	
S07_59366675	7	59366675	3.80E-17	35.9829798	
S07_59404098	7	59404098	4.00E-16	35.05231585	
S07_59396111	7	59396111	5.63E-16	35.39298664	
S07_59519118	7	59519118	3.71E-15	20.12108814	
S07_59417972	7	59417972	2.33E-13	31.08293979	
S07_59439884	7	59439884	9.85E-13	30.48284523	
S07_59456813	7	59456813	2.02E-12	16.04872783	
S07_59858203	7	59858203	6.99E-11	30.11164071	
S07_59456807	7	59456807	6.99E-11	28.06369392	
S07_59512451	7	59512451	4.96E-10	32.72978253	
S07_59177463	7	59177463	7.96E-07	22.57499564	
S07_59419274	7	59419274	1.60E-06	23.16714808	
S07_59867803	7	59867803	1.90E-06	26.88128747	
S07_59867807	7	59867807	1.90E-06	26.88128747	
S07_59867808	7	59867808	1.90E-06	26.88128747	
S07_59867811	7	59867811	1.90E-06	26.88128747	
S07_61080813	7	61080813	5.83E-06	22.62566997	
S07_60179636	7	60179636	2.87E-05	22.22426852	
S07_60104728	7	60104728	2.95E-05	22.02893349	
S07_59953003	7	59953003	3.80E-05	24.99925212	
S07_61098841	7	61098841	5.11E-05	20.3324984	
S07_59808206	7	59808206	5.11E-05	24.82767244	Dw3 (Sobic.007G163800)
S07_60734373	7	60734373	7.19E-05	21.36083259	
S03_12923320	3	12923320	0.000136873	24.98433788	
S03_12923423	3	12923423	0.000197993	23.61926533	
S03_12923421	3	12923421	0.000313052	23.00766472	

Table B.3 Top 30 significant SNPs for ADB identified by GWAS using the MLM model. The SNPs identified *Dw3* are highlighted in red color.

SNP	Chromosome	Position	FDR_Adjusted_P-values	Effect	Candidate Gene
S07_59768820	7	59768820	7.23E-12	118.6496394	
S07_59406473	7	59406473	4.65E-10	113.3968863	
S07_59406503	7	59406503	4.65E-10	113.3968863	
S07_59418009	7	59418009	1.77E-09	110.0597141	
S07_59519118	7	59519118	2.31E-09	64.50796374	
S07_59366675	7	59366675	3.56E-09	106.4584363	
S07_59404098	7	59404098	9.55E-09	104.5896615	
S07_59396111	7	59396111	1.87E-08	104.4990046	
S07_59456813	7	59456813	5.68E-08	52.25569666	
S07_59417972	7	59417972	6.78E-08	97.00163759	
S07_59858203	7	59858203	2.03E-07	101.2938716	
S07_59439884	7	59439884	9.24E-07	91.11319191	
S07_59456807	7	59456807	9.24E-07	90.36344323	
S07_59512451	7	59512451	3.01E-06	106.1016626	
S07_60179636	7	60179636	9.09E-06	91.34288674	
S07_59867803	7	59867803	1.60E-05	99.74843046	
S07_59867807	7	59867807	1.60E-05	99.74843046	
S07_59867808	7	59867808	1.60E-05	99.74843046	
S07_59867811	7	59867811	1.60E-05	99.74843046	
S03_12923423	3	12923423	0.000526931	91.29719661	
S07_60734373	7	60734373	0.00067338	77.95376467	
S07_59812218	7	59812218	0.001303313	86.93278687	Dw3 (Sobic.007G163800)
S07_59808206	7	59808206	0.001542928	87.12364901	Dw3 (Sobic.007G163800)
S07_61080813	7	61080813	0.001592638	73.35416016	
S03_12923421	3	12923421	0.002078499	85.1698318	
S07_59419274	7	59419274	0.003182467	69.94142254	
S07_60104728	7	60104728	0.005268951	71.33627934	
S07_60042381	7	60042381	0.006828875	97.80326848	
S07_59811910	7	59811910	0.006828875	80.0502064	Dw3 (Sobic.007G163800)
S07_59788255	7	59788255	0.012359118	96.30598947	

Table B.4 Significant SNPs and candidate genes for moisture identified by GWAS using the MLM model.

SNP	Chromosome	Position	FDR_Adjusted_P-values	Effect	Candidate Gene
S06_50914827	6	50914827	0.004339062	0.0123007	Sobic.006G147450 D locus (Sobic.006G147400)
S06_50914738	6	50914738	0.041508039	0.011026165	Sobic.006G147450 D locus (Sobic.006G147400)

Table B.5 Significant SNPs and candidate genes for apex height identified by GWAS using the FarmCPU model at FDR 0.05.

SNP	Chromosome	Position	FDR_Adjusted_P-values	Effect	Candidate Gene
S09_57212498	9	57212498	2.14E-13	19.36432133	Sobic.009G231900
					Sobic.009G232000
					Sobic.009G232100
					Sobic.009G232200
					Sobic.009G232266
S07_59366675	7	59366675	1.04E-09	19.3624711	Sobic.007G158800
					Sobic.007G158900
					Sobic.007G159000
					Sobic.007G159100
					Sobic.007G159200
S07_59768820	7	59768820	8.11E-05	15.25066826	Sobic.007G163300
S07_5435798	7	5435798	0.002566026	11.83594916	Sobic.007G053500
					Sobic.007G053600
					Sobic.007G053700
					Sobic.007G053800
					Sobic.007G053900
					Sobic.007G054000
S02_73983796	2	73983796	0.004214251	-16.20805182	Sobic.002G384500
					Sobic.002G384600
					Sobic.002G384700
					Sobic.002G384800
					Sobic.002G384900
					Sobic.002G385000
					Sobic.002G385100
					Sobic.002G385200
S07_162826	7	162826	0.004214251	14.17623088	Sobic.007G001800
					Sobic.007G001900
					Sobic.007G002000
S03_4997705	3	4997705	0.006740849	13.06907546	Sobic.003G055500
					Sobic.003G055600
					Sobic.003G055700
					Sobic.003G055800
					Sobic.003G055900
					Sobic.003G056000
S03_19146851	3	19146851	0.008286311	-24.04725933	Sobic.003G160500
					Sobic.003G160600
					Sobic.003G160700
					Sobic.003G160800
					Sobic.003G160900

					Sobic.003G161000
S07_60179636	7	60179636	0.008984154	11.37533094	Sobic.007G166600
					Sobic.007G166701
					Sobic.007G166800
					Sobic.007G166900
S05_65547442	5	65547442	0.015412995	18.47867137	NA
S10_2514019	10	2514019	0.015412995	-19.82035373	Sobic.010G030900
					Sobic.010G031000
					Sobic.010G031100
					Sobic.010G031300
S02_64340809	2	64340809	0.015412995	-14.79558451	Sobic.002G257500
					Sobic.002G257600
					Sobic.002G257750
S10_7243966	10	7243966	0.015412995	-10.61215355	Sobic.010G084800
					Sobic.010G084900
					Sobic.010G085000
					Sobic.010G085100
S02_69475078	2	69475078	0.024599745	-5.968266738	Sobic.002G323400
					Sobic.002G323500
					Sobic.002G323600
					Sobic.002G323700
					Sobic.002G323800
					Sobic.002G324000
S04_64174744	4	64174744	0.028531137	19.30975	Sobic.004G302800
					Sobic.004G302900
					Sobic.004G303000
					Sobic.004G303100

Table B.6 Significant SNPs and candidate genes for ADB identified by GWAS using the FarmCPU model at FDR 0.05. maf is the minor allele frequency.

SNP	Chr.	Position	maf	FDR_Adjusted_P-values	Effect	Candidate Gene
S07_59768820	7	59768820	0.18	2.84E-12	88.39048698	Sobic.007G163300
S03_60588984	3	60588984	0.44	0.0030591	-72.50751714	Sobic.003G268900
						Sobic.003G269000
						Sobic.003G269100
						Sobic.003G269200
S07_61080813	7	61080813	0.18	0.0030591	49.22520134	Sobic.007G176900
						Sobic.007G177000
						Sobic.007G177100
						Sobic.007G177150
S01_30652981	1	30652981	0.05	0.009021874	-70.94533737	Sobic.001G258200
						Sobic.001G258300
S05_66379531	5	66379531	0.05	0.009021874	-60.1349911	Sobic.005G180700
						Sobic.005G180800
						Sobic.005G180850
						Sobic.005G180900
						Sobic.005G181000
						Sobic.005G181100
S09_54144857	9	54144857	0.14	0.00919189	-42.93501107	Sobic.009G189400
						Sobic.009G189501
						Sobic.009G189600
						Sobic.009G189700
S08_59178415	8	59178415	0.35	0.00919189	48.62032508	Sobic.008G158666
						Sobic.008G158732
						Sobic.008G158800
						Sobic.008G158900
						Sobic.008G159000
S01_62076176	1	62076176	0.18	0.010002105	-45.72432058	Sobic.001G332000
						Sobic.001G332050
						Sobic.001G332100
						Sobic.001G332200
						Sobic.001G332300
						Sobic.001G332400
S08_2579008	8	2579008	0.39	0.010002105	-62.26467186	Sobic.008G028700
						Sobic.008G028800
						Sobic.008G028850
						Sobic.008G028900
S01_ 74145303	1	74145303	0.12	0.010002105	61.18914483	Sobic.001G468400
						Sobic.001G468500
						Sobic.001G468600

						Sobic.001G468700
S09_56521150	9	56521150	0.31	0.01480418	20.52168866	Sobic.009G222200
						Sobic.009G222400
						Sobic.009G222500
						Sobic.009G222600
S06_2686264	6	2686264	0.03	0.015488734	83.18787512	Sobic.006G017000
						Sobic.006G017100
						Sobic.006G017200
S02_2417641	2	2417641	0.04	0.026634424	54.5982114	Sobic.002G026200
						Sobic.002G026300

Table B.7 Top 30 significant SNPs for LiDAR height at 600GDD identified by GWAS using the MLM model. The SNPs identified *Dw3* are highlighted in red color.

SNP	Chromosome	Position	FDR_Adjusted _P-values	Effect	Candidate Gene
S07_59768820	7	59768820	1.42E-18	0.193708677	
S07_59418009	7	59418009	7.83E-18	0.198339872	
S07_59366675	7	59366675	4.55E-17	0.190969365	
S07_59406473	7	59406473	1.37E-16	0.189838032	
S07_59406503	7	59406503	1.37E-16	0.189838032	
S07_59404098	7	59404098	3.58E-16	0.185543836	
S07_59519118	7	59519118	1.74E-15	0.107365342	
S07_59396111	7	59396111	2.07E-15	0.183684273	
S07_59417972	7	59417972	6.75E-15	0.17253425	
S07_59858203	7	59858203	5.46E-13	0.172278952	
S07_59439884	7	59439884	5.23E-12	0.156668435	
S07_59456813	7	59456813	1.01E-11	0.082473882	
S07_59512451	7	59512451	5.33E-11	0.179885772	
S07_59456807	7	59456807	3.97E-10	0.143383264	
S07_59419274	7	59419274	1.58E-07	0.129497825	
S07_59808206	7	59808206	6.99E-07	0.149449048	Dw3 (Sobic.007G163800)
S07_59177463	7	59177463	3.18E-06	0.114571749	
S07_59811910	7	59811910	1.84E-05	0.134234256	Dw3 (Sobic.007G163800)
S07_59867803	7	59867803	1.84E-05	0.132657602	
S07_59867807	7	59867807	1.84E-05	0.132657602	
S07_59867808	7	59867808	1.84E-05	0.132657602	
S07_59867811	7	59867811	1.84E-05	0.132657602	
S07_59812218	7	59812218	1.92E-05	0.133698204	Dw3 (Sobic.007G163800)
S07_59995136	7	59995136	2.15E-05	-0.098264052	
S03_12923320	3	12923320	2.38E-05	0.139438609	
S07_59953003	7	59953003	3.30E-05	0.131859822	
S07_59995132	7	59995132	3.30E-05	-0.09648988	
S07_59995134	7	59995134	3.30E-05	-0.09648988	
S07_61080813	7	61080813	3.30E-05	0.112397406	
S07_59995137	7	59995137	5.08E-05	-0.095243569	

Table B.8 Top 30 significant SNPs for LiDAR height at 800GDD identified by GWAS using the MLM model. The SNPs identified *Dw3* are highlighted in red color.

SNP	Chromosome	Position	FDR_Adjusted _P-values	Effect	Candidate Gene
S07_59418009	7	59418009	7.05E-17	0.358474554	
S07_59366675	7	59366675	4.12E-16	0.343620962	
S07_59519118	7	59519118	1.76E-15	0.197134459	
S07_59404098	7	59404098	1.76E-15	0.33387843	
S07_59406473	7	59406473	1.76E-15	0.336866713	
S07_59406503	7	59406503	1.76E-15	0.336866713	
S07_59768820	7	59768820	1.76E-15	0.31900568	
S07_59396111	7	59396111	2.88E-15	0.336268672	
S07_59417972	7	59417972	1.61E-14	0.313185539	
S07_59439884	7	59439884	3.83E-11	0.279056642	
S07_59456813	7	59456813	1.59E-10	0.144728095	
S07_59512451	7	59512451	1.77E-10	0.323593629	
S07_59858203	7	59858203	5.53E-10	0.28007516	
S07_59456807	7	59456807	2.62E-09	0.253943097	
S07_59808206	7	59808206	1.06E-06	0.271401013	Dw3 (Sobic.007G163800)
S07_59419274	7	59419274	4.44E-06	0.218155383	
S07_59177463	7	59177463	2.37E-05	0.19858549	
S07_61080813	7	61080813	2.37E-05	0.211524129	
S07_61098841	7	61098841	3.02E-05	0.201820446	
S07_59812218	7	59812218	3.02E-05	0.242568708	Dw3 (Sobic.007G163800)
S07_59811910	7	59811910	6.44E-05	0.23647455	Dw3 (Sobic.007G163800)
S07_60179636	7	60179636	8.66E-05	0.207567627	
S03_12923320	3	12923320	0.000233034	0.237619148	
S07_60036945	7	60036945	0.000277129	0.144571087	
S07_60104728	7	60104728	0.0003568	0.195326671	
S07_59995136	7	59995136	0.0003568	-0.163629241	
S03_12923423	3	12923423	0.000371423	0.222975898	
S07_60853629	7	60853629	0.000392736	0.182663559	
S07_59995132	7	59995132	0.00058065	-0.159987334	
S07_59995134	7	59995134	0.00058065	-0.159987334	

Table B.9 Top 30 significant SNPs for LiDAR height at 1000GDD identified by GWAS using the MLM model. The SNPs identified *Dw3* are highlighted in red color.

SNP	Chromosome	Position	FDR_Adjusted _P-values	Effect	Candidate Gene
S07_59418009	7	59418009	4.45E-15	0.334797294	
S07_59406473	7	59406473	1.47E-14	0.324542936	
S07_59406503	7	59406503	1.47E-14	0.324542936	
S07_59366675	7	59366675	1.47E-14	0.319555126	
S07_59519118	7	59519118	4.57E-14	0.186425955	
S07_59396111	7	59396111	4.59E-14	0.319059542	
S07_59404098	7	59404098	4.59E-14	0.313631686	
S07_59768820	7	59768820	6.34E-14	0.29881646	
S07_59417972	7	59417972	1.75E-12	0.287606289	
S07_59439884	7	59439884	1.45E-10	0.267969007	
S07_59456813	7	59456813	3.05E-10	0.140652223	
S07_59456807	7	59456807	6.76E-09	0.24586367	
S07_59512451	7	59512451	8.02E-09	0.295657397	
S07_59858203	7	59858203	1.09E-08	0.259798574	
S07_61080813	7	61080813	3.37E-06	0.220950541	
S07_59808206	7	59808206	8.73E-06	0.252537589	Dw3 (Sobic.007G163800)
S07_60179636	7	60179636	1.62E-05	0.216922618	
S07_59177463	7	59177463	3.41E-05	0.193099312	
S07_59419274	7	59419274	4.31E-05	0.200080004	
S07_61098841	7	61098841	4.31E-05	0.196199472	
S03_12923320	3	12923320	0.00016134	0.238262923	
S07_60104728	7	60104728	0.000236365	0.196276839	
S07_59812218	7	59812218	0.000314729	0.220551477	Dw3 (Sobic.007G163800)
S07_59867803	7	59867803	0.000475918	0.213811681	
S07_59867807	7	59867807	0.000475918	0.213811681	
S07_59867808	7	59867808	0.000475918	0.213811681	
S07_59867811	7	59867811	0.000475918	0.213811681	
S03_12923423	3	12923423	0.000492644	0.21748174	
S07_60734373	7	60734373	0.000676201	0.188044712	
S07_59811910	7	59811910	0.000706599	0.211843924	Dw3 (Sobic.007G163800)

Table B.10 Significant SNPs and candidate genes for LiDAR height at 600GDD identified by GWAS using the FarmCPU model at FDR 0.01-0.05.

SNP	Chromosome	Position	FDR_Adjusted_P-values	Effect	Candidate Gene
S04_19708160	4	19708160	0.013817917	-0.10	Sobic.004G132100
S07_6406155	7	6406155	0.016738529	-0.05	Sobic.007G060900
					Sobic.007G061000
					Sobic.007G061100
S01_19694712	1	19694712	0.017085552	0.07	Sobic.001G213100
					Sobic.001G213150
					Sobic.001G213200
					Sobic.001G213300
					Sobic.001G213400
					Sobic.001G213500
					Sobic.001G213666
S05_2405371	5	2405371	0.02598287	0.09	Sobic.005G026700
					Sobic.005G026800
					Sobic.005G026900
					Sobic.005G026966
					Sobic.005G027032
					Sobic.005G027100
					Sobic.005G027200
S05_878607	5	878607	0.02598287	-0.05	Sobic.005G010000
					Sobic.005G010100
					Sobic.005G010200
S05_25002895	5	25002895	0.037074903	-0.05	NA

Table B.11 Significant SNPs and candidate genes for LiDAR height at 800GDD identified by GWAS using the FarmCPU model at FDR 0.01-0.05.

SNP	Chromosome	Position	FDR_Adjusted_P-values	Effect	Candidate Gene
S05_878607	5	878607	0.022839766	-0.10	Sobic.005G010000
					Sobic.005G010100
					Sobic.005G010200
S01_13896487	1	13896487	0.035231064	-0.14	Sobic.001G166800
					Sobic.001G166900
					Sobic.001G167000
					Sobic.001G167100
S02_3316734	2	3316734	0.042744968	-0.13	NA
S01_75602579	1	75602579	0.046834208	0.09	Sobic.001G485200
					Sobic.001G485300

Table B.12 Significant SNPs and candidate genes for LiDAR height at 1000GDD identified by GWAS using the FarmCPU model at FDR 0.01-0.05.

SNP	Chromosome	Position	FDR_Adjusted_P-values	Effect	Candidate Gene
S02_68931676	2	68931676	0.010926168	-0.19	Sobic.002G315700
					Sobic.002G315800
					Sobic.002G315900
					Sobic.002G316000
					Sobic.002G316100
					Sobic.002G316200
					Sobic.002G316301
					Sobic.002G316400
S07_60739929	7	60739929	0.010926168	-0.15	Sobic.007G172200
					Sobic.007G172300
					Sobic.007G172400
					Sobic.007G172500
S10_7243966	10	7243966	0.010926168	-0.11	Sobic.010G084800
					Sobic.010G084900
					Sobic.010G085000
					Sobic.010G085100
S01_78384379	1	78384379	0.037993818	-0.11	Sobic.001G517400
					Sobic.001G517500
					Sobic.001G517600
					Sobic.001G517700
					Sobic.001G517800
S03_19146851	3	19146851	0.040134739	-0.22	Sobic.003G160500
					Sobic.003G160600
					Sobic.003G160700
					Sobic.003G160800
					Sobic.003G160900
					Sobic.003G161000

APPENDIX C. CHAPTER 4

Table C.1 SRUE and ADB values for each genotype in the SbDIV TC in 2018, 2019, 2020, and the average across three years. SRUE is seasonal radiation use efficiency. ADB is aboveground dry biomass.

ID	Genotype	ADB18	ADB19	ADB20	Avg.ADB	SRUE18	SRUE19	SRUE20	Avg.SRUE
			g/m^2				g/MJ		
1	BOK11	1919.38	1427.94	1469.92	1605.75	1.48	1.05	1.10	1.21
2	BQL41	1349.74	1640.69	1495.98	1495.47	1.13	1.30	1.17	1.20
3	BTx2752	1565.50	1458.54	1644.45	1556.16	1.18	1.11	1.27	1.19
4	BTx3042	1280.80	1769.19	1531.07	1527.02	0.95	1.37	1.16	1.16
5	BTx3197	1359.35	1461.40	1522.33	1447.69	1.07	1.14	1.18	1.13
6	BTx378	1756.96	1687.96	1486.50	1643.80	1.38	1.29	1.13	1.27
7	BTx399	1292.62	1453.84	1493.22	1413.23	1.01	1.11	1.11	1.08
8	BTx615	1708.46	1548.29	1574.72	1610.49	1.31	1.18	1.20	1.23
9	BTx641	2247.45	1585.19	1352.92	1728.52	1.78	1.19	1.03	1.33
10	BTx642	1653.35	1615.15	1634.73	1634.41	1.23	1.24	1.25	1.24
11	BTx643	1529.42	1395.64	1061.27	1328.78	1.24	1.04	0.86	1.05
12	BTx645	1765.94	1446.45	1524.00	1578.79	1.43	1.19	1.25	1.29
13	Caprock	1374.18	1359.94	1253.22	1329.11	1.05	1.00	0.95	1.00
14	Comb7078	1614.38	1540.49	1494.62	1549.83	1.22	1.19	1.18	1.20
15	Day	1623.19	1673.52	1500.51	1599.08	1.25	1.24	1.13	1.21
16	Dorado	1782.55	1755.70	1796.43	1778.23	1.38	1.35	1.37	1.37
17	DwfYellMilo	3271.80	2204.50	2549.05	2675.12	2.31	1.60	1.80	1.91
18	KS19	1696.08	1459.37	1540.65	1565.37	1.26	1.13	1.15	1.18
19	Martin	1507.03	1404.56	1249.55	1387.05	1.18	1.10	0.99	1.09
20	MR732	2024.03	1631.28	1821.88	1825.73	1.59	1.28	1.43	1.43
21	P_721	1950.09	1487.95	1531.04	1656.36	1.42	1.14	1.17	1.24
22	P9517	1715.82	1599.43	1356.70	1557.32	1.32	1.25	1.01	1.19
23	Redbine	1511.53	1417.31	1477.68	1468.84	1.11	1.09	1.11	1.10
24	RTAM2566	1509.10	1427.53	1319.78	1418.80	1.20	1.11	1.01	1.10
25	RTAM428	1535.04	1376.44	1356.34	1422.61	1.26	1.06	1.12	1.15
26	RTx2917	1980.95	1334.00	1454.04	1589.66	1.55	1.06	1.11	1.24
27	RTx434	1757.38	1468.42	1700.32	1642.04	1.31	1.12	1.25	1.23
28	RTx437	1994.13	1556.85	1534.26	1695.08	1.57	1.19	1.22	1.33
29	SanChiSan	1896.21	1786.18	2074.94	1919.11	1.45	1.37	1.57	1.47
30	SC0002	1627.94	1755.34	1487.72	1623.67	1.22	1.32	1.12	1.22
31	SC0003	1544.82	1376.73	1800.34	1573.96	1.17	1.08	1.45	1.23
32	SC0004	1337.92	1608.99	1542.31	1496.41	1.04	1.24	1.20	1.16
33	SC0007	1954.46	1702.63	1877.96	1845.01	1.48	1.29	1.39	1.39
34	SC0012	1894.40	1776.62	1741.87	1804.30	1.50	1.48	1.33	1.44

35	SC0013	1605.21	1454.39	1664.86	1574.82	1.20	1.06	1.28	1.18
36	SC0015	1647.87	1696.09	1666.97	1670.31	1.27	1.30	1.23	1.27
37	SC0016	2132.49	1662.56	1902.13	1899.06	1.65	1.26	1.43	1.45
38	SC0017	1494.42	1518.46	1729.36	1580.75	1.18	1.21	1.34	1.24
39	SC0019	2014.61	1854.36	1902.51	1923.83	1.66	1.47	1.45	1.53
40	SC0020	1689.74	1692.56	1628.40	1670.23	1.30	1.31	1.22	1.28
41	SC0021	1809.38	1630.79	1686.99	1709.05	1.41	1.27	1.38	1.35
42	SC0022	1998.48	1654.55	1620.25	1757.76	1.57	1.23	1.18	1.33
43	SC0027	1907.80	1707.81	1894.39	1836.66	1.46	1.23	1.44	1.38
44	SC0033	1691.97	1553.88	1484.10	1576.65	1.26	1.26	1.19	1.24
45	SC0035	1857.32	1452.16	1590.24	1633.24	1.39	1.12	1.19	1.23
46	SC0037	1807.05	1708.78	1583.12	1699.65	1.48	1.31	1.21	1.33
47	SC0041	1952.17	1742.26	1633.01	1775.81	1.51	1.40	1.27	1.39
48	SC0042	1766.94	1616.73	1731.45	1705.04	1.40	1.32	1.35	1.35
49	SC0043	1793.10	1678.35	1809.19	1760.22	1.46	1.26	1.40	1.37
50	SC0044	2049.46	1639.58	2374.65	2021.23	1.57	1.31	1.74	1.54
51	SC0048	1077.01	1440.02	1743.59	1420.20	0.84	1.15	1.31	1.10
52	SC0049	1917.68	1425.13	1875.78	1739.53	1.50	1.04	1.44	1.33
53	SC0050	1388.45	1541.58	1792.37	1574.13	1.11	1.23	1.42	1.25
54	SC0051	1299.98	1568.56	1613.63	1494.05	0.97	1.19	1.20	1.12
55	SC0052	1578.38	1834.68	1552.52	1655.19	1.27	1.44	1.19	1.30
56	SC0053	2022.04	1922.69	2026.82	1990.52	1.48	1.44	1.49	1.47
57	SC0054	2256.63	1769.61	2008.57	2011.60	1.70	1.35	1.55	1.53
58	SC0056	1543.82	1550.39	1667.87	1587.36	1.21	1.16	1.36	1.24
59	SC0058	1467.37	1683.98	1775.71	1642.35	1.10	1.28	1.38	1.25
60	SC0059	2237.18	1759.96	2195.84	2064.32	1.65	1.35	1.71	1.57
61	SC0060	2089.50	2056.20	1720.29	1955.33	1.53	1.51	1.31	1.45
62	SC0062	1358.22	1429.86	1505.52	1431.20	1.08	1.15	1.17	1.14
63	SC0063	2128.48	1533.35	1852.04	1837.96	1.63	1.13	1.36	1.38
64	SC0066	1467.09	1662.79	1436.16	1522.01	1.18	1.28	1.17	1.21
65	SC0067	2024.11	2131.21	2214.11	2123.14	1.46	1.51	1.60	1.52
66	SC0068	1205.24	1646.75	1737.88	1529.96	0.97	1.25	1.33	1.18
67	SC0069	2221.95	2251.31	1568.28	2013.85	1.73	1.76	1.16	1.55
68	SC0072	2247.74	1970.97	2111.26	2109.99	1.72	1.48	1.60	1.60
69	SC0073	1431.25	1568.51	1621.46	1540.41	1.15	1.29	1.28	1.24
70	SC0074	1524.02	1287.26	1446.60	1419.29	1.21	1.01	1.19	1.14
71	SC0075	1567.32	1752.70	1557.33	1625.79	1.23	1.36	1.21	1.27
72	SC0077	2343.92	1863.35	2027.73	2078.33	1.81	1.43	1.55	1.60
73	SC0078	1848.56	1519.86	1698.11	1688.85	1.44	1.18	1.36	1.33
74	SC0079	1781.35	1711.60	1760.87	1751.28	1.48	1.36	1.38	1.41
75	SC0080	1881.97	2062.96	1963.94	1969.62	1.45	1.62	1.54	1.54
76	SC0083	1688.93	2004.12	2031.14	1908.06	1.30	1.62	1.55	1.49
77	SC0085	1635.60	1577.64	1489.61	1567.62	1.24	1.31	1.22	1.26

78	SC0086	1548.32	1428.43	1563.96	1513.57	1.22	1.16	1.22	1.20
79	SC0087	2218.89	1843.92	2027.50	2030.10	1.67	1.38	1.51	1.52
80	SC0091	2353.49	1775.78	2254.13	2127.80	1.89	1.29	1.76	1.64
81	SC0092	2136.41	1818.74	2221.27	2058.81	1.61	1.34	1.60	1.51
82	SC0093	1300.74	1780.47	1711.81	1597.67	1.02	1.38	1.29	1.23
83	SC0094	1703.21	1758.68	1725.46	1729.12	1.26	1.35	1.27	1.30
84	SC0097	1462.00	1520.46	1696.12	1559.53	1.17	1.21	1.29	1.22
85	SC0098	2020.12	1712.97	2173.77	1968.95	1.52	1.26	1.58	1.45
86	SC0101	1242.06	1627.08	1623.23	1497.46	0.98	1.27	1.27	1.17
87	SC0103	1698.91	1763.42	1656.47	1706.27	1.33	1.31	1.24	1.29
88	SC0105	1319.96	1724.20	1565.73	1536.63	1.01	1.35	1.17	1.18
89	SC0106	1517.21	1693.60	1789.61	1666.81	1.14	1.29	1.38	1.27
90	SC0108	1641.09	1601.06	1602.26	1614.80	1.29	1.23	1.28	1.27
91	SC0109	1220.99	1351.45	1371.80	1314.75	0.91	1.05	1.03	1.00
92	SC0110	1649.56	1528.00	1530.57	1569.38	1.26	1.15	1.21	1.21
93	SC0111	2004.15	1808.04	1839.41	1883.86	1.46	1.32	1.36	1.38
94	SC0112	1855.30	1770.20	1615.68	1747.06	1.44	1.33	1.30	1.36
95	SC0113	1271.67	1440.31	1507.02	1406.33	1.08	1.16	1.17	1.14
96	SC0114	1920.82	1948.10	2038.08	1969.00	1.49	1.40	1.49	1.46
97	SC0115	1745.64	1569.54	1483.36	1599.51	1.32	1.25	1.13	1.23
98	SC0118	1026.91	1723.75	1723.60	1491.42	0.78	1.33	1.27	1.13
99	SC0119	1529.51	1649.86	1492.01	1557.13	1.18	1.25	1.14	1.19
100	SC0121	2158.55	1837.96	1950.48	1982.33	1.62	1.39	1.45	1.49
101	SC0123	1488.60	1919.84	1917.51	1775.32	1.14	1.44	1.47	1.35
102	SC0124	1743.16	1686.82	2015.99	1815.32	1.27	1.24	1.41	1.31
103	SC0126	1715.73	1945.26	1840.03	1833.67	1.36	1.47	1.41	1.41
104	SC0127	1253.22	1717.20	1561.96	1510.79	0.99	1.28	1.21	1.16
105	SC0131	1673.27	1597.38	1834.18	1701.61	1.30	1.21	1.41	1.31
106	SC0134	1451.96	1686.53	1847.04	1661.84	1.11	1.33	1.41	1.28
107	SC0136	1483.23	1621.83	1505.32	1536.79	1.24	1.32	1.22	1.26
108	SC0137	1710.82	1649.84	1741.50	1700.72	1.32	1.29	1.30	1.30
109	SC0138	1258.36	1916.42	1733.57	1636.12	0.99	1.46	1.37	1.27
110	SC0139	1504.58	1857.94	1656.29	1672.94	1.17	1.47	1.34	1.33
111	SC0140	2059.76	1639.65	1908.40	1869.27	1.56	1.25	1.45	1.42
112	SC0142	1288.40	1506.75	1480.94	1425.36	1.00	1.16	1.15	1.11
113	SC0146	1548.39	1521.82	1474.87	1515.03	1.23	1.15	1.12	1.17
114	SC0147	1920.30	1760.79	1687.50	1789.53	1.42	1.34	1.26	1.34
115	SC0150	1444.02	1747.38	1773.58	1654.99	1.07	1.38	1.34	1.26
116	SC0154	1608.99	1407.22	1508.61	1508.27	1.25	1.08	1.16	1.16
117	SC0156	2112.11	1501.01	1778.05	1797.05	1.66	1.10	1.35	1.37
118	SC0157	1604.27	1430.33	2003.79	1679.46	1.25	1.10	1.52	1.29
119	SC0159	2297.96	1354.56	1956.97	1869.83	1.82	1.02	1.48	1.44
120	SC0161	2101.49	2338.91	2166.27	2202.22	1.55	1.68	1.56	1.60

121	SC0165	1641.65	1658.84	1790.85	1697.11	1.22	1.21	1.33	1.25
122	SC0166	1746.88	1479.52	1719.43	1648.61	1.37	1.17	1.28	1.27
123	SC0171	1945.25	1805.73	1504.03	1751.67	1.59	1.36	1.14	1.36
124	SC0172	1548.51	1370.88	1488.12	1469.17	1.14	1.05	1.25	1.15
125	SC0173	1516.68	1566.39	1259.42	1447.49	1.21	1.24	1.04	1.16
126	SC0175	1922.96	2015.88	2231.16	2056.67	1.49	1.48	1.67	1.55
127	SC0176	1478.31	1706.72	1453.71	1546.25	1.14	1.30	1.15	1.20
128	SC0178	1473.84	1651.83	1611.79	1579.16	1.17	1.25	1.17	1.20
129	SC0179	1472.47	1682.33	1853.64	1669.48	1.15	1.23	1.37	1.25
130	SC0181	1694.04	1718.98	1615.24	1676.08	1.28	1.29	1.19	1.26
131	SC0182	1888.73	1332.64	1424.92	1548.76	1.38	0.98	1.04	1.13
132	SC0183	2060.35	1684.83	1510.70	1751.96	1.71	1.30	1.13	1.38
133	SC0184	1379.47	1541.18	1597.35	1506.00	1.09	1.19	1.17	1.15
134	SC0186	1484.05	1507.25	1590.88	1527.39	1.16	1.14	1.21	1.17
135	SC0187	1212.61	1575.21	1671.45	1486.42	0.94	1.19	1.22	1.12
136	SC0188	1546.83	2056.07	1859.02	1820.64	1.17	1.54	1.35	1.35
137	SC0191	1870.44	1676.10	2184.15	1910.23	1.41	1.27	1.62	1.43
138	SC0192	1448.04	1689.71	1702.15	1613.30	1.12	1.25	1.28	1.22
139	SC0201	2980.58	1869.62	1988.82	2279.67	2.22	1.32	1.43	1.66
140	SC0202	1382.26	1513.70	1404.28	1433.41	1.02	1.17	1.14	1.11
141	SC0207	1960.59	1595.31	1395.99	1650.63	1.47	1.24	1.06	1.26
142	SC0208	1754.93	1475.76	1716.94	1649.21	1.35	1.16	1.33	1.28
143	SC0210	1871.03	1703.12	1543.18	1705.78	1.47	1.35	1.13	1.32
144	SC0211	1535.41	1556.96	1391.15	1494.51	1.17	1.20	1.07	1.15
145	SC0212	1324.56	1724.65	1750.39	1599.87	1.07	1.32	1.34	1.24
146	SC0214	1276.85	1577.56	1358.45	1404.29	0.95	1.18	1.11	1.08
147	SC0215	1691.45	1463.45	1352.29	1502.39	1.33	1.12	1.10	1.18
148	SC0217	1829.14	1807.27	1953.19	1863.20	1.43	1.36	1.47	1.42
149	SC0218	1902.99	1705.19	1591.89	1733.36	1.46	1.28	1.30	1.35
150	SC0221	1503.04	1489.09	1602.40	1531.51	1.12	1.11	1.18	1.14
151	SC0223	1566.57	1809.29	1505.16	1627.01	1.25	1.35	1.13	1.24
152	SC0224	2598.63	1961.36	2155.78	2238.59	2.00	1.56	1.63	1.73
153	SC0226	1793.55	1767.02	1613.25	1724.61	1.45	1.38	1.31	1.38
154	SC0228	1480.97	1729.36	1821.38	1677.24	1.17	1.35	1.38	1.30
155	SC0230	1981.35	1600.53	1322.91	1634.93	1.63	1.25	1.08	1.32
156	SC0233	1441.92	1581.74	1474.51	1499.39	1.22	1.30	1.21	1.24
157	SC0235	1383.36	1718.02	1700.93	1600.77	1.10	1.38	1.33	1.27
158	SC0236	2257.51	1862.67	1967.55	2029.24	1.74	1.38	1.46	1.53
159	SC0239	2533.67	1932.34	1533.16	1999.73	1.90	1.47	1.21	1.53
160	SC0241	1600.84	1765.51	1890.34	1752.23	1.23	1.43	1.41	1.36
161	SC0243	1823.22	1850.91	1966.17	1880.10	1.42	1.46	1.49	1.46
162	SC0244	1397.78	1559.04	1536.99	1497.94	1.08	1.27	1.25	1.20
163	SC0247	1466.07	1566.02	1730.73	1587.61	1.09	1.16	1.24	1.16

164	SC0249	2235.56	1865.57	2077.78	2059.64	1.68	1.39	1.57	1.55
165	SC0250	1850.64	1776.84	1886.89	1838.12	1.36	1.34	1.45	1.38
166	SC0253	1992.27	1575.18	2045.21	1870.89	1.51	1.17	1.53	1.40
167	SC0254	2205.88	1717.23	1728.23	1883.78	1.69	1.25	1.31	1.42
168	SC0256	1622.35	1613.21	1763.69	1666.42	1.22	1.24	1.33	1.26
169	SC0257	1964.69	1907.84	2146.26	2006.26	1.49	1.47	1.59	1.52
170	SC0258	1736.38	1898.01	1645.04	1759.81	1.33	1.44	1.27	1.35
171	SC0259	1786.12	1404.13	1802.44	1664.23	1.37	1.09	1.32	1.26
172	SC0261	1788.25	1521.04	1965.20	1758.16	1.38	1.27	1.53	1.39
173	SC0262	1753.04	1504.31	1948.68	1735.34	1.36	1.18	1.51	1.35
174	SC0265	1716.23	1690.93	1588.59	1665.25	1.35	1.37	1.28	1.33
175	SC0266	1895.86	1788.63	2070.11	1918.20	1.49	1.40	1.52	1.47
176	SC0268	1604.17	1588.06	1607.38	1599.87	1.36	1.21	1.30	1.29
177	SC0269	1856.79	1798.37	1658.76	1771.31	1.41	1.41	1.30	1.37
178	SC0270	2427.80	2208.98	2116.07	2250.95	1.82	1.65	1.54	1.67
179	SC0272	1554.68	1733.66	1812.37	1700.24	1.18	1.40	1.37	1.32
180	SC0273	2076.02	1757.99	2126.47	1986.83	1.56	1.31	1.57	1.48
181	SC0275	1623.98	1712.82	1768.58	1701.79	1.24	1.36	1.32	1.30
182	SC0276	1994.03	1946.06	2334.81	2091.63	1.51	1.48	1.75	1.58
183	SC0277	1677.76	1727.81	2185.11	1863.56	1.31	1.34	1.62	1.42
184	SC0278	1321.56	1631.10	1416.65	1456.44	1.06	1.28	1.12	1.15
185	SC0279	1484.12	1704.83	1723.70	1637.55	1.15	1.27	1.30	1.24
186	SC0280	1661.79	2089.21	2156.52	1969.17	1.31	1.56	1.66	1.51
187	SC0282	1819.46	1694.86	1665.99	1726.77	1.52	1.33	1.22	1.36
188	SC0283	1969.85	1719.16	1552.55	1747.19	1.47	1.32	1.20	1.33
189	SC0284	1430.29	1539.39	1900.31	1623.33	1.09	1.18	1.44	1.24
190	SC0287	2400.60	1515.76	1589.75	1835.37	1.87	1.21	1.20	1.42
191	SC0289	1846.38	1392.71	1804.70	1681.26	1.39	1.05	1.32	1.25
192	SC0290	2486.92	1213.93	1834.64	1845.16	1.89	0.92	1.35	1.38
193	SC0291	1735.49	1855.88	1886.33	1825.90	1.30	1.40	1.44	1.38
194	SC0292	1649.21	1944.01	1869.07	1820.77	1.27	1.48	1.45	1.40
195	SC0293	2157.90	1574.20	1646.38	1792.83	1.62	1.17	1.55	1.45
196	SC0295	2352.46	1957.54	2171.07	2160.36	1.68	1.43	1.61	1.57
197	SC0296	1166.81	1444.85	1330.03	1313.90	0.89	1.17	1.02	1.03
198	SC0297	1552.14	1459.61	2217.03	1742.93	1.26	1.12	1.71	1.36
199	SC0298	2463.06	1295.12	1994.50	1917.56	1.81	0.99	1.46	1.42
200	SC0299	1996.18	2020.13	1901.41	1972.57	1.45	1.49	1.37	1.44
201	SC0300	1603.73	1466.50	1421.64	1497.29	1.21	1.11	1.13	1.15
202	SC0301	1742.68	1343.46	2154.13	1746.76	1.31	1.04	1.53	1.29
203	SC0303	1665.41	2156.62	1955.09	1925.71	1.30	1.61	1.49	1.47
204	SC0305	1752.14	1411.30	1601.25	1588.23	1.34	1.09	1.18	1.20
205	SC0308	1601.54	1642.95	1824.73	1689.74	1.17	1.27	1.37	1.27
206	SC0309	1774.96	1543.21	1815.41	1711.19	1.35	1.21	1.34	1.30

207	SC0311	1828.09	1550.10	1671.86	1683.35	1.41	1.17	1.29	1.29
208	SC0314	1987.62	1664.41	1779.05	1810.36	1.53	1.25	1.34	1.37
209	SC0315	1916.69	1898.54	1644.45	1819.89	1.52	1.39	1.23	1.38
210	SC0317	2359.29	2065.79	1934.36	2119.81	1.78	1.57	1.42	1.59
211	SC0319	2111.37	1526.68	1815.11	1817.72	1.57	1.12	1.40	1.36
212	SC0320	1388.22	1458.99	1497.83	1448.35	1.07	1.11	1.12	1.10
213	SC0322	1264.52	1517.12	1547.02	1442.89	1.01	1.18	1.19	1.13
214	SC0323	2187.41	1667.54	2150.48	2001.81	1.77	1.30	1.63	1.57
215	SC0325	1775.28	1407.14	1724.54	1635.66	1.39	1.10	1.29	1.26
216	SC0328	2013.14	2085.54	2409.72	2169.47	1.52	1.63	1.79	1.65
217	SC0329	1964.03	1804.87	1900.48	1889.80	1.45	1.40	1.46	1.43
218	SC0330	2498.67	2159.53	2047.17	2235.12	1.88	1.63	1.53	1.68
219	SC0331	1803.59	1933.46	1747.52	1828.19	1.45	1.48	1.34	1.42
220	SC0333	1874.87	1516.81	1757.78	1716.49	1.46	1.19	1.26	1.30
221	SC0334	1715.73	1745.89	2030.70	1830.77	1.35	1.33	1.51	1.40
222	SC0335	1692.21	1980.45	1850.49	1841.05	1.24	1.48	1.43	1.38
223	SC0336	1231.96	1483.52	1473.12	1396.20	0.94	1.15	1.15	1.08
224	SC0337	1756.96	1870.22	1801.58	1809.58	1.38	1.43	1.44	1.42
225	SC0338	2101.52	1992.89	1579.30	1891.24	1.50	1.45	1.25	1.40
226	SC0340	1556.23	1550.67	1445.79	1517.57	1.22	1.22	1.15	1.20
227	SC0343	2189.16	2178.54	1481.80	1949.83	1.63	1.53	1.03	1.40
228	SC0344	1351.92	1452.93	1486.28	1430.38	1.08	1.11	1.15	1.11
229	SC0345	1754.56	1516.24	1710.28	1660.36	1.32	1.21	1.32	1.28
230	SC0348	1900.03	1447.51	1558.85	1635.47	1.59	1.10	1.26	1.32
231	SC0349	1927.77	1913.51	1538.54	1793.27	1.42	1.43	1.18	1.35
232	SC0351	1256.87	2296.97	1816.25	1790.03	0.95	1.75	1.39	1.36
233	SC0352	1707.94	1813.90	1792.00	1771.28	1.31	1.36	1.33	1.33
234	SC0353	1768.09	1873.64	1827.26	1823.00	1.30	1.41	1.37	1.36
235	SC0354	1620.62	1917.47	1466.58	1668.23	1.41	1.48	1.18	1.36
236	SC0356	1141.21	1683.43	1739.86	1521.50	0.87	1.27	1.34	1.16
237	SC0358	1697.47	1812.66	1764.27	1758.13	1.27	1.38	1.32	1.32
238	SC0362	1377.31	1594.61	1637.48	1536.47	1.13	1.20	1.25	1.20
239	SC0366	1424.92	1773.81	1498.61	1565.78	1.17	1.43	1.19	1.26
240	SC0367	2002.36	1784.47	1884.75	1890.53	1.52	1.31	1.38	1.40
241	SC0368	1867.51	1694.51	2031.22	1864.41	1.42	1.29	1.57	1.43
242	SC0369	1699.30	1883.68	1967.79	1850.26	1.27	1.39	1.48	1.38
243	SC0371	1459.74	1686.30	1740.75	1628.93	1.20	1.25	1.36	1.27
244	SC0373	2080.27	1998.80	2062.60	2047.22	1.59	1.48	1.53	1.54
245	SC0374	1277.28	1492.52	1776.58	1515.46	1.00	1.16	1.30	1.15
246	SC0377	1736.43	1770.60	1895.62	1800.88	1.42	1.40	1.44	1.42
247	SC0380	1220.34	1868.91	1728.32	1605.86	0.96	1.36	1.31	1.21
248	SC0382	1408.97	1949.03	1901.90	1753.30	1.09	1.45	1.46	1.33
249	SC0384	1605.21	1580.15	1459.52	1548.29	1.26	1.24	1.15	1.22

250	SC0386	1658.34	1829.98	2118.41	1868.91	1.29	1.38	1.57	1.41
251	SC0388	1324.77	1483.97	1549.10	1452.61	1.03	1.13	1.21	1.12
252	SC0391	1561.73	1575.94	2065.35	1734.34	1.22	1.18	1.56	1.32
253	SC0393	1296.83	1594.48	1498.69	1463.33	0.99	1.15	1.13	1.09
254	SC0394	1762.17	1634.03	1824.70	1740.30	1.35	1.25	1.39	1.33
255	SC0396	2034.15	1620.28	2046.56	1900.33	1.62	1.21	1.53	1.45
256	SC0397	1241.91	1338.80	1600.32	1393.68	0.98	1.08	1.22	1.09
257	SC0399	2254.45	1959.77	2136.52	2116.91	1.79	1.50	1.57	1.62
258	SC0400	2130.99	1722.01	1978.36	1943.79	1.61	1.28	1.51	1.47
259	SC0401	1514.05	1973.72	1966.01	1817.92	1.18	1.50	1.50	1.39
260	SC0402	1925.29	1894.38	1837.59	1885.75	1.42	1.47	1.47	1.45
261	SC0403	2012.90	2053.04	1642.93	1902.96	1.50	1.56	1.20	1.42
262	SC0405	1572.78	1498.59	1811.43	1627.60	1.18	1.13	1.30	1.20
263	SC0406	1573.82	1776.14	1943.89	1764.62	1.29	1.42	1.41	1.37
264	SC0407	2027.83	2339.78	2255.25	2207.62	1.57	1.74	1.67	1.66
265	SC0408	1806.99	1676.15	1936.45	1806.53	1.39	1.29	1.42	1.37
266	SC0409	2343.85	1663.57	2224.29	2077.24	1.79	1.26	1.62	1.55
267	SC0411	1538.36	1534.58	1443.73	1505.55	1.17	1.16	1.13	1.15
268	SC0412	1815.66	1633.32	1484.03	1644.34	1.45	1.26	1.18	1.29
269	SC0413	1654.33	1840.71	2088.40	1861.15	1.32	1.39	1.61	1.44
270	SC0418	1946.96	1770.40	1860.31	1859.22	1.48	1.36	1.40	1.41
271	SC0420	2131.04	1886.11	2037.80	2018.32	1.60	1.43	1.53	1.52
272	SC0422	1633.24	1867.24	1597.40	1699.29	1.33	1.46	1.23	1.34
273	SC0423	2022.42	1656.98	1730.74	1803.38	1.50	1.24	1.32	1.35
274	SC0424	1624.28	1596.64	1531.97	1584.30	1.27	1.22	1.21	1.23
275	SC0426	2226.14	2022.57	2040.47	2096.39	1.65	1.50	1.48	1.54
276	SC0430	1826.57	1518.17	1693.10	1679.28	1.39	1.12	1.29	1.27
277	SC0432	1669.92	1721.27	2130.19	1840.46	1.27	1.38	1.64	1.43
278	SC0436	1692.57	1423.40	1389.68	1501.88	1.33	1.10	1.06	1.16
279	SC0438	1541.40	1657.33	1403.51	1534.08	1.14	1.30	1.05	1.16
280	SC0449	1778.98	2195.09	1951.90	1975.32	1.32	1.70	1.45	1.49
281	SC0452	1730.37	1412.99	1623.05	1588.80	1.38	1.10	1.25	1.24
282	SC0456	1444.27	1748.99	1736.82	1643.36	1.07	1.35	1.37	1.26
283	SC0457	1458.80	1596.34	1598.57	1551.24	1.25	1.35	1.21	1.27
284	SC0458	1362.53	1576.99	1607.68	1515.73	1.09	1.17	1.23	1.16
285	SC0462	1473.94	1818.08	1490.03	1594.02	1.13	1.43	1.19	1.25
286	SC0463	1670.99	1968.76	1778.48	1806.08	1.28	1.53	1.50	1.44
287	SC0465	2099.66	1805.27	2189.56	2031.50	1.62	1.36	1.62	1.53
288	SC0466	1392.47	1419.79	1588.56	1466.94	1.11	1.05	1.22	1.13
289	SC0467	1462.24	1544.61	1350.88	1452.58	1.17	1.22	1.07	1.15
290	SC0468	1552.70	1427.19	1551.52	1510.47	1.18	1.09	1.19	1.15
291	SC0470	1754.04	1956.17	1779.41	1829.87	1.36	1.49	1.34	1.40
292	SC0472	1624.05	1491.12	1795.18	1636.78	1.26	1.20	1.36	1.28

293	SC0475	2027.97	1986.85	2055.67	2023.50	1.54	1.42	1.49	1.48
294	SC0477	1546.63	1832.60	1300.24	1559.82	1.20	1.36	1.01	1.19
295	SC0490	1845.41	1676.13	1604.11	1708.55	1.36	1.34	1.24	1.31
296	SC0497	1538.76	1591.22	1699.75	1609.91	1.19	1.23	1.30	1.24
297	SC0501	1148.45	1646.74	1381.09	1392.09	0.87	1.35	1.00	1.07
298	SC0502	929.21	1626.52	1631.00	1395.58	0.74	1.27	1.25	1.09
299	SC0504	1436.61	1346.56	1510.26	1431.14	1.16	1.04	1.21	1.13
300	SC0505	1870.04	1603.59	1789.57	1754.40	1.41	1.22	1.33	1.32
301	SC0508	1773.29	1491.32	1903.00	1722.54	1.36	1.12	1.41	1.30
302	SC0512	1708.65	1515.03	1469.80	1564.49	1.35	1.18	1.13	1.22
303	SC0514	2318.09	2142.57	1986.39	2149.02	1.87	1.59	1.44	1.63
304	SC0516	1521.63	2039.21	1771.57	1777.47	1.15	1.51	1.31	1.32
305	SC0517	1672.92	1624.20	1722.07	1673.06	1.29	1.27	1.30	1.29
306	SC0519	1602.16	1758.46	1685.80	1682.14	1.23	1.37	1.29	1.29
307	SC0521	2029.02	1847.10	1942.56	1939.56	1.52	1.38	1.47	1.45
308	SC0522	1524.90	1580.68	1707.41	1604.33	1.15	1.18	1.30	1.21
309	SC0523	1613.64	2098.99	1775.84	1829.49	1.21	1.58	1.34	1.38
310	SC0525	1293.06	1688.45	1564.67	1515.39	1.09	1.31	1.20	1.20
311	SC0526	1998.35	1786.76	1786.79	1857.30	1.54	1.33	1.34	1.40
312	SC0528	1507.14	1716.93	1824.70	1682.93	1.11	1.27	1.38	1.25
313	SC0534	1188.71	1656.16	1833.85	1559.57	0.94	1.33	1.42	1.23
314	SC0537	1804.83	1908.37	1589.46	1767.55	1.36	1.52	1.22	1.37
315	SC0538	1421.67	1977.43	1470.00	1623.03	1.15	1.51	1.11	1.25
316	SC0540	1454.30	2006.55	1838.91	1766.59	1.10	1.53	1.37	1.33
317	SC0541	1998.90	1848.73	1704.18	1850.60	1.65	1.40	1.27	1.44
318	SC0542	1513.34	1675.47	1763.39	1650.74	1.16	1.25	1.34	1.25
319	SC0543	1489.76	2123.95	1891.98	1835.23	1.12	1.59	1.41	1.37
320	SC0544	1929.44	2036.44	1894.04	1953.31	1.40	1.55	1.37	1.44
321	SC0545	1924.45	1855.98	1688.33	1822.92	1.41	1.35	1.23	1.33
322	SC0546	1666.04	1593.65	1369.35	1543.01	1.33	1.21	1.06	1.20
323	SC0547	1659.68	2066.17	1593.86	1773.24	1.30	1.53	1.19	1.34
324	SC0549	2138.81	1822.28	2121.36	2027.49	1.65	1.37	1.53	1.52
325	SC0550	1828.65	1789.25	1972.72	1863.54	1.52	1.37	1.53	1.47
326	SC0551	1427.25	1972.86	1560.85	1653.65	1.11	1.50	1.30	1.30
327	SC0556	1444.65	1760.04	1528.98	1577.89	1.12	1.38	1.18	1.23
328	SC0557	1918.90	1819.05	2100.78	1946.24	1.44	1.44	1.56	1.48
329	SC0559	1578.33	1553.31	1433.60	1521.75	1.19	1.16	1.10	1.15
330	SC0562	1466.58	1731.92	1726.92	1641.81	1.14	1.37	1.33	1.28
331	SC0563	1813.66	1646.69	1855.48	1771.95	1.50	1.24	1.44	1.39
332	SC0565	2207.18	1821.22	1913.31	1980.57	1.71	1.41	1.78	1.63
333	SC0566	1797.34	1796.18	1638.77	1744.10	1.49	1.49	1.32	1.43
334	SC0567	1519.30	1379.87	1633.54	1510.90	1.23	1.13	1.25	1.20
335	SC0568	1918.04	1490.01	1775.81	1727.95	1.59	1.13	1.38	1.37

336	SC0569	1745.34	1562.84	1517.67	1608.62	1.36	1.23	1.20	1.26
337	SC0572	1742.45	1723.31	1786.92	1750.89	1.36	1.26	1.43	1.35
338	SC0574	1543.94	1689.46	1779.50	1670.97	1.16	1.32	1.35	1.28
339	SC0575	1987.15	1681.09	1828.44	1832.23	1.44	1.22	1.37	1.34
340	SC0577	1869.76	1689.77	2066.76	1875.43	1.37	1.23	1.49	1.36
341	SC0578	1371.14	1953.10	1841.31	1721.85	1.09	1.55	1.43	1.35
342	SC0584	1961.37	1544.19	1792.18	1765.91	1.50	1.17	1.42	1.36
343	SC0590	1899.08	1817.76	1836.56	1851.13	1.49	1.38	1.42	1.43
344	SC0593	1594.27	1903.07	1648.64	1715.33	1.29	1.52	1.27	1.36
345	SC0599	1717.15	1506.70	1459.29	1561.04	1.25	1.12	1.11	1.16
346	SC0600	1542.93	1598.51	1529.26	1556.90	1.18	1.23	1.16	1.19
347	SC0601	1673.05	1704.22	1649.39	1675.55	1.24	1.26	1.27	1.25
348	SC0602	1426.87	1774.44	1612.26	1604.52	1.08	1.38	1.29	1.25
349	SC0603	1597.93	1388.46	1525.35	1503.91	1.22	1.05	1.17	1.15
350	SC0604	2359.36	2031.79	2054.77	2148.64	1.80	1.48	1.52	1.60
351	SC0605	1675.44	1718.04	2125.79	1839.76	1.31	1.30	1.61	1.41
352	SC0606	2094.99	1439.51	1943.74	1826.08	1.64	1.12	1.47	1.41
353	SC0609	1186.78	1699.62	1454.28	1446.89	0.95	1.36	1.15	1.16
354	SC0610	1570.31	2214.09	1871.80	1885.40	1.22	1.58	1.41	1.40
355	SC0614	1904.61	1509.86	1597.15	1670.54	1.46	1.18	1.21	1.28
356	SC0615	1469.82	1561.60	1590.12	1540.51	1.24	1.30	1.22	1.25
357	SC0618	1788.14	1466.26	1578.04	1610.82	1.47	1.19	1.29	1.32
358	SC0621	1755.07	2116.79	1684.64	1852.17	1.33	1.58	1.32	1.41
359	SC0623	1802.46	1436.21	2185.57	1808.08	1.38	1.10	1.61	1.36
360	SC0625	1813.44	1513.09	1511.76	1612.77	1.41	1.16	1.16	1.25
361	SC0626	1826.50	1942.14	1943.76	1904.13	1.41	1.51	1.40	1.44
362	SC0627	1430.59	1621.21	1364.37	1472.06	1.18	1.25	1.08	1.17
363	SC0628	1469.18	1340.20	1448.04	1419.14	1.18	1.07	1.19	1.15
364	SC0629	1426.81	1737.34	1359.19	1507.78	1.05	1.33	1.04	1.14
365	SC0630	1649.63	1982.12	1549.18	1726.98	1.25	1.51	1.20	1.32
366	SC0631	1431.43	1359.09	1614.03	1468.18	1.19	1.18	1.24	1.21
367	SC0632	1519.98	1227.12	1568.12	1438.41	1.20	1.00	1.21	1.14
368	SC0635	1389.17	1490.34	1381.29	1420.27	1.11	1.16	1.07	1.11
369	SC0636	1367.37	1518.69	1928.91	1604.99	1.04	1.18	1.53	1.25
370	SC0637	2074.46	2422.85	2132.33	2209.88	1.50	1.75	1.62	1.62
371	SC0639	1667.41	1702.26	1673.01	1680.89	1.23	1.34	1.23	1.27
372	SC0641	1873.04	1773.31	1933.53	1859.96	1.47	1.34	1.41	1.41
373	SC0642	1995.07	1667.81	1752.36	1805.08	1.48	1.22	1.29	1.33
374	SC0643	2150.79	1370.35	1994.04	1838.39	1.63	1.03	1.51	1.39
375	SC0644	1377.67	1564.04	1642.05	1527.92	1.02	1.18	1.27	1.16
376	SC0645	2074.78	1964.93	1961.15	2000.29	1.61	1.47	1.45	1.51
377	SC0646	1451.08	1519.72	1664.15	1544.98	1.18	1.21	1.26	1.22
378	SC0647	1593.40	1458.06	1508.26	1519.91	1.19	1.09	1.14	1.14

379	SC0648	1467.01	1534.11	1537.26	1512.79	1.15	1.14	1.15	1.15
380	SC0649	1412.74	1854.67	1768.55	1678.65	1.09	1.42	1.40	1.31
381	SC0652	1363.69	1686.44	1366.82	1472.32	1.03	1.31	1.08	1.14
382	SC0653	1307.68	1813.84	1709.23	1610.25	1.01	1.42	1.31	1.25
383	SC0655	1911.03	1941.46	2004.68	1952.39	1.45	1.41	1.48	1.45
384	SC0657	1470.59	1563.14	1631.09	1554.94	1.10	1.18	1.27	1.19
385	SC0659	1306.31	1594.61	1544.64	1481.85	0.98	1.18	1.17	1.11
386	SC0663	1777.76	1655.17	1797.78	1743.57	1.35	1.28	1.35	1.33
387	SC0671	1496.99	1516.72	1627.62	1547.11	1.14	1.17	1.24	1.18
388	SC0672	1667.06	1693.64	1732.77	1697.82	1.34	1.34	1.43	1.37
389	SC0673	1385.92	1726.43	1682.02	1598.12	1.08	1.27	1.30	1.22
390	SC0679	1425.61	1647.48	1721.07	1598.06	1.13	1.31	1.35	1.26
391	SC0680	1428.74	1527.89	1489.87	1482.17	1.07	1.17	1.13	1.12
392	SC0682	1248.82	1650.04	1580.69	1493.18	1.00	1.30	1.26	1.18
393	SC0683	2397.07	1822.88	1909.31	2043.09	1.82	1.43	1.43	1.56
394	SC0685	1945.07	1752.06	1798.54	1831.89	1.47	1.32	1.32	1.37
395	SC0686	2304.59	1989.41	2213.02	2169.01	1.67	1.48	1.63	1.59
396	SC0687	1679.10	1451.42	1526.78	1552.43	1.28	1.09	1.17	1.18
397	SC0689	2433.53	2208.76	2017.89	2220.06	1.79	1.65	1.53	1.65
398	SC0691	1935.96	2016.25	1620.95	1857.72	1.58	1.56	1.29	1.48
399	SC0692	1848.71	1956.24	1964.86	1923.27	1.42	1.48	1.52	1.47
400	SC0693	2104.61	1787.05	1915.49	1935.72	1.69	1.38	1.55	1.54
401	SC0694	2055.39	2180.04	1813.36	2016.26	1.55	1.67	1.40	1.54
402	SC0695	2015.93	1570.70	1821.74	1802.79	1.53	1.21	1.39	1.38
403	SC0700	1455.49	1524.06	1436.80	1472.12	1.19	1.19	1.10	1.16
404	SC0701	2162.52	2079.96	1795.38	2012.62	1.65	1.51	1.30	1.48
405	SC0704	1919.14	2077.37	1985.02	1993.84	1.43	1.52	1.46	1.47
406	SC0705	1342.77	1495.72	1211.14	1349.87	1.04	1.15	1.02	1.07
407	SC0706	1929.95	1676.57	1942.78	1849.77	1.42	1.28	1.44	1.38
408	SC0708	3308.81	2254.54	1863.72	2475.69	2.45	1.65	1.35	1.81
409	SC0709	1273.52	1658.88	1529.57	1487.32	0.95	1.27	1.15	1.12
410	SC0713	1544.70	1458.49	1195.21	1399.46	1.29	1.25	0.98	1.17
411	SC0715	1862.20	1777.91	1705.89	1782.00	1.37	1.32	1.26	1.32
412	SC0716	2171.98	1915.96	2013.90	2033.95	1.59	1.51	1.48	1.53
413	SC0720	2034.81	1741.38	2284.37	2020.19	1.52	1.30	1.69	1.50
414	SC0723	1393.27	1711.80	1121.23	1408.77	1.04	1.28	0.82	1.05
415	SC0724	1311.98	1355.67	1416.67	1361.44	1.05	0.97	1.08	1.03
416	SC0725	1779.57	1423.50	1822.41	1675.16	1.28	1.09	1.33	1.23
417	SC0726	2044.57	1860.27	1780.56	1895.13	1.49	1.35	1.31	1.39
418	SC0727	1768.98	2288.17	2303.43	2120.19	1.29	1.63	1.64	1.52
419	SC0728	1866.87	2113.59	1993.11	1991.19	1.39	1.55	1.49	1.48
420	SC0730	2310.44	1645.92	1975.05	1977.14	1.71	1.21	1.49	1.47
421	SC0731	2112.85	1866.23	1475.92	1818.33	1.57	1.40	1.10	1.36

422	SC0732	2199.06	1758.93	2142.50	2033.50	1.57	1.26	1.54	1.45
423	SC0733	1583.85	1412.06	1564.46	1520.12	1.23	1.14	1.21	1.19
424	SC0734	1854.91	1471.19	1539.84	1621.98	1.37	1.09	1.14	1.20
425	SC0736	1463.52	1565.12	1571.07	1533.23	1.12	1.18	1.21	1.17
426	SC0738	1853.23	2057.47	1912.19	1940.96	1.43	1.55	1.43	1.47
427	SC0741	1824.61	2096.80	1756.05	1892.49	1.44	1.70	1.38	1.51
428	SC0747	1701.54	1499.38	1084.91	1428.61	1.23	1.15	0.86	1.08
429	SC0748	1943.65	2145.88	2007.22	2032.25	1.41	1.57	1.48	1.49
430	SC0749	2009.62	1739.38	1676.52	1808.51	1.47	1.31	1.26	1.35
431	SC0751	2128.56	2170.01	1849.36	2049.31	1.60	1.60	1.38	1.53
432	SC0753	1281.28	1428.97	1466.12	1392.12	1.03	1.08	1.10	1.07
433	SC0755	2063.38	1771.84	2021.59	1952.27	1.66	1.33	1.52	1.50
434	SC0756	2242.07	2547.93	1977.37	2255.79	1.69	1.93	1.46	1.69
435	SC0757	1193.89	1415.93	1112.62	1240.82	0.96	1.15	0.85	0.98
436	SC0760	1589.45	1845.00	2007.48	1813.98	1.17	1.32	1.49	1.33
437	SC0761	1737.37	1693.29	1433.17	1621.28	1.34	1.28	1.06	1.23
438	SC0762	2351.12	1700.62	2088.74	2046.83	1.74	1.23	1.58	1.52
439	SC0763	1360.77	1554.13	1537.12	1484.01	1.10	1.19	1.17	1.15
440	SC0764	1780.08	1484.04	1491.26	1585.13	1.32	1.10	1.07	1.16
441	SC0770	2197.93	1995.28	1778.69	1990.64	1.65	1.45	1.34	1.48
442	SC0773	1968.72	1873.25	1870.66	1904.21	1.47	1.37	1.40	1.41
443	SC0774	2515.65	1642.49	1971.92	2043.35	1.91	1.28	1.44	1.55
444	SC0781	2098.00	1407.46	1795.91	1767.12	1.61	1.08	1.33	1.34
445	SC0782	2290.29	2051.80	2191.98	2178.03	1.70	1.63	1.65	1.66
446	SC0784	2186.84	2088.19	2041.01	2105.35	1.66	1.60	1.53	1.60
447	SC0790	1908.17	1778.32	1483.15	1723.21	1.44	1.35	1.17	1.32
448	SC0797	2252.32	2074.45	1756.79	2027.86	1.74	1.50	1.36	1.53
449	SC0800	1738.72	1852.02	1909.72	1833.49	1.35	1.34	1.41	1.37
450	SC0803	1852.02	1658.51	1749.47	1753.33	1.36	1.23	1.32	1.31
451	SC0804	1555.68	1524.25	1638.05	1572.66	1.22	1.18	1.26	1.22
452	SC0807	1431.55	1646.23	1338.26	1472.01	1.14	1.30	1.08	1.17
453	SC0808	1617.47	1533.70	1717.18	1622.78	1.23	1.25	1.29	1.26
454	SC0810	1719.29	1942.50	1935.02	1865.60	1.36	1.50	1.50	1.45
455	SC0814	1591.70	1627.14	1840.07	1686.30	1.29	1.24	1.42	1.32
456	SC0817	1682.79	1903.14	1825.95	1803.96	1.25	1.49	1.40	1.38
457	SC0823	1878.15	1636.08	1684.21	1732.81	1.44	1.24	1.25	1.31
458	SC0830	1599.66	1805.88	1897.62	1767.72	1.21	1.36	1.42	1.33
459	SC0832	2524.60	1732.13	1851.29	2036.01	2.06	1.37	1.49	1.64
460	SC0833	1708.12	1877.30	1627.44	1737.62	1.33	1.43	1.28	1.35
461	SC0835	1497.30	1625.76	1626.06	1583.04	1.19	1.22	1.21	1.21
462	SC0837	1283.54	1500.94	1199.59	1328.03	1.02	1.15	0.91	1.03
463	SC0839	1334.37	1553.83	1879.01	1589.07	1.02	1.17	1.42	1.20
464	SC0841	1873.48	1608.53	1986.88	1822.96	1.47	1.24	1.46	1.39

465	SC0842	2646.96	2390.88	2184.41	2407.42	1.90	1.73	1.63	1.75
466	SC0847	1694.07	1791.64	1875.48	1787.06	1.37	1.33	1.43	1.38
467	SC0851	1342.64	1693.09	1395.30	1477.01	1.05	1.37	1.16	1.19
468	SC0852	1922.71	1850.50	2082.80	1952.00	1.52	1.45	1.60	1.52
469	SC0854	2003.98	2173.76	1965.37	2047.70	1.55	1.63	1.48	1.55
470	SC0855	1674.76	1808.61	1662.41	1715.26	1.26	1.38	1.26	1.30
471	SC0859	1627.27	1535.20	1530.41	1564.29	1.29	1.14	1.19	1.21
472	SC0860	1569.63	1732.84	1888.91	1730.46	1.18	1.34	1.42	1.31
473	SC0864	1890.72	1940.39	1861.81	1897.64	1.43	1.46	1.39	1.43
474	SC0865	1900.71	1633.26	1827.22	1787.06	1.55	1.23	1.39	1.39
475	SC0868	1358.06	1725.53	1582.88	1555.49	1.09	1.34	1.23	1.22
476	SC0876	1582.27	1824.84	1719.62	1708.91	1.27	1.41	1.29	1.32
477	SC0877	1709.54	1833.95	1980.21	1841.23	1.29	1.39	1.48	1.39
478	SC0878	1781.17	2024.32	1996.47	1933.99	1.45	1.48	1.51	1.48
479	SC0891	1470.72	1537.84	1528.97	1512.51	1.17	1.09	1.15	1.14
480	SC0893	2097.31	1634.07	1921.08	1884.15	1.65	1.21	1.48	1.45
481	SC0895	2242.04	1361.14	2380.78	1994.65	1.72	0.97	1.80	1.50
482	SC0902	1476.61	1635.37	1518.31	1543.43	1.13	1.28	1.20	1.20
483	SC0906	1868.33	1564.10	2002.27	1811.57	1.38	1.11	1.44	1.31
484	SC0913	1893.29	1774.14	2232.63	1966.69	1.46	1.34	1.60	1.47
485	SC0914	1290.38	1569.61	1411.56	1423.85	0.97	1.26	1.07	1.10
486	SC0919	1763.72	1760.75	1884.92	1803.13	1.36	1.40	1.45	1.40
487	SC0921	1952.48	1616.52	1734.03	1767.68	1.49	1.28	1.31	1.36
488	SC0923	1492.31	1457.73	1392.14	1447.39	1.21	1.10	1.05	1.12
489	SC0929	1442.89	1615.43	1553.01	1537.11	1.09	1.20	1.18	1.16
490	SC0937	1680.13	1724.29	2058.48	1820.97	1.33	1.41	1.77	1.50
491	SC0942	1734.71	1554.12	1689.92	1659.58	1.33	1.26	1.36	1.32
492	SC0947	1345.41	1639.17	1618.48	1534.36	1.05	1.35	1.30	1.23
493	SC0949	1601.89	1859.14	1756.30	1739.11	1.31	1.48	1.39	1.39
494	SC0950	1651.64	1771.56	1666.09	1696.43	1.24	1.33	1.29	1.29
495	SC0951	1949.53	1958.70	2172.98	2027.07	1.48	1.45	1.64	1.52
496	SC0958	1941.27	2187.64	2094.85	2074.59	1.44	1.67	1.54	1.55
497	SC0963	1949.62	1869.38	1902.65	1907.22	1.45	1.35	1.47	1.42
498	SC0964	2135.07	1943.59	1792.99	1957.22	1.57	1.46	1.38	1.47
499	SC0965	1377.56	1325.62	1434.87	1379.35	1.15	1.10	1.15	1.13
500	SC0968	1619.82	1564.12	1696.24	1626.73	1.21	1.17	1.28	1.22
501	SC0975	1673.80	1737.45	1734.44	1715.23	1.28	1.36	1.37	1.34
502	SC0979	2169.79	1913.34	1860.49	1981.21	1.67	1.41	1.42	1.50
503	SC0982	2298.28	1479.16	1829.33	1868.92	1.70	1.13	1.37	1.40
504	SC0987	1756.93	1820.46	1770.27	1782.55	1.34	1.36	1.33	1.34
505	SC0991	1469.92	1859.13	1820.31	1716.45	1.13	1.39	1.40	1.31
506	SC0998	1541.09	1722.69	1795.43	1686.40	1.20	1.32	1.37	1.30
507	SC0999	2232.71	1723.89	1686.02	1880.87	1.83	1.30	1.27	1.47

508	SC1014	1286.41	1695.86	1983.72	1655.33	1.03	1.28	1.49	1.27
509	SC1015	1722.75	1658.92	1481.46	1621.04	1.31	1.26	1.14	1.24
510	SC1017	1664.40	1745.36	1481.13	1630.30	1.25	1.33	1.07	1.22
511	SC1019	1978.30	2252.64	1836.61	2022.52	1.48	1.65	1.38	1.50
512	SC1021	1862.41	1846.17	1854.99	1854.53	1.44	1.42	1.45	1.43
513	SC1022	1546.15	1788.47	1600.34	1644.99	1.17	1.37	1.26	1.27
514	SC1023	1211.24	1624.55	1821.99	1552.59	0.89	1.21	1.32	1.14
515	SC1024	2058.23	1991.42	2046.45	2032.03	1.54	1.51	1.49	1.51
516	SC1025	1709.65	1595.74	1756.40	1687.27	1.23	1.18	1.27	1.23
517	SC1031	1362.41	1557.31	1681.55	1533.76	1.04	1.18	1.34	1.19
518	SC1038	1445.43	1789.63	1636.98	1624.01	1.15	1.34	1.24	1.25
519	SC1039	1543.85	1578.55	1727.66	1616.69	1.16	1.21	1.30	1.23
520	SC1040	1544.66	1517.35	1427.13	1496.38	1.18	1.19	1.12	1.16
521	SC1046	1872.39	1684.16	1766.03	1774.19	1.38	1.33	1.35	1.36
522	SC1055	2255.12	2354.98	1610.66	2073.59	1.75	1.75	1.24	1.58
523	SC1056	2157.05	1965.92	1674.05	1932.34	1.59	1.41	1.33	1.44
524	SC1063	1476.32	1568.08	1654.52	1566.31	1.11	1.23	1.25	1.20
525	SC1067	2047.79	1495.25	2152.18	1898.41	1.53	1.09	1.64	1.42
526	SC1069	1679.21	1872.93	1553.86	1702.00	1.44	1.42	1.23	1.36
527	SC1072	1376.18	1607.63	1506.14	1496.65	1.06	1.22	1.17	1.15
528	SC1074	1459.28	1791.34	1794.56	1681.73	1.12	1.39	1.38	1.30
529	SC1076	1142.01	1710.12	1988.61	1613.58	1.12	1.30	1.47	1.30
530	SC1077	1965.75	1639.86	1979.61	1861.74	1.46	1.26	1.45	1.39
531	SC1079	2020.11	1944.29	1888.44	1950.95	1.50	1.46	1.40	1.45
532	SC1080	1760.65	1531.09	1680.93	1657.56	1.32	1.17	1.27	1.25
533	SC1083	1896.92	1318.20	1718.02	1644.38	1.59	0.99	1.25	1.28
534	SC1084	1935.93	1491.17	1370.30	1599.13	1.50	1.06	1.05	1.20
535	SC1089	2081.23	1873.30	2149.12	2034.55	1.58	1.36	1.71	1.55
536	SC1097	1977.55	1449.82	1903.11	1776.83	1.51	1.10	1.45	1.35
537	SC1101	1815.72	1655.72	2035.10	1835.51	1.37	1.24	1.56	1.39
538	SC1104	1738.30	1524.03	1699.44	1653.92	1.40	1.24	1.26	1.30
539	SC1107	2295.24	2097.96	2179.52	2190.91	1.74	1.56	1.61	1.64
540	SC1111	1782.41	1724.68	1806.25	1771.12	1.35	1.32	1.37	1.35
541	SC1114	1401.41	1596.45	1867.88	1621.91	1.05	1.16	1.36	1.19
542	SC1116	1469.91	1403.30	1574.93	1482.71	1.11	1.09	1.17	1.12
543	SC1117	1902.39	1846.63	1819.51	1856.18	1.47	1.37	1.32	1.39
544	SC1118	1445.59	1347.63	1315.44	1369.55	1.11	1.06	1.57	1.25
545	SC1119	1494.14	1925.03	1653.66	1690.94	1.17	1.50	1.27	1.31
546	SC1120	1976.94	2263.76	1929.30	2056.67	1.52	1.66	1.45	1.54
547	SC1123	1817.53	1599.99	1740.51	1719.34	1.40	1.22	1.31	1.31
548	SC1124	1540.71	1723.33	1921.00	1728.35	1.22	1.37	1.43	1.34
549	SC1125	2123.29	2168.32	1657.48	1983.03	1.54	1.59	1.20	1.44
550	SC1133	1444.44	1810.58	1971.90	1742.30	1.17	1.42	1.56	1.38

551	SC1154	1533.72	1807.33	1610.32	1650.46	1.13	1.38	1.24	1.25
552	SC1155	2014.97	1631.49	1912.12	1852.86	1.53	1.22	1.43	1.40
553	SC1156	1190.93	1571.27	1476.53	1412.91	0.92	1.26	1.22	1.13
554	SC1157	1803.56	2056.11	1969.18	1942.95	1.38	1.55	1.51	1.48
555	SC1158	1355.45	1505.71	1430.45	1430.54	1.05	1.11	1.13	1.10
556	SC1159	1879.76	2226.03	2381.66	2162.49	1.43	1.61	1.75	1.59
557	SC1160	1800.36	2097.69	1614.60	1837.55	1.38	1.59	1.29	1.42
558	SC1166	1708.16	1488.77	1517.33	1571.42	1.33	1.14	1.22	1.23
559	SC1170	2068.86	1854.51	1881.16	1934.85	1.54	1.43	1.46	1.48
560	SC1172	1660.31	1744.62	1996.40	1800.44	1.23	1.32	1.45	1.33
561	SC1177	1703.93	1888.67	1613.61	1735.40	1.31	1.51	1.21	1.34
562	SC1178	1494.16	1511.83	1573.89	1526.63	1.23	1.15	1.23	1.20
563	SC1186	1742.88	1440.34	1326.35	1503.19	1.32	1.11	1.13	1.19
564	SC1203	2001.24	1516.36	1746.72	1754.77	1.55	1.24	1.36	1.38
565	SC1205	1901.10	1652.75	2002.86	1852.24	1.48	1.24	1.46	1.39
566	SC1211	1878.63	2139.19	2279.61	2099.14	1.46	1.61	1.67	1.58
567	SC1212	1658.14	1835.12	1520.85	1671.37	1.20	1.41	1.12	1.24
568	SC1214	1859.04	1516.34	1829.48	1734.95	1.42	1.17	1.35	1.31
569	SC1215	1455.14	1747.07	1875.77	1692.66	1.11	1.40	1.48	1.33
570	SC1222	1710.17	1641.68	1811.27	1721.04	1.33	1.23	1.34	1.30
571	SC1229	1602.47	1689.29	1641.57	1644.44	1.29	1.38	1.23	1.30
572	SC1237	1593.36	1772.69	1718.51	1694.86	1.25	1.46	1.38	1.36
573	SC1251	1790.66	1258.08	1404.77	1484.50	1.36	1.01	1.08	1.15
574	SC1261	1646.26	1534.71	1765.49	1648.82	1.29	1.21	1.39	1.30
575	SC1262	1378.37	1614.90	1687.12	1560.13	1.08	1.27	1.31	1.22
576	SC1271	1918.04	1809.18	1900.54	1875.92	1.45	1.31	1.45	1.41
577	SC1277	2409.50	2002.18	2227.79	2213.16	1.90	1.48	1.62	1.67
578	SC1287	2494.28	2108.07	2010.68	2204.34	1.84	1.61	1.45	1.64
579	SC1293	1543.05	1854.34	1869.79	1755.73	1.22	1.41	1.41	1.35
580	SC1300	1443.23	1484.82	1431.48	1453.18	1.13	1.12	1.07	1.11
581	SC1302	1805.25	1411.14	1683.03	1633.14	1.36	1.09	1.31	1.25
582	SC1305	1502.92	1675.72	1603.21	1593.95	1.17	1.27	1.21	1.22
583	SC1307	1554.01	1652.70	1737.29	1648.00	1.15	1.24	1.42	1.27
584	SC1313	1912.90	2119.85	1861.36	1964.71	1.51	1.59	1.43	1.51
585	SC1314	1977.22	1941.05	1852.53	1923.60	1.55	1.46	1.38	1.46
586	SC1317	2369.64	1858.33	1956.19	2061.39	1.81	1.39	1.43	1.54
587	SC1318	2661.59	1697.88	1679.03	2012.83	1.98	1.29	1.33	1.53
588	SC1319	1729.74	1763.84	1916.39	1803.32	1.33	1.32	1.42	1.36
589	SC1320	2257.04	1927.28	1856.97	2013.76	1.65	1.42	1.39	1.49
590	SC1321	1491.40	1481.37	1562.66	1511.81	1.13	1.10	1.20	1.14
591	SC1322	2704.04	1804.36	2105.41	2204.60	2.12	1.34	1.53	1.66
592	SC1325	1892.44	1842.66	1935.55	1890.22	1.44	1.35	1.48	1.42
593	SC1328	1609.56	1718.33	1753.69	1693.86	1.25	1.30	1.29	1.28

594	SC1329	2307.01	1818.01	2191.92	2105.65	1.64	1.30	1.60	1.51
595	SC1330	2176.30	2217.42	2036.93	2143.55	1.62	1.66	1.52	1.60
596	SC1332	2181.95	1545.69	1973.68	1900.44	1.66	1.19	1.46	1.44
597	SC1333	1784.05	2134.26	1999.80	1972.70	1.37	1.60	1.47	1.48
598	SC1337	1994.76	2231.59	1985.25	2070.53	1.49	1.71	1.46	1.55
599	SC1341	1407.55	1951.98	2098.89	1819.47	1.11	1.48	1.56	1.38
600	SC1342	1724.29	1731.28	1856.79	1770.79	1.35	1.31	1.36	1.34
601	SC1345	2279.83	1922.98	1303.51	1835.44	1.78	1.41	0.93	1.37
602	SC1351	1383.49	1486.50	1874.22	1581.40	1.15	1.20	1.48	1.27
603	SC1356	1435.30	1647.22	1585.25	1555.92	1.19	1.30	1.23	1.24
604	SC1416	1951.72	2100.93	1993.37	2015.34	1.49	1.53	1.49	1.50
605	SC1426	1436.95	1962.59	1724.34	1707.96	1.22	1.56	1.34	1.37
606	SC1429	2139.86	1446.78	2138.70	1908.45	1.68	1.09	1.62	1.46
607	SC1441	1353.95	1708.68	1702.68	1588.44	1.04	1.29	1.29	1.21
608	SC1442	1495.03	1827.67	1770.17	1697.62	1.17	1.34	1.38	1.29
609	SC1446	1859.75	2247.52	1794.88	1967.39	1.43	1.74	1.42	1.53
610	SC1471	2136.84	1772.95	1780.39	1896.72	1.62	1.34	1.39	1.45
611	SC1476	1779.77	1414.45	1928.46	1707.56	1.32	1.11	1.44	1.29
612	SC1484	1681.10	1729.39	1517.86	1642.78	1.34	1.31	1.13	1.26
613	SC1489	1614.05	1294.39	1381.64	1430.03	1.23	1.01	1.11	1.12
614	SC1494	2346.21	2269.62	2110.08	2241.97	1.78	1.64	1.58	1.66
615	Soberano	2238.19	1858.61	1863.44	1986.75	1.79	1.41	1.47	1.55
616	SpurFeter	2537.90	2458.35	1935.70	2310.65	1.92	1.86	1.63	1.81
617	SRN39	1761.50	1858.09	1850.27	1823.29	1.39	1.42	1.38	1.40
618	Tx2741	1497.98	1558.04	1580.98	1545.67	1.18	1.21	1.21	1.20
619	Tx2911	1583.77	1386.49	1658.58	1542.94	1.16	1.06	1.23	1.15

REFERENCES

Anbarjafari, Gholamreza. 2018. *1. Introduction to Image Processing*.

Adhikari, Pragya, Santiago X. Mideros, and Tiffany M. Jamann. 2021. "Differential Regulation of Maize and Sorghum Orthologs in Response to the Fungal Pathogen Exserohilum Turcicum." *Frontiers in Plant Science* 12:930. doi: 10.3389/fpls.2021.675208.

Aisawi, K. a. B., M. P. Reynolds, R. P. Singh, and M. J. Foulkes. 2015. "The Physiological Basis of the Genetic Progress in Yield Potential of CIMMYT Spring Wheat Cultivars from 1966 to 2009." *Crop Science* 55(4):1749–64. doi: 10.2135/cropsci2014.09.0601.

Alam, M. M., E. S. Mace, E. J. van Oosterom, A. Cruickshank, C. H. Hunt, G. L. Hammer, and D. R. Jordan. 2014. "QTL Analysis in Multiple Sorghum Populations Facilitates the Dissection of the Genetic and Physiological Control of Tillering." *Theoretical and Applied Genetics* 127(10):2253–66. doi: 10.1007/s00122-014-2377-9.

Alam, Mohammad Mobashwer, Graeme L. Hammer, Erik J. van Oosterom, Alan W. Cruickshank, Colleen H. Hunt, and David R. Jordan. 2014. "A Physiological Framework to Explain Genetic and Environmental Regulation of Tillering in Sorghum." *New Phytologist* 203(1):155–67. doi: 10.1111/nph.12767.

Anderson, Steven L., Seth C. Murray, Yuanyuan Chen, Lonesome Malambo, Anjin Chang, Sorin Popescu, Dale Cope, and Jinha Jung. 2020. "Unoccupied Aerial System Enabled Functional Modeling of Maize Height Reveals Dynamic Expression of Loci." *Plant Direct* 4(5):e00223. doi: 10.1002/pld3.223.

Arendt, Elke K., and Emanuele Zannini. 2013. *Cereal Grains for the Food and Beverage Industries*. Elsevier.

Asseng, Senthold, Pierre Martre, Frank Ewert, M. Fernanda Dreccer, Brian L. Beres, Matthew Reynolds, Hans-Joachim Braun, Peter Langridge, Jacques Le Gouis, Jérôme Salse, and P. Stephen Baenziger. 2019. "Model-Driven Multidisciplinary Global Research to Meet Future Needs: The Case for 'Improving Radiation Use Efficiency to Increase Yield.'" *Crop Science* 59(3):843–49. doi: 10.2135/cropsci2018.09.0562.

Atwell, Susanna, Yu S. Huang, Bjarni J. Vilhjálmsson, Glenda Willems, Matthew Horton, Yan Li, Dazhe Meng, Alexander Platt, Aaron M. Tarone, Tina T. Hu, Rong Jiang, N. Wayan Muliyati, Xu Zhang, Muhammad Ali Amer, Ivan Baxter, Benjamin Brachi, Joanne Chory, Caroline Dean, Marilyne Debieu, Juliette de Meaux, Joseph R. Ecker, Nathalie Faure, Joel M. Kniskern, Jonathan D. G. Jones, Todd Michael, Adnane Nemri, Fabrice Roux, David E. Salt, Chunlao Tang, Marco Todesco, M. Brian Traw, Detlef Weigel, Paul Marjoram, Justin O. Borevitz, Joy Bergelson, and Magnus Nordborg. 2010. "Genome-Wide Association Study of 107 Phenotypes in Arabidopsis Thaliana Inbred Lines." *Nature* 465(7298):627–31. doi: 10.1038/nature08800.

Bai, Chunming, Chunyu Wang, Ping Wang, Zhenxing Zhu, Ling Cong, Dan Li, Yifei Liu, Wenjing Zheng, and Xiaochun Lu. 2017. "QTL Mapping of Agronomically Important Traits in Sorghum (Sorghum Bicolor L.)." *Euphytica* 213(12):285. doi: 10.1007/s10681-017-2075-1.

Bangbol Sangma, Harriet. 2013. "Genetic Characterization of Flowering Time in Sorghum."

Baret, Frederic, Simon Madec, Kamran Irfan, Jeremy Lopez, Alexis Comar, Matthieu Hemmerlé, Dan Dutartre, Sebastien Praud, and Marie Helene Tixier. 2018. "Leaf-Rolling in Maize Crops: From Leaf Scoring to Canopy-Level Measurements for Phenotyping." *Journal of Experimental Botany* 69(10):2705–16. doi: 10.1093/jxb/ery071.

Bates, Douglas, Martin Mächler, Ben Bolker, and Steve Walker. 2015. "Fitting Linear Mixed-Effects Models Using Lme4." *Journal of Statistical Software* 67(1):1–48. doi: 10.18637/jss.v067.i01.

Benjamini, Yoav, and Yosef Hochberg. 1995. "Controlling the False Discovery Rate: A Practical and Powerful Approach to Multiple Testing." *Journal of the Royal Statistical Society: Series B (Methodological)* 57(1):289–300. doi: 10.1111/j.2517-6161.1995.tb02031.x.

Beveridge, Christine A. 2006. "Axillary Bud Outgrowth: Sending a Message." *Current Opinion in Plant Biology* 9(1):35–40. doi: 10.1016/j.pbi.2005.11.006.

Biddington, Norman L. 1986. "The Effects of Mechanically-Induced Stress in Plants — a Review." *Plant Growth Regulation* 4(2):103–23. doi: 10.1007/BF00025193.

Blancon, Justin, Dan Dutartre, Marie-Hélène Tixier, Marie Weiss, Alexis Comar, Sébastien Praud, and Frédéric Baret. 2019. "A High-Throughput Model-Assisted Method for Phenotyping Maize Green Leaf Area Index Dynamics Using Unmanned Aerial Vehicle Imagery." *Frontiers in Plant Science* 10. doi: 10.3389/fpls.2019.00685.

Boote, Kenneth J., James W. Jones, and Nigel B. Pickering. 1996. "Potential Uses and Limitations of Crop Models." *Agronomy Journal* 88(5):704–16. doi: 10.2134/agronj1996.00021962008800050005x.

Borrell, Andrew K., Graeme L. Hammer, and Andrew C. L. Douglas. 2000a. "Does Maintaining Green Leaf Area in Sorghum Improve Yield under Drought? I. Leaf Growth and Senescence." *Crop Science* 40(4):1026–37. doi: 10.2135/cropsci2000.4041026x.

Borrell, Andrew K., John E. Mullet, Barbara George-Jaeggli, Erik J. van Oosterom, Graeme L. Hammer, Patricia E. Klein, and David R. Jordan. 2014. "Drought Adaptation of Stay-Green Sorghum Is Associated with Canopy Development, Leaf Anatomy, Root Growth, and Water Uptake." *Journal of Experimental Botany* 65(21):6251–63. doi: 10.1093/jxb/eru232.

Borrell, Andrew K., Erik J. van Oosterom, John E. Mullet, Barbara George-Jaeggli, David R. Jordan, Patricia E. Klein, and Graeme L. Hammer. 2014. "Stay-Green Alleles Individually Enhance Grain Yield in Sorghum under Drought by Modifying Canopy Development and Water Uptake Patterns." *New Phytologist* 203(3):817–30. doi: 10.1111/nph.12869.

Borrell, Andrew, Erik van Oosterom, Barbara George-Jaeggli, Daniel Rodriguez, Joe Eyre, David J. Jordan, Emma Mace, Vijaya Singh, Vincent Vadez, Mike Bell, Ian Godwin, Alan Cruickshank, Yongfu Tao, and Graeme Hammer. 2021. "Chapter 5 - Sorghum." Pp. 196–221 in *Crop Physiology Case Histories for Major Crops*, edited by V. O. Sadras and D. F. Calderini. Academic Press.

Botstein, D., R. L. White, M. Skolnick, and R. W. Davis. 1980. "Construction of a Genetic Linkage Map in Man Using Restriction Fragment Length Polymorphisms." *American Journal of Human Genetics* 32(3):314–31.

Bouman, B. a. M. 1995. "Crop Modelling and Remote Sensing for Yield Prediction." *Netherlands Journal of Agricultural Science* 43(2):143–61. doi: 10.18174/njas.v43i2.573.

Bouman, B. A. M., H. van Keulen, H. H. van Laar, and R. Rabbinge. 1996. "The 'School of de Wit' Crop Growth Simulation Models: A Pedigree and Historical Overview." *Agricultural Systems* 52(2):171–98. doi: 10.1016/0308-521X(96)00011-X.

Boyles, Richard E., Brian K. Pfeiffer, Elizabeth A. Cooper, Kelsey J. Zielinski, Matthew T. Myers, William L. Rooney, and Stephen Kresovich. 2017. "Quantitative Trait Loci Mapping of Agronomic and Yield Traits in Two Grain Sorghum Biparental Families." *Crop Science* 57(5):2443–56. doi: 10.2135/cropsci2016.12.0988.

Brown, Patrick J., William L. Rooney, Cleve Franks, and Stephen Kresovich. 2008. "Efficient Mapping of Plant Height Quantitative Trait Loci in a Sorghum Association Population With Introgressed Dwarfing Genes." *Genetics* 180(1):629–37. doi: 10.1534/genetics.108.092239.

Browning, Sharon R., and Brian L. Browning. 2007. "Rapid and Accurate Haplotype Phasing and Missing-Data Inference for Whole-Genome Association Studies By Use of Localized Haplotype Clustering." *The American Journal of Human Genetics* 81(5):1084–97. doi: 10.1086/521987.

Burks, Payne S., Chris M. Kaiser, Elizabeth M. Hawkins, and Patrick J. Brown. 2015. "Genomewide Association for Sugar Yield in Sweet Sorghum." *Crop Science* 55(5):2138–48. doi: 10.2135/cropsci2015.01.0057.

Byrt, Caitlin S., Christopher P. L. Grof, and Robert T. Furbank. 2011. "C4 Plants as Biofuel Feedstocks: Optimising Biomass Production and Feedstock Quality from a Lignocellulosic PerspectiveFree Access." *Journal of Integrative Plant Biology* 53(2):120–35. doi: 10.1111/j.1744-7909.2010.01023.x.

Cai, Enyu, Sriram Baireddy, Changye Yang, Melba Crawford, and Edward J. Delp. 2020. "Deep Transfer Learning for Plant Center Localization." Pp. 62–63 in.

Cai, Enyu, Sriram Baireddy, Changye Yang, Edward J. Delp, and Melba Crawford. 2021. "Panicle Counting in UAV Images for Estimating Flowering Time in Sorghum." Pp. 6280–83 in *2021 IEEE International Geoscience and Remote Sensing Symposium IGARSS*.

Campbell, Malachy, Mehdi Momen, Harkamal Walia, and Gota Morota. 2019. "Leveraging Breeding Values Obtained from Random Regression Models for Genetic Inference of Longitudinal Traits." *The Plant Genome* 12(2):180075. doi: https://doi.org/10.3835/plantgenome2018.10.0075.

Campos, H., M. Cooper, J. E. Habben, G. O. Edmeades, and J. R. Schussler. 2004. "Improving Drought Tolerance in Maize: A View from Industry." *Field Crops Research* 90(1):19–34. doi: 10.1016/j.fcr.2004.07.003.

Carberry, P. S., R. C. Muchow, and G. L. Hammer. 1993. "Modelling Genotypic and Environmental Control of Leaf Area Dynamics in Grain Sorghum. II. Individual Leaf Level - ScienceDirect." *Field Crops Research* 33(3):311–28.

Carpita, Nicholas C., and Maureen C. McCann. 2008. "Maize and Sorghum: Genetic Resources for Bioenergy Grasses." *Trends in Plant Science* 13(8):415–20. doi: 10.1016/j.tplants.2008.06.002.

Casa, R., F. Baret, S. Buis, R. Lopez-Lozano, S. Pascucci, A. Palombo, and H. G. Jones. 2010. "Estimation of Maize Canopy Properties from Remote Sensing by Inversion of 1-D and 4-D Models." *Precision Agriculture* 11(4):319–34. doi: 10.1007/s11119-010-9162-9.

Casto, Anna L., Ashley J. Mattison, Sara N. Olson, Manish Thakran, William L. Rooney, and John E. Mullet. 2019. "Maturity2, a Novel Regulator of Flowering Time in Sorghum Bicolor, Increases Expression of SbPRR37 and SbCO in Long Days Delaying Flowering." *PLOS ONE* 14(4):e0212154. doi: 10.1371/journal.pone.0212154.

Castro, Fernanda Maria Rodrigues, Adriano Teodoro Bruzi, José Airton Rodrigues Nunes, Rafael Augusto Costa Parrella, Gabrielle Maria Romeiro Lombardi, Carlos Juliano Brant Albuquerque, and Maurício Lopes. 2015. "Agronomic and Energetic Potential of Biomass Sorghum Genotypes." *American Journal of Plant Sciences* 06(11):1862. doi: 10.4236/ajps.2015.611187.

Chapman, S. C., M. Cooper, D. G. Butler, and R. G. Henzell. 2000. "Genotype by Environment Interactions Affecting Grain Sorghum. I. Characteristics That Confound Interpretation of Hybrid Yield." *Australian Journal of Agricultural Research* 51(2):197–208. doi: 10.1071/ar99020.

Chapman, S. C., M. Cooper, G. L. Hammer, and D. G. Butler. 2000. "Genotype by Environment Interactions Affecting Grain Sorghum. II. Frequencies of Different Seasonal Patterns of Drought Stress Are Related to Location Effects on Hybrid Yields." *Australian Journal of Agricultural Research* 51(2):209–22. doi: 10.1071/ar99021.

Chapman, S. C., G. L. Hammer, D. G. Butler, and M. Cooper. 2000. "Genotype by Environment Interactions Affecting Grain Sorghum. III. Temporal Sequences and Spatial Patterns in the Target Population of Environments." *Australian Journal of Agricultural Research* 51(2):223–34. doi: 10.1071/ar99022.

Chapman, Scott C. 2008. “Use of Crop Models to Understand Genotype by Environment Interactions for Drought in Real-World and Simulated Plant Breeding Trials.” *Euphytica* 161(1–2):195–208. doi: 10.1007/s10681-007-9623-z.

Chapman, Scott, Mark Cooper, Dean Podlich, and Graeme Hammer. 2003. “Evaluating Plant Breeding Strategies by Simulating Gene Action and Dryland Environment Effects.” *Agronomy Journal* 95(1):99–113. doi: 10.2134/agronj2003.9900.

Charles-Edwards, D. A. 1982. “Physiological Determinants of Crop Growth.” 25.

Chehab, E. Wassim, Elizabeth Eich, and Janet Braam. 2009. “Thigmomorphogenesis: A Complex Plant Response to Mechano-Stimulation.” *Journal of Experimental Botany* 60(1):43–56. doi: 10.1093/jxb/ern315.

Chen, Yuhao. 2019. “ESTIMATING PLANT PHENOTYPIC TRAITS FROM RGB IMAGERY.” thesis, Purdue University Graduate School.

Chen, Yuhao, Sriram Baireddy, Enyu Cai, Changye Yang, and Edward J. Delp. 2019. “Leaf Segmentation by Functional Modeling.” Pp. 0–0 in.

Chen, Yuhao, Javier Ribera, Christopher Boomsma, and Edward Delp. 2017. “Locating Crop Plant Centers From UAV-Based RGB Imagery.” Pp. 2030–37 in.

Chen, Yuhao, Javier Ribera, Christopher Boomsma, and Edward J. Delp. 2017. “Plant Leaf Segmentation for Estimating Phenotypic Traits.” Pp. 3884–88 in *2017 IEEE International Conference on Image Processing (ICIP)*.

Chen, Yuhao, Javier Ribera, and Edward J. Delp. 2018. “Estimating Plant Centers Using A Deep Binary Classifier.” Pp. 105–8 in *2018 IEEE Southwest Symposium on Image Analysis and Interpretation (SSIAI)*.

Chenu, K., E. J. Van Oosterom, G. McLean, K. S. Deifel, A. Fletcher, G. Geetika, A. Tirfessa, E. S. Mace, D. R. Jordan, R. Sulman, and G. L. Hammer. 2018. “Integrating Modelling and Phenotyping Approaches to Identify and Screen Complex Traits: Transpiration Efficiency in Cereals.” *Journal of Experimental Botany* 69(13):3181–94. doi: 10.1093/jxb/ery059.

Chenu, Karine, Scott C. Chapman, Graeme L. Hammer, Greg Mclean, Halim Ben Haj Salah, and François Tardieu. 2008. “Short-Term Responses of Leaf Growth Rate to Water Deficit Scale up to Whole-Plant and Crop Levels: An Integrated Modelling Approach in Maize.” *Plant, Cell & Environment* 31(3):378–91. doi: 10.1111/j.1365-3040.2007.01772.x.

Childs, K. L., F. R. Miller, M. M. Cordonnier-Pratt, L. H. Pratt, P. W. Morgan, and J. E. Mullet. 1997. “The Sorghum Photoperiod Sensitivity Gene, Ma3, Encodes a Phytochrome B.” *Plant Physiology* 113(2):611–19. doi: 10.1104/pp.113.2.611.

Cho, Young Yeol, and Jung Eek Son. 2007. “Estimation of Leaf Number and Leaf Area of Hydroponic Pak-Choi Plants (<Emphasis Type="Italic">Brassica Campestns</Emphasis> Ssp,<Emphasis Type="Italic">chinensis</Emphasis>) Using Growing Degree-Days.” *Journal of Plant Biology* 50(1):8. doi: 10.1007/BF03030593.

Chu, Tianxing, Michael J. Starek, Michael J. Brewer, Seth C. Murray, and Luke S. Pruter. 2018. “Characterizing Canopy Height with UAS Structure-from-Motion Photogrammetry—Results Analysis of a Maize Field Trial with Respect to Multiple Factors.” *Remote Sensing Letters* 9(8):753–62. doi: 10.1080/2150704X.2018.1475771.

Ciampitti, Ignacio A., and P. V. Vara Prasad. 2020. *Sorghum: State of the Art and Future Perspectives*. John Wiley & Sons.

Clerget, B., M. Dingkuhn, E. Gozé, H. F. W. Rattunde, and B. Ney. 2008. “Variability of Phyllochron, Plastochron and Rate of Increase in Height in Photoperiod-Sensitive Sorghum Varieties.” *Annals of Botany* 101(4):579–94. doi: 10.1093/aob/mcm327.

Cobb, Joshua N., Genevieve DeClerck, Anthony Greenberg, Randy Clark, and Susan McCouch. 2013. “Next-Generation Phenotyping: Requirements and Strategies for Enhancing Our Understanding of Genotype–Phenotype Relationships and Its Relevance to Crop Improvement.” *Theoretical and Applied Genetics* 126(4):867–87. doi: 10.1007/s00122-013-2066-0.

Cobb, Joshua N., Roselyne U. Juma, Partha S. Biswas, Juan D. Arbelaez, Jessica Rutkoski, Gary Atlin, Tom Hagen, Michael Quinn, and Eng Hwa Ng. 2019. “Enhancing the Rate of Genetic Gain in Public-Sector Plant Breeding Programs: Lessons from the Breeder’s Equation.” *Theoretical and Applied Genetics* 132(3):627–45. doi: 10.1007/s00122-019-03317-0.

Cockram, James, Jon White, Diana L. Zuluaga, David Smith, Jordi Comadran, Malcolm Macaulay, Zewei Luo, Mike J. Kearsey, Peter Werner, David Harrap, Chris Tapsell, Hui Liu, Peter E. Hedley, Nils Stein, Daniela Schulte, Burkhard Steuernagel, David F. Marshall, William T. B. Thomas, Luke Ramsay, Ian Mackay, David J. Balding, The AGOUEB Consortium, Robbie Waugh, and Donal M. O’Sullivan. 2010. “Genome-Wide Association Mapping to Candidate Polymorphism Resolution in the Unsequenced Barley Genome.” *Proceedings of the National Academy of Sciences* 107(50):21611–16. doi: 10.1073/pnas.1010179107.

Condon, A. G., R. A. Richards, G. J. Rebetzke, and G. D. Farquhar. 2002. “Improving Intrinsic Water-Use Efficiency and Crop Yield.” *Crop Science* 42(1):122–31. doi: 10.2135/cropsci2002.1220.

Cooper, JP. 1970. “Potential Production and Energy Conversion in Temperate and Tropical Grasses.” *Herb Abstr* 40:1–15.

Cooper, Mark, Carlos D. Messina, Dean Podlich, L. Radu Totir, Andrew Baumgarten, Neil J. Hausmann, Deanne Wright, Geoffrey Graham, Mark Cooper, Carlos D. Messina, Dean Podlich, L. Radu Totir, Andrew Baumgarten, Neil J. Hausmann, Deanne Wright, and Geoffrey Graham. 2014. "Predicting the Future of Plant Breeding: Complementing Empirical Evaluation with Genetic Prediction." *Crop and Pasture Science* 65(4):311–36. doi: 10.1071/CP14007.

Cooper, Mark, Tom Tang, Carla Gho, Tim Hart, Graeme Hammer, and Carlos Messina. 2020. "Integrating Genetic Gain and Gap Analysis to Predict Improvements in Crop Productivity." *Crop Science* 60(2):582–604. doi: 10.1002/csc2.20109.

Cooper, Mark, Frank Technow, Carlos Messina, Carla Gho, and L. Radu Totir. 2016. "Use of Crop Growth Models with Whole-Genome Prediction: Application to a Maize Multienvironment Trial." *Crop Science* 56(5):2141–56. doi: 10.2135/cropsci2015.08.0512.

Crasta, O. R., W. W. Xu, D. T. Rosenow, J. Mullet, and H. T. Nguyen. 1999. "Mapping of Post-Flowering Drought Resistance Traits in Grain Sorghum: Association between QTLs Influencing Premature Senescence and Maturity." *Molecular and General Genetics MGG* 262(3):579–88. doi: 10.1007/s004380051120.

Crossa, José, Paulino Pérez-Rodríguez, Jaime Cuevas, Osval Montesinos-López, Diego Jarquín, Gustavo de los Campos, Juan Burgueño, Juan M. González-Camacho, Sergio Pérez-Elizalde, Yoseph Beyene, Susanne Dreisigacker, Ravi Singh, Xuecai Zhang, Manje Gowda, Manish Roorkiwal, Jessica Rutkoski, and Rajeev K. Varshney. 2017. "Genomic Selection in Plant Breeding: Methods, Models, and Perspectives." *Trends in Plant Science* 22(11):961–75. doi: 10.1016/j.tplants.2017.08.011.

Cruet-Burgos, Clara, Sarah Cox, Brian P. Ioerger, Ramasamy Perumal, Zhenbin Hu, Thomas J. Herald, Scott R. Bean, and Davina H. Rhodes. 2020. "Advancing Provitamin A Biofortification in Sorghum: Genome-Wide Association Studies of Grain Carotenoids in Global Germplasm." *The Plant Genome* 13(1):e20013. doi: 10.1002/tpg2.20013.

Cuevas, Hugo E., and Louis K. Prom. 2020. "Evaluation of Genetic Diversity, Agronomic Traits, and Anthracnose Resistance in the NPGS Sudan Sorghum Core Collection." *BMC Genomics* 21(1):88. doi: 10.1186/s12864-020-6489-0.

Cuevas, Hugo E., Chengbo Zhou, Haibao Tang, Prashant P. Khadke, Sayan Das, Yann-Rong Lin, Zhengxiang Ge, Thomas Clemente, Hari D. Upadhyaya, C. Thomas Hash, and Andrew H. Paterson. 2016. "The Evolution of Photoperiod-Insensitive Flowering in Sorghum, A Genomic Model for Panicoid Grasses." *Molecular Biology and Evolution* 33(9):2417–28. doi: 10.1093/molbev/msw120.

Curt, M. D., J. Fernandez, and M. Martinez. 1998. "Productivity and Radiation Use Efficiency of Sweet Sorghum (Sorghum Bicolor (L.) Moench) Cv. Keller in Central Spain." *Biomass and Bioenergy* 14(2):169–78. doi: 10.1016/S0961-9534(97)10025-3.

Dale, Laura M., André Thewis, Christelle Boudry, Ioan Rotar, Pierre Dardenne, Vincent Baeten, and Juan A. Fernández Pierna. 2013. “Hyperspectral Imaging Applications in Agriculture and Agro-Food Product Quality and Safety Control: A Review.” *Applied Spectroscopy Reviews* 48(2):142–59. doi: 10.1080/05704928.2012.705800.

Deery, David, Jose Jimenez-Berni, Hamlyn Jones, Xavier Sirault, and Robert Furbank. 2014. “Proximal Remote Sensing Buggies and Potential Applications for Field-Based Phenotyping.” *Agronomy* 4(3):349–79. doi: 10.3390/agronomy4030349.

Demarez, Valérie, Sylvie Duthoit, Frédéric Baret, Marie Weiss, and Gérard Dedieu. 2008. “Estimation of Leaf Area and Clumping Indexes of Crops with Hemispherical Photographs.” *Agricultural and Forest Meteorology* 148(4):644–55. doi: 10.1016/j.agrformet.2007.11.015.

Desta, Zeratsion Abera, and Rodomiro Ortiz. 2014. “Genomic Selection: Genome-Wide Prediction in Plant Improvement.” *Trends in Plant Science* 19(9):592–601. doi: 10.1016/j.tplants.2014.05.006.

DeWit, C. T. de. 1965. *Photosynthesis of Leaf Canopies*. 663. Wageningen: Pudoc.

Dharmasiri, Nihal, Sunethra Dharmasiri, Dolf Weijers, Esther Lechner, Masashi Yamada, Lawrence Hobbie, Jasmin S. Ehrismann, Gerd Jürgens, and Mark Estelle. 2005. “Plant Development Is Regulated by a Family of Auxin Receptor F Box Proteins.” *Developmental Cell* 9(1):109–19. doi: 10.1016/j.devcel.2005.05.014.

Diepen, C. A. van, J. Wolf, H. van Keulen, and C. Rappoldt. 1989. “WOFOST: A Simulation Model of Crop Production.” *Soil Use and Management* 5(1):16–24. doi: 10.1111/j.1475-2743.1989.tb00755.x.

Dreccer, M. F., M. van Oijen, A. H. C. M. Schapendonk, C. S. Pot, and R. Rabbinge. 2000. “Dynamics of Vertical Leaf Nitrogen Distribution in a Vegetative Wheat Canopy. Impact on Canopy Photosynthesis.” *Annals of Botany* 86(4):821–31. doi: 10.1006/anbo.2000.1244.

Duan, Si-Bo, Zhao-Liang Li, Hua Wu, Bo-Hui Tang, Lingling Ma, Enyu Zhao, and Chuanrong Li. 2014. “Inversion of the PROSAIL Model to Estimate Leaf Area Index of Maize, Potato, and Sunflower Fields from Unmanned Aerial Vehicle Hyperspectral Data.” *International Journal of Applied Earth Observation and Geoinformation* 26:12–20. doi: 10.1016/j.jag.2013.05.007.

Duan, T., S. C. Chapman, E. Holland, G. J. Rebetzke, Y. Guo, and B. Zheng. 2016. “Dynamic Quantification of Canopy Structure to Characterize Early Plant Vigour in Wheat Genotypes.” *Journal of Experimental Botany* 67(15):4523–34. doi: 10.1093/jxb/erw227.

Duan, T., S. C. Chapman, Y. Guo, and B. Zheng. 2017. “Dynamic Monitoring of NDVI in Wheat Agronomy and Breeding Trials Using an Unmanned Aerial Vehicle.” *Field Crops Research* 210:71–80. doi: 10.1016/j.fcr.2017.05.025.

Duncan, W. G. 1971. “Leaf Angles, Leaf Area, and Canopy Photosynthesis 1.” *Crop Science* 11(4):482–85. doi: 10.2135/cropsci1971.0011183X001100040006x.

El Mannai, Yousra, Tariq Shehzad, and Kazutoshi Okuno. 2011. “Variation in Flowering Time in Sorghum Core Collection and Mapping of QTLs Controlling Flowering Time by Association Analysis.” *Genetic Resources and Crop Evolution* 58(7):983. doi: 10.1007/s10722-011-9737-y.

Elshire, Robert J., Jeffrey C. Glaubitz, Qi Sun, Jesse A. Poland, Ken Kawamoto, Edward S. Buckler, and Sharon E. Mitchell. 2011. “A Robust, Simple Genotyping-by-Sequencing (GBS) Approach for High Diversity Species.” *PLOS ONE* 6(5):e19379. doi: 10.1371/journal.pone.0019379.

Escolà, Alexandre, Santiago Planas, Joan Ramon Rosell, Jesús Pomar, Ferran Camp, Francesc Solanelles, Felip Gracia, Jordi Llorens, and Emilio Gil. 2011. “Performance of an Ultrasonic Ranging Sensor in Apple Tree Canopies.” *Sensors* 11(3):2459–77. doi: 10.3390/s110302459.

Esechie, H. A., J. W. Maranville, and W. M. Ross. 1977. “Relationship of Stalk Morphology and Chemical Composition to Lodging Resistance in Sorghum1.” *Crop Science* 17(4):cropsci1977.0011183X001700040032x. doi: 10.2135/cropsci1977.0011183X001700040032x.

Falster, Daniel S., and Mark Westoby. 2003. “Leaf Size and Angle Vary Widely across Species: What Consequences for Light Interception?” *New Phytologist* 158(3):509–25. doi: 10.1046/j.1469-8137.2003.00765.x.

Farquhar, G. D., J. R. Ehleringer, and K. T. Hubick. 1989. “Carbon Isotope Discrimination and Photosynthesis.” *Annual Review of Plant Physiology and Plant Molecular Biology* 40(1):503–37. doi: 10.1146/annurev.pp.40.060189.002443.

Felderhoff, T. J., S. C. Murray, P. E. Klein, A. Sharma, M. T. Hamblin, S. Kresovich, W. Vermerris, and W. L. Rooney. 2012. “QTLs for Energy-Related Traits in a Sweet × Grain Sorghum [Sorghum Bicolor (L.) Moench] Mapping Population.” *Crop Science* 52(5):2040–49. doi: 10.2135/cropsci2011.11.0618.

Feltus, F. A., G. E. Hart, K. F. Schertz, A. M. Casa, S. Kresovich, S. Abraham, P. E. Klein, P. J. Brown, and A. H. Paterson. 2006. “Alignment of Genetic Maps and QTLs between Inter- and Intra-Specific Sorghum Populations.” *Theoretical and Applied Genetics* 112(7):1295. doi: 10.1007/s00122-006-0232-3.

Ferraris, R. 1981. “Early Assessment of Sweet Sorghum as an Agro-Industrial Crop. I. Varietal Evaluation.” *Australian Journal of Experimental Agriculture* 21(108):75–82. doi: 10.1071/ea9810075.

Fernandes, Samuel B., Kaio O. G. Dias, Daniel F. Ferreira, and Patrick J. Brown. 2018. "Efficiency of Multi-Trait, Indirect, and Trait-Assisted Genomic Selection for Improvement of Biomass Sorghum." *Theoretical and Applied Genetics* 131(3):747–55. doi: 10.1007/s00122-017-3033-y.

Fiedler, Karin, Wubishet A. Bekele, Ria Duensing, Susann Gründig, Rod Snowdon, Hartmut Stützel, Arndt Zacharias, and Ralf Uptmoor. 2014. "Genetic Dissection of Temperature-Dependent Sorghum Growth during Juvenile Development." *Theoretical and Applied Genetics* 127(9):1935–48. doi: 10.1007/s00122-014-2350-7.

Fiedler, Karin, Wubishet A. Bekele, Claudia Matschegewski, Rod Snowdon, Silke Wieckhorst, Arndt Zacharias, and Ralf Uptmoor. 2016. "Cold Tolerance during Juvenile Development in Sorghum: A Comparative Analysis by Genomewide Association and Linkage Mapping." *Plant Breeding* 135(5):598–606. doi: 10.1111/pbr.12394.

Furbank, Robert T. 2009. "Plant Phenomics: From Gene to Form and Function." *Funct. Plant Biol. 2009* 10–11.

Furbank, Robert T., Jose A. Jimenez-Berni, Barbara George-Jaeggli, Andries B. Potgieter, and David M. Deery. 2019. "Field Crop Phenomics: Enabling Breeding for Radiation Use Efficiency and Biomass in Cereal Crops." *New Phytologist* 223(4):1714–27. doi: 10.1111/nph.15817.

Furbank, Robert T., and Mark Tester. 2011. "Phenomics – Technologies to Relieve the Phenotyping Bottleneck." *Trends in Plant Science* 16(12):635–44. doi: 10.1016/j.tplants.2011.09.005.

Gelli, Malleswari, Sharon E. Mitchell, Kan Liu, Thomas E. Clemente, Donald P. Weeks, Chi Zhang, David R. Holding, and Ismail M. Dweikat. 2016. "Mapping QTLs and Association of Differentially Expressed Gene Transcripts for Multiple Agronomic Traits under Different Nitrogen Levels in Sorghum." *BMC Plant Biology* 16(1):16. doi: 10.1186/s12870-015-0696-x.

George-Jaeggli, B., D. R. Jordan, E. J. van Oosterom, I. J. Broad, and G. L. Hammer. 2013. "Sorghum Dwarfing Genes Can Affect Radiation Capture and Radiation Use Efficiency." *Field Crops Research* 149:283–90. doi: 10.1016/j.fcr.2013.05.005.

George-Jaeggli, B., D. R. Jordan, E. J. van Oosterom, and G. L. Hammer. 2011. "Decrease in Sorghum Grain Yield Due to the Dw3 Dwarfing Gene Is Caused by Reduction in Shoot Biomass." *Field Crops Research* 124(2):231–39. doi: 10.1016/j.fcr.2011.07.005.

Gill, John R., Payne S. Burks, Scott A. Staggenborg, Gary N. Odvody, Ron W. Heiniger, Bisoondat Macoon, Ken J. Moore, Michael Barrett, and William L. Rooney. 2014. "Yield Results and Stability Analysis from the Sorghum Regional Biomass Feedstock Trial." *BioEnergy Research* 7(3):1026–34. doi: 10.1007/s12155-014-9445-5.

Girma, Gezahegn, Habte Nida, Amare Seyoum, Moges Mekonen, Amare Nega, Dagnachew Lule, Kebede Dessalegn, Alemnesh Bekele, Adane Gebreyohannes, Adedayo Adeyanju, Alemu Tirfessa, Getachew Ayana, Taye Taddese, Firew Mekbib, Ketema Belete, Tesfaye Tesso, Gebisa Ejeta, and Tesfaye Mengiste. 2019. "A Large-Scale Genome-Wide Association Analyses of Ethiopian Sorghum Landrace Collection Reveal Loci Associated With Important Traits." *Frontiers in Plant Science* 10. doi: 10.3389/fpls.2019.00691.

Goodstein, David M., Shengqiang Shu, Russell Howson, Rochak Neupane, Richard D. Hayes, Joni Fazo, Therese Mitros, William Dirks, Uffe Hellsten, Nicholas Putnam, and Daniel S. Rokhsar. 2012. "Phytozome: A Comparative Platform for Green Plant Genomics." *Nucleic Acids Research* 40(Database issue):D1178–86. doi: 10.1093/nar/gkr944.

Gouache, David, Katia Beauchêne, Agathe Mini, Antoine Fournier, Benoit de Solan, Fred Baret, and Alexis Comar. 2016. "Applying Remote Sensing Expertise to Crop Improvement: Progress and Challenges to Scale up High Throughput Field Phenotyping from Research to Industry." P. 986604 in *Autonomous Air and Ground Sensing Systems for Agricultural Optimization and Phenotyping*. Vol. 9866. International Society for Optics and Photonics.

Goudriaan, J. 1982. "Potential Production Processes." Pp. 98–113 in *Simulation of plant growth and crop production*. Pudoc.

Griebel, Stefanie, Adeyanju Adedayo, and Mitchell R. Tuinstra. 2021. "Genetic Diversity for Starch Quality and Alkali Spreading Value in Sorghum." *The Plant Genome* 14(1):e20067. doi: 10.1002/tpg2.20067.

Großkinsky, Dominik K., Jesper Svensgaard, Svend Christensen, and Thomas Roitsch. 2015. "Plant Phenomics and the Need for Physiological Phenotyping across Scales to Narrow the Genotype-to-Phenotype Knowledge Gap." *Journal of Experimental Botany* 66(18):5429–40. doi: 10.1093/jxb/erv345.

Guan, Yan-an, Hai-lian Wang, Ling Qin, Hua-wen Zhang, Yan-bing Yang, Feng-ju Gao, Ru-yu Li, and Hong-gang Wang. 2011. "QTL Mapping of Bio-Energy Related Traits in Sorghum." *Euphytica* 182(3):431. doi: 10.1007/s10681-011-0528-5.

Guindo, Diarah, Niaba Teme, Michel Vaksmann, Mohamed Doumbia, Ingrid Vilmus, Baptiste Guitton, Aliou Sissoko, Christian Mestres, Fabrice Davrieux, Geneviève Fliedel, Mamoutou Kouressy, Brigitte Courtois, and Jean-Francois Rami. 2019. "Quantitative Trait Loci for Sorghum Grain Morphology and Quality Traits: Toward Breeding for a Traditional Food Preparation of West-Africa." *Journal of Cereal Science* 85:256–72. doi: 10.1016/j.jcs.2018.11.012.

Guo, Wei, Bangyou Zheng, Tao Duan, Tokihiro Fukatsu, Scott Chapman, and Seishi Ninomiya. 2017. "EasyPCC: Benchmark Datasets and Tools for High-Throughput Measurement of the Plant Canopy Coverage Ratio under Field Conditions." *Sensors* 17(4):798. doi: 10.3390/s17040798.

Habib, Ayman, Tian Zhou, Ali Masjedi, Zhou Zhang, John Evan Flatt, and Melba Crawford. 2018. "Boresight Calibration of GNSS/INS-Assisted Push-Broom Hyperspectral Scanners on UAV Platforms." *IEEE Journal of Selected Topics in Applied Earth Observations and Remote Sensing* 11(5):1734–49. doi: 10.1109/JSTARS.2018.2813263.

Habyarimana, Ephrem, Paolo De Franceschi, Sezai Ercisli, Faheem Shehzad Baloch, and Michela Dall'Agata. 2020. "Genome-Wide Association Study for Biomass Related Traits in a Panel of Sorghum Bicolor and S. Bicolor × S. Halepense Populations." *Frontiers in Plant Science* 11:1796. doi: 10.3389/fpls.2020.551305.

Hamby, R. Keith, and Elizabeth A. Zimmer. 1988. "Ribosomal RNA Sequences for Inferring Phylogeny within the Grass Family (Poaceae)." *Plant Systematics and Evolution* 160(1):29–37. doi: 10.1007/BF00936707.

Hammer, G. L., P. S. Carberry, and R. C. Muchow. 1993. "Modelling Genotypic and Environmental Control of Leaf Area Dynamics in Grain Sorghum. I. Whole Plant Level." *Field Crops Research* 33(3):293–310. doi: 10.1016/0378-4290(93)90087-4.

Hammer, G. L., and R. C. Muchow. 1994. "Assessing Climatic Risk to Sorghum Production in Water-Limited Subtropical Environments I. Development and Testing of a Simulation Model - ScienceDirect." *Field Crops Research* 36(3):221–34.

Hammer, Graeme L., Zhanshan Dong, Greg McLean, Al Doherty, Carlos Messina, Jeff Schussler, Chris Zinselmeier, Steve Paszkiewicz, and Mark Cooper. 2009. "Can Changes in Canopy and/or Root System Architecture Explain Historical Maize Yield Trends in the U.S. Corn Belt?" *Crop Science* 49(1):299–312. doi: 10.2135/cropsci2008.03.0152.

Hammer, Graeme L., Greg McLean, Scott Chapman, Bangyou Zheng, Al Doherty, Matthew T. Harrison, Erik van Oosterom, and David Jordan. 2014. "Crop Design for Specific Adaptation in Variable Dryland Production Environments." *Crop and Pasture Science* 65(7):614–26. doi: 10.1071/CP14088.

Hammer, Graeme L., Erik van Oosterom, Greg McLean, Scott C. Chapman, Ian Broad, Peter Harland, and Russell C. Muchow. 2010. "Adapting APSIM to Model the Physiology and Genetics of Complex Adaptive Traits in Field Crops." *Journal of Experimental Botany* 61(8):2185–2202. doi: 10.1093/jxb/erq095.

Han, Yucui, Peng Lv, Shenglin Hou, Suying Li, Guisu Ji, Xue Ma, Ruiheng Du, and Guoqing Liu. 2015. "Combining Next Generation Sequencing with Bulked Segregant Analysis to Fine Map a Stem Moisture Locus in Sorghum (Sorghum Bicolor L. Moench)." *PLOS ONE* 10(5):e0127065. doi: 10.1371/journal.pone.0127065.

Harlan, J. R., and J. M. J. de Wet. 1972. "A Simplified Classification of Cultivated Sorghum1." *Crop Science* 12(2):cropsci1972.0011183X001200020005x. doi: 10.2135/cropsci1972.0011183X001200020005x.

Hart, G. E., K. F. Schertz, Y. Peng, and N. H. Syed. 2001. “Genetic Mapping of Sorghum Bicolor (L.) Moench QTLs That Control Variation in Tillering and Other Morphological Characters.” *Theoretical and Applied Genetics* 103(8):1232–42. doi: 10.1007/s001220100582.

Hasheminasab, Seyyed Meghdad, Tian Zhou, and Ayman Habib. 2020. “GNSS/INS-Assisted Structure from Motion Strategies for UAV-Based Imagery over Mechanized Agricultural Fields.” *Remote Sensing* 12(3):351. doi: 10.3390/rs12030351.

Hasheminasab, Seyyed Meghdad, Tian Zhou, Lisa M. LaForest, and Ayman Habib. 2021. “Multiscale Image Matching for Automated Calibration of UAV-Based Frame and Line Camera Systems.” *IEEE Journal of Selected Topics in Applied Earth Observations and Remote Sensing* 14:3133–50. doi: 10.1109/JSTARS.2021.3062573.

Hatfield, Jerry L., and Christian Dold. 2019. “Chapter 1 - Photosynthesis in the Solar Corridor System.” Pp. 1–33 in *The Solar Corridor Crop System*, edited by C. L. Deichman and R. J. Kremer. Academic Press.

Haussmann, B., V. Mahalakshmi, B. Reddy, N. Seetharama, C. Hash, and H. Geiger. 2002. “QTL Mapping of Stay-Green in Two Sorghum Recombinant Inbred Populations.” *Theoretical and Applied Genetics* 106(1):133–42. doi: 10.1007/s00122-002-1012-3.

Hayes, Chad M., Gloria B. Burow, Patrick J. Brown, Carrie Thurber, Zhanguo Xin, and John J. Burke. 2015. “Natural Variation in Synthesis and Catabolism Genes Influences Dhurrin Content in Sorghum.” *The Plant Genome* 8(2):plantgenome2014.09.0048. doi: 10.3835/plantgenome2014.09.0048.

He, Fangning, Tian Zhou, Weifeng Xiong, Seyyed Meghdad Hasheminnasab, and Ayman Habib. 2018. “Automated Aerial Triangulation for UAV-Based Mapping.” *Remote Sensing* 10(12):1952. doi: 10.3390/rs10121952.

He, Jiangfeng, Xiaoqing Zhao, André Laroche, Zhen-Xiang Lu, HongKui Liu, and Ziqin Li. 2014. “Genotyping-by-Sequencing (GBS), an Ultimate Marker-Assisted Selection (MAS) Tool to Accelerate Plant Breeding.” *Frontiers in Plant Science* 5:484. doi: 10.3389/fpls.2014.00484.

He, Jin. 2017. “Conserved Water Use Improves the Yield Performance of Soybean (Glycine Max (L.) Merr.) under Drought.” *Agricultural Water Management* v. 179:236–45. doi: 10.1016/j.agwat.2016.07.008.

Higgins, R. H., C. S. Thurber, I. Assaranurak, and P. J. Brown. 2014. “Multiparental Mapping of Plant Height and Flowering Time QTL in Partially Isogenic Sorghum Families.” *G3 Genes|Genomes|Genetics* 4(9):1593–1602. doi: 10.1534/g3.114.013318.

Hilley, Josie, Sandra Truong, Sara Olson, Daryl Morishige, and John Mullet. 2016. “Identification of Dw1, a Regulator of Sorghum Stem Internode Length.” *PLoS ONE* 11(3). doi: 10.1371/journal.pone.0151271.

Hirano, Ko, Mayuko Kawamura, Satoko Araki-Nakamura, Haruka Fujimoto, Kozue Ohmae-Shinohara, Miki Yamaguchi, Akihiro Fujii, Hiroaki Sasaki, Shigemitsu Kasuga, and Takashi Sazuka. 2017. "Sorghum DW1 Positively Regulates Brassinosteroid Signaling by Inhibiting the Nuclear Localization of BRASSINOSTEROID INSENSITIVE 2." *Scientific Reports* 7(1):126. doi: 10.1038/s41598-017-00096-w.

Hoffmeister, D., G. Waldhoff, W. Korres, C. Curdt, and G. Bareth. 2016. "Crop Height Variability Detection in a Single Field by Multi-Temporal Terrestrial Laser Scanning." *Precision Agriculture* 17(3):296–312.

Holzworth, Dean, N. I. Huth, J. Fainges, H. Brown, E. Zurcher, R. Cichota, S. Verrall, N. I. Herrmann, B. Zheng, and V. Snow. 2018. "APSIM Next Generation: Overcoming Challenges in Modernising a Farming Systems Model." *Environmental Modelling & Software* 103:43–51. doi: 10.1016/j.envsoft.2018.02.002.

Holzworth, Dean P. 2014. "APSIM – Evolution towards a New Generation of Agricultural Systems Simulation." *Environmental Modelling & Software* v. 62:327–50. doi: 10.1016/j.envsoft.2014.07.009.

Hoyos-Villegas, V., J. h. Houx, S. k. Singh, and F. b. Fritschi. 2014. "Ground-Based Digital Imaging as a Tool to Assess Soybean Growth and Yield." *Crop Science* 54(4):1756–68. doi: 10.2135/cropsci2013.08.0540.

Huang, Xuehui, and Bin Han. 2014. "Natural Variations and Genome-Wide Association Studies in Crop Plants." *Annual Review of Plant Biology* 65(1):531–51. doi: 10.1146/annurev-arplant-050213-035715.

Huang, Xuehui, Yan Zhao, Xinghua Wei, Canyang Li, Ahong Wang, Qiang Zhao, Wenjun Li, Yunli Guo, Liuwei Deng, Chuanrang Zhu, Danlin Fan, Yiqi Lu, Qijun Weng, Kunyan Liu, Taoying Zhou, Yufeng Jing, Lizhen Si, Guojun Dong, Tao Huang, Tingting Lu, Qi Feng, Qian Qian, Jiayang Li, and Bin Han. 2012. "Genome-Wide Association Study of Flowering Time and Grain Yield Traits in a Worldwide Collection of Rice Germplasm." *Nature Genetics* 44(1):32–39. doi: 10.1038/ng.1018.

Ines, Amor V. M., Narendra N. Das, James W. Hansen, and Eni G. Njoku. 2013. "Assimilation of Remotely Sensed Soil Moisture and Vegetation with a Crop Simulation Model for Maize Yield Prediction." *Remote Sensing of Environment* 138:149–64. doi: 10.1016/j.rse.2013.07.018.

J. R. Williams, C. A. Jones, J. R. Kiniry, and D. A. Spanel. 1989. "The EPIC Crop Growth Model." *Transactions of the ASAE* 32(2):0497–0511. doi: 10.13031/2013.31032.

Janick, Jules. 2010. *Plant Breeding Reviews*. John Wiley & Sons.

Jiang, Rong, Wentian He, Wei Zhou, Yunpeng Hou, J. Y. Yang, and Ping He. 2019. "Exploring Management Strategies to Improve Maize Yield and Nitrogen Use Efficiency in Northeast China Using the DNDC and DSSAT Models." *Computers and Electronics in Agriculture* 166:104988. doi: 10.1016/j.compag.2019.104988.

Jimenez-Berni, Jose A., David M. Deery, Pablo Rozas-Larraondo, Anthony (Tony) G. Condon, Greg J. Rebetzke, Richard A. James, William D. Bovill, Robert T. Furbank, and Xavier R. R. Sirault. 2018. "High Throughput Determination of Plant Height, Ground Cover, and Above-Ground Biomass in Wheat with LiDAR." *Frontiers in Plant Science* 9. doi: 10.3389/fpls.2018.00237.

Jonas, Elisabeth, and Dirk-Jan de Koning. 2013. "Does Genomic Selection Have a Future in Plant Breeding?" *Trends in Biotechnology* 31(9):497–504. doi: 10.1016/j.tibtech.2013.06.003.

Jones, J. W., G. Hoogenboom, C. H. Porter, K. J. Boote, W. D. Batchelor, L. A. Hunt, P. W. Wilkens, U. Singh, A. J. Gijsman, and J. T. Ritchie. 2003. "The DSSAT Cropping System Model." *European Journal of Agronomy* 18(3–4):235–65. doi: 10.1016/S1161-0301(02)00107-7.

Jones, James W., John M. Antle, Bruno Basso, Kenneth J. Boote, Richard T. Conant, Ian Foster, H. Charles J. Godfray, Mario Herrero, Richard E. Howitt, Sander Janssen, Brian A. Keating, Rafael Munoz-Carpena, Cheryl H. Porter, Cynthia Rosenzweig, and Tim R. Wheeler. 2017. "Brief History of Agricultural Systems Modeling." *Agricultural Systems* 155:240–54. doi: 10.1016/j.agsy.2016.05.014.

Jordan, D. R., C. H. Hunt, A. W. Cruickshank, A. K. Borrell, and R. G. Henzell. 2012. "The Relationship Between the Stay-Green Trait and Grain Yield in Elite Sorghum Hybrids Grown in a Range of Environments." *Crop Science* 52(3):1153–61. doi: 10.2135/cropsci2011.06.0326.

Kapanigowda, Mohankumar H., William A. Payne, William L. Rooney, John E. Mullet, Maria Balota, Mohankumar H. Kapanigowda, William A. Payne, William L. Rooney, John E. Mullet, and Maria Balota. 2014. "Quantitative Trait Locus Mapping of the Transpiration Ratio Related to Preflowering Drought Tolerance in Sorghum (Sorghum Bicolor)." *Functional Plant Biology* 41(11):1049–65. doi: 10.1071/FP13363.

Karami, Azam, Melba Crawford, and Edward J. Delp. 2020a. "A Weakly Supervised Deep Learning Approach for Plant Center Detection and Counting." Pp. 1584–87 in *IGARSS 2020 - 2020 IEEE International Geoscience and Remote Sensing Symposium*.

Karami, Azam, Melba Crawford, and Edward J. Delp. 2020b. "Automatic Plant Counting and Location Based on a Few-Shot Learning Technique." *IEEE Journal of Selected Topics in Applied Earth Observations and Remote Sensing* 13:5872–86. doi: 10.1109/JSTARS.2020.3025790.

Karami, Azam, Karoll Quijano, and Melba Crawford. 2021. "Advancing Tassel Detection and Counting: Annotation and Algorithms." *Remote Sensing* 13(15):2881. doi: 10.3390/rs13152881.

Kasampalis, Dimitrios A., Thomas K. Alexandridis, Chetan Deva, Andrew Challinor, Dimitrios Moshou, and Georgios Zalidis. 2018. "Contribution of Remote Sensing on Crop Models: A Review." *Journal of Imaging* 4(4):52. doi: 10.3390/jimaging4040052.

Kavuluko, Jacinta, Magdaline Kibe, Irine Sugut, Willy Kibet, Joel Masanga, Sylvia Mutinda, Mark Wamalwa, Titus Magomere, Damaris Odeny, and Steven Runo. 2021. "GWAS Provides Biological Insights into Mechanisms of the Parasitic Plant (Striga) Resistance in Sorghum." *BMC Plant Biology* 21(1):392. doi: 10.1186/s12870-021-03155-7.

Keating, B. A., M. J. Robertson, R. C. Muchow, and N. I. Huth. 1999. "Modelling Sugarcane Production Systems I. Development and Performance of the Sugarcane Module." *Field Crops Research* 61(3):253–71. doi: 10.1016/S0378-4290(98)00167-1.

Keating, B. A., P. S. Carberry, G. L. Hammer, M. E. Probert, M. J. Robertson, D. Holzworth, N. I. Huth, J. N. G. Hargreaves, H. Meinke, Z. Hochman, G. McLean, K. Verburg, V. Snow, J. P. Dimes, M. Silburn, E. Wang, S. Brown, K. L. Bristow, S. Asseng, S. Chapman, R. L. McCown, D. M. Freebairn, and C. J. Smith. 2003. "An Overview of APSIM, a Model Designed for Farming Systems Simulation." *European Journal of Agronomy* 18(3–4):267–88. doi: 10.1016/S1161-0301(02)00108-9.

Kebede, H., P. K. Subudhi, D. T. Rosenow, and H. T. Nguyen. 2001. "Quantitative Trait Loci Influencing Drought Tolerance in Grain Sorghum (Sorghum Bicolor L. Moench)." *Theoretical and Applied Genetics* 103(2):266–76. doi: 10.1007/s001220100541.

Kenga, R., A. Tenkouano, S. C. Gupta, and S. O. Alabi. 2006. "Genetic and Phenotypic Association between Yield Components in Hybrid Sorghum (Sorghum Bicolor (L.) Moench) Populations." *Euphytica* 150(3):319–26. doi: 10.1007/s10681-006-9108-5.

Kim, Hae Koo, Delphine Luquet, Erik van Oosterom, Michael Dingkuhn, and Graeme Hammer. 2010. "Regulation of Tillering in Sorghum: Genotypic Effects." *Annals of Botany* 106(1):69–78. doi: 10.1093/aob/mcq080.

Kiniry, J. R., C. A. Jones, J. C. O'toole, R. Blanchet, M. Cabelguenne, and D. A. Spanel. 1989. "Radiation-Use Efficiency in Biomass Accumulation Prior to Grain-Filling for Five Grain-Crop Species." *Field Crops Research* 20(1):51–64. doi: 10.1016/0378-4290(89)90023-3.

Konare, D., S. Pierre, J. Y. Weng, and E. Morand. 2003. "Real-Time Image Processing for Remote Sensing." Pp. 699–702 vol.2 in *CCECE 2003 - Canadian Conference on Electrical and Computer Engineering. Toward a Caring and Humane Technology (Cat. No.03CH37436)*. Vol. 2.

Kong, Wenqian, Hui Guo, Valorie H. Goff, Tae-Ho Lee, Changsoo Kim, and Andrew H. Paterson. 2014. "Genetic Analysis of Vegetative Branching in Sorghum." *Theoretical and Applied Genetics* 127(11):2387–2403. doi: 10.1007/s00122-014-2384-x.

Kong, Wenqian, Huizhe Jin, Valorie H. Goff, Susan A. Auckland, Lisa K. Rainville, and Andrew H. Paterson. 2020. "Genetic Analysis of Stem Diameter and Water Contents To Improve Sorghum Bioenergy Efficiency." *G3 Genes|Genomes|Genetics* 10(11):3991–4000. doi: 10.1534/g3.120.401608.

Kong, WenQian, Changsoo Kim, Dong Zhang, Hui Guo, Xu Tan, Huizhe Jin, Chengbo Zhou, Lan-shuan Shuang, Valorie Goff, Uzay Sezen, Gary Pierce, Rosana Compton, Cornelia Lemke, Jon Robertson, Lisa Rainville, Susan Auckland, and Andrew H. Paterson. 2018. "Genotyping by Sequencing of 393 Sorghum Bicolor BTx623 × IS3620C Recombinant Inbred Lines Improves Sensitivity and Resolution of QTL Detection." *G3 Genes|Genomes|Genetics* 8(8):2563–72. doi: 10.1534/g3.118.200173.

Konieczny, Andrzej, and Frederick M. Ausubel. 1993. "A Procedure for Mapping Arabidopsis Mutations Using Co-Dominant Ecotype-Specific PCR-Based Markers." *The Plant Journal* 4(2):403–10. doi: 10.1046/j.1365-313X.1993.04020403.x.

Kumar, Gaurav, and Pradeep Kumar Bhatia. 2014. "A Detailed Review of Feature Extraction in Image Processing Systems." Pp. 5–12 in *2014 Fourth International Conference on Advanced Computing & Communication Technologies*. Rohtak, India: IEEE.

Lafarge, T. A., and G. L. Hammer. 2002. "Predicting Plant Leaf Area Production:: Shoot Assimilate Accumulation and Partitioning, and Leaf Area Ratio, Are Stable for a Wide Range of Sorghum Population Densities." *Field Crops Research* 77(2):137–51. doi: 10.1016/S0378-4290(02)00085-0.

Lande, R., and R. Thompson. 1990. "Efficiency of Marker-Assisted Selection in the Improvement of Quantitative Traits." *Genetics* 124(3):743–56.

Lin, Y. R., K. F. Schertz, and A. H. Paterson. 1995. "Comparative Analysis of QTLs Affecting Plant Height and Maturity across the Poaceae, in Reference to an Interspecific Sorghum Population." *Genetics* 141(1):391–411.

Lin, Yi-Chun, and Ayman Habib. 2021. "Quality Control and Crop Characterization Framework for Multi-Temporal UAV LiDAR Data over Mechanized Agricultural Fields." *Remote Sensing of Environment* 256:112299. doi: 10.1016/j.rse.2021.112299.

Lin, Yi-Chun, Tian Zhou, Taojun Wang, Melba Crawford, and Ayman Habib. 2021. "New Orthophoto Generation Strategies from UAV and Ground Remote Sensing Platforms for High-Throughput Phenotyping." *Remote Sensing* 13(5):860. doi: 10.3390/rs13050860.

Lindquist, John L., Timothy J. Arkebauer, Daniel T. Walters, Kenneth G. Cassman, and Achim Dobermann. 2005. "Maize Radiation Use Efficiency under Optimal Growth Conditions." *Agronomy Journal* 97(1):72–78. doi: 10.2134/agronj2005.0072.

Lipka, Alexander E., Feng Tian, Qishan Wang, Jason Peiffer, Meng Li, Peter J. Bradbury, Michael A. Gore, Edward S. Buckler, and Zhiwu Zhang. 2012. "GAPIT: Genome Association and Prediction Integrated Tool." *Bioinformatics* 28(18):2397–99. doi: 10.1093/bioinformatics/bts444.

Litt, M., and J. A. Luty. 1989. "A Hypervariable Microsatellite Revealed by in Vitro Amplification of a Dinucleotide Repeat within the Cardiac Muscle Actin Gene." *American Journal of Human Genetics* 44(3):397–401.

Liu, Huanhuan, Hangqin Liu, Leina Zhou, and Zhongwei Lin. 2019. “Genetic Architecture of Domestication- and Improvement-Related Traits Using a Population Derived from Sorghum Virgatum and Sorghum Bicolor.” *Plant Science* 283:135–46. doi: 10.1016/j.plantsci.2019.02.013.

Liu, Xiaolei, Meng Huang, Bin Fan, Edward S. Buckler, and Zhiwu Zhang. 2016. “Iterative Usage of Fixed and Random Effect Models for Powerful and Efficient Genome-Wide Association Studies.” *PLOS Genetics* 12(2):e1005767. doi: 10.1371/journal.pgen.1005767.

Llorens, Jordi, Emilio Gil, Jordi Llop, and Alexandre Escolà. 2011. “Ultrasonic and LIDAR Sensors for Electronic Canopy Characterization in Vineyards: Advances to Improve Pesticide Application Methods.” *Sensors* 11(2):2177–94. doi: 10.3390/s110202177.

Löffler, Carlos M., Jun Wei, Tim Fast, Joe Gogerty, Steve Langton, Marlin Bergman, Bob Merrill, and Mark Cooper. 2005. “Classification of Maize Environments Using Crop Simulation and Geographic Information Systems.” *Crop Science* 45(5):1708–16. doi: 10.2135/cropsci2004.0370.

Luque, Sergio F., Alfredo G. Cirilo, and María E. Otegui. 2006. “Genetic Gains in Grain Yield and Related Physiological Attributes in Argentine Maize Hybrids.” *Field Crops Research* 95(2):383–97. doi: 10.1016/j.fcr.2005.04.007.

Mace, E. S., C. H. Hunt, and D. R. Jordan. 2013. “Supermodels: Sorghum and Maize Provide Mutual Insight into the Genetics of Flowering Time.” *Theoretical and Applied Genetics* 126(5):1377–95. doi: 10.1007/s00122-013-2059-z.

Mace, E., Innes, D., Hunt, C., Wang, X., Tao, Y., Baxter, J., ... & Jordan, D. (2019). The Sorghum QTL Atlas: a powerful tool for trait dissection, comparative genomics and crop improvement. *Theoretical and applied genetics*, *132*(3), 751-766.

Madec, Simon, Fred Baret, Benoît de Solan, Samuel Thomas, Dan Dutartre, Stéphane Jezequel, Matthieu Hemmerlé, Gallian Colombeau, and Alexis Comar. 2017. “High-Throughput Phenotyping of Plant Height: Comparing Unmanned Aerial Vehicles and Ground LiDAR Estimates.” *Frontiers in Plant Science* 8:2002. doi: 10.3389/fpls.2017.02002.

Madhusudhana, R., and J. V. Patil. 2013. “A Major QTL for Plant Height Is Linked with Bloom Locus in Sorghum [Sorghum Bicolor (L.) Moench].” *Euphytica* 191(2):259–68. doi: 10.1007/s10681-012-0812-z.

Marla, Sandeep R., Gloria Burow, Ratan Chopra, Chad Hayes, Marcus O. Olatoye, Terry Felderhoff, Zhenbin Hu, Rubi Raymundo, Ramasamy Perumal, and Geoffrey P. Morris. 2019. “Genetic Architecture of Chilling Tolerance in Sorghum Dissected with a Nested Association Mapping Population.” *G3 Genes|Genomes|Genetics* 9(12):4045–57. doi: 10.1534/g3.119.400353.

Masjedi, Ali. 2020. “MULTI-TEMPORAL MULTI-MODAL PREDICTIVE MODELLING OF PLANT PHENOTYPES.”

Masjedi, Ali, and Melba M. Crawford. 2020. “PREDICTION OF SORGHUM BIOMASS USING TIME SERIES UAV-BASED HYPERSPECTRAL AND LIDAR DATA.” Pp. 3912–15 in *IGARSS 2020 - 2020 IEEE International Geoscience and Remote Sensing Symposium*.

Masjedi, Ali, Melba M. Crawford, Neal R. Carpenter, and Mitchell R. Tuinstra. 2020. “Multi-Temporal Predictive Modelling of Sorghum Biomass Using UAV-Based Hyperspectral and LiDAR Data.” *Remote Sensing* 12(21):3587. doi: 10.3390/rs12213587.

Masjedi, Ali, Neal R. Carpenter, Melba M. Crawford, and Mitch R. Tuinstra. 2019. “Prediction of Sorghum Biomass Using Uav Time Series Data and Recurrent Neural Networks.” Pp. 0–0 in.

Masjedi, Ali, Jieqiong Zhao, Addie M. Thompson, Kai-Wei Yang, John E. Flatt, Melba M. Crawford, David S. Ebert, Mitchell R. Tuinstra, Graeme Hammer, and Scott Chapman. 2018. “Sorghum Biomass Prediction Using Uav-Based Remote Sensing Data and Crop Model Simulation.” Pp. 7719–22 in *IGARSS 2018 - 2018 IEEE International Geoscience and Remote Sensing Symposium*.

McCormick, Ryan F., Sandra K. Truong, and John E. Mullet. 2016. “3D Sorghum Reconstructions from Depth Images Identify QTL Regulating Shoot Architecture.” *Plant Physiology* 172(2):823–34. doi: 10.1104/pp.16.00948.

McCormick, Ryan F., Sandra K. Truong, Avinash Sreedasyam, Jerry Jenkins, Shengqiang Shu, David Sims, Megan Kennedy, Mojgan Amirebrahimi, Brock D. Weers, Brian McKinley, Ashley Mattison, Daryl T. Morishige, Jane Grimwood, Jeremy Schmutz, and John E. Mullet. 2018. “The Sorghum Bicolor Reference Genome: Improved Assembly, Gene Annotations, a Transcriptome Atlas, and Signatures of Genome Organization.” *The Plant Journal* 93(2):338–54. doi: 10.1111/tpj.13781.

McGrath, Justin M., and Stephen P. Long. 2014. “Can the Cyanobacterial Carbon-Concentrating Mechanism Increase Photosynthesis in Crop Species? A Theoretical Analysis.” *Plant Physiology* 164(4):2247–61. doi: 10.1104/pp.113.232611.

Meki, Manyowa N., Richard M. Ogoshi, Jim R. Kiniry, Susan E. Crow, Adel H. Youkhana, Mae H. Nakahata, and Kerrie Littlejohn. 2017. “Performance Evaluation of Biomass Sorghum in Hawaii and Texas.” *Industrial Crops and Products* 103:257–66. doi: 10.1016/j.indcrop.2017.04.014.

Messina, Carlos, G. Hammer, Zhanshan Dong, Dean Podlich, and Mark Cooper. 2009. “Modelling Crop Improvement in a G×E×M Framework via Gene–Trait–Phenotype Relationships.” *Crop Physiology: Applications for Genetic Improvement and Agronomy* 235–65. doi: 10.1016/B978-0-12-374431-9.00010-4.

Miao, Chenyong, Yuhang Xu, Sanzhen Liu, Patrick S. Schnable, and James C. Schnable. 2020. “Increased Power and Accuracy of Causal Locus Identification in Time Series Genome-Wide Association in Sorghum.” *Plant Physiology* 183(4):1898–1909. doi: 10.1104/pp.20.00277.

Mocoeur, Anne, Yu-Miao Zhang, Zhi-Quan Liu, Xin Shen, Li-Min Zhang, Søren K. Rasmussen, and Hai-Chun Jing. 2015. "Stability and Genetic Control of Morphological, Biomass and Biofuel Traits under Temperate Maritime and Continental Conditions in Sweet Sorghum (Sorghum Bicolour)." *Theoretical and Applied Genetics* 128(9):1685–1701. doi: 10.1007/s00122-015-2538-5.

Monk, R. L., F. R. Miller, and G. G. McBee. 1984. "Sorghum Improvement for Energy Production." *Biomass* 6(1):145–53. doi: 10.1016/0144-4565(84)90017-9.

Monteith, J. L., Moss C. J., Cooke George William, Pirie Norman Wingate, and Bell George Douglas Hutton. 1977. "Climate and the Efficiency of Crop Production in Britain." *Philosophical Transactions of the Royal Society of London. B, Biological Sciences* 281(980):277–94. doi: 10.1098/rstb.1977.0140.

Morris, Geoffrey P., Punna Ramu, Santosh P. Deshpande, C. Thomas Hash, Trushar Shah, Hari D. Upadhyaya, Oscar Riera-Lizarazu, Patrick J. Brown, Charlotte B. Acharya, Sharon E. Mitchell, James Harriman, Jeffrey C. Glaubitz, Edward S. Buckler, and Stephen Kresovich. 2013. "Population Genomic and Genome-Wide Association Studies of Agroclimatic Traits in Sorghum." *Proceedings of the National Academy of Sciences* 110(2):453–58. doi: 10.1073/pnas.1215985110.

Muchow, R. C. 1989. "Comparative Productivity of Maize, Sorghum and Pearl Millet in a Semi-Arid Tropical Environment I. Yield Potential." *Field Crops Research* 20(3):191–205. doi: 10.1016/0378-4290(89)90079-8.

Muchow, R. C., and R. Davis. 1988. "Effect of Nitrogen Supply on the Comparative Productivity of Maize and Sorghum in a Semi-Arid Tropical Environment II. Radiation Interception and Biomass Accumulation." *Field Crops Research* 18(1):17–30. doi: 10.1016/0378-4290(88)90056-1.

Muchow, R. C., and P. S. Carberry. 1990. "Phenology and Leaf-Area Development in a Tropical Grain Sorghum - ScienceDirect." *Field Crops Research* 23(3–4):221–37.

Muchow, R. C., and T. R. Sinclair. 1994. "Nitrogen Response of Leaf Photosynthesis and Canopy Radiation Use Efficiency in Field-Grown Maize and Sorghum." *Crop Science* 34(3):721–27. doi: 10.2135/cropsci1994.0011183X003400030022x.

Mullet, John, Daryl Morishige, Ryan McCormick, Sandra Truong, Josie Hilley, Brian McKinley, Robert Anderson, Sara N. Olson, and William Rooney. 2014. "Energy Sorghum—a Genetic Model for the Design of C4 Grass Bioenergy Crops." *Journal of Experimental Botany* 65(13):3479–89. doi: 10.1093/jxb/eru229.

Multani, Dilbag S., Steven P. Briggs, Mark A. Chamberlin, Joshua J. Blakeslee, Angus S. Murphy, and Gurmukh S. Johal. 2003. "Loss of an MDR Transporter in Compact Stalks of Maize Br2 and Sorghum Dw3 Mutants." *Science* 302(5642):81–84. doi: 10.1126/science.1086072.

Murchie, Erik H., Shawn Kefauver, Jose Luis Araus, Onno Muller, Uwe Rascher, Pádraic J. Flood, and Tracy Lawson. 2018. "Measuring the Dynamic Photosynthome." *Annals of Botany* 122(2):207–20. doi: 10.1093/aob/mcy087.

Murphy, Rebecca L., Robert R. Klein, Daryl T. Morishige, Jeff A. Brady, William L. Rooney, Frederick R. Miller, Diana V. Dugas, Patricia E. Klein, and John E. Mullet. 2011. "Coincident Light and Clock Regulation of Pseudoresponse Regulator Protein 37 (PRR37) Controls Photoperiodic Flowering in Sorghum." *Proceedings of the National Academy of Sciences* 108(39):16469–74. doi: 10.1073/pnas.1106212108.

Murphy, Rebecca L., Daryl T. Morishige, Jeff A. Brady, William L. Rooney, Shanshan Yang, Patricia E. Klein, and John E. Mullet. 2014. "Ghd7 (Ma6) Represses Sorghum Flowering in Long Days: Ghd7 Alleles Enhance Biomass Accumulation and Grain Production." *The Plant Genome* 7(2):plantgenome2013.11.0040. doi: 10.3835/plantgenome2013.11.0040.

Murray, Seth C., William L. Rooney, Sharon E. Mitchell, Arun Sharma, Patricia E. Klein, John E. Mullet, and Stephen Kresovich. 2008. "Genetic Improvement of Sorghum as a Biofuel Feedstock: II. QTL for Stem and Leaf Structural Carbohydrates." *Crop Science* 48(6):2180–93. doi: 10.2135/cropsci2008.01.0068.

Myles, Sean, Jason Peiffer, Patrick J. Brown, Elhan S. Ersoz, Zhiwu Zhang, Denise E. Costich, and Edward S. Buckler. 2009. "Association Mapping: Critical Considerations Shift from Genotyping to Experimental Design." *The Plant Cell* 21(8):2194–2202. doi: 10.1105/tpc.109.068437.

Nagaraja Reddy, R., R. Madhusudhana, S. Murali Mohan, D. V. N. Chakravarthi, S. P. Mehtre, N. Seetharama, and J. V. Patil. 2013. "Mapping QTL for Grain Yield and Other Agronomic Traits in Post-Rainy Sorghum [Sorghum Bicolor (L.) Moench]." *Theoretical and Applied Genetics* 126(8):1921–39. doi: 10.1007/s00122-013-2107-8.

Narayanan, Sruthi, Robert M. Aiken, P. V. Vara Prasad, Zhanguo Xin, and Jianming Yu. 2013. "Water and Radiation Use Efficiencies in Sorghum." *Agronomy Journal* 105(3):649. doi: 10.2134/agronj2012.0377.

Neumann, K., B. Kobiljski, S. Denčić, R. K. Varshney, and A. Börner. 2011. "Genome-Wide Association Mapping: A Case Study in Bread Wheat (Triticum Aestivum L.)." *Molecular Breeding* 27(1):37–58. doi: 10.1007/s11032-010-9411-7.

Oakey, Helena, Arūnas P. Verbyla, Brian R. Cullis, Xianming Wei, and Wayne S. Pitchford. 2007. "Joint Modeling of Additive and Non-Additive (Genetic Line) Effects in Multi-Environment Trials." *Theoretical and Applied Genetics* 114(8):1319–32. doi: 10.1007/s00122-007-0515-3.

de Oliveira, Amanda Avelar, Marcio F. R. Resende, Luís Felipe Ventorim Ferrão, Rodrigo Rampazo Amadeu, Lauro José Moreira Guimarães, Claudia Teixeira Guimarães, Maria Marta Pastina, and Gabriel Rodrigues Alves Margarido. 2020. "Genomic Prediction Applied to Multiple Traits and Environments in Second Season Maize Hybrids." *Heredity* 125(1):60–72. doi: 10.1038/s41437-020-0321-0.

Olsen, Peder A., Karthikeyan Natesan Ramamurthy, Javier Ribera, Yuhao Chen, Addie M. Thompson, Ronny Luss, Mitch Tuinstra, and Naoki Abe. 2018. "Detecting and Counting Panicles in Sorghum Images." Pp. 400–409 in *2018 IEEE 5th International Conference on Data Science and Advanced Analytics (DSAA)*.

Olson, Sara N., Kimberley Ritter, William Rooney, Armen Kemanian, Bruce A. McCarl, Yuquan Zhang, Susan Hall, Dan Packer, and John Mullet. 2012. "High Biomass Yield Energy Sorghum: Developing a Genetic Model for C4 Grass Bioenergy Crops." *Biofuels, Bioproducts and Biorefining* 6(6):640–55. doi: 10.1002/bbb.1357.

Ongaro, Veronica, Katherine Bainbridge, Lisa Williamson, and Ottoline Leyser. 2008. "Interactions between Axillary Branches of Arabidopsis." *Molecular Plant* 1(2):388–400. doi: 10.1093/mp/ssn007.

Onogi, Akio, Maya Watanabe, Toshihiro Mochizuki, Takeshi Hayashi, Hiroshi Nakagawa, Toshihiro Hasegawa, and Hiroyoshi Iwata. 2016. "Toward Integration of Genomic Selection with Crop Modelling: The Development of an Integrated Approach to Predicting Rice Heading Dates." *Theoretical and Applied Genetics* 129(4):805–17. doi: 10.1007/s00122-016-2667-5.

van Oosterom, E. J., P. S. Carberry, and G. J. O'Leary. 2001. "Simulating Growth, Development, and Yield of Tillering Pearl Millet: I. Leaf Area Profiles on Main Shoots and Tillers - ScienceDirect." *Field Crops Research* 72(1):51–66.

van Oosterom, E. J., A. K. Borrell, K. S. Deifel, and G. L. Hammer. 2011. "Does Increased Leaf Appearance Rate Enhance Adaptation to Postanthesis Drought Stress in Sorghum?" *Crop Science* 51(6):2728–40. doi: 10.2135/cropsci2011.01.0031.

van Oosterom, E. J., and G. L. Hammer. 2008. "Determination of Grain Number in Sorghum." *Field Crops Research* 108(3):259–68. doi: 10.1016/j.fcr.2008.06.001.

Ortiz, Diego, Jieyun Hu, and Maria G. Salas Fernandez. 2017. "Genetic Architecture of Photosynthesis in Sorghum Bicolor under Non-Stress and Cold Stress Conditions." *Journal of Experimental Botany* 68(16):4545–57. doi: 10.1093/jxb/erx276.

Pareek, Chandra Shekhar, Rafal Smoczynski, and Andrzej Tretyn. 2011. "Sequencing Technologies and Genome Sequencing." *Journal of Applied Genetics* 52(4):413–35. doi: 10.1007/s13353-011-0057-x.

Parent, Boris, Emilie J. Millet, and François Tardieu. 2019. "The Use of Thermal Time in Plant Studies Has a Sound Theoretical Basis Provided That Confounding Effects Are Avoided." *Journal of Experimental Botany* 70(9):2359–70. doi: 10.1093/jxb/ery402.

Pauli, Duke, Scott C. Chapman, Rebecca Bart, Christopher N. Topp, Carolyn J. Lawrence-Dill, Jesse Poland, and Michael A. Gore. 2016. "The Quest for Understanding Phenotypic Variation via Integrated Approaches in the Field Environment." *Plant Physiology* 172(2):622–34. doi: 10.1104/pp.16.00592.

Pereira, M. G., and M. Lee. 1995. “Identification of Genomic Regions Affecting Plant Height in Sorghum and Maize.” *Theoretical and Applied Genetics* 90(3):380–88. doi: 10.1007/BF00221980.

Pfeiffer, Brian K., Dennis Pietsch, Ronnie W. Schnell, and William L. Rooney. 2019. “Long-Term Selection in Hybrid Sorghum Breeding Programs.” *Crop Science* 59(1):150–64. doi: 10.2135/cropsci2018.05.0345.

Phuong, Nguyen, H. Stützel, and R. Uptmoor. 2013. “Quantitative Trait Loci Associated to Agronomic Traits and Yield Components in a Sorghum Bicolor L. Moench RIL Population Cultivated under Pre-Flowering Drought and Well-Watered Conditions.” *Agricultural Sciences* 4(12):781–91. doi: 10.4236/as.2013.412107.

Piñeiro, Gervasio, Susana Perelman, Juan Guerschman, and José Paruelo. 2008. “How to Evaluate Models: Observed vs. Predicted or Predicted vs. Observed?” *Ecological Modelling* 216(3–4):316–22. doi: 10.1016/j.ecolmodel.2008.05.006.

Pokhrel, Pramod, Nithya Rajan, John Jifon, William Rooney, Russell Jessup, Jorge da Silva, Juan Enciso, and Ahmed Attia. 2021. “Evaluation of the DSSAT-CANEGRO Model for Simulating the Growth of Energy Cane (Saccharum Spp.), a Biofuel Feedstock Crop.” *Crop Science* n/a(n/a). doi: 10.1002/csc2.20648.

Potgieter, Andries B., Barbara George-Jaeggli, Scott C. Chapman, Kenneth Laws, Luz A. Suárez Cadavid, Jemima Wixted, James Watson, Mark Eldridge, David R. Jordan, and Graeme L. Hammer. 2017. “Multi-Spectral Imaging from an Unmanned Aerial Vehicle Enables the Assessment of Seasonal Leaf Area Dynamics of Sorghum Breeding Lines.” *Frontiers in Plant Science* 8:1532. doi: 10.3389/fpls.2017.01532.

Pugh, N. Ace, David W. Horne, Seth C. Murray, Geraldo Carvalho Jr, Lonesome Malambo, Jinha Jung, Anjin Chang, Murilo Maeda, Sorin Popescu, Tianxing Chu, Michael J. Starek, Michael J. Brewer, Grant Richardson, and William L. Rooney. 2018. “Temporal Estimates of Crop Growth in Sorghum and Maize Breeding Enabled by Unmanned Aerial Systems.” *The Plant Phenome Journal* 1(1):170006. doi: 10.2135/tppj2017.08.0006.

Quinby, J. R., and R. E. Karper. 1953. “Inheritance of Height in Sorghum.” *Inheritance of Height in Sorghum.*

R Core Team. 2020. “R: The R Project for Statistical Computing. R Foundation for Statistical Computing, Vienna, Austria.” Retrieved October 26, 2021 (https://www.r-project.org/).

Rafalski, Antoni. 2002. “Applications of Single Nucleotide Polymorphisms in Crop Genetics.” *Current Opinion in Plant Biology* 5(2):94–100. doi: 10.1016/S1369-5266(02)00240-6.

Rajkumar, B. Fakrudin, S. P. Kavil, Y. Girma, S. S. Arun, D. Dadakhalandar, B. H. Gurusiddesh, A. M. Patil, M. Thudi, S. B. Bhairappanavar, Y. D. Narayana, P. U. Krishnaraj, B. M. Khadi, and M. Y. Kamatar. 2013. “Molecular Mapping of Genomic Regions Harbouring QTLs for Root and Yield Traits in Sorghum (Sorghum Bicolor L. Moench).” *Physiology and Molecular Biology of Plants* 19(3):409–19. doi: 10.1007/s12298-013-0188-0.

Rama Reddy, Nagaraja Reddy, Madhusudhana Ragimasalawada, Murali Mohan Sabbavarapu, Seetharama Nadoor, and Jagannatha Vishnu Patil. 2014. "Detection and Validation of Stay-Green QTL in Post-Rainy Sorghum Involving Widely Adapted Cultivar, M35-1 and a Popular Stay-Green Genotype B35." *BMC Genomics* 15(1):909. doi: 10.1186/1471-2164-15-909.

Ravi, Radhika, Yun-Jou Lin, Magdy Elbahnasawy, Tamer Shamseldin, and Ayman Habib. 2018a. "Bias Impact Analysis and Calibration of Terrestrial Mobile LiDAR System With Several Spinning Multibeam Laser Scanners." *IEEE Transactions on Geoscience and Remote Sensing* 56(9):5261–75. doi: 10.1109/TGRS.2018.2812782.

Ravi, Radhika, Yun-Jou Lin, Magdy Elbahnasawy, Tamer Shamseldin, and Ayman Habib. 2018b. "Simultaneous System Calibration of a Multi-LiDAR Multicamera Mobile Mapping Platform." *IEEE Journal of Selected Topics in Applied Earth Observations and Remote Sensing* 11(5):1694–1714. doi: 10.1109/JSTARS.2018.2812796.

Ravi, Radhika, Yun-Jou Lin, Tamer Shamseldin, Magdy Elbahnasawy, Ali Masjedi, Melba Crawford, and Ayman Habib. 2018. "Wheel-Based Lidar Data for Plant Height and Canopy Cover Evaluation to Aid Biomass Prediction." Pp. 3242–45 in *IGARSS 2018 - 2018 IEEE International Geoscience and Remote Sensing Symposium*.

Ravi Kumar, S., Graeme Hammer, Ian Broad, Peter Harland, and Greg McLean. 2009. "Modelling Environmental Effects on Phenology and Canopy Development of Diverse Sorghum Genotypes - ScienceDirect." *Field Crops Research* 111(1–2):157–65.

Reddy, Belum VS, S. Ramesh, P. Sanjana Reddy, B. Ramaiah, P. M. Salimath, and Rajashekar Kachapur. 2005. "Sweet Sorghum - a Potential Alternate Raw Material for Bio-Ethanol and Bio-Energy." *Journal of SAT Agricultural Research*.

Rhodes, Davina H., Leo Hoffmann, William L. Rooney, Thomas J. Herald, Scott Bean, Richard Boyles, Zachary W. Brenton, and Stephen Kresovich. 2017. "Genetic Architecture of Kernel Composition in Global Sorghum Germplasm." *BMC Genomics* 18(1):15. doi: 10.1186/s12864-016-3403-x.

Ribera, Javier, Yuhao Chen, Christopher Boomsma, and Edward J. Delp. 2017. "Counting Plants Using Deep Learning." Pp. 1344–48 in *2017 IEEE Global Conference on Signal and Information Processing (GlobalSIP)*.

Ribera, Javier, Fangning He, Yuhao Chen, Ayman F. Habib, and Edward J. Delp. 2018. "Estimating Phenotypic Traits From UAV Based RGB Imagery." *ArXiv:1807.00498 [Cs]*.

Rocateli, A. C., R. L. Raper, K. S. Balkcom, F. J. Arriaga, and D. I. Bransby. 2012. "Biomass Sorghum Production and Components under Different Irrigation/Tillage Systems for the Southeastern U.S." *Industrial Crops and Products* 36(1):589–98. doi: 10.1016/j.indcrop.2011.11.007.

Rodríguez-Álvarez, María Xosé, Martin P. Boer, Fred A. van Eeuwijk, and Paul H. C. Eilers. 2018. "Correcting for Spatial Heterogeneity in Plant Breeding Experiments with P-Splines." *Spatial Statistics* 23:52–71. doi: 10.1016/j.spasta.2017.10.003.

Rooney, William L. 2004. *Advances in Agronomy*. Academic Press.

Rooney, William L., Jürg Blumenthal, Brent Bean, and John E. Mullet. 2007. "Designing Sorghum as a Dedicated Bioenergy Feedstock." *Biofuels, Bioproducts and Biorefining* 1(2):147–57. doi: 10.1002/bbb.15.

Rosenow, D. T., J. A. Dahlberg, J. C. Stephens, F. R. Miller, D. K. Barnes, G. C. Peterson, J. W. Johnson, and K. F. Schertz. 1997. "Registration of 63 Converted Sorghum Germplasm Lines from the Sorghum Conversion Program." *Crop Science* 37(4):1399–1400. doi: 10.2135/cropsci1997.0011183X003700040090x.

Rosenow, D.T., D. T. Rosenow, J. A. Dahlberg, G. C. Peterson, and L. E. Clark. 1997. "Registration of Fifty Converted Sorghums from the Sorghum Conversion Program." *Crop Science* v. 37(4):1397–98. doi: 10.2135/cropsci1997.0011183X003700040089x.

Rossi, Evandrei S., Maurício C. Kuki, Ronald J. B. Pinto, Carlos A. Scapim, Marcos V. Faria, and Natalia De Leon. 2020. "Genomic-Wide Association Study for White Spot Resistance in a Tropical Maize Germplasm." *Euphytica* 216(1):15. doi: 10.1007/s10681-019-2550-y.

Rubin, Edward M. 2008. "Genomics of Cellulosic Biofuels." *Nature* 454(7206):841–45. doi: 10.1038/nature07190.

Sabadin, P. K., M. Malosetti, M. P. Boer, F. D. Tardin, F. G. Santos, C. T. Guimarães, R. L. Gomide, C. L. T. Andrade, P. E. P. Albuquerque, F. F. Caniato, M. Mollinari, G. R. A. Margarido, B. F. Oliveira, R. E. Schaffert, A. A. F. Garcia, F. A. van Eeuwijk, and J. V. Magalhaes. 2012. "Studying the Genetic Basis of Drought Tolerance in Sorghum by Managed Stress Trials and Adjustments for Phenological and Plant Height Differences." *Theoretical and Applied Genetics* 124(8):1389–1402. doi: 10.1007/s00122-012-1795-9.

Sadras, V. O., C. Lawson, and A. Montoro. 2012. "Photosynthetic Traits in Australian Wheat Varieties Released between 1958 and 2007." *Field Crops Research* 134:19–29. doi: 10.1016/j.fcr.2012.04.012.

Sadras, Victor O., Chris Lawson, Victor O. Sadras, and Chris Lawson. 2011. "Genetic Gain in Yield and Associated Changes in Phenotype, Trait Plasticity and Competitive Ability of South Australian Wheat Varieties Released between 1958 and 2007." *Crop and Pasture Science* 62(7):533–49. doi: 10.1071/CP11060.

Salas Fernandez, Maria G., Philip W. Becraft, Yanhai Yin, and Thomas Lübberstedt. 2009. "From Dwarves to Giants? Plant Height Manipulation for Biomass Yield." *Trends in Plant Science* 14(8):454–61. doi: 10.1016/j.tplants.2009.06.005.

Salimath, Shanmukhaswami S., Antonio C. de Oliveira, Jeffrey L. Bennetzen, and Ian D. Godwin. 1995. “Assessment of Genome Origins and Genetic Diversity in the Genus Eleusine with DNA Markers.” *Genome* 38(4):757–63. doi: 10.1139/g95-096.

Sami, Rukaiya. 2013. “Heritability Studies In Some Sweet Sorghum (Sorghum Bicolor. L. Moench) Genotypes.” *Journal of Biology, Agriculture and Healthcare* 3.

Schneider, Caroline A., Wayne S. Rasband, and Kevin W. Eliceiri. 2012. “NIH Image to ImageJ: 25 Years of Image Analysis.” *Nature Methods* 9(7):671–75. doi: 10.1038/nmeth.2089.

Seyoum, Solomon, Rao Rachaputi, Yash Chauhan, Boddupalli Prasanna, and Solomon Fekybelu. 2018. “Application of the APSIM Model to Exploit G × E × M Interactions for Maize Improvement in Ethiopia.” *Field Crops Research* 217:113–24. doi: 10.1016/j.fcr.2017.12.012.

Shearman, V. J., R. Sylvester-Bradley, R. K. Scott, and M. J. Foulkes. 2005. “Physiological Processes Associated with Wheat Yield Progress in the UK.” *Crop Science* 45(1):cropsci2005.0175. doi: 10.2135/cropsci2005.0175a.

Shehzad, Tariq, and Kazutoshi Okuno. 2015. “QTL Mapping for Yield and Yield-Contributing Traits in Sorghum (Sorghum Bicolor (L.) Moench) with Genome-Based SSR Markers.” *Euphytica* 203(1):17–31. doi: 10.1007/s10681-014-1243-9.

Shiringani, Amukelani L., and Wolfgang Friedt. 2011. “QTL for Fibre-Related Traits in Grain × Sweet Sorghum as a Tool for the Enhancement of Sorghum as a Biomass Crop.” *Theoretical and Applied Genetics* 123(6):999. doi: 10.1007/s00122-011-1642-4.

Shiringani, Amukelani Lacrecia, Matthias Frisch, and Wolfgang Friedt. 2010. “Genetic Mapping of QTLs for Sugar-Related Traits in a RIL Population of Sorghum Bicolor L. Moench.” *Theoretical and Applied Genetics* 121(2):323–36. doi: 10.1007/s00122-010-1312-y.

Sieglinger, J. B. 1936. “Leaf Number of Sorghum Stalks.” *Agronomy Journal* 28(8):636–42. doi: 10.2134/agronj1936.00021962002800080005x.

Sinclair, T. R., and T. Horie. 1989. “Leaf Nitrogen, Photosynthesis, and Crop Radiation Use Efficiency: A Review.” *Crop Science* 29(1):cropsci1989.0011183X002900010023x. doi: 10.2135/cropsci1989.0011183X002900010023x.

Sinclair, Thomas R., and Russell C. Muchow. 1999. “Radiation Use Efficiency.” Pp. 215–65 in *Advances in Agronomy*. Vol. 65, edited by D. L. Sparks. Academic Press.

Singh, Piara, S. Nedumaran, P. C. S. Traore, K. J. Boote, H. F. W. Rattunde, P. V. Vara Prasad, N. P. Singh, K. Srinivas, and M. C. S. Bantilan. 2014. “Quantifying Potential Benefits of Drought and Heat Tolerance in Rainy Season Sorghum for Adapting to Climate Change.” *Agricultural and Forest Meteorology* 185:37–48. doi: 10.1016/j.agrformet.2013.10.012.

Smith, C. Wayne, and Richard A. Frederiksen. 2000. *Sorghum: Origin, History, Technology, and Production*. John Wiley & Sons.

Smith, W. H. 1986. “Biomass Energy Development.”

Soler, Cecilia Manuela Tojo, Paulo César Sentelhas, and Gerrit Hoogenboom. 2007. “Application of the CSM-CERES-Maize Model for Planting Date Evaluation and Yield Forecasting for Maize Grown off-Season in a Subtropical Environment.” *European Journal of Agronomy* 27(2):165–77. doi: 10.1016/j.eja.2007.03.002.

Srinivas, G., K. Satish, R. Madhusudhana, R. Nagaraja Reddy, S. Murali Mohan, and N. Seetharama. 2009. “Identification of Quantitative Trait Loci for Agronomically Important Traits and Their Association with Genic-Microsatellite Markers in Sorghum.” *Theoretical and Applied Genetics* 118(8):1439–54. doi: 10.1007/s00122-009-0993-6.

Stanton, Carly, Michael J. Starek, Norman Elliott, Michael Brewer, Murilo M. Maeda, and Tianxing Chu. 2017. “Unmanned Aircraft System-Derived Crop Height and Normalized Difference Vegetation Index Metrics for Sorghum Yield and Aphid Stress Assessment.” *Journal of Applied Remote Sensing* 11(2):026035. doi: 10.1117/1.JRS.11.026035.

Stefaniak, Thomas R., Jeffery A. Dahlberg, Brent W. Bean, Nilesh Dighe, Edward J. Wolfrum, and William L. Rooney. 2012. “Variation in Biomass Composition Components among Forage, Biomass, Sorghum-Sudangrass, and Sweet Sorghum Types.” *Crop Science* 52(4):1949–54. doi: 10.2135/cropsci2011.10.0534.

Stephens, J. C., F. R. Miller, and D. T. Rosenow. 1967. “Conversion of Alien Sorghums to Early Combine Genotypes 1.” *Crop Science* 7(4):396–396. doi: 10.2135/cropsci1967.0011183X000700040036x.

Stöckle, Claudio O., Marcello Donatelli, and Roger Nelson. 2003. “CropSyst, a Cropping Systems Simulation Model.” *European Journal of Agronomy* 18(3):289–307. doi: 10.1016/S1161-0301(02)00109-0.

Subudhi, P. K., D. T. Rosenow, and H. T. Nguyen. 2000. “Quantitative Trait Loci for the Stay Green Trait in Sorghum (Sorghum Bicolor L. Moench): Consistency across Genetic Backgrounds and Environments.” *Theoretical and Applied Genetics* 101(5):733–41. doi: 10.1007/s001220051538.

Sukumaran, Sivakumar, Susanne Dreisigacker, Marta Lopes, Perla Chavez, and Matthew P. Reynolds. 2015. “Genome-Wide Association Study for Grain Yield and Related Traits in an Elite Spring Wheat Population Grown in Temperate Irrigated Environments.” *TAG. Theoretical and Applied Genetics. Theoretische Und Angewandte Genetik* 128(2):353–63. doi: 10.1007/s00122-014-2435-3.

Sukumaran, Sivakumar, Xin Li, Xianran Li, Chengsong Zhu, Guihua Bai, Ramasamy Perumal, Mitchell R. Tuinstra, P. V. Vara Prasad, Sharon E. Mitchell, Tesfaye T. Tesso, and Jianming Yu. 2016. “QTL Mapping for Grain Yield, Flowering Time, and Stay-Green Traits in Sorghum with Genotyping-by-Sequencing Markers.” *Crop Science* 56(4):1429–42. doi: 10.2135/cropsci2015.02.0097.

Sukumaran, Sivakumar, Wenwen Xiang, Scott R. Bean, Jeffrey F. Pedersen, Stephen Kresovich, Mitchell R. Tuinstra, Tesfaye T. Tesso, Martha T. Hamblin, and Jianming Yu. 2012. "Association Mapping for Grain Quality in a Diverse Sorghum Collection." *Plant Genome* 5(3):126–35. doi: 10.3835/plantgenome2012.07.0016.

Taiyun. 2021. *Taiyun/Corrplot*.

Takai, Tomoyuki, Jun-ichi Yonemaru, Hirokazu Kaidai, and Shigemitsu Kasuga. 2012. "Quantitative Trait Locus Analysis for Days-to-Heading and Morphological Traits in an RIL Population Derived from an Extremely Late Flowering F1 Hybrid of Sorghum." *Euphytica* 187(3):411–20. doi: 10.1007/s10681-012-0727-8.

Tardieu, François, Llorenç Cabrera-Bosquet, Tony Pridmore, and Malcolm Bennett. 2017. "Plant Phenomics, From Sensors to Knowledge." *Current Biology* 27(15):R770–83. doi: 10.1016/j.cub.2017.05.055.

Technow, Frank, Carlos D. Messina, L. Radu Totir, and Mark Cooper. 2015. "Integrating Crop Growth Models with Whole Genome Prediction through Approximate Bayesian Computation." *PLOS ONE* 10(6):e0130855. doi: 10.1371/journal.pone.0130855.

Tian, Feng, Peter J. Bradbury, Patrick J. Brown, Hsiaoyi Hung, Qi Sun, Sherry Flint-Garcia, Torbert R. Rocheford, Michael D. McMullen, James B. Holland, and Edward S. Buckler. 2011. "Genome-Wide Association Study of Leaf Architecture in the Maize Nested Association Mapping Population." *Nature Genetics* 43(2):159–62. doi: 10.1038/ng.746.

Tilman, David, Jason Hill, and Clarence Lehman. 2006. "Carbon-Negative Biofuels from Low-Input High-Diversity Grassland Biomass." *Science* 314(5805):1598–1600. doi: 10.1126/science.1133306.

Tolley, Seth A., Amritpal Singh, and Mitchell R. Tuinstra. 2021. "Heterotic Patterns of Temperate and Tropical Maize by Ear Photometry." *Frontiers in Plant Science* 12:1117. doi: 10.3389/fpls.2021.616975.

Truong, Sandra K., Ryan F. McCormick, and John E. Mullet. 2017. "Bioenergy Sorghum Crop Model Predicts VPD-Limited Transpiration Traits Enhance Biomass Yield in Water-Limited Environments." *Frontiers in Plant Science* 8. doi: 10.3389/fpls.2017.00335.

Tumbo, S. D., M. Salyani, J. D. Whitney, T. A. Wheaton, and W. M. Miller. 2002. "Investigation of Laser and Ultrasonic Ranging Sensors for Measurements of Citrus Canopy Volume." *Applied Engineering in Agriculture*.

Turner, Stephen D. 2014. *Qqman: An R Package for Visualizing GWAS Results Using Q-Q and Manhattan Plots*. doi: 10.1101/005165.

Vanneste, Steffen, and Jiří Friml. 2009. "Auxin: A Trigger for Change in Plant Development." *Cell* 136(6):1005–16. doi: 10.1016/j.cell.2009.03.001.

Villanueva, Randle Aaron M., and Zhuo Job Chen. 2019. “Ggplot2: Elegant Graphics for Data Analysis (2nd Ed.).” *Measurement: Interdisciplinary Research and Perspectives* 17(3):160–67. doi: 10.1080/15366367.2019.1565254.

Virlet, Nicolas, Kasra Sabermanesh, Pouria Sadeghi-Tehran, Malcolm J. Hawkesford, Nicolas Virlet, Kasra Sabermanesh, Pouria Sadeghi-Tehran, and Malcolm J. Hawkesford. 2016. “Field Scanalyzer: An Automated Robotic Field Phenotyping Platform for Detailed Crop Monitoring.” *Functional Plant Biology* 44(1):143–53. doi: 10.1071/FP16163.

Vos, Pieter, Rene Hogers, Marjo Bleeker, Martin Reijans, Theo van de Lee, Miranda Hornes, Adrie Friters, Jerina Pot, Johan Paleman, Martin Kuiper, and Marc Zabeau. 1995. “AFLP: A New Technique for DNA Fingerprinting.” *Nucleic Acids Research* 23(21):4407–14. doi: 10.1093/nar/23.21.4407.

Wallach, Daniel, David Makowski, James W. Jones, and Francois Brun. 2018. *Working with Dynamic Crop Models: Methods, Tools and Examples for Agriculture and Environment*. Academic Press.

Wang, E., M. J. Robertson, G. L. Hammer, P. S. Carberry, D. Holzworth, H. Meinke, S. C. Chapman, J. N. G. Hargreaves, N. I. Huth, and G. McLean. 2002. “Development of a Generic Crop Model Template in the Cropping System Model APSIM.” *European Journal of Agronomy* 18(1):121–40. doi: 10.1016/S1161-0301(02)00100-4.

Wang, Hai-Lian, Hua-Wen Zhang, Rui-Heng Du, Gui-Ling Chen, Bin Liu, Yan-Bing Yang, Ling Qin, Er-Ying Cheng, Qiang Liu, Yan-An Guan, Hai-Lian Wang, Hua-Wen Zhang, Rui-Heng Du, Gui-Ling Chen, Bin Liu, Yan-Bing Yang, Ling Qin, Er-Ying Cheng, Qiang Liu, and Yan-An Guan. 2016. “Identification and Validation of QTLs Controlling Multiple Traits in Sorghum.” *Crop and Pasture Science* 67(2):193–203. doi: 10.1071/CP15239.

Wang, Jiabo, and Zhiwu Zhang. 2020. *GAPIT Version 3: Boosting Power and Accuracy for Genomic Association and Prediction*. doi: 10.1101/2020.11.29.403170.

Wang, Jianan, Zhenbin Hu, Hari D. Upadhyaya, and Geoffrey P. Morris. 2020. “Genomic Signatures of Seed Mass Adaptation to Global Precipitation Gradients in Sorghum.” *Heredity* 124(1):108–21. doi: 10.1038/s41437-019-0249-4.

Wang, Taojun, and Melba M. Crawford. 2021. “Multi-Year Sorghum Biomass Prediction with UAV-Based Remote Sensing Data.” Pp. 4312–15 in *2021 IEEE International Geoscience and Remote Sensing Symposium IGARSS*.

Wang, Xuemin, Emma Mace, Colleen Hunt, Alan Cruickshank, Robert Henzell, Heidi Parkes, and David Jordan. 2014. “Two Distinct Classes of QTL Determine Rust Resistance in Sorghum.” *BMC Plant Biology* 14(1):366. doi: 10.1186/s12870-014-0366-4.

Wheeler, Tim, and Joachim von Braun. 2013. “Climate Change Impacts on Global Food Security.” *Science* 341(6145):508–13. doi: 10.1126/science.1239402.

White, J. W., G. Alagarswamy, M. J. Ottman, C. H. Porter, U. Singh, and G. Hoogenboom. 2015. “An Overview of CERES–Sorghum as Implemented in the Cropping System Model Version 4.5.” *Agronomy Journal* 107(6):1987–2002. doi: 10.2134/agronj15.0102.

White, Jeffrey W., Pedro Andrade-Sanchez, Michael A. Gore, Kevin F. Bronson, Terry A. Coffelt, Matthew M. Conley, Kenneth A. Feldmann, Andrew N. French, John T. Heun, Douglas J. Hunsaker, Matthew A. Jenks, Bruce A. Kimball, Robert L. Roth, Robert J. Strand, Kelly R. Thorp, Gerard W. Wall, and Guangyao Wang. 2012. “Field-Based Phenomics for Plant Genetics Research.” *Field Crops Research* 133:101–12. doi: 10.1016/j.fcr.2012.04.003.

Williams, J. R., K. G. Renard, and P. T. Dyke. 1983. “EPIC: A New Method for Assessing Erosion’s Effect on Soil Productivity.” *Journal of Soil and Water Conservation* 38(5):381–83.

Williams, John G. K., Anne R. Kubelik, Kenneth J. Livak, J. Antoni Rafalski, and Scott V. Tingey. 1990. “DNA Polymorphisms Amplified by Arbitrary Primers Are Useful as Genetic Markers.” *Nucleic Acids Research* 18(22):6531–35. doi: 10.1093/nar/18.22.6531.

Wilson, G. L., and J. D. Eastin. 1982. “The Plant and Its Environment.” *Sorghum in the Eighties: Proceedings of the International Symposium on Sorghum. 2 7 November 1981, ICRISAT Center Patancheru, A. P. India.* 1:101–19.

Xia, Jingnu, Yunjun Zhao, Payne Burks, Markus Pauly, and Patrick J. Brown. 2018. “A Sorghum NAC Gene Is Associated with Variation in Biomass Properties and Yield Potential.” *Plant Direct* 2(7):e00070. doi: 10.1002/pld3.70.

Xu, Wenwei, Prasanta K. Subudhi, Oswald R. Crasta, Darrell T. Rosenow, John E. Mullet, and Henry T. Nguyen. 2000. “Molecular Mapping of QTLs Conferring Stay-Green in Grain Sorghum (Sorghum Bicolor L. Moench).” *Genome* 43(3):461–69. doi: 10.1139/g00-003.

Yamaguchi, Miki, Haruka Fujimoto, Ko Hirano, Satoko Araki-Nakamura, Kozue Ohmae-Shinohara, Akihiro Fujii, Masako Tsunashima, Xian Jun Song, Yusuke Ito, Rie Nagae, Jianzhong Wu, Hiroshi Mizuno, Jun-ichi Yonemaru, Takashi Matsumoto, Hidemi Kitano, Makoto Matsuoka, Shigemitsu Kasuga, and Takashi Sazuka. 2016. “Sorghum Dw1, an Agronomically Important Gene for Lodging Resistance, Encodes a Novel Protein Involved in Cell Proliferation.” *Scientific Reports* 6(1):28366. doi: 10.1038/srep28366.

Yang, Changye, Sriram Baireddy, Enyu Cai, Melba Crawford, and Edward J. Delp. 2021. “Field-Based Plot Extraction Using UAV RGB Images.” *ArXiv:2109.00632 [Cs]*.

Yang, Kai-Wei, Scott Chapman, Neal Carpenter, Graeme Hammer, Greg McLean, Bangyou Zheng, Yuhao Chen, Edward Delp, Ali Masjedi, Melba Crawford, David Ebert, Ayman Habib, Addie Thompson, Clifford Weil, and Mitchell R. Tuinstra. 2021. “Integrating Crop Growth Models with Remote Sensing for Predicting Biomass Yield of Sorghum.” *In Silico Plants* 3(1). doi: 10.1093/insilicoplants/diab001.

Yang, Shanshan, Rebecca L. Murphy, Daryl T. Morishige, Patricia E. Klein, William L. Rooney, and John E. Mullet. 2014. "Sorghum Phytochrome B Inhibits Flowering in Long Days by Activating Expression of SbPRR37 and SbGHD7, Repressors of SbEHD1, SbCN8 and SbCN12." *PLOS ONE* 9(8):e105352. doi: 10.1371/journal.pone.0105352.

Yin, Xinyou, Paul C. Struik, and Jan Goudriaan. 2021. "On the Needs for Combining Physiological Principles and Mathematics to Improve Crop Models." *Field Crops Research* 271:108254. doi: 10.1016/j.fcr.2021.108254.

Yu, Jianming, Gael Pressoir, William H. Briggs, Irie Vroh Bi, Masanori Yamasaki, John F. Doebley, Michael D. McMullen, Brandon S. Gaut, Dahlia M. Nielsen, James B. Holland, Stephen Kresovich, and Edward S. Buckler. 2006. "A Unified Mixed-Model Method for Association Mapping That Accounts for Multiple Levels of Relatedness." *Nature Genetics* 38(2):203–8. doi: 10.1038/ng1702.

Zhang, Dong, Wenqian Kong, Jon Robertson, Valorie H. Goff, Ethan Epps, Alexandra Kerr, Gabriel Mills, Jay Cromwell, Yelena Lugin, Christine Phillips, and Andrew H. Paterson. 2015. "Genetic Analysis of Inflorescence and Plant Height Components in Sorghum (Panicoidae) and Comparative Genetics with Rice (Oryzoidae)." *BMC Plant Biology* 15(1):107. doi: 10.1186/s12870-015-0477-6.

Zhang, Li-Min, Chuan-Yuan Leng, Hong Luo, Xiao-Yuan Wu, Zhi-Quan Liu, Yu-Miao Zhang, Hong Zhang, Yan Xia, Li Shang, Chun-Ming Liu, Dong-Yun Hao, Yi-Hua Zhou, Cheng-Cai Chu, Hong-Wei Cai, and Hai-Chun Jing. 2018. "Sweet Sorghum Originated through Selection of Dry, a Plant-Specific NAC Transcription Factor Gene." *The Plant Cell* 30(10):2286–2307. doi: 10.1105/tpc.18.00313.

Zhang, Xiaoxiang, Zhongrong Guan, Lei Wang, Jun Fu, Yinchao Zhang, Zhaoling Li, Langlang Ma, Peng Liu, Yanling Zhang, Min Liu, Peng Li, Chaoying Zou, Yongcong He, Haijian Lin, Guangsheng Yuan, Shibin Gao, Guangtang Pan, and Yaou Shen. 2020. "Combined GWAS and QTL Analysis for Dissecting the Genetic Architecture of Kernel Test Weight in Maize." *Molecular Genetics and Genomics* 295(2):409–20. doi: 10.1007/s00438-019-01631-2.

Zhang, Zhiwu, Elhan Ersoz, Chao-Qiang Lai, Rory J. Todhunter, Hemant K. Tiwari, Michael A. Gore, Peter J. Bradbury, Jianming Yu, Donna K. Arnett, Jose M. Ordovas, and Edward S. Buckler. 2010. "Mixed Linear Model Approach Adapted for Genome-Wide Association Studies." *Nature Genetics* 42(4):355–60. doi: 10.1038/ng.546.

Zhang, Zhou, Ali Masjedi, Jieqiong Zhao, and Melba M. Crawford. 2017. "Prediction of Sorghum Biomass Based on Image Based Features Derived from Time Series of UAV Images." Pp. 6154–57 in *2017 IEEE International Geoscience and Remote Sensing Symposium (IGARSS)*.

Zhao, Chunjiang, Ying Zhang, Jianjun Du, Xinyu Guo, Weiliang Wen, Shenghao Gu, Jinglu Wang, and Jiangchuan Fan. 2019. “Crop Phenomics: Current Status and Perspectives.” *Frontiers in Plant Science* 10:714. doi: 10.3389/fpls.2019.00714.

Zhao, Jing, Maria B. Mantilla Perez, Jieyun Hu, and Maria G. Salas Fernandez. 2016. “Genome-Wide Association Study for Nine Plant Architecture Traits in Sorghum.” *The Plant Genome* 9(2). doi: 10.3835/plantgenome2015.06.0044.

Zhou, Chengquan, Hongbao Ye, Zhifu Xu, Jun Hu, Xiaoyan Shi, Shan Hua, Jibo Yue, and Guijun Yang. 2019. “Estimating Maize-Leaf Coverage in Field Conditions by Applying a Machine Learning Algorithm to UAV Remote Sensing Images.” *Applied Sciences* 9(11). doi: 10.3390/app9112389.

Zhou, Tian, Seyyed Meghdad Hasheminasab, and Ayman Habib. 2021. “Tightly-Coupled Camera/LiDAR Integration for Point Cloud Generation from GNSS/INS-Assisted UAV Mapping Systems.” *ISPRS Journal of Photogrammetry and Remote Sensing* 180:336–56. doi: 10.1016/j.isprsjprs.2021.08.020.

Zhu, Guanglong, Shaobing Peng, Jianliang Huang, Kehui Cui, Lixiao Nie, and Fei Wang. 2016. “Genetic Improvements in Rice Yield and Concomitant Increases in Radiation- and Nitrogen-Use Efficiency in Middle Reaches of Yangtze River.” *Scientific Reports* 6(1):21049. doi: 10.1038/srep21049.

Zhu, Xin-Guang, Jonathan P. Lynch, David S. LeBauer, Andrew J. Millar, Mark Stitt, and Stephen P. Long. 2016. “Plants in Silico: Why, Why Now and What?—An Integrative Platform for Plant Systems Biology Research.” *Plant, Cell & Environment* 39(5):1049–57. doi: 10.1111/pce.12673.